

# **For Reference**

---

**NOT TO BE TAKEN FROM THIS ROOM**

Ex LIBRIS  
UNIVERSITATIS  
ALBERTAEASIS











To My Family



THE UNIVERSITY OF ALBERTA

TRANSITION METAL DITHIOPHOSPHINATES

by



E. DAVID DAY

A THESIS

SUBMITTED TO THE FACULTY OF GRADUATE STUDIES AND RESEARCH  
IN PARTIAL FULFILMENT OF THE REQUIREMENTS FOR THE DEGREE  
OF DOCTOR OF PHILOSOPHY

DEPARTMENT OF CHEMISTRY

UNIVERSITY OF ALBERTA

EDMONTON, ALBERTA

SPRING, 1972



Thesis  
1972  
22D

UNIVERSITY OF ALBERTA  
FACULTY OF GRADUATE STUDIES AND RESEARCH

The undersigned certify that they have read, and recommend  
to the Faculty of Graduate Studies and Research for acceptance,  
a thesis entitled

TRANSITION METAL DITHIOPHOSPHINATES

submitted by E. David Day in partial fulfilment of the requirements  
for the degree of Doctor of Philosophy.



## ABSTRACT

The geometry of the dithiophosphinate ion  $\text{S}_2\text{PX}_2^-$  is such that when coordinated to a metal ion by the sulfur atoms the substituents (X) occupy what is effectively the third coordination sphere of the metal ion. When the substituent groups were varied between  $\text{X} = \text{CH}_3$ ,  $\text{C}_6\text{H}_5$ ,  $\text{OC}_2\text{H}_5$ , F, and  $\text{CF}_3$ , distinct differences in physical and chemical properties were observed for the coordination complexes  $\text{M}[\text{S}_2\text{PX}_2]_n$  of the metal ions  $\text{M}^{+n} = \text{OV}^{+2}$ ,  $\text{V}^{+3}$ ,  $\text{Cr}^{+3}$ ,  $\text{Mn}^{+2}$ ,  $\text{Fe}^{+3}$ ,  $\text{Fe}^{+2}$ ,  $\text{Co}^{+3}$ ,  $\text{Co}^{+2}$ ,  $\text{Ni}^{+2}$ ,  $\text{Pd}^{+2}$ ,  $\text{Pt}^{+2}$ ,  $\text{Cu}^{+2}$ ,  $\text{Cu}^+$ ,  $\text{Zn}^{+2}$ ,  $\text{Cd}^{+2}$  and  $\text{Hg}^{+2}$ . In many cases the complexes were novel. Where the skeletal atomic cluster  $\text{M}(\text{S}_2\text{P})_n$  was maintained constant, differences in properties were attributed to the varied substituent. The chemical, thermal, spectral, and magnetic properties are described. An attempt has been made to evaluate the relative importance of the mass, steric, and electrical factors contributing to the total substituent effect upon the  $\text{M}(\text{S}_2\text{P})_n$  skeleton.

In the rationalization of the electrical substituent effects the resolved Hammett-Taft parameters,  $\sigma_I$  and  $\sigma_R^\circ$ , were found to be most useful, but with an unexpected "twist". Since much of the chemistry of transition metal complexes is determined by the metal ion and its immediate electrical "ligand field" it was of interest to consider how the substituents might electrically influence the metal atom. Consistency in interpreting the results was achieved by the novel assumption that the  $\sigma$ -,  $\pi$ -type electron polarization effects of the substituents on the  $\text{S}_2\text{PX}_2^-$  group were "transduced" into  $\pi$ ,  $\sigma$  polarization



effects on transmission through the tetrahedrally coordinated P atom. Some direct transmission of  $\sigma$ -type electron polarization effects was anticipated due to the non-directional property of the 3s orbital of the P atom. This transduction property appears to be general for tetrahedrally coordinated atoms and accounts for the Lewis  $\pi$  acidity of groups such as  $\text{PF}_3$ ,  $\text{CF}_3$  and  $\text{SnCl}_3$ , in terms of the Hammett-Taft parameters for F and Cl.

The coordination geometries of the sulfur atoms about the metal ions encountered within the set of tris complexes  $\text{M}[\text{S}_2\text{PX}_2]_3$  and bis complexes  $\text{M}[\text{S}_2\text{PX}_2]_2$  included approximately octahedral ( $\text{M}^{+3}$ ), square planar ( $\text{Ni}^{+2}$ ,  $\text{Pd}^{+2}$ ,  $\text{Pt}^{+2}$ ), square pyramidal ( $\text{OV}^{+2}$ ), and tetrahedral ( $\text{Mn}^{+2}$ ,  $\text{Fe}^{+2}$ ,  $\text{Co}^{+2}$ , etc.) configurations. The frequencies of bands assignable to M-S vibrations in the infrared spectra of the complexes were found to correlate monotonically with the ligand field band frequencies in the electronic spectra except in the tetrahedral structural category. An attempt has been made to relate the infrared data to the structural data available from crystal determinations.

The redox, thermal and mass spectral behavior of the dithiophosphinate complexes indicated that the range of isolable metal atom oxidation states was parallel to but somewhat more restricted than that obtainable in aqueous solution. Although most of the odd electron molecules behaved as normal paramagnets, the complexes  $\text{OV}[\text{S}_2\text{PF}_2]_2$ ,  $\text{OV}[\text{S}_2\text{P}(\text{CF}_3)_2]_2$  and  $\text{Co}[\text{S}_2\text{P}(\text{OC}_2\text{H}_5)_2]_2$  proved to be magnetically anomalous in the solid state. Transition metal dithiophosphinates



do not appear to possess the unusual redox properties or geometries characteristic of the 1,2-dithiolenes and are quite unambiguous as to the formal oxidation state of the metal ion.



## ACKNOWLEDGEMENTS

The author wishes to express his gratitude to Dr. R. G. Cavell for his direction and assistance in the course of this work.

Special thanks are due Drs. R. B. Jordan, A. R. Sanger and A. J. Tomlinson for their forbearance and much help during the development of this thesis.

The author is indebted to Mrs. J. Bereton and Dr. W. Byers for the preliminary preparation of many complexes  $M[S_2PX_2]_n$  where  $X = CH_3$  and  $C_6H_5$ , to Miss J. K. Schneider for preparation of the acids  $HS_2PF_2$  and  $HS_2P(CF_3)_2$ , and to both ladies for the preparation of the salt  $NaS_2P(CH_3)_2 \cdot 2H_2O$ . Much gratitude is extended to Dr. A. A. Pinkerton for preliminary preparation of many complexes  $M[S_2P(CF_3)_2]$  and to Dr. P. M. Watkins for the preparation of most and the gasimetric  $HCF_3$  analyses of all these latter compounds as well as the preparation of many  $M[S_2PF_2]_n$  complexes.

Many thanks are extended to Dr. R. E. D. McClung for helpful discussions and computer assistance in the analysis of the solution epr spectra. Voltammetric data contained herein was gratefully received from Dr. B. Kratochvil. Figures 3.1 and 3.2 are reproduced with the kind permission of Dr. M. J. Bennett. Much gratitude is due Dr. F. W. Birss for many positive interactions.

Members of the Department of Chemistry Technical Staff deserve very special thanks, especially Mr. F. Dreissigacker, for his patience and care in the construction and maintenance of the



Faraday balance; Mrs. D. Mahlow and A. Dunn for their uncorruptability in the chemical analyses; Mr. R. Swindlehurst for invaluable aid in the obtaining of the vibrational and electronic spectra; and Mr. A. Budd for enduring nauseous odors while obtaining excellent mass spectra.

Special tribute is due Mrs. R. Tarnowski for her expert translation of the author's handwriting into readable English and for her able preparation of the manuscript.

A final bouquet goes to the author's wife, Marilyn, who suffered half the tribulations encountered during this work.



## TABLE OF CONTENTS

	Page
ABSTRACT.....	iii
ACKNOWLEDGEMENTS.....	vi
LIST OF TABLES.....	xi
LIST OF FIGURES.....	xiii
1. INTRODUCTION.....	1
1.1 Intention.....	1
1.2 Nomenclature.....	2
1.3 Historical Background.....	3
1.4 Practical Applications.....	5
1.5 Academic Interest.....	7
2. EXPERIMENTAL.....	13
2.1 Instrumentation and Techniques.....	13
2.2 Syntheses.....	16
2.3 Treatment of Results.....	33
3. STRUCTURAL CONSIDERATIONS, INFRARED SPECTRA, AND SUBSTITUENT EFFECTS.....	38
3.1 Information Based on Crystallographic Data.....	38
3.2 Structural Inferences for Solution and Gas Phases....	48
3.3 Infrared Spectra.....	51
3.4 Substituent Effects in Dithiophosphinates.....	63
4. CHEMICAL, THERMAL AND MASS SPECTRAL BEHAVIOR.....	71
4.1 Redox Properties.....	71



## TABLE OF CONTENTS (cont'd)

	Page
4.2 Reactions with Lewis Bases.....	86
4.3 Sulfur Replacement by Oxygen.....	91
 5. MAGNETOCHEMISTRY.....	 96
5.1 Introduction.....	96
5.2 Results and Discussion.....	97
5.3 Summary and Conclusions.....	118
 6. ELECTRONIC SPECTRA.....	 120
6.1 Introduction.....	120
6.2 The Molecular Orbital Theory Applied to Dithiophosphinate Complexes.....	122
6.3 Results and Discussion.....	131
6.4 Summary and Conclusions.....	181
 7. CORRELATIONS AND CONCLUSIONS.....	 184
7.1 Substituent Dependence in Dithiophosphinates and Related Compounds.....	184
7.2 The Application of Hammett-Taft Parameters in Inorganic Chemistry.....	189
7.3 Indicated Further Work.....	190
 REFERENCES.....	 192
APPENDIX A. Infrared Spectral Bands of the $PX_2$ Group in the Complexes $M[S_2PX_2]_n$ .....	203



## TABLE OF CONTENTS (cont'd)

	Page
APPENDIX B. Mass Spectral Peaks Corresponding to Metal Containing Ions.....	209
APPENDIX C. Magnetic Susceptibility Data.....	214
APPENDIX D. Description of the Faraday Balance Assembly.....	222
APPENDIX E. Computer Program Listings.....	226



## LIST OF TABLES

TABLE		Page
1.1	Literature Survey of the Complexes $M[S_2PX_2]_n$ of d-block Transition Metals.....	12
2.1	Analytical Data for the Complexes $M[S_2PX_2]_n$ .....	17
3.1	Structural Parameters.....	42
3.2	Infrared Spectral Band Assignments for the $PS_2$ Group Stretching Frequencies in the Acids $HS_2PX_2$ and their Salts.....	54
3.3	Infrared Spectral Band Assignments for the M-S and P-S Stretching Frequencies in the Tris Complexes $M[S_2PX_2]_3$ .....	55
3.4	Infrared Spectral Band Assignments for the M-S and P-S Stretching Frequencies in the Tetrahedral Bis Complexes $M[S_2PX_2]_2$ .....	56
3.5	Infrared Spectral Band Assignments for the M-S and P-S Stretching Frequencies in the Planar Bis Complexes $M[S_2PX_2]_2$ .....	57
3.6	Infrared Spectral Band Assignments for the M-S and P-S Stretching Frequencies in the Vanadyl Bis Complexes $OV[S_2PX_2]_2$ .....	58
3.7	Physical Indexes of Electrical Substituent (X) Effects.	61
4.1	Redox Reactions of Dithiophosphinic Acids $HS_2PX_2$ and Derivatives.....	74
4.2	Thermal Data for the Complexes $M[S_2PX_2]_n$ .....	77
5.1	Static Field Magnetic Susceptibility Parameters for the Complexes $M[S_2PX_2]_n$ .....	99



## LIST OF TABLES (cont'd)

TABLE	Page
5.2 EPR Parameters of $\text{OV}[\text{S}_2\text{PX}_2]_2$ Systems.....	103
6.1 Electronic Spectra of the Complexes $\text{OV}[\text{S}_2\text{PX}_2]_n$ .....	136
6.2 Electronic Spectra of the Complexes $\text{V}[\text{S}_2\text{PX}_2]_3$ .....	142
6.3 Electronic Spectra of the Complexes $\text{Cr}[\text{S}_2\text{PX}_2]_3$ .....	148
6.4 Electronic Spectra of Fe(III) Complexes.....	155
6.5 Electronic Spectra of the Complexes $\text{Co}[\text{S}_2\text{PX}_2]_3$ .....	161
6.6 Electronic Spectra of the Complexes $\text{Co}[\text{S}_2\text{PX}_2]_2$ .....	166
6.7 Electronic Spectra of Planar $\text{M}[\text{S}_2\text{PX}_2]_2$ Complexes.....	173
7.1 Ligand Field-Metal-Sulfur Vibrational Frequency Correlation.....	187



## LIST OF FIGURES

FIGURE		Page
1.1	A simplified representation of the vertical $\pi$ ( $\pi_v$ ) molecular orbitals of five major ligand systems.....	9
2.1	Grease free apparatus for the preparation of volatile solid complexes.....	14
3.1	The crystal structure of $\text{Co}[\text{S}_2\text{P}(\text{CH}_3)_2]_2$ .....	43
3.2	The crystal structure of $\text{OV}[\text{S}_2\text{P}(\text{CH}_3)_2]_2$ .....	47
4.1	Mass spectral fragmentations usually resulting in metastable ions.....	95
5.1	Successive splittings of a $^3T_{1g}$ term.....	107
5.2	Successive term splittings for a Cr(III) ion.....	108
6.1	A qualitative MO diagram for a chromophore $\text{M}(\text{S}_2\text{P})_3$ of $D_3$ symmetry (pseudo-octahedral).....	125
6.2	A qualitative MO diagram for a chromophore $\text{M}(\text{S}_2\text{P})_2$ of $D_{2d}$ symmetry (pseudo-tetrahedral).....	126
6.3	Electronic absorption spectra of $\text{OV}[\text{S}_2\text{PX}_2]_2$ complexes in $\text{CH}_2\text{Cl}_2$ solution.....	135
6.4	A qualitative MO diagram for the chromophore $\text{OV}(\text{S}_2\text{P})_2$ of $C_{2v}$ symmetry.....	138
6.5	Electronic spectra of $\text{V}[\text{S}_2\text{PX}_2]_3$ complexes in $\text{CH}_2\text{Cl}_2$ solution.....	141
6.6	Electronic spectra of $\text{Cr}[\text{S}_2\text{PX}_2]_3$ complexes in $\text{CH}_2\text{Cl}_2$ solution.....	147
6.7	Electronic spectrum of $\text{Fe}[\text{S}_2\text{P}(\text{C}_6\text{H}_5)_2]_3$ in $\text{CH}_2\text{Cl}_2$ solution.....	154



## LIST OF FIGURES (cont'd)

FIGURE		Page
6.8	Diffuse reflectance spectra of $\text{Fe}[\text{S}_2\text{PX}_2]_2$ complexes...	157
6.9	Electronic spectra of the $\text{Co}[\text{S}_2\text{PX}_2]_3$ complexes in $\text{CH}_2\text{Cl}_2$ solution.....	160
6.10	Electronic spectra of $\text{Co}[\text{S}_2\text{PX}_2]_2$ complexes in $\text{CH}_2\text{Cl}_2$ solution.....	165
6.11	Electronic spectra of the $\text{CoS}_4\text{P}_2(\text{CH}_3)_4$ and $\text{CoOS}_3\text{P}_2(\text{CH}_3)_4$ complexes in alcohol solutions.....	171
6.12	Molecular coordinate system (xy plane).....	170
6.13	Electronic spectra of $\text{Ni}[\text{S}_2\text{PX}_2]_2$ complexes in $\text{CH}_2\text{Cl}_2$ solution.....	174
6.14	Electronic spectra of $\text{Pd}[\text{S}_2\text{PX}_2]_2$ complexes in $\text{CH}_2\text{Cl}_2$ solution.....	175
6.15	Electronic spectra of $\text{Pt}[\text{S}_2\text{PX}_2]_2$ complexes in $\text{CH}_2\text{Cl}_2$ solution.....	176
6.16	Electronic spectrum of $\text{Pt}_2\text{S}_6\text{P}_4(\text{CF}_3)_8$ in $\text{CH}_2\text{Cl}_2$ solution.....	177
6.17	A qualitative MO diagram for a planar chromophore $\text{M}(\text{S}_2\text{P})_2$ of $D_{2h}$ symmetry.....	178
7.1	$\nu_{\text{M-S}}^2 - \nu_{\text{l el}}$ correlation for $\text{Ni}[\text{S}_2\text{PX}_2]_2$ complexes....	186
E1	Sample Calcomp plot from MAGSUS.....	237



## CHAPTER 1

INTRODUCTION1.1 Intention

A chemical compound is well defined when the relative positions of the constituent atomic nuclei and the nature of the bonds between them are sufficiently known to enable prediction of the reactivity of the compound. In the theoretical descriptions of the bonding in transition metal complexes the electronic behavior of the monatomic or polyatomic ligands is often considered to be sufficiently understood that attention is restricted to the nature of the metal-ligand bonds. Furthermore, in an attempt to classify the chemical behavior of metal atoms and ligands separately, the physical and chemical properties of coordination compounds are often factored into functions of the central atom and the ligand group. However, it is of interest to hold the metal-ligand linkage as constant as possible and determine the effect of variation more remote from the metal atom. Thus a ligand substrate capable of supporting a wide variety of substituents while maintaining constant the first and perhaps higher coordination spheres about the central atom might be expected to provide a system of complexes with sufficiently different properties to enable inferences to be made concerning the metal-ligand and intraligand bonds.

The geometry of a dithiophosphinate ligand ion  $\text{S}_2\text{PX}_2^-$  is such that the P atom is nearly tetrahedrally coordinated and when the ligand is coordinated to a metal ion by the sulfur atoms



the substituents (X) occupy what is effectively the third coordination sphere of the metal ion. In a homologous series of complexes  $M[S_2PX_2]_n$ , varying only in X, the effects of the substituents may be monitored by the differences in physical and chemical properties primarily dependent upon the skeletal atomic cluster  $M(S_2P)_n$ . The chemistry of phosphorus is now well enough advanced that dithiophosphinic acids and salts may be obtained bearing very many different substituent groups. In view of the current interest in compounds containing metal-sulfur linkages and thiophosphorus chemistry in general, the dithiophosphinate complexes provided a potentially valuable system for study.

It is intended to describe herein the chemical, thermal, spectral, and magnetic results obtained for most of the transition metal dithiophosphinates  $M[S_2PX_2]_n$  with X =  $CH_3$ ,  $C_6H_5$ ,  $OC_2H_5$ , F and  $CF_3$  and  $M^{+n} = OV^{+2}$ ,  $V^{+3}$ ,  $Cr^{+3}$ ,  $Mn^{+2}$ ,  $Fe^{+3}$ ,  $Fe^{+2}$ ,  $Co^{+3}$ ,  $Co^{+2}$ ,  $Ni^{+2}$ ,  $Pd^{+2}$ ,  $Pt^{+2}$ ,  $Cu^{+2}$ ,  $Cu^+$ ,  $Ag^+$ ,  $Zn^{+2}$ ,  $Cd^{+2}$  and  $Hg^{+2}$ . An attempt is made to interpret the results in terms of the substituent perturbation upon the  $M(S_2P)_n$  skeleton.

## 1.2 Nomenclature

Complexes of the type  $M[S_2PX_2]_n$  with X = F or OR(R = an organic moiety) are treated in the literature as derivatives of phosphoric acid and are variously called phosphorodifluorodithioates, difluorodithiophosphates, difluorophosphinates, 0,0'-di(organic moiety)dithiophosphates, respectively<sup>1,2</sup>. Hypophosphorous or phosphinic acid,  $HO(O)PH_2$ , yields as derivatives the di(substituent)



phosphonites or phosphinates<sup>1,2,3</sup>. The sulfur analogues of these latter acids with organic substituents are known as phosphinodisubstituent)dithioates or di(substituent)dithiophosphinates due to their initial preparation from the corresponding disubstituted phosphine and elemental sulfur<sup>1,2</sup>. For consistency herein, all the acids  $\text{HS}_2\text{PX}_2$  for all X are called di(substituent)dithiophosphinic acids and their derivative compounds  $\text{M}[\text{S}_2\text{PX}_2]_n$  are referred to as di(substituent)dithiophosphinates. Since all the compounds included in this study were homogeneous with respect to the substituents, unambiguous identification within the system is possible by noting the metal ion and substituent only. Moreover, complexes containing homogeneous ligands are referred to as "simple" as opposed to mixed ligand compounds.

### 1.3 Historical Background

The earliest mention of a dithiophosphinic acid was in 1871, but the preparation and characterization of the acid  $\text{HS}_2\text{P}(\text{C}_2\text{H}_5)_2$  its sodium and ammonium salts and the complexes  $\text{M}[\text{S}_2\text{P}(\text{C}_2\text{H}_5)_2]_n$  with  $\text{M}^{+n} = \text{Cu}^+, \text{Ag}^+, \text{Au}^+$ , and  $\text{Pb}^{+2}$  were not reported until 1892<sup>4</sup>. Dialkoxy-dithiophosphinic acids were first reported in 1908 while the first mention of transition metal complexes awaited the preparation of the Fe(III), Co(III), and Ni(II) compounds with  $\text{X} = \text{OCH}_3$  and  $\text{OC}_2\text{H}_5$  by Malatesta and Pizzotti<sup>5</sup> in 1945. Two years later (1947), Malatesta<sup>7</sup> reported the acids  $\text{HS}_2\text{P}(\text{C}_6\text{H}_5)_2$ ,  $\text{HS}_2\text{P}(\text{CH}_3)_2$ , and their sodium, ammonium, and Ni(II) salts. Further development of the chemistry of alkyl, aryl, alkoxy and aryloxy substituted dithiophosphinic



acids with all combinations of substituents included the syntheses of a number of complexes useful in the characterization of the acids<sup>2,8-10</sup>.

In 1959, Jorgensen<sup>11,14</sup> became interested in the electronic spectral properties of diethoxydithiophosphinates while Kuchen and coworkers<sup>13</sup> began to report their systematic study of the properties of a large number of dialkyl and diaryl acids and derivatives.

The work reported up to 1969 has been summarized in reviews<sup>12,13</sup>.

Prior to 1967, no isolated complexes of scandium, titanium, vanadium, manganese, iron(II), or copper(II) had been reported.

The initial studies leading to this thesis were begun with the intention of investigating the electronic spectral and temperature dependent magnetic properties of transition metal complexes derived from the acids  $\text{HS}_2\text{P}(\text{CH}_3)_2$  and  $\text{HS}_2\text{P}(\text{C}_6\text{H}_5)_2$ . Although several complexes of the latter acid were known, few of their physical properties had been reported<sup>14</sup>. Crystals of  $\text{OV}[\text{S}_2\text{P}(\text{CH}_3)_2]_2$ ,  $\text{Cr}[\text{S}_2\text{P}(\text{CH}_3)_2]_3$ , and  $\text{Co}[\text{S}_2\text{P}(\text{CH}_3)_2]_2$  were provided for structural determinations which have since been completed<sup>15</sup>. Suitable methods for large scale preparations of salts of the dithiophosphinic acids  $\text{HS}_2\text{PX}_2$  with  $\text{X} = \text{F}^{16}$ ,  $\text{N}_3^{16a}$ ,  $\text{CN}^{16a}$ ,  $\text{CSNH}_2^{16a}$  were described in 1967 and the subsequent discovery of the acid  $\text{HS}_2\text{P}(\text{CF}_3)_2^{17}$  led to the inclusion of the two fluoroacids in an expanded field of study.

Many new transition metal complexes derived from  $\text{HS}_2\text{PF}_2$  were described by Tebbe and Muetterties<sup>18</sup> but with only a summary account of the electronic properties. Roesky<sup>19</sup> has prepared several complexes of the acids  $\text{HS}_2\text{P}(\text{F})\text{R}$ , where  $\text{R} = \text{CH}_3$  or  $\text{C}_2\text{H}_5$ .



Between 1967 and 1971, crystal and molecular structures were published for the complexes:  $\text{Ni}[\text{S}_2\text{PX}_2]_2$  where  $\text{X} = \text{CH}_3^{20}$ ,  $\text{C}_6\text{H}_5^{21}$ ,  $\text{OCH}_3^{22}$ ,  $\text{OC}_2\text{H}_5^{23}$ ;  $\text{M}[\text{S}_2\text{PX}_2]_2$  where  $\text{M} = \text{Zn}^{24}$ ,  $\text{Cd}^{24}$ ,  $\text{Hg}^{25}$ ,  $\text{X} = \text{O}-\text{C}_3\text{H}_7$ , and  $\text{M} = \text{Zn}$ ,  $\text{X} = \text{C}_2\text{H}_5^{26}$  and  $\text{OC}_2\text{H}_5^{27}$ ; and  $\text{V}[\text{S}_2\text{P}(\text{OC}_2\text{H}_5)_2]_3^{28}$ . The structural systematics of dithioacid complexes have been recently and extensively reviewed<sup>29,30</sup>.

Oriented single crystal spectra have been reported for the complexes  $\text{M}[\text{S}_2\text{P}(\text{OC}_2\text{H}_5)_2]_n$  of  $\text{V}(\text{III})^{28,31\text{a,b}}$ ,  $\text{Cr}(\text{III})^{31\text{a,b}}$ ,  $\text{Co}(\text{III})^{31\text{a,b}}$ ,  $\text{Rh}(\text{III})^{31\text{a}}$ ,  $\text{Ir}(\text{III})^{31\text{a}}$  and  $\text{Ni}(\text{II})^{32}$ . A single magnetic circular dichroism (MCD) study has been reported<sup>33</sup> for  $\text{Ni}[\text{S}_2\text{P}(\text{OC}_2\text{H}_5)_2]_2$ . Spectral results have been published for series of dialkoxydithiophosphinates of  $\text{Cr}(\text{III})^{34}$  and  $\text{Ni}(\text{II})^{35}$ . Very recently the  $\text{V}(\text{III})$  and  $\text{OV}(\text{IV})$  complexes derived from the acids  $\text{HS}_2\text{P}(\text{C}_6\text{H}_5)_2^{36}$ ,  $\text{HS}_2\text{P}(\text{C}_2\text{H}_5)_2^{37}$  and  $\text{HS}_2\text{P}(\text{C}_3\text{H}_7)_2^{37}$  were described together with the complexes of the first acid with  $\text{Co}(\text{III})$ ,  $\text{Rh}(\text{III})$ ,  $\text{Ir}(\text{III})$ ,  $\text{Pd}(\text{II})$ ,  $\text{Pt}(\text{II})$ , and  $\text{Au}(\text{III})^{38}$ . Prior to the latter reports, electron paramagnetic resonance (epr) spectra had been observed<sup>39</sup> in solution for  $\text{Cu}(\text{II})$  and  $\text{OV}(\text{IV})$  dithiophosphinates with a variety of alkyl, aryl, and alkoxy substituents, but without further isolation and characterization of the complexes. No  $\text{Cu}(\text{II})$  dithiophosphinate has yet been isolated.

#### 1.4 Practical Application

Metal derivatives of dithiophosphinic acids are important as lubricating oil additives with metal and substituent dependent anti-oxidant and antiwear properties<sup>13,24,40</sup>. In particular, the



Zn(II) derivatives are widely used as lubricant additives to reduce wear under boundary or thin-film lubrication conditions as well as to inhibit oxidation and corrosion<sup>24,40</sup>. Further industrial applications as described in several patents are vulcanization accelerators, stabilizers for polyolefin molding compositions, and coloring additives for plastics due to outstanding color- and lightfastness<sup>12,13</sup>.

Analytical advantage can be taken of the dependence of the formation constants of the complexes on the metal ion and substituent in aqueous solution<sup>13,41</sup>. Metal ions can be selectively extracted from aqueous solution into a water immiscible organic solvent as the electrically neutral dithiophosphinate complex. For example, Cd(II), Hg(II), Pb(II), and Bi(III) have been quantitatively extracted as their diethyldithiophosphinates from acidic aqueous solutions into carbon tetrachloride<sup>13</sup>. However, Mn(II), Ni(II), Cd(II), Cr(III), Zn(II), Mg(II), and other metals can be extracted incompletely or not at all<sup>13</sup>. The dialkyldithiophosphinate salts are quite stable in non-oxidizing acid solutions in contrast to the dialkoxydithiophosphinates or dithiocarbamates<sup>13</sup>.

The biological significance of phosphorus compounds has possibly gained the greatest notoriety through their association with the so-called "nerve gases". In fact, derivatives of dialkoxy-dithiophinic acids are known to inhibit hydrolysis of the enzyme acetylcholinesterase to its substrate acetylcholine, thus causing muscular paralysis<sup>35</sup>. Esters of the type  $(X)_2P(S)SY$  (Y = substituted acetylphenyl or alkylurea) are known for their insecticidal, rodenticidal, and fungicidal activity believed to result from



enzyme inhibition<sup>35</sup>. Salts of the type  $[PX_4][X_2PS_2]$  are effective fungicides and bacteriocides<sup>35</sup>. The Ni, Pd, and Pt complexes  $M[S_2P(OCH_3)_2]_2$  show promising carcinostatic activity in preliminary tests<sup>35</sup>.

### 1.5 Academic Interest

Since the early studies of Werner the coordination chemistry of chelating ligands has been dominated by those ligands possessing O and N donor atoms<sup>42</sup>. Many of the bidentate ligands were the conjugate bases of oxo-acids. While nearly cubic coordination geometry about the metal atom is usually maintained, oxo-acid ligands often perform bridging functions resulting in polymeric structures<sup>43,44,45</sup> which have stimulated much interest especially in the cases of the magnetically anomalous dinuclear chromous and cupric carboxylates<sup>45</sup>.

Within the last decade it has been discovered that general replacement of oxygen by sulfur in bidentate ligand systems forming five-membered unsaturated chelate "rings" (in particular the 1,2-dithiolenes<sup>46,47</sup>) resulted in (i) complexes that undergo readily reversible redox reactions, (ii) stable complexes with a square-planar coordination geometry with many metal ions, (iii) trigonal prismatic six-coordinate tris complexes in many cases, and (iv) a marked dependence of the ligand  $\pi$ -acidity upon the substituents<sup>29,30,46,47</sup>. This revelation has intensified the interest in established dithio-ligand systems and has led to the development of new systems to test the generality or limitations of the above behavior.

A somewhat "*a posteriori*" classification of five major



dithioacid ligand systems is indicated in Figure 1.1. These are:

the imidodithiodiphosphinates<sup>48</sup> and dithioacetylacetones<sup>30,49</sup> (1), the 1,2-dithiolenes and benzene-1,2 dithiolenes<sup>29,30,46,47</sup> (2), the dithioxalates<sup>30,50</sup> (3), the dithiocarbimates, trithiocarbonates, and ethene-1,1 dithiolates<sup>30,51</sup> (4), the dithiocarbamates, xanthates, dithiocarboxylates<sup>30,51</sup>, and (last but not least) the dithiophosphinates (5). Although all these ligands possess  $\pi$ -electron systems extended over the atoms forming the backbone of the metal-chelate ring, the dianionic ligands are shown in their classical formulation in Figure 1.1, where R = H, an alkyl, aryl, or some more exotic organic substituent. Combinations of substituents do occur but the substitutions are indicated as being symmetrical for simplicity of representation.

Schrauzer<sup>47</sup> has classified bidentate ligands as "even" or "odd" by the even or odd number of  $\pi$  atomic orbitals contributing to the  $\pi$ -type molecular orbital (MO) network ( $\pi_v$ ) perpendicular to the plane of the ligand backbone. The  $\pi_v$  MO diagrams and their occupation with varying formal charge on the ligands are included in Figure 1.1. If no unoccupied low-lying  $\pi_v$  MO's are present, the "odd" ligands are not expected to accept additional electrons and thus should behave as "normal" monoanions. However, if the lowest unoccupied  $\pi_v$  MO of an "even" ligand is only weakly antibonding, the ligand may behave as an electron acceptor or donor in much the same way as nitric oxide<sup>3</sup> (NO). The existence of a small energy difference between the highest occupied and lowest unoccupied  $\pi_v$  MO of the metal-1,2 dithiolenes has been cited<sup>47</sup> as the explanation of their semiconducting properties and high electron affinities. Jorgensen<sup>12</sup>



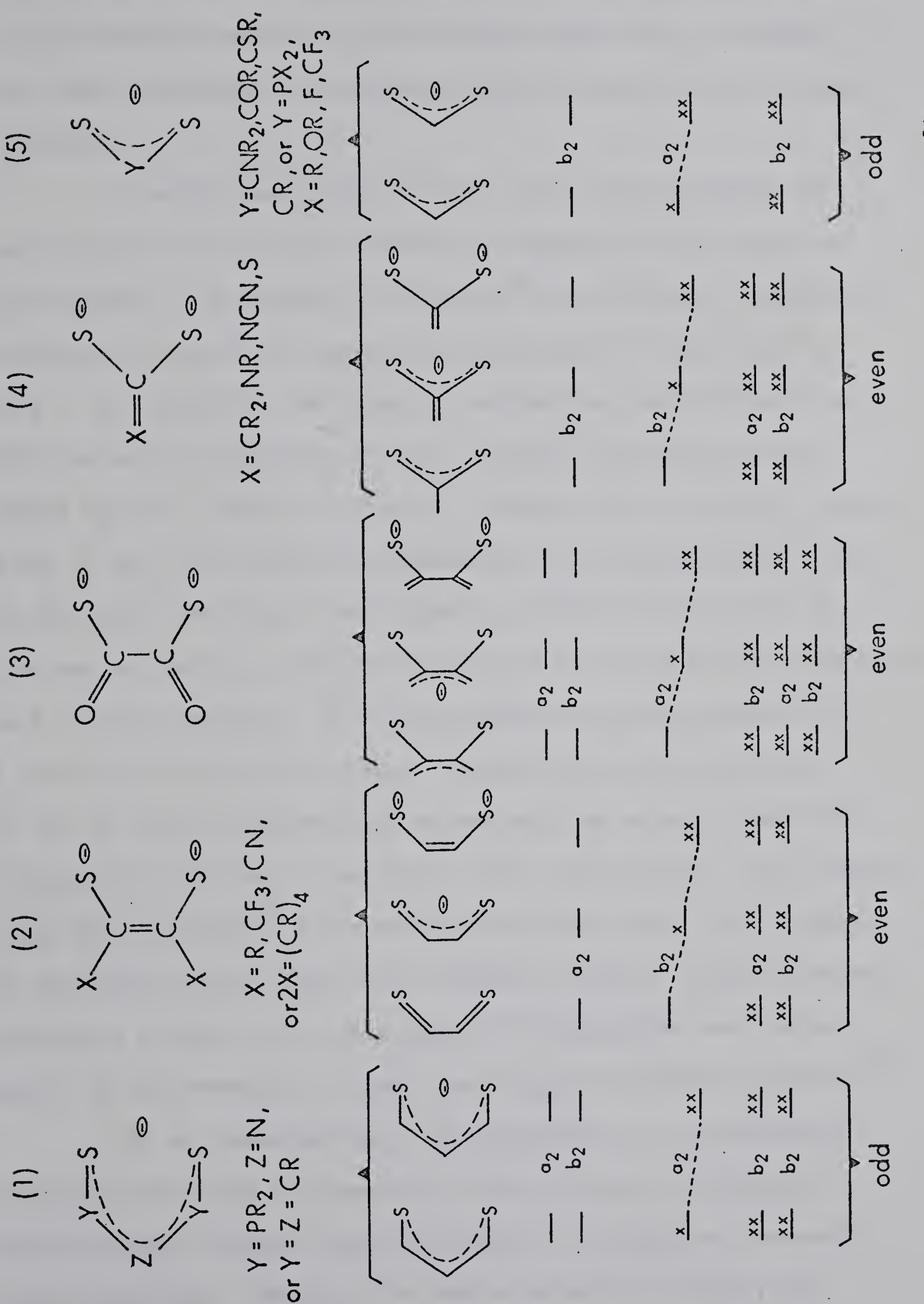


FIGURE 1.1: A simplified representation of the vertical  $\pi$  ( $\pi_V$ ) molecular orbitals of five major ligand systems ( $\text{C}_{2v}$  symmetry).

major ligand systems ( $\text{C}_{2v}$  symmetry).



calls "suspect" those conjugated sulfur containing ligands for which a fixed valence formalism cannot be given while those for which the formal oxidation state remains a useful classification he terms "innocent".

Possibly the greatest single factor distinguishing the metal-ligand bonding in the dithioacid complexes is the extent of metal-ligand  $\pi$ -type bonding. Eisenberg<sup>29</sup> has discussed  $\pi$  bonding in dithioacid complexes in terms of the symmetries of the ligand  $\pi_v$  MO's. In order for the ligand  $\pi_v$  orbitals to overlap significantly with the metal  $d_{\pi}$  functions, it was thought<sup>29</sup> necessary that the ligand  $\pi_v$  MO's should be of the  $b_2$  symmetry type (in the  $C_{2v}$  point group of the free-ligand) and nonbonding or antibonding with respect to the ligand skeleton. The crucial  $b_2$  orbitals (Figure 1.1) in the case of neutral 1,2-dithiolene ligands are empty and thus available as  $\pi$  acceptor orbitals. In all the remaining ligand systems, the  $\pi_v$  orbitals eligible for  $\pi_v$ -type overlap with metal orbitals are of the  $a_2$  type or energetically unfavorable for strong interaction. Geometrical constraints also impose their restrictions. Four membered rings are postulated<sup>29</sup> to be strained and hence limit the closeness of approach of sulfur atoms from different ligands. There is strong structural evidence that interligand S-S interactions are instrumental in the formation of planar and trigonal prismatic geometries<sup>29</sup>.

In an investigation of the properties of 1,1-dithioacid complexes containing four-membered chelate rings, the dithiophosphate ligands present unique advantages in testing the "even-odd" ligand hypothesis. Firstly, the charge (electron) transfer and



intraligand bands in the electronic spectra occur at higher energies than those observed for other dithioacid complexes, leaving a greater spectral range clear for observation of ligand field bands.

Secondly, the nuclear spin ( $I = 1/2$ ) of the phosphorus atoms provides an intramolecular probe of the bonding in conjunction with magnetic resonance techniques (nmr and epr). Thirdly, two substituents in what is effectively the third coordination sphere of the metal atom might be expected to produce more readily observed effects than the one substituent available with the dithiocarboxylates. Fourthly, the larger size of the P atom over a C atom should relieve some of the strain postulated in four membered chelate rings<sup>29</sup>.

In order to place the discussion to follow in perspective an abbreviated survey of the relevant literature to date is presented in Table 1.1.



TABLE I.1  
Literature Survey of the Complexes  $M[S_2P(X)X']_n$  of d-Block Transition Metals\*

$X,X' = R,R'$	R,Ar	R,OR'	R,OAr	R,F	Ar,Ar'	Ar,OR	OR,OR'	F,F	CF <sub>3</sub> ,CF <sub>3</sub>
$X^n$									
0V <sup>+2</sup>	37 <sup>m</sup> ,S,V,SSC,e, <sup>m</sup> ,MS,S,V				36 <sup>m</sup> ,S,V,SS <sup>e</sup> , <sup>m</sup> ,MS,S,V	39 <sup>e</sup> ,U,55 <sup>e</sup> , <sup>m</sup> ,MS,S,V	55e,M,MS,R,S,V		
V <sup>+3</sup>	37 <sup>m</sup> ,S,V,54 <sup>c</sup> , <sup>m</sup> ,MS,R,S,V				36 <sup>m</sup> ,S,V,54 <sup>e</sup> , <sup>m</sup> ,MS,S,V	28 <sup>c</sup> , <sup>m</sup> ,S,SC,V,54 <sup>m</sup> ,MS,S,V	54 <sup>e</sup> , <sup>m</sup> ,MS,R,S,V		
Cr <sup>+3</sup>	12 <sup>s</sup> ,53 <sup>c</sup> , <sup>m</sup> ,MS,R,S,V,12 <sup>m</sup> ,S,V				12 <sup>s</sup> ,53 <sup>m</sup> ,MS,S,V,142 <sup>e</sup>	12 <sup>s</sup> ,31 <sup>c</sup> ,S,SC,34 <sup>m</sup> ,S,53 <sup>m</sup> ,MS,S,V,120 <sup>e</sup>	12 <sup>s</sup> ,18 <sup>m</sup> ,MS,V,53 <sup>m</sup> ,MS,S,V		
O <sup>+6</sup>	60 <sup>m</sup> ,n,s,V (also X=X'=OAr)					60 <sup>m</sup> ,n,s,V (also X=X'=OAr)	91 <sup>m</sup> ,MS,R,S,V		
Mo <sup>+3</sup>							91 <sup>m</sup> ,MS,S,V		
N <sub>2</sub> <sup>+2</sup>	57 <sup>c</sup> , <sup>m</sup> ,MS,V						18 <sup>m</sup> ,BS,V,57 <sup>m</sup> ,MS,V	57 <sup>m</sup> ,BS,V	
Fe <sup>+3</sup>	13 <sup>m</sup> ,R,57 <sup>m</sup> ,MS,R,U						18 <sup>U</sup>	57 <sup>m</sup> ,S,V	
Fe <sup>+2</sup>	57 <sup>c</sup> , <sup>m</sup> ,MS,R,S,V						18 <sup>m</sup> ,MS,R,V,57 <sup>m</sup> ,MS,R,S,V	57 <sup>m</sup> ,MS,S,V	
Fe <sup>+3</sup>									
Rs <sup>+3</sup>	13 <sup>m</sup>								
Co <sup>+3</sup>	13 <sup>m</sup> ,R,57 <sup>c</sup> , <sup>m</sup> ,MS,R,S,V								
Co <sup>+2</sup>	13 <sup>d</sup> , <sup>m</sup> ,S,26 <sup>c</sup> ,57 <sup>c</sup> , <sup>m</sup> ,MS,S,V								
Rh <sup>+3</sup>	13 <sup>m</sup>								
Ir <sup>+3</sup>	13 <sup>m</sup>								
Ni <sup>+2</sup>	12 <sup>s</sup> ,13 <sup>d</sup> , <sup>m</sup> ,S,20 <sup>c</sup> ,56 <sup>m</sup> ,MS,S,R,V	9	10	10	19 <sup>s</sup> ,V	14 <sup>m</sup> ,V,21 <sup>c</sup> ,S,32 <sup>s</sup> ,SC,56 <sup>m</sup> ,MS,S,V	10	12 <sup>s</sup> ,23 <sup>c</sup> ,31 <sup>s</sup> ,SC,35 <sup>m</sup> ,MS,S,V,56 <sup>m</sup> ,MS,S,V	56 <sup>m</sup> ,MS,R,S,V
Pd <sup>+2</sup>	13 <sup>m</sup> ,56 <sup>m</sup> ,MS,S,V					38 <sup>m</sup> ,S,V,56 <sup>m</sup> ,MS,S,V		12 <sup>s</sup> ,23 <sup>c</sup> ,56 <sup>m</sup> ,MS,S,V	56 <sup>m</sup> ,MS,R,S,V
Pt <sup>+2</sup>	13 <sup>m</sup> ,56 <sup>m</sup> ,MS,S,V					36 <sup>m</sup> ,S,V,56 <sup>m</sup> ,MS,S,V		18 <sup>m</sup> ,MS,R,V,56 <sup>m</sup> ,MS,S,V	56 <sup>m</sup> ,MS,U
Cu <sup>+2</sup>	39 <sup>c</sup> ,U					14 <sup>r</sup> ,U,39 <sup>e</sup> ,U	39 <sup>e</sup> ,U	18 <sup>r</sup> ,U	57 <sup>r</sup> ,U
Cu <sup>+1</sup>	13 <sup>m</sup> ,R					13 <sup>m</sup> ,R	39	18 <sup>c</sup> ,N,V	57
A <sup>2+</sup>	13 <sup>m</sup>					13 <sup>m</sup> ,R		18 <sup>n</sup>	
Au <sup>+3</sup>						38 <sup>v</sup>			
Au <sup>+1</sup>	13 <sup>m</sup>					13 <sup>m</sup>			
Zn <sup>+2</sup>	13 <sup>d</sup> , <sup>m</sup> ,27 <sup>c</sup> ,57 <sup>c</sup> , <sup>m</sup> ,MS,V				19 <sup>n</sup> ,V	57 <sup>m</sup> ,MS,V	24 <sup>c</sup> ,27 <sup>c</sup> ,57 <sup>m</sup> ,MS,V,83 <sup>v</sup>	18 <sup>m</sup> ,N,V,44 <sup>m</sup> ,MS,V	57 <sup>m</sup> ,MS,N,V
Cd <sup>+2</sup>	13 <sup>m</sup> ,57 <sup>m</sup> ,MS,V				19 <sup>v</sup>	57 <sup>m</sup> ,MS,V	24 <sup>c</sup> ,41 <sup>r</sup>	18 <sup>n</sup> ,V	57 <sup>m</sup> ,S,N,V
Hg <sup>+2</sup>	13 <sup>m</sup> ,57 <sup>m</sup> ,MS,V					57 <sup>m</sup> ,MS,V	25 <sup>c</sup>		

\* The ions  $M^{+n}$  are restricted to simple metal ions or the mono-oxo ions while R is an aliphatic or olefinic carbon chain substituent and Ar is an aromatic substituent. Table entries are reference numbers of reviews or recent publications containing relevant back references. The reference numbers are sequential in the text. Not included in the table are the complexes with ligands other than dithiophosphinate and oxo anions (see references 60, 91, and 92 for expanded Ligand systems).

Superscript letter code  
of available data:  
c = crystal structure  
d = electric dipole  
e = epr spectrum  
m = magnetic susceptibility

md = magnetic circular dichroism spectrum  
ms = mass spectrum  
n = nmr spectrum  
r = redox behavior

s = electronic spectrum  
sc = oriented single crystal spectrum  
u = not isolated or uncharacterized analytically  
v = vibrational spectrum



## CHAPTER 2

EXPERIMENTAL2.1 Instrumentation and Techniques

Standard Pyrex high vacuum apparatus and techniques were employed operating at pressures of about  $10^{-2}$  torr. Fractional sublimations of volatile solid materials were achieved in vacuo with a long (~60 cm) vertical Pyrex tube closed at the bottom (containing the sample), connected to a vacuum line at the top, and enclosed in a close fitting jacket of copper tubing to reduce the thermal gradient up the length of the tube when heated at the bottom in a bath of paraffin oil or Wood's metal. Efficient collection and separation of very volatile (vapor pressure > 10 torr, at 100°C) solids were achieved by use of grease-free vacuum apparatus schematically illustrated in Figure 2.1, for the preparations.

Air stable compounds were handled with typical bench-top techniques. Transfers and other manipulations of air sensitive materials were carried out under nitrogen in polyethylene glove bags. Chlorocarbon solvents were dried and deoxygenated by vacuum distillation from  $P_4O_{10}$ , when necessary for the preparation of solutions of air sensitive materials.

Electronic spectra were measured on a Cary 14 spectrometer equipped with the Cary 1411 diffuse reflectance attachment operated in Type II mode. Infrared (ir) spectra were obtained using



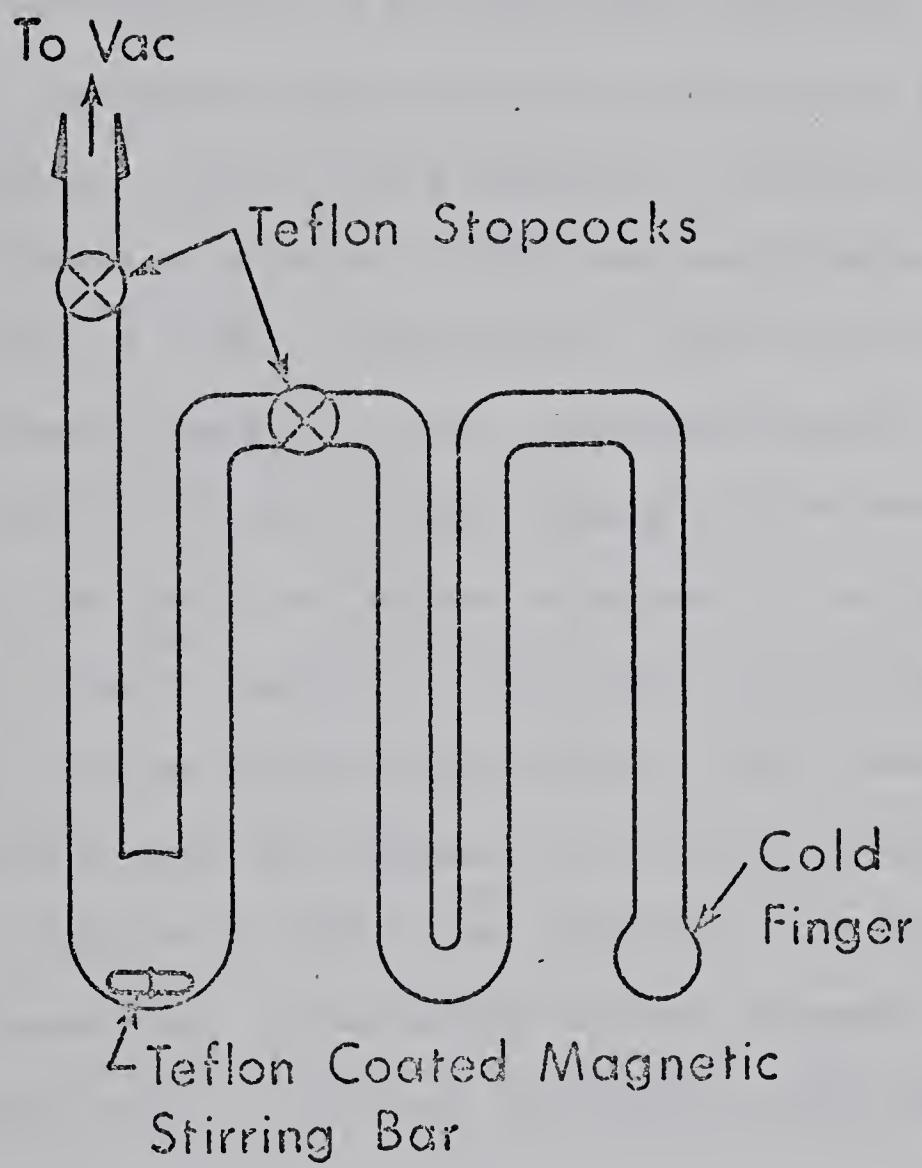


FIGURE 2.1: Grease free apparatus for the preparation of volatile solid complexes.



Perkin-Elmer 337, 421, 457, and Beckmann IR-11 instruments. Raman spectra were observed on a Spectra Research Ltd., Ramalog instrument with photon counting. Circular dichroism (CD) and optical rotatory dispersion (ORD) effects were investigated using a Jasco ORD/UV-5 instrument with a CD measurement capability. The nuclear magnetic resonance (nmr) spectra were obtained on a Varian A56/60 spectrometer. The electron paramagnetic resonance (epr) spectra were obtained on a Varian V-4502X-band spectrometer. Mass spectra were obtained by direct probe sample insertion into an AEI MS9 mass spectrometer operated at 70eV. Thermogravimetric analyses were carried out under vacuum using the Dupont Model 950 Thermogravimetric Analyzer as a module attachment to the Dupont 900 Differential Thermal Analyzer. X-ray powder patterns were obtained using a Philips Debije-Scherrer PW1024 powder camera. Magnetic susceptibilities were obtained by the Faraday method over the temperature range 90 - 300°K, using  $\text{HgCo}(\text{NCS})_4^{52}$  as a field calibrant. A description of the Faraday balance components and cryostat assembled prior to, but made operational during this investigation is contained in Appendix A.

Chemical analyses for elements other than C and H were performed by Schwartzkopf Laboratories, Woodside, N.Y., U.S.A. Analyses for C, H, and in some cases S, as well as osmometric solution molecular weight measurements were performed by the microanalytical service at the University of Alberta, Department



of Chemistry. Gasimetric analyses of the  $\text{CF}_3\text{H}$  evolved on alkaline hydrolysis of the  $\text{CF}_3$  containing complexes were performed by an associate, Dr. P. M. Watkins. Each  $(\text{CF}_3)_2\text{P}^{\text{V}}$  unit yields one unit of  $\text{CF}_3\text{H}$ <sup>53-57</sup>.

## 2.2 Syntheses

Commercially available chemicals of "Reagent" grade were used without further purification. Unless otherwise specified, preparations were carried out on a 2-10 mmole scale. Analytical data are contained in Table 2.1.

### Dithiophosphinic Acids and Salts

(a)  $\text{NaS}_2\text{P}(\text{CH}_3)_2 \cdot 2\text{H}_2\text{O}$  was prepared by Mrs. J. Bereton and Miss J. K. Schneider using a variation of the method employed in the syntheses<sup>58</sup> of the  $\text{C}_2\text{H}_5$  and  $\text{C}_3\text{H}_7$  substituted acid salts.

The salt was dehydrated when required by heating to 100°C in vacuo.

(b)  $\text{NH}_4\text{S}_2\text{P}(\text{C}_6\text{H}_5)_2$  was formed as a white precipitate on bubbling gaseous ammonia into a benzene solution of the crude commercial acid (Columbia Organic Chemicals Co.). When dichloromethane was used in place of benzene, continued addition of ammonia resulted in dissolution of the precipitated salt which, however, was recovered on removal of the dichloromethane and excess ammonia on a rotary evaporator. After washing with benzene or dichloromethane, the salt was dried and used without further purification.

(c)  $\text{NaS}_2\text{P}(\text{OC}_2\text{H}_5)_2$  was prepared by addition of slightly



TABLE 2.1  
Analytical Data for the Complexes  $M[S_2PX_2]_n^a$

X	$M^{+n}$	Color	Molecular Weight		% Constitution				
			Solution	Mass Spec.	M	C	H	P	S
$CH_3$	$OV^{+2}$	Blue	335(317) <sup>b</sup>	316.8680(316.8686)	16.04(16.1)	15.30(15.14)	3.68(3.81)	19.78(19.56)	40.7 (40.3)
	$V^{+3}$	Brown		426(426)	12.13(11.95)	16.5 (16.9)	4.05(4.25)	21.69(21.79)	45.61(45.11)
	$Cr^{+3}$	Dark-blue	415(428) <sup>b</sup>	427(427)		16.76(16.86)	4.44(4.24)		
	$Mn^{+2}$	Cream		305(305)	17.84(18.00)	15.96(15.74)	4.14(3.96)	20.48(20.29)	42.2 (42.0)
	$Fe^{+2}$	Yellow		306(306)	17.85(18.24)	15.54(15.69)	3.81(3.95)	19.8 (20.2)	42.2 (41.9)
	$Co^{+3}$	Brown				16.61(16.59)	4.13(4.18)	21.1 (21.4)	
	$Co^{+2}$	Green		309(309)		15.68(15.53)	4.12(3.91)		
	$Ni^{+2}$	Dark-blue	304(309) <sup>b</sup>	308(308)		15.68(15.55)	4.17(3.91)		
	$Pd^{+2}$	Orange-red	385(357) <sup>b</sup>	356(356)		13.65(13.47)	3.44(3.39)		
	$Pt^{+2}$	Orange-yellow	522(445) <sup>b</sup>	445(445)		10.82(10.79)	2.95(2.72)		
	$Zn^{+2}$	White		314(314)		15.47(15.22)	3.92(3.83)		
$COOS_2P(CH_3)_4$	$Cd^{+2}$	White		364(364)		13.36(13.24)	3.56(3.34)		
	$Hg^{+2}$	White		452(452)		10.73(10.65)	2.84(2.68)		
	$NaS_2P(CH_3)_2 \cdot 2H_2O$	Blue				16.34(16.39)	4.13(4.13)		
	$C_6H_5$	White				12.76(13.04)	5.48(5.43)		
	$OV^{+2}$	Blue		565(565)	9.2 (8.9)	50.94(50.97)	3.59(3.56)	10.8 (10.8)	23.0 (22.3)
	$V^{+3}$	Brown		798(798)		54.0 (54.1)	4.2 (3.8)	11.7 (11.7)	20.4 (24.0)
	$Cr^{+3}$	Blue-purple	729(799) <sup>b</sup>	799(799)		53.6 (54.0)	3.89(3.78)		25.15(24.05)
	$Mn^{+2}$	Pale green		553(553)	9.73(9.92)	51.98(52.08)	3.54(3.64)	11.1 (11.2)	22.9 (23.2)
	$Fe^{+3}$	Black				53.65(53.79)	3.98(3.76)	11.68(11.56)	23.7 (23.9)
	$Fe^{+2}$	Yellow		554(554)	10.6 (10.0)	51.86(51.99)	3.87(3.64)	10.7 (11.2)	23.9 (23.1)
	$Co^{+3}$	Brown	795(806) <sup>d</sup>			53.74(53.59)	3.87(3.75)		
$NaS_2P(OC_2H_5)_2$	$Co^{+2}$	Green		557(557)		51.86(51.70)	3.83(3.62)		
	$Ni^{+2}$	Purple	558(557) <sup>b</sup>	556(556)		51.77(51.72)	3.82(3.62)		
	$Pd^{+2}$	Red-orange	623(605) <sup>b</sup>	604(604)		47.53(47.65)	3.43(3.33)		
	$Pt^{+2}$	Orange	674(694) <sup>b</sup>	693(693)		41.44(41.55)	3.09(2.91)		
	$Zn^{+2}$	White		562(562)		50.99(51.11)	3.71(3.58)		
	$Cd^{+2}$	White		612(612)		47.16(47.18)	3.40(3.30)		
	$Hg^{+2}$	White		700(700)		41.32(41.23)	2.82(2.88)		
	$NH_4S_2P(C_6H_5)_2$	White			N:5.12(5.25)	53.99(53.91)	5.29(5.28)		
	$OC_2H_5$	$OV^{+2}$	Violet	437(437)	11.3 (11.7)	21.91(21.97)	4.61(4.61)	14.7 (14.2)	30.0 (29.3)
	$V^{+3}$	Red-orange		606(606)		23.68(23.76)	5.17(4.99)		
	$Cr^{+3}$	Deep-purple	729(799) <sup>b</sup>	799(799)		53.56(54.05)	3.89(3.78)		
$NaS_2P(NH_4)_2$	$Co^{+3}$	Brown				53.74(53.59)	3.87(3.75)		
	$Co^{+2}$	Green		557(557)		51.86(51.70)	3.83(3.62)		
	$Ni^{+2}$	Deep-purple	407(429)	428(428)		22.44(22.39)	4.57(4.70)		
	$Pd^{+2}$	Red-orange	431(477)	476(476)		20.31(20.15)	4.19(4.23)		
	$Pt^{+2}$	Orange-yellow	513(566)	565(100)		16.66(16.99)	3.63(3.56)		
	$Zn^{+2}$	White		434(434)		21.0 (22.0)	4.65(4.63)		28.6 (29.4)
	$NaS_2P(OC_2H_5)_2$	White				22.76(23.07)	4.50(4.84)		
$NH_4S_2P(OC_2H_5)_2$	$NH_4S_2P(OC_2H_5)_2$	White			N:6.84(6.89)	22.56(23.64)	6.94(6.94)		33.1 (31.6)



TABLE 2.1 (cont'd)  
Analytical Data for the Complexes  $M[S_2PX_2]_n^a$

X	$M^{+n}$	Color	Molecular Weight		$\frac{Cr}{Cr_3}^1$	Constitution
			Solution	Mass Spec.		
P	OV <sup>+2</sup>	Black		332.7681(332.7679)		
	V <sup>+3</sup>	Deep red		499.6886(499.6884)		
	Cr <sup>+3</sup>	Deep blue		451(451)		
	Mn <sup>+2</sup>	Pale pink	325(321) <sup>f</sup>	320.7672(320.7675)		
	Fe <sup>+2</sup>	Orange-yellow	343(322) <sup>g</sup>	321.7659(321.7648)		
	Co <sup>+3</sup>	Brown		457.6765(457.6773)		
	Co <sup>+2</sup>	Green		324.7620(324.7626)		
	Ni <sup>+2</sup>	Dark green	329(325) <sup>h</sup>	323.7641(323.7659)		
	Pd <sup>+2</sup>	Red-orange	384(373) <sup>f</sup>	372.7333(372.7326)		
	Pt <sup>+2</sup>	Orange-yellow		460.7935(460.7942)		
	Zn <sup>+2</sup>	White		329.7580(329.7575)		
	Hg <sup>+2</sup>	White		467.8002(467.8002)		
CrF <sub>3</sub>	OV <sup>+2</sup>	Black		532.7550(532.7555)	26.0 (26.25)	
	V <sup>+3</sup>	Deep red		749.6692(749.6689)	25.3 (25.5)	
	Cr <sup>+3</sup>	Deep purple		751(751)	27.2 (27.0)	
	Mn <sup>+2</sup>	Pale green		520.7535(520.7545)	26.4 (26.5)	
	Fe <sup>+3</sup>	Black		754.6623(754.6598)		
	Fe <sup>+2</sup>	Yellow		521.7500(521.7515)	26.8 (26.4)	
	Co <sup>+3</sup>	Brown		757.6613(757.6581)		
	Co <sup>+2</sup>	Green		524.7526(524.7498)	26.4 (26.3)	
	Ni <sup>+2</sup>	Blue-green	507(520) <sup>e</sup>	523.7523(523.7519)	26.1 (26.2)	24.88(24.42)
	Pd <sup>+2</sup>	Orange-red	633(572) <sup>e</sup>	571.7190(571.7198)	24.0 (24.1)	22.39(22.39)
	Pt <sup>+2</sup>	dimer Yellow	>1000(1258) <sup>e</sup>	1257.6160(1257.6181)	21.3 (21.9)	15.31(15.28)
	Zn <sup>+2</sup>	White		529.7460(529.7467)	26.3 (26.3)	
	Cd <sup>+2</sup>	White		579.7175(579.7202)		
	Hg <sup>+2</sup>	White		667.7886(667.7872)		

<sup>a</sup> The entries are found values followed by the value calculated for the presumed formulation in parentheses.

<sup>b</sup> Osmometrically in  $CH_2Br_2$ .

<sup>c</sup> Osmometrically in acetone.

<sup>d</sup> Osmometrically in  $CHCl_3$ , reference 38.

<sup>e</sup> Osmometrically in  $CCl_4$ .

<sup>f</sup> In 1,2-dichloroethane, reference 18.

<sup>g</sup> In toluene, reference 18.

<sup>h</sup> By gas density at 160°C, reference 18.

<sup>i</sup> Calculated from the  $ECF_3$  evolved on base hydrolysis of the compound, assuming one mole of  $HCF_3$  evolved per mole of P present.



less than the stoichiometric amount of either  $\text{NaOCH}_3$  or anhydrous  $\text{Na}_2\text{CO}_3$  to the ethanolic solution of  $\text{HS}_2\text{P}(\text{OC}_2\text{H}_5)_2$  formed upon dissolution of  $\text{P}_4\text{S}_{10}$  in ethanol<sup>59</sup>. All reactions were vigorously exothermic. The white salt was precipitated by and washed well with diethyl ether, dried at 70°C, and then used without further purification.

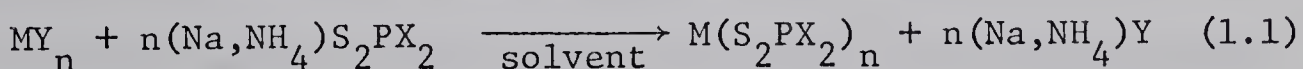
(d)  $\text{NH}_4\text{S}_2\text{P}(\text{OC}_2\text{H}_5)_2$  was obtained by bubbling gaseous ammonia into an ethanolic solution of the acid prepared as in (c). The white salt was precipitated as lustrous flakes on addition of diethyl ether to the reaction mixture. The salt was used without further purification after being washed well with ether and dried at 70°C.

(e)  $\text{HS}_2\text{PF}_2$  was prepared by published methods<sup>16</sup>.

(f)  $\text{HS}_2\text{P}(\text{CF}_3)_2$  was prepared by Miss J. K. Schneider according to published methods<sup>17c</sup>.

#### Complexes Formed through Metathetical Salt Reactions

Preparations included in this category are of the general type



where  $\text{MY}_n$  is a transition metal ion  $\text{M}^{+n}$  salt and  $\text{X} = \text{CH}_3$ ,  $\text{C}_6\text{H}_5$  or  $\text{OC}_2\text{H}_5$ .

(a)  $\text{OV}[\text{S}_2\text{P}(\text{CH}_3)_2]_2$ . Powdered  $\text{OVSO}_4 \cdot 2\text{H}_2\text{O}$  (5 mmoles) was stirred with 10 mmoles of  $\text{NaS}_2\text{P}(\text{CH}_3)_2 \cdot 2\text{H}_2\text{O}$  in ~25 ml of methanol until dissolution of the sulfate salt. After removal of the



methanol in vacuo, the vanadyl complex was extracted into chloroform yielding a deep blue solution. Slow removal of the chloroform in vacuo gave lustrous blue crystals which were washed quickly with cold acetone, diethyl ether and then dried in vacuo.

(b)  $\text{OV}[\text{S}_2\text{P}(\text{C}_6\text{H}_5)_2]_2$ . The light blue finely divided product precipitated immediately on mixing concentrated, filtered aqueous solutions containing stoichiometric amounts of  $\text{OVSO}_4 \cdot 2\text{H}_2\text{O}$  and  $\text{NH}_4\text{S}_2\text{P}(\text{C}_6\text{H}_5)_2$ , respectively. After washing with water and ethanol, recrystallization was effected as in (a) from chloroform.

(c)  $\text{OV}[\text{S}_2\text{P}(\text{OC}_2\text{H}_5)_2]_2$ . The deep purple complex precipitated immediately on mixing concentrated aqueous solutions of  $\text{OVSO}_4 \cdot 2\text{H}_2\text{O}$  and  $\text{NaS}_2\text{P}(\text{OC}_2\text{H}_5)_2$ . Extraction into cyclohexane from the aqueous mixture produced deep blue-purple solutions from which fine, needle-like, blue-purple crystals (m.p.  $65^\circ\text{C}$ , uncorr.) were obtained on removal of the solvent in vacuo. The complex was distilled at  $\sim 100^\circ\text{C}$  in a sublimer under vacuum from its melt onto a water cooled probe at  $15^\circ\text{C}$ , leaving a small residue of  $\text{V}[\text{S}_2\text{P}(\text{OC}_2\text{H}_5)_2]_3$  identified by its color, infrared and mass spectra. Solutions of  $\text{OV}[\text{S}_2\text{P}(\text{OC}_2\text{H}_5)_2]_2$  appeared more stable exposed to air than the isolated solid which rapidly formed oily black intractable mixtures which produced no colored solutions on extraction with non-polar organic solvents.

When oxygen was bubbled into organic solvent ( $\text{C}_6\text{H}_{12}$ ,  $\text{CHCl}_3$ ) solutions of either  $\text{OV}[\text{S}_2\text{P}(\text{CH}_3)_2]_2$  or  $\text{OV}[\text{S}_2\text{P}(\text{C}_6\text{H}_5)_2]_2$ , the initially blue solutions over a period of  $\sim 30$  min turned green and eventually



colorless leaving a deposit of dark material. In chloroform, a deep blue-purple solution of  $\text{OV}[\text{S}_2\text{P}(\text{OC}_2\text{H}_5)_2]_2$  turned bright red within  $\sim 10$  min before eventual decolorization and deposition of a dark solid. Removal of the chloroform from this latter solution at the red stage left only the original complex. The dark solids uniformly gave low C, H, and S analyses, proved insoluble to the extent of imparting color to non-polar solvents, but dissolved in water giving blue solutions characteristic of the ion  $\text{OV(OH)}_2^5^{+2}$ .

(d)  $\text{OMo}[\text{S}_2\text{P}(\text{CH}_3)_2]_2$  and  $\text{OMo}[\text{S}_2\text{P}(\text{C}_6\text{H}_5)_2]_2$  were prepared as air sensitive (turned black on exposure) pale purple crystalline solids from the reaction of the respective ligand salt with  $\text{K}_3\text{MoCl}_6$  in dilute HCl solution as has been described<sup>60</sup> for  $\text{OMo}[\text{S}_2\text{P}(\text{O}-\text{C}_3\text{H}_7)_2]_2$ . The reaction solution containing the components of the methyl-substituted complex was chilled in a stoppered flask at  $\sim -10^\circ\text{C}$  for several days in a refrigerator before crystallization was observed. Apart from observation of bands characteristic of Mo-O stretches ( $944$  and  $920 \text{ cm}^{-1}$ , respectively) and coordinated ligand vibrations in their infrared spectra, these complexes were uncharacterized.

(e)  $\text{O}_2\text{U}[\text{S}_2\text{P}(\text{CH}_3)_2]_2$  and  $\text{O}_2\text{U}[\text{S}_2\text{P}(\text{C}_6\text{H}_5)_2]_2$ . Mixing of concentrated aqueous solutions of  $\text{O}_2\text{U}(\text{NO}_3)_2 \cdot 6\text{H}_2\text{O}$  with the respective concentrated solution of the ligand salt resulted in the immediate precipitation of  $\text{O}_2\text{U}[\text{S}_2\text{P}(\text{C}_6\text{H}_5)_2]_2$  only. The yellow-orange aqueous solution containing the methyl substituted complex components was evaporated to dryness in vacuo leaving a yellow-orange solid. Both



complexes were recrystallized from diethylether and proved generally soluble in organic solvents. Apart from obtaining their infrared spectra, observation of the parent molecule ions in the mass spectra and preliminary chemical analyses, these complexes were uncharacterized.

The complex  $O_2U[S_2P(C_6H_5)_2]_2$  had been reported previously<sup>146</sup>.

(f)  $V[S_2P(CH_3)_2]_3$  was prepared under anaerobic conditions by vacuum distillation of 50 ml of ethanol onto stoichiometric amounts (5:15 mmoles) of solid  $VCI_3$  and  $NaS_2P(CH_3)_2$  (anhyd.) in a flask connected to a vacuum line. After stirring for several minutes the ethanolic solution became deep red-brown and deposited some lustrous red-brown crystals. The ethanol was distilled off and the residual solid was extracted with ~50 ml of carbon tetrachloride in a Soxhlet extractor under an atmosphere of nitrogen in a glove bag. The resultant saturated, deep red-brown solution containing flat needle-like red-brown crystals was evaporated to dryness in vacuo to yield crude  $V[S_2P(CH_3)_2]_3$ . Final purification was effected by fractional sublimation in vacuo at ~200°C yielding dark brown crystals. The preliminary steps in this procedure were also carried out using acetonitrile, however, the limited solubility of the salt  $Na[S_2P(CH_3)_2]_2$  necessitated a much longer stirring time (~12 hrs). The complex rapidly turned blue on exposure to air.

(g)  $V[S_2P(C_6H_5)_2]_3$  precipitated as a greenish-yellow solid on addition of  $VCI_3$  (1 mmole) to a filtered, concentrated aqueous solution of  $NH_4S_2P(C_6H_5)_2$  (>3 mmoles in 5 ml). The product was washed with freshly boiled water stored under nitrogen and then dried in vacuo. Recrystallization from chloroform or carbon



tetrachloride yielded larger brown crystals. The solid complex is remarkably stable in air, but solutions exposed to air rapidly turned blue.

(h)  $\text{Cr}[\text{S}_2\text{P}(\text{CH}_3)_2]_3$  and  $\text{Cr}[\text{S}_2\text{P}(\text{C}_6\text{H}_5)_2]_3$ . Concentrated methanolic solutions of the respective ligand salts were mixed with concentrated methanolic solutions of  $\text{CrCl}_3 \cdot 6\text{H}_2\text{O}$ . Blue-purple  $\text{Cr}[\text{S}_2\text{P}(\text{C}_6\text{H}_5)_2]_3$  precipitated immediately while approximately 12 hours later a significant quantity of purple  $\text{Cr}[\text{S}_2\text{P}(\text{CH}_3)_2]_3$  was deposited. Both complexes were extracted into and crystallized from dichloromethane. Alternative preparative procedures developed by Dr. W. Byers are described elsewhere<sup>53</sup>.

(i)  $\text{Mn}[\text{S}_2\text{P}(\text{CH}_3)_2]_2$ . Mixing of concentrated ethanolic solutions containing stoichiometric amounts of  $\text{MnCl}_2 \cdot 4\text{H}_2\text{O}$  and  $\text{NaS}_2\text{P}(\text{CH}_3)_2 \cdot 2\text{H}_2\text{O}$  resulted in the immediate and nearly quantitative precipitation of NaCl. The solution was filtered and evaporated to dryness on a rotary evaporator using a hot water bath, leaving a pale-pink residue. Fractional sublimation at 200°C in vacuo separated an off-white product. Accidental sublimation in air during an attempted Soxhlet extraction resulted in no apparent damage to the complex. Attempts to prepare the complex by concentration of aqueous solutions containing the metal and ligand salts simply resulted in the reprecipitation of the ligand salt without complex formation.

(j)  $\text{Mn}[\text{S}_2\text{P}(\text{C}_6\text{H}_5)_2]_2$  precipitated immediately as a white solid on mixing of concentrated, filtered aqueous solutions of  $\text{MnCl}_2 \cdot 4\text{H}_2\text{O}$  and  $\text{NH}_4\text{S}_2\text{P}(\text{C}_6\text{H}_5)_2$  in stoichiometric amounts. After washing



well with water, the complex was dried in vacuo. The dried solid had a very pale green hue.

(k)  $\text{Fe}[\text{S}_2\text{P}(\text{C}_6\text{H}_5)_2]_3$  precipitated immediately as a black solid on mixing concentrated, filtered aqueous solutions of  $\text{FeCl}_3 \cdot 6\text{H}_2\text{O}$  and  $\text{NH}_4\text{S}_2\text{P}(\text{C}_6\text{H}_5)_2$  in stoichiometric amounts. The complex was washed with water, 2-propanol, and then dried in vacuo. Dichloromethane and 2-propanol solutions were deep green in color.

(l)  $\text{Fe}[\text{S}_2\text{P}(\text{CH}_3)_2]_2$  and  $\text{Fe}[\text{S}_2\text{P}(\text{C}_6\text{H}_5)_2]_2$ . Aqueous solutions containing Fe(II) were prepared by bubbling  $\text{SO}_2$  for ~20 min into hot solutions of 5 mmoles of  $\text{FeSO}_4 \cdot 7\text{H}_2\text{O}$  dissolved in 50 ml of water. Excess  $\text{SO}_2$  was removed by boiling the solutions to half-volume in air after which the flasks containing the solutions were stoppered and stored under nitrogen until cool. Under nitrogen, freshly boiled methanolic solutions of the respective and stoichiometric amount of ligand salt, 10 mmoles in 25 ml, were mixed with the Fe(II) solutions. On standing,  $\text{Fe}[\text{S}_2\text{P}(\text{C}_6\text{H}_5)_2]_2$  crystallized from the mother solution as small pale-yellow clusters of crystals distributed over the surface of the flask. Mustard yellow  $\text{Fe}[\text{S}_2\text{P}(\text{CH}_3)_2]_2$  could only be induced to precipitate from solution by reduction of the volume to ~10 ml by removal of the solvent in vacuo. Both complexes were washed with cold, oxygen-free water and were dried in vacuo (yields were 30 - 50%). When dry,  $\text{Fe}[\text{S}_2\text{P}(\text{CH}_3)_2]_2$  appeared to be remarkably resistant to aerial oxidation in contrast with  $\text{Fe}[\text{S}_2\text{P}(\text{C}_6\text{H}_5)_2]_2$  which rapidly turned green and then black. Both complexes proved only very sparingly soluble in non-polar organic solvents yielding solutions which were particularly susceptible to oxidation turning the green



color characteristic of the more soluble Fe(III) complex. The green (oxidized) solutions of  $\text{Fe}[\text{S}_2\text{P}(\text{CH}_3)_2]_2$  were unstable, continuously fading while depositing a tan colored material.

(m)  $\text{Ru}[\text{S}_2\text{P}(\text{CH}_3)_2]_3$  and  $\text{Ru}[\text{S}_2\text{P}(\text{C}_6\text{H}_5)_2]_3$  were formed as dark purple and mauve precipitates, respectively, on mixing concentrated aqueous solutions of  $\text{RuCl}_3$  with concentrated aqueous solutions of the respective ligand salt. These compounds were further characterized by Dr. W. Byers.

(n)  $\text{Co}[\text{S}_2\text{P}(\text{CH}_3)_2]_3$  and  $\text{Co}[\text{S}_2\text{P}(\text{C}_6\text{H}_5)_2]_3$  were precipitated on addition of concentrated aqueous solutions of  $\text{Na}_3\text{Co}(\text{NO}_2)_6$  to the respective dry ligand salt. The dark brown solids were extracted from the aqueous mixture into dichloromethane from which they were recovered by removal of the solvent on a rotary evaporator, without heating. After washing with cold 2-propanol, the two complexes were dried in vacuo.

(o)  $\text{Co}[\text{S}_2\text{P}(\text{CH}_3)_2]_2$  crystallized out of aqueous solutions 0.1M in  $\text{CoCl}_2 \cdot 6\text{H}_2\text{O}$  and 0.2M in  $\text{NaS}_2\text{P}(\text{CH}_3)_2 \cdot \text{H}_2\text{O}$  as bright emerald green plates. It was also prepared on mixing ethanolic solutions of the dehydrated metal and ligand salts, and as a thermal decomposition product of a blue complex to be described in section (r). Final purification was achieved by fractional sublimation in vacuo at 200°C.

(p)  $\text{Co}[\text{S}_2\text{P}(\text{C}_6\text{H}_5)_2]_2$  immediately precipitated as a light green solid on mixing of ethanolic or aqueous solutions of  $\text{CoCl}_2 \cdot 6\text{H}_2\text{O}$  (~1 gm/10 mls) and  $\text{NH}_4\text{S}_2\text{P}(\text{C}_6\text{H}_5)_2$ . The complex was washed well with ethanol and dried in vacuo.



(q)  $\text{Co}[\text{S}_2\text{P}(\text{OC}_2\text{H}_5)_2]_2$  was precipitated on adding dry  $\text{NaS}_2\text{P}(\text{OC}_2\text{H}_5)_2$  to a concentrated, freshly boiled aqueous solution of  $\text{CoCl}_2 \cdot 6\text{H}_2\text{O}$  and then extracted into dichloromethane. Removal of the solvent slowly under vacuum precipitated the complex as lustrous, flat, blue needles. Surface Co(III) complex and water soluble materials were readily removed by consecutively washing with acetone, water, acetone, and finally ether. No halide was detected in samples of the solid. In the solid state the complex could be kept in air for periods of hours without apparent change, however, solutions were readily oxidized in air turning from an initial blue to an eventual red-brown characteristic of the Co(III) complex.

(r)  $\text{CoOS}_3\text{P}_2(\text{CH}_3)_4$ . Attempted preparation of green  $\text{Co}[\text{S}_2\text{P}(\text{CH}_3)_2]_2$  in alcohol, acetone, or acetonitrile using hydrated salts, produced instead precipitates of varying shades of blue. A crystalline blue material was prepared by mixing hot 25 ml ethanolic solutions containing 5 mmoles of  $\text{CoY}_2 \cdot 6\text{H}_2\text{O}$  ( $\text{Y} = \text{Cl}$  or  $\text{Br}$ ) and 10 mmoles of  $\text{NaS}_2\text{P}(\text{CH}_3)_2 \cdot 2\text{H}_2\text{O}$ , respectively, and setting the reaction mixture aside to cool. Halide contamination of the crystals was minimized (3%) by use of  $\text{CoBr}_2 \cdot 6\text{H}_2\text{O}$ . Carbon and sulfur analyses on the blue crystals gave a mole ratio C/S of 1.36 (calc. C/S = 1.33 for  $\text{CoOS}_3\text{P}_2(\text{CH}_3)_4$ ). Soxhlet extraction of the blue crystals into methanol, ethanol, dichloromethane, or chloroform yielded blue solutions and removed the halide contamination while retaining the C/S ratio and the ir spectrum observed for the crystals. Recrystallization could not be effected from these solvents, although the complex could be reprecipitated. Extraction



of the blue material into benzene, carbon tetrachloride or carbon disulfide gave green colored solutions from which blue-to-green colored solids were recovered, on removal of the solvent, showing irregular but decreased C/S ratios. Since this complex is an odd member in the set of dithiophosphinates studied, the infrared spectrum of a nujol mull is given here separately: 1422(w), 1415(w), 1399(w), 1298(w), 1285(m), 1100(wsh), 1058(s), 947(m), 934(msh), 901(s), 861(msh), 855(m), 849(wsh), 745(w), 716(s), 593(msh), 578(s), 550(m), 488(m), 428(m), 363(m), 326(m), 315(msh), 253(w), 215(wsh), 205(m).

(s)  $M[S_2PX_2]_2$  with M = Ni, Pd, Pt, and X =  $\text{CH}_3$  and  $\text{C}_6\text{H}_5$ .

Mixing of concentrated aqueous solutions of the respective ligand salt with a concentrated aqueous solution of the respective metal salt ( $\text{NiCl}_2 \cdot 6\text{H}_2\text{O}$ ,  $(\text{NH}_4)_2\text{PdCl}_4$ ,  $\text{K}_2\text{PtCl}_4$ ) resulted in the precipitation of purple nickel complexes, orange palladium complexes and yellow platinum complexes. Crystallization was effected by extraction of the metal complex into dichloromethane (~1 gm/10 ml), addition of an equal volume of 2-propanol, followed by boiling off half of the solvent mixture at ~1 atm pressure and setting the solution enriched in 2-propanol aside to cool. Attempted preparations of the Pd and Pt complexes from dilute aqueous solutions often resulted in the precipitation of a brown material (presumably the metal sulfide) accompanied by the readily detectable evolution of  $\text{H}_2\text{S}$ . The complex  $\text{Pt}[\text{S}_2\text{P}(\text{CH}_3)_2]_2$  was fractionally sublimed at 250°C while the remaining complexes were washed with 2-propanol and dried in vacuo.



(t)  $\text{Pt}[\text{S}_2\text{P}(\text{OC}_2\text{H}_5)_2]_2$  was prepared and crystallized as described above in section (s) starting from  $\text{K}_2\text{PtCl}_4$  and  $\text{NaS}_2\text{P}(\text{OC}_2\text{H}_5)_2$ . The yellow crystals were washed with 2-propanol and dried in vacuo.

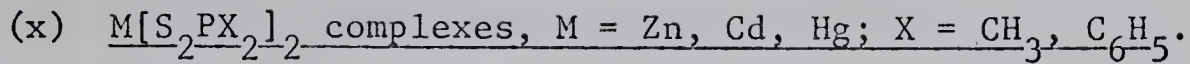
(u)  $\text{CuS}_2\text{P}(\text{CH}_3)_2$ . All attempts to prepare a Cu(II) complex from  $\text{CuCl}_2 \cdot 2\text{H}_2\text{O}$ ,  $\text{CuSO}_4 \cdot 5\text{H}_2\text{O}$  and  $\text{NaS}_2\text{P}(\text{CH}_3)_2 \cdot 2\text{H}_2\text{O}$  in water, methanol, ethanol, or acetone in air or in vacuo resulted in the immediate formation of the Cu(I) complex as a white precipitate. The stoichiometric amount of NaCl expected from the formation of a Cu(II) complex was collected in a quantitative experiment. In water or methanol  $\text{SO}_2$  and  $(\text{CH}_3)_2\text{P}(\text{S})\text{OP}(\text{S})(\text{CH}_3)_2$  are two of the overall reaction products which were identified by their infrared and mass spectra.

(v)  $\text{CuS}_2\text{P}(\text{C}_6\text{H}_5)_2$ . Mixing in air of solutions of  $\text{CuCl}_2 \cdot 2\text{H}_2\text{O}$  and  $\text{NH}_4\text{S}_2\text{P}(\text{C}_6\text{H}_5)_2$  in water, ethanol, or acetonitrile resulted in a transient orange color which lightened in time leaving an off-white precipitate of the Cu(I) complex. An interface reaction between a concentrated aqueous solution of  $\text{CuCl}_2 \cdot 2\text{H}_2\text{O}$  and a concentrated solution of  $\text{HS}_2\text{P}(\text{C}_6\text{H}_5)_2$  in chloroform resulted in the chloroform layer becoming deep red-brown. This chloroform solution proved to be metastable, continuously depositing the Cu(I) complex, but did produce an epr spectrum characteristic of a Cu(II) complex, including hyperfine structure attributable to  $^{31}\text{P}$  couplings<sup>39</sup>.  $\text{CuCl}_2 \cdot 2\text{H}_2\text{O}$  is insufficiently soluble in chloroform to produce a detectable epr spectrum.

(w)  $\text{AgS}_2\text{P}(\text{CH}_3)_2$  was prepared as the white precipitate resulting on mixture of aqueous solutions of  $\text{AgNO}_3$  and  $\text{NaS}_2\text{P}(\text{CH}_3)_2 \cdot 2\text{H}_2\text{O}$ . The complex was light sensitive turning black, but was not



characterized.

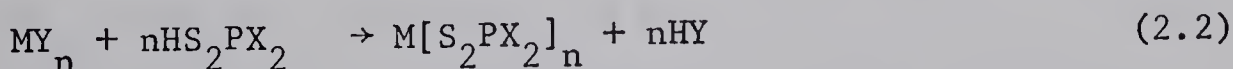


These complexes formed white precipitates on mixing 2 mmoles of the metal (II) chlorides in 20 ml of alcohol to 4 mmoles of the respective ligand salt in 20 ml of alcohol. The methyl-substituted complexes were prepared in methanol while the phenyl-substituted complexes were prepared in ethanol so that the solubilities of the salts NaCl and NH<sub>4</sub>Cl would not be exceeded and co-precipitate. The complex Hg[S<sub>2</sub>P(CH<sub>3</sub>)<sub>2</sub>]<sub>2</sub> must be immediately collected, washed with methanol, and dried in vacuo, otherwise it rapidly turns yellow, brown, and then dark brown (presumably due to formation of the metal sulfide). While the phenyl substituted complexes required only washing with alcohol, and drying in vacuo, the methyl substituted complexes required fractional sublimation in vacuo at 250°C in order to achieve a satisfactory analysis.

(y) Zn[S<sub>2</sub>P(OC<sub>2</sub>H<sub>5</sub>)<sub>2</sub>]<sub>2</sub> was precipitated as a white solid on addition of a concentrated aqueous solution of ZnCl<sub>2</sub> to dry NH<sub>4</sub>S<sub>2</sub>P(OC<sub>2</sub>H<sub>5</sub>)<sub>2</sub> or NaS<sub>2</sub>P(OC<sub>2</sub>H<sub>5</sub>)<sub>2</sub>. The wet mixture was extracted with dichloromethane. Concentration of the dichloromethane solution on a rotary evaporator with a warm water bath precipitated large white flakes which were twice recrystallized from benzene.

#### Complexes Formed through Metathetical Acid-Metal Salt Reactions

This category includes reactions of the general type



where MY<sub>n</sub> is a salt of the metal ion M<sup>+n</sup> and X = OC<sub>2</sub>H<sub>5</sub>, F, or CF<sub>3</sub>.



(a)  $\underline{M[S_2P(OC_2H_5)_2]_n}$  complexes, where  $M^{+n} = V^{+3}, Cr^{+3}, Ni^{+2}, Pd^{+2}$  and  $Co^{+3}$ . The general method of preparation of complexes from the acid  $HS_2P(OC_2H_5)_2$  in ethanol solution is described elsewhere<sup>59</sup>. In all cases the ethanolic solutions of  $HS_2P(OC_2H_5)_2$  were generated by dissolution of  $P_4S_{10}$  in ethanol. To these hot solutions,  $VCl_3$ ,  $CrCl_3 \cdot 6H_2O$ ,  $NiCl_2 \cdot 6H_2O$ ,  $(NH_4)_2PdCl_4$ , and  $CoCl_2 \cdot 2H_2O$  were added in stoichiometric amounts, respectively. On cooling, the initially hot reaction mixtures gave  $V[S_2P(OC_2H_5)_2]_3$  as orange-red crystals,  $Cr[S_2P(OC_2H_5)_2]_3$  as purple crystals,  $Ni[S_2P(OC_2H_5)_2]_3$  as purple crystals, and  $Pd[S_2P(OC_2H_5)_2]_2$  as orange crystals, respectively. The formation of brown, crystalline  $Co[S_2P(OC_2H_5)_2]_3$  required aerial oxidation of the initially formed Co(II) complex. Recrystallization was achieved through a dichloromethane/2-propanol mixture as described in section 2.2 (s). The crystals were washed with 2-propanol and dried in vacuo. As previously observed, all these complexes are air stable except  $V[S_2P(OC_2H_5)_2]_3$ <sup>26</sup> which slowly darkens in color leaving an intractable black tarry mixture within a period of hours.

(b)  $\underline{M[S_2PX_2]_n}$  complexes, where  $M^{+n} = OV^{+2}, V^{+3}$  and  $X = F$  and  $CF_3$ . These complexes were prepared from reaction of  $OVCl_3$  and  $VCl_3$  with the respective acid in a vacuum system by Dr. P. M. Watkins as described elsewhere<sup>54,55</sup> and purified by fractional sublimation.

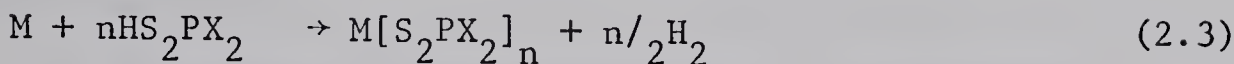
(c)  $\underline{M[S_2PX_2]_2}$  complexes, where  $M^{+2} = Pd^{+2}, Pt^{+2}, Cd^{+2}, Hg^{+2}$ ;  $X = F$  and  $CF_3$  but not  $Pt[S_2P(CF_3)_2]_2$ . The metal salts reacted<sup>56,57</sup> with the respective acids were  $(NH_4)_2PdCl_4$ ,  $PtCl_2$ ,  $K_2PtCl_4$ ,  $CdCl_2$  and  $HgCl_2$  as described by Tebbe and Meutterties<sup>18</sup>. The apparatus illustrated in Figure 2.1 proved useful in the preparation of the



volatile Pd and Pt complexes.

#### Complexes Formed through Acid-Metal Redox Reactions

Included in this category are the reactions



as observed by Tebbe and Muetterties<sup>18</sup> for X = F. Complexes of Cr(III), Mn(II), Fe(II), Co(II), Ni(II) and Zn(II), where X = F and CF<sub>3</sub> were prepared according to reaction (2.3) in vacuo. The compounds Fe[S<sub>2</sub>P(CF<sub>3</sub>)<sub>2</sub>]<sub>3</sub>, Co[S<sub>2</sub>PF<sub>2</sub>]<sub>3</sub> and Co[S<sub>2</sub>P(CF<sub>3</sub>)<sub>2</sub>]<sub>3</sub> were formed by oxidation of the M(II) complexes either by molecular oxygen or the respective thiophosphoryldisulfide [S<sub>2</sub>PX<sub>2</sub>]<sub>2</sub> herein called "diligand".

#### Unsuccessful Preparative Attempts

(a) Sc[S<sub>2</sub>P(CH<sub>3</sub>)<sub>2</sub>]<sub>3</sub> and Sc[S<sub>2</sub>P(C<sub>6</sub>H<sub>5</sub>)<sub>2</sub>]<sub>3</sub>. Concentrated aqueous solutions of ScCl<sub>3</sub>·6H<sub>2</sub>O with NaS<sub>2</sub>P(CH<sub>3</sub>)<sub>2</sub>·2H<sub>2</sub>O or NH<sub>4</sub>S<sub>2</sub>P(C<sub>6</sub>H<sub>5</sub>)<sub>2</sub> were evaporated to dryness in vacuo and the residual solid was extracted with chloroform producing pale green solutions. On concentration of the chloroform solutions, green oils remained from which white solids precipitated on addition of diethyl ether. In neither case did the mass spectra or infrared spectra correspond with a Sc[S<sub>2</sub>PX<sub>2</sub>]<sub>3</sub> complex. Attempted reactions in diglyme (1,2-dimethoxyethane) resulted in vigorously exothermic reaction of the diglyme with the ligand salt accompanied by the precipitation of elemental sulfur.

(b) OTi[S<sub>2</sub>P(CH<sub>3</sub>)<sub>2</sub>]<sub>2</sub>. Concentrated aqueous solutions of TiOSO<sub>4</sub>·2H<sub>2</sub>O with NaS<sub>2</sub>P(CH<sub>3</sub>)<sub>2</sub>·2H<sub>2</sub>O were evaporated to dryness in vacuo and the residual solid was extracted with chloroform yielding a pale green solution. Evaporation of the chloroform in vacuo left



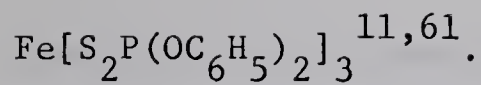
a yellowish oil from which separated a green solid on addition of diethyl ether. Neither the mass spectrum nor the ir spectrum of the green solid corresponded to a  $\text{OTi}[\text{S}_2\text{P}(\text{CH}_3)_2]_2$  complex and the attempt was terminated.

(c)  $\text{V}[\text{S}_2\text{P}(\text{CH}_3)_2]_2$  and  $\text{V}[\text{S}_2\text{P}(\text{C}_6\text{H}_5)_2]_2$ . Electrolytic reduction of 0.2 M solutions of  $\text{OVSO}_4 \cdot 2\text{H}_2\text{O}$  in  $\sim 2$  M HCl at 4.7V with a current density of  $\sim 0.1$  amps/cm<sup>2</sup> resulted in deep purple solutions of V(II). Addition of  $\text{NaS}_2\text{P}(\text{CH}_3)_2 \cdot 2\text{H}_2\text{O}$  or  $\text{NH}_4\text{S}_2\text{P}(\text{C}_6\text{H}_5)_2$  to these solutions resulted in the immediate precipitation of solids of appearance very similar to that of the corresponding dithiophosphinic acid. The correspondence was confirmed by the coincidence of the ir spectra in the case of  $\text{HS}_2\text{P}(\text{C}_6\text{H}_5)_2$ .

(d)  $\text{Cr}[\text{S}_2\text{P}(\text{CH}_3)_2]_2$  or  $\text{Cr}[\text{S}_2\text{P}(\text{C}_6\text{H}_5)_2]_2$ . Addition of  $\text{NaS}_2\text{P}(\text{CH}_3)_2 \cdot 2\text{H}_2\text{O}$  or  $\text{NH}_4\text{S}_2\text{P}(\text{C}_6\text{H}_5)_2$  to blue acidic aqueous solutions of Cr(II) prepared electrolytically resulted in the formation of purple precipitates and a solution color change from the blue of Cr(II) to the green of Cr(III). The purple precipitates were identified as the Cr(III) dithiophosphinates by comparison of infrared spectra with authenticated samples.

(e)  $\text{Fe}[\text{S}_2\text{P}(\text{CH}_3)_2]_3$ . Addition of  $\text{FeCl}_3 \cdot 6\text{H}_2\text{O}$  to a concentrated aqueous solution of  $\text{NaS}_2\text{P}(\text{CH}_3)_2 \cdot 2\text{H}_2\text{O}$  followed by extraction with dichloromethane resulted in deep green dichloromethane solutions which proved to be unstable in the presence or absence of air and from which only light tan colored solids could be recovered on removal of the solvent. The complex should be black in the solid state by analogy with the complexes  $\text{Fe}[\text{S}_2\text{P}(\text{C}_6\text{H}_5)_2]_3$  and





(f)  $\text{Ru}[\text{S}_2\text{P}(\text{CH}_3)_2]_2$ . Addition of a large excess of  $\text{NaS}_2\text{P}(\text{CH}_3)_2 \cdot 2\text{H}_2\text{O}$  to an aqueous solution of Ru(II) oxalate did not result in an immediate precipitate and investigation was discontinued.

### 2.3 Treatment of Results

#### Thermogravimetric Data

The Dupont instrument used records the weight of unvolatilized material as a function of temperature at a constant heating rate. A typical thermogram consisted of a descending series of plateaus connected by as many distinct slopes as there were distinct weight-loss processes. The arbitrary (but sufficient for present purposes) procedure followed herein was to assign the temperature at the point of intersection of the extrapolated plateau and slope to the weight-loss process. These points were found to be reproducible to within  $\pm 2^\circ\text{C}$  for the same sample in vacuo at heating rates of 3-15 degrees/min. Furthermore, these points correspond to an inflection point on the low temperature side of a peak in a plot of  $dW/dt$  vs  $t$ , where  $W$  is the weight and  $t$  the temperature.

#### Mass Spectral Data

In this study of the mass spectral fragmentation patterns of the complexes  $M[\text{S}_2\text{PX}_2]_n$ , interest was mainly focused on the fate of the metal atoms and on the presence or absence of a diligand ion  $[\text{S}_2\text{PX}_2]_2^+$ . Thus only peaks in the mass spectra assignable to metal atom containing or diligand ions are included in Appendix B. The assignment of relative intensities to mass spectral peaks is



somewhat tedious when the atoms M possess a number of isotopes.

This latter difficulty was circumvented by simply scaling the spectra such that one of the metal containing ion peaks of interest (usually the most intense) was arbitrarily assigned an intensity of 100 for comparison of intensity data between different complexes.

Peak assignments were facilitated by the use of the computer program MASPEC (Appendix E) which took peak intensities and m/e values as input and made assignments by considering all possible fragmentations of the parent molecule excluding internal breakdown in the X-group except when  $X = CF_3$ . MASPEC also performed the intensity scaling. Where ambiguities in peak assignments were not resolved by accurate mass measurement, arbitrary choices were made exercising some "chemical intuition". Only peaks assignable within the restriction of no fragmentation are included in Tables B1 - B4. While this further arbitrariness results in the neglect of some more intense peaks where  $X = C_6H_5$  and  $CF_3$  the complete assignment in these cases was not judged to be of sufficient relevance in a comparative study to warrant the extra expense and effort.

#### Magnetic Data

##### (a) Static Field Magnetic Susceptibility Results

In the Faraday method of determining magnetic susceptibilities, the force of interaction between an isotopic magnetic sample and a magnetic field  $\vec{H}$  is given by the equation<sup>63,64</sup>

$$f = m\chi_g \left( \frac{\vec{H} \cdot \vec{\partial H}}{\partial s} \right) \quad (2.4)$$

where f is the force component in the direction of the s coordinate,



$m$  and  $\chi_g$  are respectively the mass and magnetic susceptibility per unit mass of the sample. Since all samples were powdered and the geometry of the apparatus was maintained constant in this work, at a given field the "gram-susceptibility" ( $\chi_g$ ) was determined relative to a standard of known mass and susceptibility through the relation

$$\chi_g = \frac{fm_{\text{std}}}{f_{\text{std}}^m} \chi_{g\text{ std.}} \quad (2.5)$$

For "normal" paramagnets, the temperature dependence of the molar magnetic susceptibility ( $\chi_M$ ) may be expressed in the form<sup>66,67</sup>

$$\chi_M = \chi_g \cdot M = \frac{C}{T-\theta} + \chi_M^D + \text{TIP}, \quad (2.6)$$

where  $M$  is the gram molecular weight,  $C$  and  $\theta$  are the Curie and Weiss constants, respectively,  $\chi_M^D$  is the molar diamagnetic susceptibility, and TIP is the temperature independent paramagnetic susceptibility. In practice, the data were fit to an equation of the form

$$\frac{1}{\chi_M^{-D}} = AT + B, \quad (2.7)$$

where  $D = \chi_M^D + \text{TIP}$ ,  $A = 1/C$ , and  $B = -\theta/C$ . The raw experimental data consisting of forces and thermocouple voltages were processed by the computer program MAGSUS (Appendix E) which converted the forces into magnetic susceptibilities, voltages into temperatures, and calculated linear least squares values of  $A$  and  $B$  using an input value of  $D$ . An "empirical" TIP ( $= D - \chi_M^D$ ) value was derived through a computerized algorithm which minimized the sum of squared residuals with respect to  $D$  in a fit of the experimental data to



equation (7) and assuming a "known" value for  $\chi_M^D$ . The gram susceptibility data are collected in Tables C1 - C7 while a description of the apparatus is contained in Appendix D.

(b) Epr Data

The isotopic coupling constants for vanadium A<sup>V</sup> and phosphorus A<sup>P</sup> in the vanadyl complexes OV[S<sub>2</sub>PX<sub>2</sub>]<sub>2</sub> in solution at ambient temperatures were obtained as those values which reproduced the observed spectrum most closely on simulation using the computer program SAMESRLQ provided by Dr. R. E. D. McClung of this department.

(c) Precision of Results

Since the uncertainty in the magnetic susceptibility of the field calibrant used HgCo(NCS)<sub>4</sub><sup>52</sup> is ~0.5% and the uncertainties in temperature and positioning are estimated each to contribute ~0.1%, the total uncertainty in the static field magnetic susceptibility data is estimated to be ~1%. The reproducibility was observed to be within 0.5% on widely time separated determinations of the temperature dependent susceptibilities of different samples of HgCo(NCS)<sub>4</sub>.

Observable and significant changes in the simulated epr spectra of the complexes OV[S<sub>2</sub>PX<sub>2</sub>]<sub>2</sub> were observed for coupling constant changes of 0.1 gauss so that this is taken as the absolute uncertainty in the coupling constants obtained.

Electronic Spectral Data

The spectra obtained from a Cary 14 chart recording are plots of absorbance versus wavelength, both on linear scales. The manually digitized spectrum, concentration, and optical path length were input to the computer program BIGAUSS which produced a plot of



molar absorptivity vs wavenumber together with component peak parameters. This FORTRAN program was developed from an original ALGOL program obtained from Dr. J. P. Fackler, Case Western Reserve U., by Dr. R. G. Cavell. The program is listed in Appendix E.

The reliability of resolved band areas (and therefore oscillator strengths) are unknown and may be indeterminate up to a factor of five where overlap of peaks is large<sup>68</sup>. However band positions may be found with much more precision<sup>68</sup>. Solution concentrations were generally obtained from weights of samples known to four significant figures, however, intermediate dilutions, decomposition, evaporation of solvent, etc. reduce the confidence in which they are held to about 2%. Generally, the faith in numerical accuracy will be indicated by the number of figures expressed.

#### Units

Usually Gaussian or electrostatic units are used which are basically cgs units. Following C. K. Jorgensen<sup>64</sup>, spectral energies will be expressed in units or multiples of the "kayser" ( $K = \text{cm}^{-1}$ ,  $kK = 10^3 \text{ cm}^{-1}$ )<sup>5</sup>. Temperatures are presented in degrees Celsius ( $^{\circ}\text{C}$ ) or Kelvin ( $^{\circ}\text{K}$ ) where the latter notation is used to prevent confusion with "kaysers".

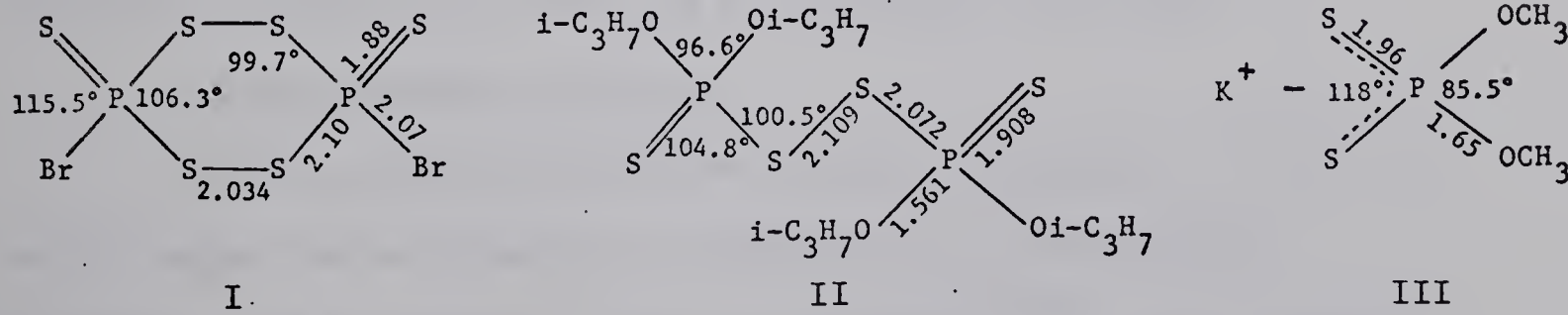


## CHAPTER 3

STRUCTURAL CONSIDERATIONS, INFRARED SPECTRA, AND SUBSTITUENT EFFECTS3.1 Information Based on Crystallographic Data

Knowledge of the crystal and molecular structures is crucial for the interpretation of physical and chemical properties of dithiophosphinates due to configurational variations observed in other dithioacid systems<sup>29,30</sup>. It has been suggested<sup>11,12</sup> that the strength (length) of the M-S and P-S bonds are related to the availability of the lone electron pairs on the sulfur atoms such that an increased P-S bond order leads to a reduced M-S bond order. Furthermore, the P-S bond order was thought<sup>11,12</sup> to be near unity making all the sulfur atom lone pairs available for bonding. Both inferences are in conflict with experimental results now available and a new interpretation is outlined below.

In discussing P-S bond orders it is useful to examine structures in which the P-S bonds may be well described in terms of single or double bond limits. Using data given by Pauling<sup>65</sup> the calculated double and single P-S bond lengths are 1.94 and 2.14 $\text{\AA}$ , respectively.





Structure I<sup>66</sup> is of particular general interest because of the skewed boat conformation, but in addition there is a clear difference between the isolated and ring P-S bond lengths. The difference in length between the isolated and chain P-S linkages in the dithiophosphoryl disulfide (diligand) of structure II<sup>40</sup> is only slightly less than for compound I. In view of the structural analogy between  $P_2S_6Br_2$  and cyclohexane it is notable that  $[S_2P(Oi-C_3H_7)_2]_2$  does not form a six-membered, planar, conjugated heterocycle analogous to benzene. The  $a_2$ -type symmetry of the upper occupied M.O. in the  $\pi_v$  system of the neutral, radical, half-dimer unit (see Figure 1.1) is wrong for aromatic ring formation. Structure III<sup>62</sup> of potassium dimethoxydithiophosphinate represents the only structure of a principally ionic dithiophosphinate salt. The sulfur atoms are not closely associated with a metal atom in compound III. An intermediate  $\pi$ -bond character is indicated by the equal P-S bond lengths in structure III which lie slightly less than mid-way between the extremes represented in structures I and II. In addition to the specific examples discussed (I-III) there have been a large number of structural determinations<sup>68</sup> which indicate that the lengths of isolated (double) P=S bonds lie in the range 1.85-1.96 $\text{\AA}$  while catenating (single) P-S bonds lie in the range 2.08-2.19 $\text{\AA}$ .

#### Tris Complexes $M[S_2PX_2]_3$

If an isolated and regular molecule  $M[S_2PX_2]_3$  in which all sulfur atoms are coordinating is considered as a three-bladed propeller with the chelate rings as the blades<sup>29,31a</sup>, then only two



angles are required to describe the angular distribution of S atoms about the central atom M. The two easily visualized angles used by Tomlinson<sup>31a</sup> are the SMS bond angle ( $\alpha$ ) within the chelate ring (i.e. the angle subtended by the "bite" of the bidentate ligand at the metal atom) and the torsional angle,  $\beta$ , between the plane of a chelate ring and a plane containing the molecular C<sub>3</sub> axis and the P atom of the chelate ring (i.e. the "twist" of the propeller blade). Since  $\beta$  is not usually directly accessible from published crystallographic data it was calculated herein from the angles  $\alpha$  and the trans SMS angle ( $\hat{S}MS^t$ ) using the equation

$$\sin \beta = \frac{\sqrt{3} \sin \alpha - \sqrt{3 \sin^2 \alpha + 12a(a+2c+1)}}{6a} \quad (8)$$

where  $a = \frac{\sin^2 \alpha}{2}$  and  $c = \cos(\hat{S}MS^t)$ . For a regular octahedron of S atoms,  $\alpha = 90^\circ$ ,  $\hat{S}MS^t = 180^\circ$ , so that  $\sin \beta = \frac{1}{\sqrt{3}} = 0.577$  and  $\beta = 35.3^\circ$ , while in the trigonal prismatic limit  $\beta = \sin \beta = 0$ . Thus for a complex lying between an octahedron and a trigonal prism,  $0 < \sin \beta < 0.577$ .

At present complete crystal and molecular structures of tris complexes have been determined only for Cr[S<sub>2</sub>P(CH<sub>3</sub>)<sub>2</sub>]<sub>3</sub> ( $\alpha_{av} = 82.7^\circ$ ,  $\hat{S}MS^t = 170.1^\circ$ )<sup>15</sup> and V[S<sub>2</sub>P(OC<sub>2</sub>H<sub>5</sub>)<sub>2</sub>]<sub>3</sub> ( $\alpha_{av} = 81.9^\circ$ ,  $\hat{S}MS^t = 164.9^\circ$ )<sup>28</sup> leading to values for  $\sin \beta$  of 0.501 and 0.477, respectively, i.e.  $\beta = 30.0^\circ$  and  $28.5^\circ$ . The X-ray powder patterns of V[S<sub>2</sub>P(CH<sub>3</sub>)<sub>2</sub>]<sub>3</sub> and Co[S<sub>2</sub>P(OC<sub>2</sub>H<sub>5</sub>)<sub>2</sub>]<sub>3</sub> and In[S<sub>2</sub>P(OC<sub>2</sub>H<sub>5</sub>)<sub>2</sub>]<sub>3</sub> are reported<sup>31</sup> to be isostructural with V[S<sub>2</sub>P(OC<sub>2</sub>H<sub>5</sub>)<sub>2</sub>]<sub>3</sub>. These results indicate that tris dithiophosphinato complexes are only slightly



distorted towards a trigonal prism of sulfur atoms and are thus representative of  $D_3$  symmetry. The consequent potential of optical isomerism was not mentioned in the discussion of the structural determination of  $V[S_2P(OC_2H_5)_2]_3^{28}$ , but the resolution of atomic positions in the crystal of  $Cr[S_2P(CH_3)_2]_3$  studied was improved by assuming the presence of one enantiomer<sup>15</sup>.

It is considered significant (*vide infra*) that the P-S bond lengths are shorter for the ethoxy substituted complex than for the methyl substituted complex (Table 3.1) although a distinction between the M-S bond lengths is not meaningful within the precision of the numbers obtained. The P-S bond lengths of both complexes indicate some  $\pi$  character.

#### Tetrahedral bis Complexes $M[S_2PX_2]_2$

X-ray powder patterns of the complexes  $M[S_2P(CH_3)_2]_2$  with  $M = Mn, Fe, Co$ , and  $Zn$  indicate that they are isostructural as are  $Cd[S_2P(CH_3)_2]_2$  and  $Hg[S_2P(CH_3)_2]_2$ , however, comparison between the two sets was uncertain due to intensity differences introduced by the larger metal atoms in the latter complexes. The structural determination<sup>15</sup> of  $Co[S_2P(CH_3)_2]_2$  has shown that it is polymeric consisting of infinite independent chains of Co atoms linked by opposed pairs of bridging ligands alternating by  $90^\circ$  and each chain lying along a two-fold screw axis as illustrated in Figure 3.1. This structure is similar to that observed<sup>44</sup> for complexes of the oxyacids  $HO_2PX_2$ , but is in notable contrast to the isostructural compounds  $Zn[S_2P(C_2H_5)_2]_2$  and  $Co[S_2P(C_2H_5)_2]_2$  which were determined<sup>26</sup> to exist in two crystallographically non-equivalent doubly bridged dimeric



TABLE 3.1  
Structural Parameters<sup>a</sup>

Chromophore	Complex	M-S	Y-S	Y-X	ŜMS	M̂SY	ŜYS	X̂X	Ref.
MS <sub>6</sub> (~octahedral)	V[S <sub>2</sub> P(OC <sub>2</sub> H <sub>5</sub> ) <sub>2</sub> ] <sub>3</sub>	2.45	1.982	1.58	81.8	85.3	108.1	95.3	28
	Cr[S <sub>2</sub> P(CH <sub>3</sub> ) <sub>2</sub> ] <sub>3</sub>	2.44	2.011	1.813	82.74	85.24	106.20	106.0	15
	Co[S <sub>2</sub> P(CH <sub>3</sub> ) <sub>2</sub> ] <sub>2</sub> <sup>b</sup>	(2.32)	(2.016)	1.813	-	(109.46)	(107.03)	105.2	15
	Zn[S <sub>2</sub> P(C <sub>2</sub> H <sub>5</sub> ) <sub>2</sub> ] <sub>2</sub>	2.34	2.02	1.86	86.0	82.1	109.6	103.0	26
	Zn[S <sub>2</sub> P(OC <sub>2</sub> H <sub>5</sub> ) <sub>2</sub> ] <sub>2</sub>	2.36	1.99	1.57	85.9	82.0	109.7	94.5	27
	Zn[S <sub>2</sub> P(Oi-C <sub>3</sub> H <sub>7</sub> ) <sub>2</sub> ] <sub>2</sub>	2.34	1.970	1.58	85.5	82.0	109.7	94.9	24
	Cd[S <sub>2</sub> P(Oi-C <sub>3</sub> H <sub>7</sub> ) <sub>2</sub> ] <sub>2</sub>	2.53	1.965	1.58	79.1	83.9	112.2	95.2	24
	Hg[S <sub>2</sub> P(Oi-C <sub>3</sub> H <sub>7</sub> ) <sub>2</sub> ] <sub>2</sub>	2.39 2.82	2.02 1.94	1.62 1.53	76.3	91.6 79.7	112.1	94.6	25
	Ni[S <sub>2</sub> P <sub>2</sub> (CH <sub>3</sub> ) <sub>4</sub> N] <sub>2</sub>	2.28	2.02	1.58 <sup>c</sup>	109.5	104.6		107.6 <sup>d</sup>	48
	Ni[S <sub>2</sub> P(CH <sub>3</sub> ) <sub>2</sub> ] <sub>2</sub>	2.236	2.01	1.81	87.7	85.8	101.3	104.9	20
MS <sub>4</sub> (~tetrahedral)	Ni[S <sub>2</sub> P(C <sub>2</sub> H <sub>5</sub> ) <sub>2</sub> ] <sub>2</sub>	2.23	2.00	1.84	87.6	86.1	100.2	101.7	29
	Ni[S <sub>2</sub> P(C <sub>6</sub> H <sub>5</sub> ) <sub>2</sub> ] <sub>2</sub>	2.238	2.01	1.78	88.3	85.2	101.3	107.2	21
	Ni[S <sub>2</sub> P(OC <sub>2</sub> H <sub>5</sub> ) <sub>2</sub> ] <sub>2</sub>	2.222	1.986	1.563	88.3	84.5	102.7	95.9	22
	Ni[S <sub>2</sub> P(OC <sub>2</sub> H <sub>5</sub> ) <sub>2</sub> ] <sub>2</sub>	2.233	1.990	1.575	88.5	84.2	103.1	96.6	23
	Ni[S <sub>2</sub> CNH <sub>2</sub> ] <sub>2</sub>	2.21	1.69	1.38	78.5	84.8	112		29,30
	Ni[S <sub>2</sub> CN(C <sub>2</sub> H <sub>5</sub> ) <sub>2</sub> ] <sub>2</sub>	2.202	1.706	1.33	79.2	85.0	110.6		29,30
	Ni[S <sub>2</sub> CNCN] <sub>2</sub> <sup>-2</sup>	2.188	1.72	1.29	79.2	86.2	108		29,30
	Ni[S <sub>2</sub> CS] <sub>2</sub> <sup>-2</sup>	2.21	1.70	1.68	76.9	87.9	107.3		29,30
	Ni[S <sub>2</sub> CO(C <sub>2</sub> H <sub>5</sub> ) <sub>2</sub> ] <sub>2</sub>	2.235	1.69	1.38	79.5	82.2	116		29,30
	Ni[S <sub>2</sub> C <sub>2</sub> (CN) <sub>2</sub> ] <sub>2</sub> <sup>-2</sup>	2.166	1.75		91.5	103.8			29,30
OVS <sub>4</sub> (~square pyramidal)	OV[S <sub>2</sub> P(CH <sub>3</sub> ) <sub>2</sub> ] <sub>2</sub> <sup>e</sup>	2.419	2.014	1.810	85.2	84.51	105.11	106.4	15

<sup>a</sup> Parameters for ligands forming closed chelate rings with one metal atom. Y = P or C, X = substituent(s) on Y. Bond lengths in angstroms, bond angles in degrees.

<sup>b</sup> Crystal does not contain any non-bridging ligands.

<sup>c</sup> P-N bond length.

<sup>d</sup> SPN = 116.6°.

<sup>e</sup> OV bond length is 1.583 Å.



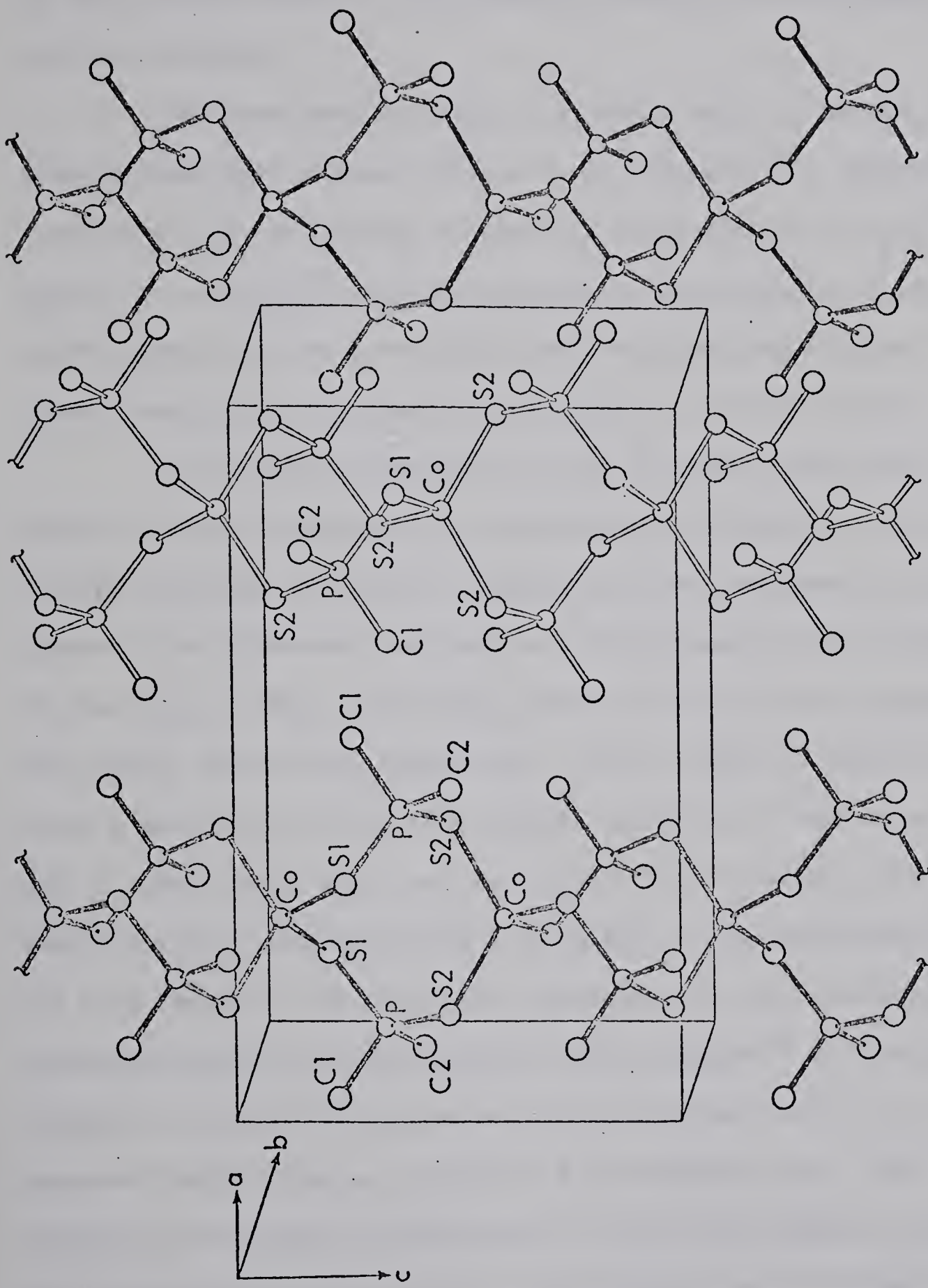


FIGURE 3.1: The crystal structure of  $\text{Co}[\text{S}_2\text{P}(\text{CH}_3)_2]^2$ .



conformations. A bridged dimeric unit may be compared to one link of the infinite chain of  $\text{Co}[\text{S}_2\text{P}(\text{CH}_3)_2]_2$  capped by non-bridging terminal ligands.

The complexes of Zn(II) and Cd(II) with  $\text{X} = \text{O}-\text{C}_3\text{H}_7$  also contain "one-link" dimers, which are all equivalent<sup>24</sup>. However, a different type of linkage is found in the Zn(II),  $\text{X} = \text{OC}_2\text{H}_5$ <sup>27</sup> and Hg(II),  $\text{X} = \text{O}-\text{C}_3\text{H}_7$ <sup>25</sup> complexes where each metal atom is coordinated by sulfur atoms from one non-bridging and two branching bridging ligand groups resulting in the formation of infinite zig-zag chains.

The relative importance of the electronic and steric effects of the substituents in determining the formation of a particular structure or type of bridging in these complexes is not clear. However, the difference in electronic substituent effects between  $\text{CH}_3$  and  $\text{C}_2\text{H}_5$  or  $\text{OC}_2\text{H}_5$  and  $\text{O}-\text{C}_3\text{H}_7$  cannot be very large, implying that steric effects are significant. Such a range of ligand functions makes a comparison of M-S bond lengths exceedingly complicated even with a common metal atom, but as with the tris complexes, the more electronegative substituents are consistently associated with shorter P-S bond lengths. The structural parameters of the tetrahedral tetramethylimidodithiodiphosphinato Ni(II) complex<sup>48</sup> are included for comparison purposes to emphasize the constraining nature of a four-membered chelate ring as opposed to a six-membered one. The unexpected tetrahedral coordination of this latter compound must be intimately connected with the "odd" property of the ligand in conjunction with the nearly tetrahedral MSP bond angle.

An X-ray powder pattern of blue  $\text{CoOS}_3\text{P}_2(\text{CH}_3)_4$  shows that



this complex is isostructural with green  $\text{Co}[\text{S}_2\text{P}(\text{CH}_3)_2]_2$  as confirmed<sup>69</sup> by a more detailed X-ray examination of the blue complex. Non-observation of the O atoms is indicative of a random distribution in contrast to the monothiophosphinates of Zn(II) and Cd(II) with X = n-C<sub>4</sub>H<sub>9</sub> and C<sub>6</sub>H<sub>5</sub> which consist<sup>43</sup> of triply-bridged, dinuclear units, "beads", connected by a "thread" of bridging ligands and in which the O/S ratio in the coordination sphere of the metal atoms alternates from 3:1 to 1:3.

#### Planar bis Complexes M[S<sub>2</sub>PX<sub>2</sub>]<sub>2</sub>

An extensive series of crystal structures (Table 3.1) is available for Ni[S<sub>2</sub>PX<sub>2</sub>]<sub>2</sub> complexes. No crystal structures have been reported for Pt(II) dithiophosphinates but the palladium and platinum complexes with X = CH<sub>3</sub> yield superimposable X-ray powder patterns which are quite different from the cadmium and mercury complexes with the same ligands. The complex Pd[S<sub>2</sub>P(OC<sub>2</sub>H<sub>5</sub>)<sub>2</sub>]<sub>2</sub> is both reported to be isostructural<sup>23a</sup> and not isomorphous<sup>70</sup> with its nickel analogue. The crystal structures of the nickel complexes are consistent in showing<sup>29</sup> that the ligand groups are all bidentate and nonbridging such that the molecules are required to possess either a crystallographic center of symmetry or at least a twofold symmetry axis.

From the data collected in Table 3.1 it is reasonably clear for at least the Ni(II) series of dithiophosphinates that both the M-S and P-S bond lengths are shorter for the more electronegative substituents. Thus a strong M-S bond does not imply a weak P-S bond or vice versa. The existence of metal-ligand π-type



bonding in these planar complexes is supported by an increase of the Ni-S bond lengths ( $X = C_6H_5^{71}$ ,  $OC_2H_5^{72}$ ) upon trans coordination by two pyridine molecules. It is notable that the M-S bond lengths in the adducts ( $\sim 2.50\text{\AA}^{71,72}$ ) are of the same order of magnitude as observed in tris complexes of Cr(III)<sup>15</sup> and V(III)<sup>28</sup> while the intraligand bond lengths are essentially unchanged from those in the original complex. However, the SPS and XPX bond angles in the adduct  $Ni[S_2P(OC_2H_5)_2]_2 \cdot 2(NC_5H_5)$  appear to approach more closely the ligand anion bond angles of structure III above.

A preliminary single crystal X-ray examination<sup>69</sup> of the complex  $Pt_2S_6P_4(CF_3)_8$  has confirmed its dinuclear formulation. The coordination geometry about each Pt atom is most probably planar.

#### Pyramidal bis Complexes $OV[S_2PX_2]_2$

The only crystal and molecular structure available of an oxovanadium(IV) dithiophosphinate complex has been that of  $OV[S_2P(CH_3)_2]_2^{15}$  which is illustrated in Figure 3.2. The crystal is composed of discrete molecules stacked so as to apparently preclude direct or superexchange magnetic interaction between the V atoms. Similarity of electronic spectra (Chapter 6) and normal solid state magnetism (Chapter 5) of the blue complexes with  $X = CH_3$ ,  $C_6H_5$  and  $OC_2H_5$  and the black colors of the complexes with  $X = F$  and  $CF_3$  of similar but anomalous magnetism reasonably indicate different solid state structures between the two color sets but possible similarity within each set. Both  $OV[S_2PF_2]_2$  and  $OV[S_2P(CF_3)_2]_2$  were observed to undergo a reversible color change from black to blue when



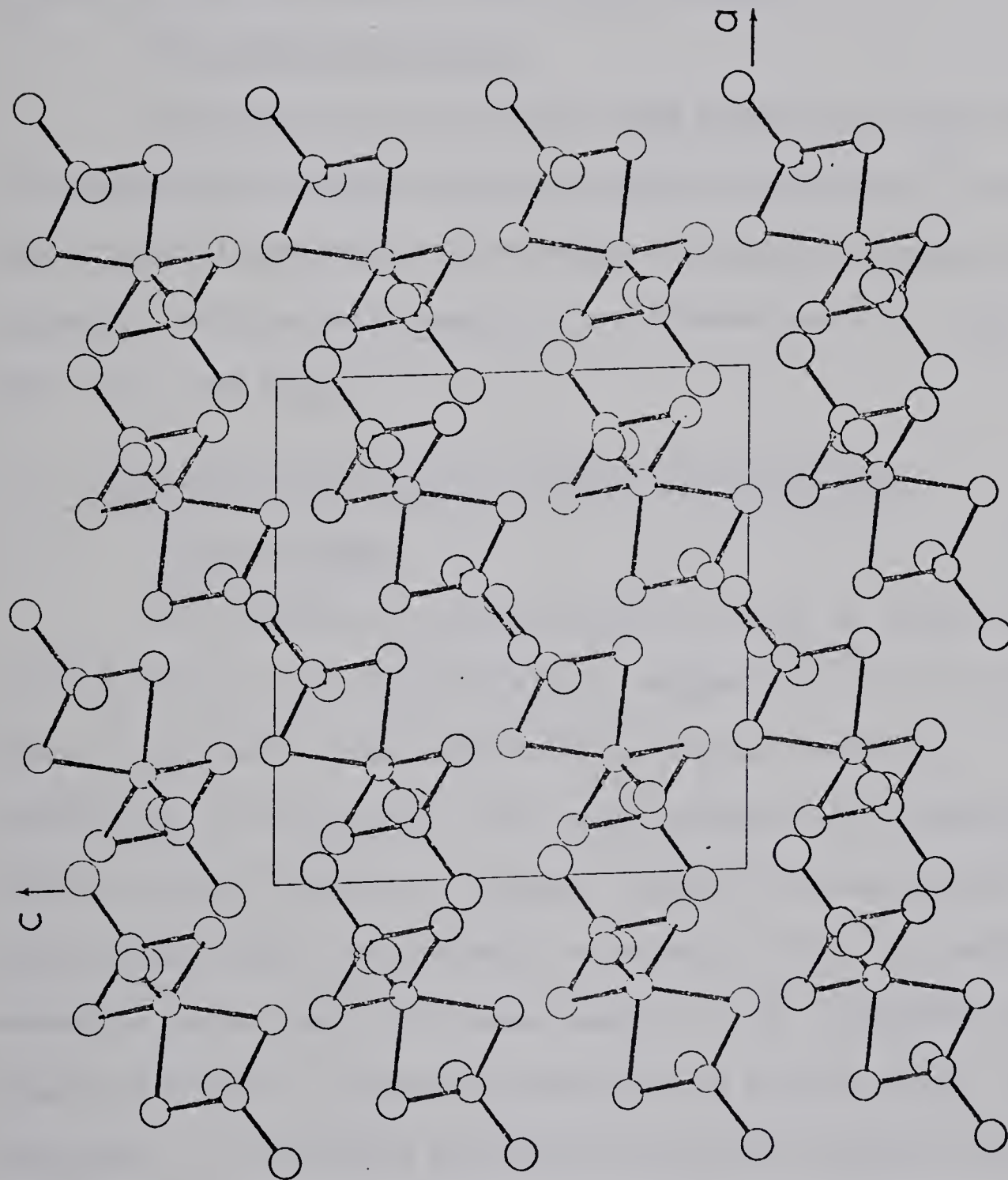


FIGURE 3.2: The crystal structure of  $\text{OV}[\text{S}_2\text{P}(\text{CH}_3)_2]^2$ .



sublimed in vacuo with strong heating. It is believed herein that the color change to blue is due to the formation of a metastable "normal" solid state crystal phase of structure similar to that of the blue complexes with  $X = \text{CH}_3$ ,  $\text{C}_6\text{H}_5$ , or  $\text{OC}_2\text{H}_5$ .

### M(I) Complexes $\text{MS}_2\text{PX}_2$

No crystal structures have been reported for this class of compound but solution molecular weight determinations<sup>73</sup> indicate that the Cu(I) compounds are tetramers, the Ag(I) compounds are polymeric, and the Au(I) compounds are dimeric where  $X = \text{C}_2\text{H}_5$ ,  $\text{C}_3\text{H}_7$ ,  $\text{C}_4\text{H}_9$ ,  $\text{C}_6\text{H}_5$ , and  $\text{OC}_2\text{H}_5$ .

### 3.2 Structural Inferences for Solution and Gas Phases

#### Tris Complexes

The packing of discrete molecular units in single crystals of  $\text{Cr}[\text{S}_2\text{P}(\text{CH}_3)_2]_3$  and  $\text{V}[\text{S}_2\text{P}(\text{OC}_2\text{H}_5)_2]_3$  suggest that the tris complexes should be monomeric when freed from the crystal lattice by dissolution or vaporization. The tris complexes were generally found to readily dissolve in organic solvents and measurements have demonstrated them to be monomeric in solution (Table 2.1) while monomeric parent ions in the mass spectra of the thermally stable complexes support a monomeric formulation in the gas phase. General similarity of the diffuse reflectance electronic spectra with those obtained from solutions (Chapter 6) is strong evidence for retention of coordination geometry through the phase transitions. Attempts to determine optical rotatory effects in chloroform solutions prepared from single crystals of  $\text{Cr}[\text{S}_2\text{P}(\text{CH}_3)_2]_3$ ,  $\text{Cr}[\text{S}_2\text{P}(\text{C}_6\text{H}_5)_2]_3$ ,



and  $\text{Cr}[\text{S}_2\text{P}(\text{OC}_2\text{H}_5)_2]_3$  were uniformly unsuccessful. Although rapid racemization in solution, unresolved enantiomers in the crystals, or inherently small specific rotations may account for the negative observations it is noted that the molar absorptivities of the ligand field bands of Cr(III) dithiophosphinates are some 6000 times as large as those of the tris ethylene-diammine Cr(III) complex<sup>74</sup>. Hence, at concentrations sufficiently small to observe the absorption spectrum the rotations would become negligible even assuming reasonably large specific rotations.

#### Tetrahedral Bis Complexes

Although dialkyldithiophosphinate complexes are usually quite soluble in organic solvents<sup>13</sup>, the tetrahedral bis complexes  $\text{M}[\text{S}_2\text{PX}_2]_2$  with  $\text{X} = \text{CH}_3$  and  $\text{C}_6\text{H}_5$  proved too insoluble in all common organic solvents for solution molecular weight determinations. Thus the degree of molecular aggregation in solutions of these latter complexes remains unknown. Where  $\text{X} = \text{C}_2\text{H}_5$  and  $\text{C}_3\text{H}_7$ , the complexes were monomeric up to  $10^{-2}$  M concentrations in benzene<sup>75</sup>. Since  $\text{Zn}[\text{S}_2\text{P}(\text{OC}_2\text{H}_5)_2]_2$  is polymeric in the solid state but monomeric in solution<sup>27</sup>, it is assumed that isostructural  $\text{Co}[\text{S}_2\text{P}(\text{OC}_2\text{H}_5)_2]_2$  should behave similarly. Due to the similar crystal structures within the  $\text{X} = \text{CH}_3$  series with Mn, Fe, Co, and Zn it is anticipated that the complexes of the same metals within the  $\text{X} = \text{F}$  series should also be isostructural. Since  $\text{Mn}[\text{S}_2\text{PF}_2]_2$  is the least volatile member of the  $\text{X} = \text{F}$  series and has been shown<sup>18</sup> to be monomeric in a  $3.4 \times 10^{-2}$  M 1,2-dichloroethane solution the remaining members are



assumed to be monomeric at similar concentration levels. The volatility and ready solubilities of the  $X = CF_3$  complexes suggests behavior parallel to that in the  $X = F$  series. Where the degree of association has been investigated, it was found<sup>13</sup> to be nearly independent of temperature between 37 and 60°C and decreased with the solvent order  $CCl_4 > C_6H_6 > CHCl_3$ . Molecular association is anticipated to be even further reduced in  $CH_2Cl_2$  solutions. The diffuse reflectance spectra of  $Co[S_2P(CH_3)_2]_2$  and  $Co[S_2P(C_6H_5)_2]_2$  were quite similar to their solution spectra with respect to band positions which would be expected on retention of approximate tetrahedral coordination of the  $Co^{+2}$  ion whatever the degree of polymerization. All the tetrahedral bis dithiophosphinates studied herein appear to behave as monomers in the mass spectrometer.

#### Planar Bis Complexes

The ready solubilities and measured solution molecular weights (Table 2.1) together with a vapor density measurement<sup>18</sup> of  $Ni[S_2PF_2]_2$  at 160°C and the mass spectra (Chapter 4) indicate that these complexes as a class are monomeric in both organic solution and vapor phases. This behavior is consistent with the molecular packing revealed in the crystal structures. General agreement between the diffuse reflectance and solution electronic spectra (Chapter 6) suggests that the planar coordination geometry is retained through phase transitions.

Due to the immense mass (1258 a m u ) of the unit  $Pt_2S_6P_4(CF_3)_8$  an attempted solution molecular weight measurement<sup>58</sup> only demonstrated that the molecular weight of the species in



solution exceeded 1000. The mass spectrum<sup>56</sup> (Chapter 4) indicated retentions of the dinuclear structure in the vapor phase.

### Pyramidal Bis Complexes

The blue vanadyl complexes  $\text{OV}[\text{S}_2\text{PX}_2]_2$  with  $\text{X} = \text{CH}_3$ ,  $\text{C}_6\text{H}_5$ , or  $\text{OC}_2\text{H}_5$  showed no marked color changes upon dissolution in non-polar organic solvents but the black complexes with  $\text{C} = \text{F}$  or  $\text{CF}_3$  dissolved in the same solvents to give respectively mauve and purple colored solutions. The electronic spectra of the complexes in solution are reasonably similar (Chapter 6) which in conjunction with the monomeric behavior of the  $\text{X} = \text{CH}_3$  and  $\text{C}_6\text{H}_5$  compounds (Table 2.1) suggest a general monomeric existence in solution.

Magnetic susceptibility measurements<sup>55</sup> on solutions of the F and  $\text{CF}_3$  substituted compounds indicated that the interaction responsible for the magnetic anomaly in the solid state is removed on dissolution. All these vanadyl complexes behave as monomers in the mass spectrometer (Chapter 4).

### 3.3 Infrared Spectra

The qualitative inverse relationship between bond lengths and vibrational frequencies is now empirically well established<sup>76</sup>. Thus for a homologous series of complexes  $\text{M}[\text{S}_2\text{PX}_2]_n$  varying only in X, it might be anticipated that vibrational frequency changes within the skeleton  $\text{M}(\text{S}_2\text{P})_n$  consisting of only M-S and P-S linkages would reflect structural differences. However, the M-S and P-S bonds are bases for the same representations and have at least one representation in common with the P-X bonds in all molecules



of  $C_{2v}$  and higher point group symmetry. Hence these bonds participate in concerted vibrations which are assigned as a first approximation to the linkage making the greatest energetic contribution.

Much effort has been expended in attempting to define the spectral regions in which bands due principally to P-X, P-S, and M-S vibrations may be expected. Corbridge<sup>77</sup> has summarized much of the present knowledge concerning  $P-X_n$  and  $P-S_n$  group vibrations.

Adams and Cornell<sup>70</sup> have assigned M-S vibrations in the range 190-330K and P-S vibrations in the range 532-640K for an extensive series of tris, tetrahedral bis, and planar bisdiethoxydithiophosphinates.

Nyquist<sup>78</sup> has reported a detailed analysis of the vibrational spectra of the acid  $HS_2P(OC_2H_5)_2$ . Kuchen and Hertel<sup>13</sup> define the frequency ranges 556-591K for  $\nu_{as}(PS_2)$  and 476-497K for  $\nu_s(PS_2)$  from a study of dialkyldithiophosphinates. Müller, et al.<sup>36,38</sup> investigated an extensive series of diphenyldithiophosphinates and found  $\nu_{as}(PS_2)$  in the range 619-650K,  $\nu_s(PS_2)$  in the range 523-578K while M-S vibrations were assigned to the region 251-345K on the basis of the metal ion dependence of the band positions. These latter authors postulate that the mean frequency  $\frac{1}{2}[\nu_{as}(PS_2) + \nu_s(PS_2)]$  should be similar for the acid  $HS_2PX_2$ , anion  $S_2^-PX_2$ , and the complexes  $M[S_2PX_2]_n$  and further estimate that the M-S bond order is less than unity from simple "two-mass" model force constant calculations.

Coates and Mukherjee<sup>79</sup> found the regions 585-606K and 493-505K to respectively contain the  $\nu_{as}(PS_2)$  and  $\nu_s(PS_2)$  group vibrations of dimethyldithiophosphinates.



Due to their more recent discovery the vibrational spectra of  $M[S_2PF_2]_n$  and  $M[S_2P(CF_3)_2]_n$  complexes have not received as much attention as their alkyl, aryl, and alkoxy substituted precursors. Tebbe and Muetterties<sup>18</sup> assigned only P-F stretching frequencies in their report on  $M[S_2PF_2]_n$  complexes, however, detailed assignments of the vibrational spectra of  $HS_2PF_2$  and  $CsS_2PF_2$  have been carried out by Mitchell et al.<sup>16b</sup> and were used herein as guides for the present assignments for these complexes. Similarly an assignment of the ir spectrum of the acid  $HS_2P(CF_3)_2$  has been made by Gosling and Burg<sup>17a</sup> upon which the assignments for the ir spectra of the  $M[S_2P(CF_3)_2]_n$  complexes have been based.

Since the  $M(S_2P)_n$  skeletal vibrations are of primary interest in this study, the  $PX_2$  group vibrational bands are relegated to Appendix A. For reference purposes and a test of the constancy of the mean  $PS_2$  group stretching frequencies, the assigned values of  $\nu_{as}(PS_2)$  and  $\nu_s(PS_2)$  with their mean values for the acids and ionic salts used in this study are listed in Table 3.2. Group theoretical considerations predict three infrared active fundamental M-S and P-S vibrations for the tris and pyramidal bis dithiophosphinates while only two of each are predicted for the tetrahedral and planar bis complexes. The M-S and P-S vibrational band assignments for the infrared spectra are given in Tables 3.3-3.6. The profusion of bands occurring in the range 200-400K in some cases and variable intensities make the assignment of M-S vibrations exceedingly difficult. Nevertheless an attempt was made to identify the bands of highest frequency and/or intensity which could be attributed to the same



TABLE 3.2

Infrared Spectral Band Assignments for the  $\text{PS}_2$  Group Stretching  
 Frequencies in the Acids  $\text{HS}_2\text{PX}_2$  and Their Salts

X	Compound	$\nu_{\text{P-S}} \text{as}$ (K)	$\nu_{\text{P-S}} \text{s}$ (K)	$\frac{1}{2}(\nu_{\text{P-S}} \text{as} + \nu_{\text{P-S}} \text{s})$ (K)
$\text{CH}_3$	$\text{HS}_2\text{P}(\text{CH}_3)_2$ <sup>a,b</sup>	608m	462m	535
	$\text{NaS}_2\text{P}(\text{CH}_3)_2$ <sup>c</sup>	606s	505s	555
	$\text{CsS}_2\text{P}(\text{CH}_3)_2$ <sup>c,d</sup>	606vs	505vs	555
	$\text{Al}[\text{S}_2\text{P}(\text{CH}_3)_2]_3$ <sup>c,d</sup>	601s (581s)	501m	551
$\text{C}_6\text{H}_5$	$\text{HS}_2\text{P}(\text{C}_6\text{H}_5)_2$ <sup>e</sup>	650s	530s	590
	$\text{NaS}_2\text{P}(\text{C}_6\text{H}_5)_2$ <sup>e</sup>	648s	565s	606
	$\text{NH}_4\text{S}_2\text{P}(\text{C}_6\text{H}_5)_2$	642vs	561vs	601
$\text{OC}_2\text{H}_5$	$\text{HS}_2\text{P}(\text{OC}_2\text{H}_5)_2$ <sup>a</sup>	655s	540m	597
	$\text{NaS}_2\text{P}(\text{OC}_2\text{H}_5)_2$ <sup>c</sup>	681s	560m	620
F	$\text{HS}_2\text{PF}_2$ <sup>f,g</sup>	725vs	531s	628
	$\text{CsS}_2\text{PF}_2$ <sup>c,g</sup>	722vs	561s	641
$\text{CF}_3$	$\text{HS}_2\text{P}(\text{CF}_3)_2$ <sup>b,f</sup>	731s	522m	626
	$\text{NaS}_2\text{P}(\text{CF}_3)_2$ <sup>c,h</sup>	719vs	535m	627

<sup>a</sup>  $\text{CS}_2$  solution ( $\sim 10\%$  by weight).

<sup>f</sup> Vapor.

<sup>b</sup> Reference 80.

<sup>g</sup> Reference 20b.

<sup>c</sup> Nujol mull.

<sup>h</sup> Reference 81.

<sup>d</sup> Reference 79.

<sup>e</sup> Reference 39.



TABLE 3.3

Infrared Spectral Band Assignments for the M-S and P-S Stretching Frequencies in the Tris Complexes  $M[S_2PX_2]_3^a$

X	M	$\nu_1(\text{PS})$	$\nu_2(\text{PS})$	$\nu_3(\text{PS})$	$\frac{1}{2}[\nu_1(\text{PS}) + \nu_3(\text{PS})]$	$\nu_{1-3}(\text{MS})^b$
$\text{CH}_3$	V	592s	585s	505s	548	359m, <u>305msh</u> , <u>296s</u> , 267m, 238w
	Cr	590s	585sh	505s	547	314s, <u>308ssh</u> , <u>288w</u> , 271m, 241w
	Co	592wsh	580s	510m	551	<u>305s</u> , <u>279s</u> , 267msh, 235w
$\text{C}_6\text{H}_5$	V	641m	612m	567s	604	<u>280s</u> , 207w
	Cr	640s	610s	570s	605	<u>316ssh</u> , <u>305s</u> , 287sh, ?
	Fe	639s	609m	569s	604	301s, 264m, ?
$\text{OC}_2\text{H}_5$	Co	640w	607w	573s	606	<u>316vw</u> , <u>302w</u> , 243w, ?
	V	663s	642sh	(549m, 536m)	606-599	<u>295s</u> , 212w
	Cr	658s	642s	(550w, 536m)	604-597	<u>315s</u> , ?
F	Co	646wsh	629m	(555wsh, 541m)	600-593	<u>307m</u> , ?
	V	694	694msh	558m	626	302msh, <u>294s</u>
	Cr	695s	695s	559s	627	<u>316s</u>
$\text{CF}_3$	Co	684m	?	564m	624	<u>309m</u> , ?
	V	689s	615s	540s	614	285s, <u>273s</u> , 210w
	Cr	683s	618s	539s	611	<u>307s</u> , <u>286sh</u> , 240w
	Fe	695sh	?	534m	614	-
	Co	611m	?	533m	597	320w, <u>297w</u> , ?

<sup>a</sup> Nujol mulls.

<sup>b</sup> Underlined bands are presumed to be attributable to the same M-S vibrational mode.



TABLE 3.4

Infrared Spectral Band Assignments for the M-S and P-S Stretching Frequencies in the  
Tetrahedral Bis Complexes  $M[S_2PX_2]_2^a$

X	M	$\nu_1$ (PS)	$\nu_2$ (PS)	$\frac{1}{2}[\nu_1$ (PS)+ $\nu_2$ (PS)]	$\nu$ (MS)	?
$CH_3$	Mn	590s	495s	542	(324msh, 215s, 204ssh, 299ssh, 281msh)	
	Fe	578s	488s	533	(333m, 314s, 307ssh, 285w, 212msh, 204s)	
	Co	578s	490m	534	(336msh, 326s, <u>314s</u> , 287w, 214wsh, 202s)	
	Zn	583s	495m	539	(331msh, 325m, 315wsh, 306wsh, 301w, 287w, 276wsh)	
	Cd	585s	496m	540	(312s, 302sh, 288m, 279m)	
	Hg	583s	493s	538	(318wsh, 312w, 304w, 284wsh, 271w)	
$C_6H_5$	Mn	634s	564s	599	(316s, 288m, 267m, 240w)	
	Fe	636m	565s	600	(317w, 300m, 277w, 231w)	
	Co	634s	564s	599	(323m, 301m, 284m, 240m, 231w)	
	Zn	640s	563s	601	(328w, 302m, 274m, 254m)	
	Cd	636s	568s	602	(327w, 282s, 260s, 255ssh, 241wsh)	
	Hg	633s	566s	599	(315wsh, 302m, 259w, 241m, 230m)	
$OC_2H_5$	Co	661s(640msh)	539m	600	(313m, ? )	
	Zn	688s(649msh)	541m	604	(310m, ? )	
	Hg <sup>b</sup>	658sh(637s)	548wm	603	(318w, 280vs,br, 239sh)	
F	Mn	720s(699s)	550m	635	(320w, 285w)	
	Fe	718ssh(702s)	559m	638	(311w )	
	Co	715vs	559m	637	(314w )	
	Zn	704vs(697ssh)	558m	631	-	
$CF_3$	Mn	696s(686msh)	541m	618	(328w, 285s)	
	Fe	691s(679msh)	541m	616	(305w, 286w)	
	Co	665w ?	538m	(601)	(311w, 288m, 277w)	
	Zn	691s	541m	616	(337w, 325w, 306w, 289w, 260w)	
	Cd	680ssh(673s)	533m	606	-	
	Hg	675s(664ssh)	536m	605	(335w, 297s, 284wsh, 263w, 246w, 200w)	

<sup>a</sup> Nujol mulls.

<sup>b</sup> Reference 70.



TABLE 3.5

Infrared Spectral Band Assignments for the M-S and P-S Stretching Frequencies  
in the Planar Bis Complexes  $M[S_2PX_2]_2$ <sup>a</sup>

X	M	$\nu_1$ (PS)	$\nu_2$ (PS)	$\frac{1}{2}[\nu_1$ (PS)+ $\nu_2$ (PS)]	$\nu(MS)$ <sup>b</sup>
$CH_3$	Ni	586s	513s		
	Pd	576s	506s		<u>347s</u> , 283m, 271m
	Pt	568s	502s		<u>309s</u> , 283m, 268m
$C_6H_5$	Ni	625m	576s		<u>300s</u> , 267m
	Pd	621m	573s		
	Pt	616m	565s		
$OC_2H_5$	Ni	640s	546m		
	Pd	625s	534m		<u>354s</u> , 332wsh, 326w
	Pt	623s	530m		<u>311s</u> , 305msh
F	Ni	703s	570m		<u>304s</u> , 290wsh
	Pd	688s	561m		
	Pt	688s	557m		
$CF_3$	Ni	685s	(537msh, 534m)	610	
	Pd	671m	(538m, 534msh)	604	<u>334s</u> , 332ssh, 284wsh, 278s <u>303s</u> , 279w

a Nujol mulls.

b Underlined  $\nu(MS)$  bands are presumed to be attributable to the same vibrational mode.



TABLE 3.6

Infrared Spectral Band Assignments for the M-S, P-S and V-O Stretching Frequencies in the Vanadyl Bis Complexes  $\text{OV}[\text{S}_2\text{PX}_2]_2$ <sup>a</sup>

X	$\nu(\text{VO})$	$\nu_1(\text{PS})$	$\nu_2(\text{PS})$	$\nu_3(\text{PS})$	$\nu(\text{MS})$ <sup>b</sup>
$\text{CH}_3$	991s	596s	?	503s	<u>365vs</u> , <u>358vs</u> , <u>343s</u> , <u>297w</u> <u>290w</u> , <u>276mw</u> , <u>267mw</u> , <u>238mw</u>
$\text{C}_6\text{H}_5$	998s	639m	612m	568s	<u>361m</u> , <u>340m</u> , <u>330w</u> , <u>230w</u>
$\text{OC}_2\text{H}_5$	(obscured) <sup>c</sup>	650s	?	530s	<u>367s</u> , <u>300m</u> , <u>200w</u>
F	(1024s) <sup>d</sup>	700s	695sh	560m	<u>377sh</u> , <u>370m</u> , <u>355m</u> , <u>335mw</u> , <u>307w</u> , <u>294w</u> , <u>283w</u> , <u>260w</u>
$\text{CF}_3$	(1023s) <sup>d</sup>	692ms	682m	538ms	<u>382mw</u> , <u>356ms</u> , <u>317w</u> , <u>286m</u> , <u>277m</u> , <u>205w</u>

<sup>a</sup> Nujol nulls.

<sup>b</sup> Underlined  $\nu(\text{MS})$  bands are presumed to be attributable to the same vibrational mode.

<sup>c</sup> Strong P-O stretching bands occur in this region.

<sup>d</sup> Free V-O stretching bands resulting from dissolution of the complex in  $\text{CS}_2$ <sup>41</sup>.

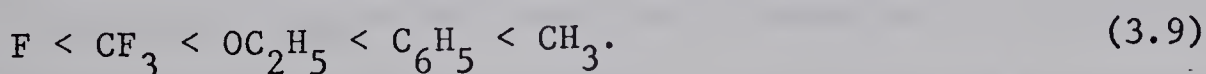


M-S vibrational mode.

Corbridge<sup>77</sup> has noted that  $\nu_{as}(PO_2)$  of phosphinates is more sensitive than  $\nu_s(PO_2)$  to changes of substituents (X) and shifts to higher frequency as the Hammett function increases. Thus the  $\nu_{as}(PS_2)$  vibration is anticipated to be coupled with a  $PX_2$  group vibration of the same symmetry. From an investigation of compounds of the type  $SPX_3$  and  $PX_3$ , Goubeau<sup>80</sup> has inferred that S-P bond force constants increase with increasing phosphorus 3s orbital character and observed that there is a roughly direct dependence of the SP stretching frequency and force constant upon substituent (X) electronegativity. Goubeau<sup>80</sup> also noted that larger substituent atoms bonded to the P atom displace the S-P stretching frequency to higher values.

Since most of the ir spectral results discussed herein were obtained from Nujol mulls of the solid compounds it is necessary to show that reflection loss errors<sup>81</sup> are not significant. The best evidence that reflection loss errors are negligible is given by the results of Table 7.1 which show close agreement between band maxima observed in mull and solution spectra of the planar bis complexes (*vide infra*).

If the highest frequency ir active  $PS_2$  group vibration is taken as an index of the P-S bond length, the assignments made in Tables 3.2 - 3.6 imply the order of P-S bond lengths:



Sequence (3.9) is also the order of group electronegativities<sup>82</sup>

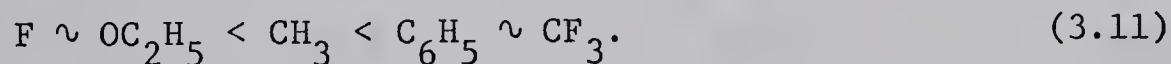


of the substituents (Table 3.7) and agrees with the order of P-S bond lengths determined in compounds with the latter three substituents (Table 3.1). No such regularity is observed for the lowest frequency ir-active  $\text{PS}_2$  group vibrations which would indicate the order of P-S bond lengths in the complexes (by substituent)



However, since the frequency range from which sequence (3.9) was deduced ( $\sim 100\text{K}$ ) is greater than the frequency range from which sequence (3.10) was deduced ( $\sim 50\text{K}$ ), the former ( $\nu_{\text{as}}(\text{PS}_2)$ ) is inferred to be a better index of substituent effects.

The difficulties in conclusively identifying bands due to M-S vibrations precludes firm generalizations based on their frequencies at this point. Initial indications are that the M-S bond lengths in the complexes follow the order by substituent



A more firm basis for decision is introduced in Chapter 6 and elaborated in Chapter 7. While sequences (3.9) and (3.10) are valid for the four stereochemical configurations indicated in Tables 3.3-3.6, no simple correlation of M-S bond lengths with M-S stretching frequencies (sequence (3.11)) is readily apparent or expected for the tetrahedral bis complexes due to the known variations in ligand function with variations of substituents.

It has been suggested<sup>83</sup> that the ir spectrum is insufficiently sensitive to distinguish between chelating, bridging, and unidentate ligand functions. However, the spectra of the complexes  $\text{Cr}[\text{S}_2\text{P}(\text{CH}_3)_2]_3$ ,



TABLE 3.7

## Physical Indexes of Electrical Substituent (X) Effects

X	Group Electronegativities <sup>a</sup>	Hammett-Taft Bond Charge Polarization "Potentials" <sup>b</sup>	
		$\sigma(\sigma_I)$	$\pi(\sigma_R^\circ)$
CH <sub>3</sub>	2.06	-0.05	-0.10
C <sub>6</sub> H <sub>5</sub>	2.43	0.10	-0.09
OCH <sub>3</sub>	2.89	0.26	-0.41
F	3.95	0.51	-0.34
CF <sub>3</sub>	3.31	0.41	+0.13
H	2.55	0.00	-0.00
Cl	3.06	0.47	-0.20
Br	2.81	0.45	-0.16
I	~2.5	0.39	-0.12
OC <sub>2</sub> H <sub>5</sub>	2.91	0.27 <sup>c</sup>	(-0.42) <sup>d</sup>
SCH <sub>3</sub>	~2.8	0.19	-0.17
SC <sub>2</sub> H <sub>5</sub>	2.83	-	-
NH <sub>2</sub>	2.3	0.10	-0.48
N(CH <sub>3</sub> ) <sub>2</sub>	2.96	0.05	-0.52
CN	3.34	0.52	+0.14

<sup>a</sup> From reference 85, page 126. The values were determined from the substituent effects upon the P=0 stretching vibrational frequency in compounds of the type X<sub>1</sub>X<sub>2</sub>X<sub>3</sub>P=0.

<sup>b</sup> From reference 86. Positive numbers correspond to an electron density shift from the substrate to substituent.

<sup>c</sup> Reference 85 and references therein.

<sup>d</sup> Estimated from  $\sigma_I$  and values for OCH<sub>3</sub>.



$\text{Ni}[\text{S}_2\text{P}(\text{CH}_3)_2]_2$ ,  $\text{OV}[\text{S}_2\text{P}(\text{CH}_3)_2]_2$ , and  $\text{Co}[\text{S}_2\text{P}(\text{CH}_3)_2]_2$  which are representative complexes of known structures clearly indicate that the ir spectra can be used to distinguish between bridging and non-bridging ligand functions as well as stereochemistry. Following  $\nu_{as}(\text{PS}_2)$  and  $\nu_s(\text{PS}_2)$  values, both frequencies are lowered by  $\sim 15\text{K}$  in  $\text{Co}[\text{S}_2\text{P}(\text{CH}_3)_2]_2$  where all ligands are bridging relative to the Cr(III) and OV(IV) complexes where all ligands are non-bridging. A value of  $\nu_s(\text{PS}_2)$  less than  $500\text{K}$  is apparently characteristic of a bridging  $\text{S}_2\text{P}(\text{CH}_3)_2$  group. In view of the high values of  $\nu_{as}(\text{PS}_2)$  in the ionic salts a monodentate  $\text{S}_2\text{P}(\text{CH}_3)_2$  group is anticipated to possess a P-S stretching frequency in excess of  $600\text{K}$ . A planar geometry appears to be characterized by a smaller frequency difference between  $\nu_{as}(\text{PS}_2)$  and  $\nu_s(\text{PS}_2)$  than for other geometries. Similar considerations hold for complexes bearing other substituents. Differences of structural significance can be seen even in the  $\text{PX}_2$  group vibrations (Tables A1-A5, Appendix).

In the course of preparation of the tetrahedral bis complexes  $\text{M}[\text{S}_2\text{P}(\text{CH}_3)_2]_2$  from the hydrated metal salts in polar organic solvents, it was found that the ir spectra of the crude products generally contained a broad absorption at  $1020\text{-}1080\text{K}$  and a sharp absorption of lesser intensity at  $550\text{-}520\text{K}$ . The first band is assigned to the P-O stretching mode and the second to a P-S stretching mode of a  $\text{P}(\text{O})\text{S}$  group. The ir spectrum is a sensitive analytical indicator for this type of sulfur replacement (see Chapter 4).

The blue complexes  $\text{OV}[\text{S}_2\text{P}(\text{CH}_3)_2]_2$  and  $\text{OV}[\text{S}_2\text{P}(\text{C}_6\text{H}_5)_2]_2$



both possess a strong ir absorption in the range 950-1030K designated to contain the V-O stretching frequency. Intense absorptions due to P-O vibrations mask the above region too effectively for a firm assignment in the case of blue  $\text{OV}[\text{S}_2\text{P}(\text{OC}_2\text{H}_5)_2]_2$ . Nujol mulls of black  $\text{OV}[\text{S}_2\text{PF}_2]_2$  and  $\text{OV}[\text{S}_2\text{P}(\text{CF}_3)_2]_2$  are clear in the usual V-O stretching region of the ir spectrum but absorb at 860 and 870K, respectively<sup>55</sup>. However, respectively mauve and purple carbon disulfide solutions of the latter two compounds were clear in the region 860-870K but absorbed strongly at 1024 and 1023K<sup>55</sup>. The low frequency of the V-O stretch in the black complexes may be due to ...O-V-O-V... chain structures in the solid state<sup>84</sup>.

### 3.4 Substituent Effects in Dithiophosphinates

The structural and vibrational data alone clearly demonstrate that there are discernible differences in the properties of the complexes  $\text{M}[\text{S}_2\text{PX}_2]_n$  with variation of the substituent X. A comprehensive analysis of the total influence of a substituent must account separately for the mass, steric, and electronic components.

#### Mass Effects

Beyond isotopic variations, it is not possible to increase the mass of the substituent X without simultaneously altering the steric and/or electronic properties. The substituents in this investigation were varied between X =  $\text{CH}_3$ ,  $\text{C}_6\text{H}_5$ ,  $\text{OC}_2\text{H}_5$ , F, and  $\text{CF}_3$  which are all bound to the P atom by an element from the first



short period. Probably the best evidence that the mass effect component has negligible influence upon the  $MS_n$  chromophore for this range of substituents is provided by the nearly identical electronic spectra<sup>12</sup> of  $Cr[S_2P(OC_2H_5)_2]_3$  and  $Cr[S_2P(OC_8H_{17})_2]_3$  together with numerous other examples of alkoxy substituted complexes of  $Cr(III)$ <sup>12,34</sup>,  $Co(III)$ <sup>12</sup>,  $Rh(III)$ <sup>12</sup>, and  $Ni(II)$ <sup>12,35</sup>. The oxygen and first carbon atoms largely damp the electrical effects of more remote portions of the substituent. The substituent mass effect remains largely indeterminate with respect to the  $PS_2$  group vibrational frequencies.

#### Steric Effects

The most obvious and probably the most important steric consideration dependent upon the substituents is the geminal X-X interaction within the  $PX_2$  groups. Assuming that the substituent groups adopt a conformation which minimizes their mutual interference, the minimum van der Waals radii ( $\text{\AA}$ ) perpendicular to the P-X bond axis for the groups of interest in this study are

$$\begin{aligned} H(1.20) < O(\text{ether linkage})(1.46) \sim F(1.47) &< CH_3(1.715) \\ &< C_6H_5(1.78) < CF_3(2.107). \quad (3.12) \end{aligned}$$

The concurrence of sequence (3.12) with sequence (3.11) of relative M-S bond lengths inferred from the ir spectra suggests that the M-S bond lengths may be related to the XPX bond angles. While the limited data contained in Table 3.1 suggest that within a given coordination geometry a larger XPX angle corresponds to a smaller SPS angle and *vice versa*, there is no apparent correlation between



XPX bond angles and M-S bond lengths or even SMS angles. Moreover, while the geminal X-X distances remain relatively constant ( $\pm 0.02\text{\AA}$ ) between compounds of common X groups, the O-O distance in  $\text{KS}_2\text{P}(\text{OCH}_3)_2$  is  $2.23\text{\AA}$  but  $2.32\text{\AA}$  in  $\text{Ni}[\text{S}_2\text{P}(\text{OCH}_3)_2]_2$  with an even shorter P-O bond. All the X-X distances calculated from known structures are less than twice the van der Waals radii given in sequence (3.12).

Thus the steric contribution to the total substituent effect is as yet indeterminate. Since H represents the "zero" of mass, steric, and electronic substituent effects much of the uncertainty remaining with this steric component is anticipated to be removed by knowledge of the structural parameters and physical properties of the as yet unreported complexes  $\text{M}(\text{S}_2\text{PH}_2)_n$ , especially  $\text{Ni}(\text{S}_2\text{PH}_2)_2$ .

#### Electrical Effects

The electrical effect of substituent groups of atoms bound to a molecular substrate is determined by their relative influence upon the electron density distribution within the substrate molecule. As an approximation the total substituent electrical effect,  $E_X$ , may be factored<sup>86</sup> as

$$E_X = \text{first order electrostatic term} + \sigma\text{-bond electron density polarization} + \pi\text{-bond electron density polarization}, \quad (3.13)$$

where  $\sigma$  and  $\pi$  are used in the "two-center" sense. Considerable success has been achieved in the classification of relative substituent effects upon molecular properties through the use of linear free energy relationships of the form<sup>86</sup>



$$P_X = \rho\sigma_X + \delta, \quad (3.14)$$

where  $P_X$  is some chemical or physical property dependent upon the nature of the substituent X,  $\rho$  and  $\delta$  are constants of the system (dependent on structure, conditions, etc.), and  $\sigma_X$  is the relative parameter characteristic of the X group. Taft and coworkers<sup>86</sup> found that  $\sigma_X$  could be usefully resolved into independent components  $\sigma_I$ , associated with the polarization of the  $\sigma$ -electron system, and  $\sigma_R^\circ$ , associated with polarization of the  $\pi$ -electron system, i.e.

$$P_X = \rho_I \sigma_I + \rho_R \sigma_R^\circ, \quad (\delta = 0) \quad (3.15)$$

The use of  $\sigma_I$  and  $\sigma_R^\circ$  values determined from series of substituted benzenes have been strongly supported by generalized correlations between chemical and physical determinations for substituted hydrocarbon systems<sup>86</sup>. Group electronegativities and the Hammett-Taft parameters for the atoms and substituent groups of interest in this study are collected in Table 3.7.

Although the Hammett-Taft parameters were derived<sup>86</sup> so as to be independent of the substrate molecule, the approximations involved in their determination rendered uncertain their validity in other than hydrocarbon systems. Kabachnik, et al.<sup>87</sup>, studied the ionization constants of the acids  $H_2SPX_2$  with  $X = R$  or  $OR$  ( $R$  = an alkyl or aryl group) and found small and apparently random variations of the  $pK_a$  values with substituent X. Charton<sup>88</sup> has treated the ionization constants of similarly substituted phosphonic and phosphinic acids, the rate constants for benzylation reactions of dithiophosphinates, and the ionization constants of phosphazenes



using an "extended" Hammett equation

$$P_X = \alpha \sum \sigma_I + \beta \sum \sigma_R^\circ + \delta, \quad (3.16)$$

where the summations allow for non-uniform substitution. Charton<sup>88</sup> concluded that the effects of substituents bonded to pentavalent phosphorus are adequately represented in terms of the  $\sigma_I$  and  $\sigma_R^\circ$  values derived for the substituents bonded to carbon. However, the magnitudes of the electrical effects in the phosphorus oxyacids were observed<sup>88</sup> to be somewhat less than for carboxylic acids and the benzylation rates of dithiophosphinates appeared to be independent of the substituents.

Thus, in both previous cases where attempts have been made to determine the substituent electrical effects in the  $S_2PX_2$  group the results indicated either that the  $PS_2$  group behaves as an insulator or that there is a fortuitous compensation of the  $\sigma, \pi$  effects leaving the same net electron density on the sulfur atom(s). For the range of substituents employed in the above investigations ( $X = R$  or  $OR$ ,  $R$  = an alkyl or aryl group)<sup>87,88</sup> reference to Table 3.7 indicates that the latter explanation is entirely plausible.

Since it has not been demonstrated that the Hammett-Taft parameters can be applied with any correlative consistency to the  $S_2PX_2$  group, attempts were made to fit the position of the first ligand field band  $\nu_{1e\bar{L}}$  in the electronic spectra of the  $Ni[S_2PX_2]_2$  complexes ( $X = CH_3, C_6H_5, OC_2H_5, F$ , and  $CF_3$ ) to equations (3.15) and (3.16). This particular system was chosen because (a) more molecular structures are known for this class of complexes,



(b) the electronic band maxima are well defined, and (c) since the electronic band positions are functions of both the ground and first excited states these quantities should provide a rigorous test for the substituent parameters between both states. Using the  $\nu_{1el}$  data from Table 6.7 and standard matrix procedures, a completely unsatisfactory fit of the data to equation (3.15) was achieved. However, the data fit equation (3.16) with  $\alpha = -0.803$ ,  $\beta = -3.233$ , and  $\delta = 13.393$  to a standard deviation of 0.017 in  $\nu_{1el}$  which is well within the experimental error ( $\pm 0.05$ ) associated with the spectral values. Thus it is inferred that within the validity of equation (3.16) the Hammett-Taft parameters may be applied with confidence to the interpretation of the substituent dependent variations in molecular properties of dithiophosphinate complexes. The goodness of the above fit is also taken to imply that substituent steric effects are of negligible significance relative to their electrical effects.

As the ligand field spectra of the complexes  $M[S_2PX_2]_n$  are largely determined by the nature of the metal ion  $M^{+n}$  which is physically remote from the substituents X it is of interest to consider how the substituent  $\sigma, \pi$  electron density polarization effects might be transmitted through the intervening P and S atoms. All the available structural data of dithiophosphinic acid derivatives indicate nearly tetrahedral coordination of the P atom. A consequence of tetrahedral symmetry is that the atomic p orbitals satisfy the symmetry requirements for both  $\sigma$  and  $\pi$  bonding. Although the essence of the following argument remains the same when d orbitals



are considered the basis set of phosphorus atomic orbitals is restricted to the 3s and 3p orbitals. If a p orbital is considered  $\sigma$  bonding with respect to one substituent, then the opposite lobe of the p orbital or alternatively the antibonding orbital associated with that linkage in the diatomic sense is  $\pi$  bonding with respect to the opposite substituent groups. Thus in a tetrahedral  $S_2PX_2$  group, the  $\sigma, \pi$  polarization effects of the X groups are anticipated to appear as  $\pi, \sigma$  polarization effects at the S atoms, i.e. the tetrahedrally coordinated P atom might be considered as a  $\sigma, \pi$  effect "transducer". While the transduction of  $\sigma, \pi$  effects by the central atom p orbitals is considered to be rigorous, the non-directional character of the central atom s orbitals is anticipated to allow some direct transmission of  $\sigma$ -electron density polarization effects depending upon the orbital overlaps. Since the MSP bond angles are nearly  $90^\circ$  ( $83.5 \pm 1.5^\circ$ , Table 3.1), no further transduction of the substituent effects by the sulfur atoms is expected.

The  $\sigma$  donor and  $\pi$  acceptor (synergic) capabilities of ligands are frequently cited as the factors determining strong metal-ligand bonds in transition metal complexes. If the Hammett-Taft parameters for the substituents  $X = OCH_3$  or  $OC_2H_5$  (Table 3.7) are transduced both  $\sigma$  donor and  $\pi$  acceptor behavior result in agreement with the shorter M-S bond lengths observed for these substituents in the nickel series of dithiophosphinates. While the  $CF_3$  substituent is a strong  $\sigma, \pi$  acid, its transduced effect is also  $\sigma, \pi$  acid which is expected to result in weaker M-S bond strengths (reduced synergism) relative to the other substituents used in this



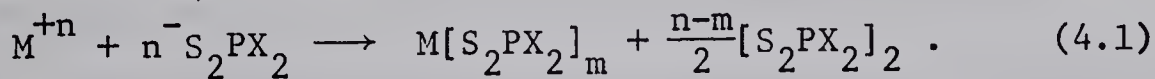
study. Possibly the most convincing cases in support for the existence and generality of a transducer effect in tetrahedral molecules are the groups<sup>89</sup> CF<sub>3</sub>, PF<sub>3</sub>, and SnCl<sub>3</sub> which behave in their chemistry (adducts or substituents) as strong  $\pi$  acceptors as would have been predicted by the transduced Hammett-Taft parameters for the halogen atoms. A further demonstration of the plausible utility of this transducer concept is provided by the imidodithiophosphinate Ni[S<sub>2</sub>P<sub>2</sub>(CH<sub>3</sub>)<sub>4</sub>N]<sub>2</sub> which has been shown<sup>48</sup> to contain a tetrahedral NiS<sub>4</sub> chromophore in contrast to the planar configuration of the same chromophoric group with all other classes of dithioacid ligands. Both the MSP and SPN bond angles are nearly the tetrahedral angle (Table 3.1). If the electrical effects of the N atom and CH<sub>3</sub> groups are transduced twice (by the P and S atoms), the net  $\pi$ -electron density polarization experienced by the Ni atom is of the  $\pi$ -base type. This is not conducive to the formation of the strong  $\pi$  bonds which are believed<sup>29,30,46,47</sup> to be instrumental in the formation of planar dithioacid complexes and thus explains the tetrahedral conformation.



## CHAPTER 4

CHEMICAL, THERMAL AND MASS SPECTRAL BEHAVIOR4.1 Redox Properties

The acids  $\text{HS}_2\text{PX}_2$  have generally been established to be strong Bronsted acids. Where  $\text{X} = \text{R}$  or  $\text{OR}$  ( $\text{R}$  = an alkyl or aryl group) the  $\text{pK}_a$  values were respectively found<sup>87</sup> to be  $1.7 \pm 0.1$  and  $2.6 \pm 0.1$  in 7 and 80% ethanol-water solvent mixtures. The  $\text{pK}_a$  of  $\text{HS}_2\text{PF}_2$  (presumably in water) is reported<sup>16d</sup> to be 1.0 while the acid  $\text{HS}_2\text{P}(\text{CF}_3)_2$  is not displaced<sup>16c</sup> from its ammonium salts by anhydrous HCl. Higher valent coinage metals ( $\text{X} = \text{R}^{13}$ ,  $\text{OR}^{39}$ ,  $\text{F}^{18}$ ,  $\text{CF}_3^{57}$ ), vanadium ( $\text{X} = \text{OR}^{28,39}$ ,  $\text{F}^{54,55,90}$ ,  $\text{CF}_3^{54,55}$ ), chromium, molybdenum, and tungsten ( $\text{X} = \text{F}^{91}$ ), iron and cobalt ( $\text{X} = \text{R}^{13}$ ,  $\text{OR}^{11}$ ) all have been observed to suffer reduction in the presence of at least one of the dithiophosphinic acids or acid anions. No simple dithiophosphinate complex has been isolated in the course of this work or reported elsewhere in which the cation can be assigned a formal charge greater than +3. Thus the dithiophosphinic acids have been called "reducing acids"<sup>13</sup>. Where the reductions at the metal ion are not complicated by the presence of bound oxygen<sup>91</sup>, the formation of a lower-valent metal ion complex is usually accompanied by production of the "diligand" species  $[\text{S}_2\text{PX}_2]_2$  according to the general equation



The diligand compounds are also readily obtained by oxidation of the free acids or their salts with bromine gas<sup>18,68,92</sup>.



The acids  $\text{HS}_2\text{PF}_2$  and  $\text{HS}_2\text{P}(\text{CF}_3)_2$  react directly with first row transition metals following vanadium with nearly quantitative evolution of hydrogen (see equation (2.3)). However, further reduction of the acid  $\text{HS}_2\text{P}(\text{CF}_3)_2$  has sometimes been observed<sup>57</sup> leading to the secondary reaction



A clear manifestation of the stereochemical influence of the substituent groups is provided by the compounds  $\text{F}_2\overset{\text{V}}{\text{P}}(\text{S})\text{H}$  and  $(\text{CF}_3)_2\overset{\text{III}}{\text{P}}\text{SH}$  resulting from reaction of the respective acid  $\text{HS}_2\text{PX}_2$  with  $\text{HI}^{16c}$ . If the substituent groups ( $\text{X} = \text{F}$  or  $\text{CF}_3$ ) are considered as one electron radicals these latter products are formally isoelectronic and the formal difference in oxidation number of the phosphorus atoms is due solely to the location of the proton. Since a proton is expected to reside near the most available concentration of negative charge, the two structural types represented by  $\text{F}_2\overset{\text{V}}{\text{P}}(\text{S})\text{H}$  and  $(\text{CF}_3)_2\overset{\text{III}}{\text{P}}\text{SH}$  are consistent with a greater negative charge on the P atom in the first compound as would have been predicted by the Hammett-Taft parameters for F and  $\text{CF}_3$  (Table 3.7).

#### Voltammetric Information

Unfortunately, electrochemical series of metals and dithiophosphinic acids in standardized environments are not available. The predictive value of such information is anticipated to parallel that in aqueous chemistry. However it is noted that the range of central metal atom oxidation states compatible with



dithiophosphinate ligands in simple complexes is a subset of the range observed for the metal ions in aqueous solution. Table 4.1 contains a summary of redox reactions observed within the dithiophosphinate system of compounds together with the corresponding aqueous couples and electrode potentials. While quantitative correlations have not been attempted and are anticipated to be difficult<sup>93</sup>, a comparison of the range of observed dithiophosphinate complexes with the corresponding range of aqueous couple electrode potentials does suggest which of the preparations not yet attempted might be successful. Thus in view of the isolation of Cr(III) and Co(III) complexes with dithiophosphinate ligands, the reduction potentials of the aqueous couples  $Ti^{+2}/Ti^{+3}$  and  $Mn^{+2}/Mn^{+3}$  leave some hope for eventual isolation of Ti(III) and Mn(III) dithiophosphinates.

Whereas the "even" ligand 1,2-dithiolene complexes form up to six-membered redox series with retention of ligand coordination (but not necessarily geometry)<sup>29,30,46,47</sup>, the "odd" classification of the dithiophosphinate ligands predicts<sup>29,47</sup> a much more restricted electron transfer series. Shetty and Fernando<sup>41</sup> have investigated the polarographic behavior of the complexes  $M[S_2P(OC_2H_5)_2]_2$  with M = Ni, Mn, Zn, Cd, and Pb in ethanol and ethanol-water media using a saturated calomel reference electrode. In each case a single well-developed but irreversible reduction wave was observed<sup>41</sup> in the range 0 to -1.8V. The behavior of these reduction waves with varying solution components was interpreted<sup>41</sup> to indicate a single-step, two electron, catalytic reduction of the metal ion.



TABLE 4.1

Redox Reactions of Dithiophosphinic Acids ( $\text{HS}_2\text{PX}_2$ ) and Derivatives

Observed Reactions <sup>a</sup>	X <sup>b</sup>	Ref.	Aqueous Couple	$E_{\text{o}}^{\text{red}}$ (volts) <sup>c</sup>
$\text{Mn} + 2\text{HL} \longrightarrow \text{MnL}_2 + \text{H}_2$	$\text{F}, \text{CF}_3$	18, 57	$\text{Ti}/\text{Ti}^{+2}$	-1.63
$\text{V} + 2\text{HL} \longrightarrow \text{No reaction}$	$\text{F}, \text{CF}_3$	54	$\text{Mn}/\text{Mn}^{+2}$	-1.029
			$\text{V}/\text{V}^{+2}$	-1.2
			$\text{S}/\text{S}^{=}$	-0.92
$\text{Zn} + 2\text{HL} \longrightarrow \text{ZnL}_2 + \text{H}_2$	$\text{F}, \text{CF}_3$	18, 57	$\text{Zn}/\text{Zn}^{+2}$	-0.763
$\text{Cr} + 3\text{HL} \longrightarrow \text{CrL}_3 + 3/2\text{H}_2$	$\text{F}, \text{CF}_3$	18, 53	$\text{Cr}/\text{Cr}^{+3}$	-0.74
$\text{Fe} + 2\text{HL} \longrightarrow \text{FeL}_2 + \text{H}_2$	$\text{F}, \text{CF}_3$	18, 57	$\text{Fe}/\text{Fe}^{+2}$	-0.44
$\text{Cr}^{+2} + 2\text{L}^- \longrightarrow \text{CrL}_3 + ?$	R,		$\text{Cr}^{+2}/\text{Cr}^{+3}$	-0.41
$\text{Cd} + 2\text{HL} \longrightarrow \text{CdL}_2 + \text{H}_2$	$\text{F}, \text{CF}_3$	18, 57	$\text{Cd}/\text{Cd}^{+2}$	-0.4026
			$\text{Ti}^{+2}/\text{Ti}^{+3}$	-0.37
$\text{Co} + 2\text{HL} \longrightarrow \text{CoL}_2 + \text{H}_2$	$\text{F}, \text{CF}_3$	18, 57	$\text{Co}/\text{Co}^{+2}$	-0.28
			$\text{V}^{+2}/\text{V}^{+3}$	-0.255
$\text{Ni} + 2\text{HL} \longrightarrow \text{Nil}_2 + \text{H}_2$	$\text{F}, \text{CF}_3$	18, 56	$\text{Ni}/\text{Ni}^{+2}$	-0.23
$\text{Mo} + 3\text{HL} \longrightarrow \text{No reaction}$	$\text{F}, \text{CF}_3$	90	$\text{Mo}/\text{Mo}^{+3}$	-0.2
$[\text{H}] + \text{HS}_2\text{PX}_2 \rightarrow \text{HSPX}_2 + \text{H}_2\text{S}$	$\text{CF}_3$	57		
$[\text{S}_2\text{PX}_2]_2 + e \rightarrow \text{S}_2\text{PX}_2 + 1/2\text{H}_2$	$\text{F}, \text{CF}_3$	18, 57	$\text{H}_2/\text{H}^+$	
$[\text{CuL}_2] \xrightarrow{\Delta} \text{CuL} + 1/2\text{L}_2$	$\text{F}, \text{CF}_3$	18, 57		
$\text{OVL}_2 \xrightarrow{\Delta} \text{VL}_3 + ?$	$\text{R}, \text{OR}, \text{F}, \text{CF}_3$	13, 39, 57	$\text{Cu}^+/ \text{Cu}^{++}$	0.158
	$\text{OR}, \text{F}, \text{CF}_3$	28, 55	$\text{V}^{+3}, \text{H}_2\text{O}/\text{OV}^{+2}, \text{H}^+$	0.337



TABLE 4.1 (cont'd)

Redox Reactions of Dithiophosphinic Acids ( $\text{HS}_2\text{PX}_2$ ) and Derivatives

Observed Reactions <sup>a</sup>	X <sup>b</sup>	Ref.	Aqueous Couple	$E_{\text{O}_{\text{red}}}^{\text{c}}$ (volts) <sup>c</sup>
$\text{Cu} + 2\text{HL} \longrightarrow [\text{CuL}_2]^? + \text{H}_2$	$\text{F}, \text{CF}_3$	18, 57	$\text{Cu}/\text{Cu}^{+2}$	0.3402
	R, OR	1, 2	$\text{Cu}/\text{Cu}^{+}$	0.522
$\text{I}_2 + \text{HL} \longrightarrow 2\text{HI} + \text{L}_2$			$\text{I}_2/\text{I}^-$	0.5335
$\text{FeL}_2 + 1/2\text{L}_2 \longrightarrow \text{FeL}_3$	$\text{F}, \text{CF}_3$		$\text{Fe}^{+2}/\text{Fe}^{+3}$	0.770
$\text{Ag} + \text{HL} \longrightarrow$ No reaction	F	91b	$\text{Ag}/\text{Ag}^{+}$	0.7996
			$\text{Rh}/\text{Rh}^{+3}$	$\sim 0.8$
$\text{Pd} + 2\text{HL} \longrightarrow$ No reaction			$\text{Pd}/\text{Pd}^{+2}$	0.987
$\text{Br}_2 + 2\text{L}^- \longrightarrow \text{L}_2 + 2\text{Br}^-$			$\text{Br}_2(\text{L})/\text{Br}^-$	1.065
$\text{Pt} + 2\text{HL} \longrightarrow$ No reaction			$\text{Pt}/\text{Pt}^{+2}$	1.2
$\text{Tl}^{+3} + 3\text{L}^- \longrightarrow \text{TlL} + \text{L}_2$	R	13	$\text{Tl}^+/ \text{Tl}^{+3}$	1.247
			$\text{Au}/\text{Au}^{+3}$	1.42
			$\text{Mn}^{+2}/\text{Mn}^{+3}$	1.51
$\text{CoL}_2 + 1/2\text{L}_2 \longrightarrow \text{CoL}_3$			$\text{Co}^{+2}/\text{Co}^{+3}$	1.842
$\text{Ag}^{+2} + 2\text{L}^- \longrightarrow \text{AgL} + 1/2\text{L}_2$	R	13	$\text{Ag}^{+}/\text{Ag}^{+2}$	1.987
$\text{CrO}_2\text{Cl}_2 + \text{HL} \longrightarrow \text{CrL}_3 + \text{OPF}_3$ , etc.	F	90		

<sup>a</sup> Where possible, the  $\text{S}_2\text{PX}_2$  group is represented simply as "L".<sup>b</sup> R is an alkyl or aryl group.<sup>c</sup> Standard reduction potentials were found in the "Handbook of Chemistry and Physics", 48th Edition (1967-1968), The Chemical Rubber Co., Cleveland, Ohio, or adapted from tables in the 45th edition of the same volume.



A voltammetric investigation by Dr. B. Kratochvil<sup>94</sup> of  $\text{Ni}[\text{S}_2\text{P}(\text{CH}_3)_2]_2$ ,  $\text{Cr}[\text{S}_2\text{P}(\text{CH}_3)_2]_3$ , and  $\text{Co}[\text{S}_2\text{P}(\text{CH}_3)_2]_2$  in acetonitrile at a rotating platinum electrode referenced to a  $\text{Ag}/\text{AgNO}_3$ , 0.1M electrode also in acetonitrile revealed no reduction of  $\text{Cr}[\text{S}_2\text{P}(\text{CH}_3)_2]_3$  but an oxidation at high voltage, while  $\text{Ni}[\text{S}_2\text{P}(\text{CH}_3)_2]_2$  showed one oxidation wave (1.8V) and two reduction waves (-0.5 and -0.8V).  $\text{Co}[\text{S}_2\text{P}(\text{CH}_3)_2]_2$  proved too insoluble in acetonitrile for useful results<sup>94</sup>.

#### Thermal and Chemical Results

Thermal data for the dithiophosphinic acids and complexes of interest herein are included in Table 4.2. While negligible thermal decomposition was detected in the vacuum sublimations of  $\text{OV}[\text{S}_2\text{P}(\text{CH}_3)_2]_2$ , a complicated decomposition of  $\text{OV}[\text{S}_2\text{P}(\text{C}_6\text{H}_5)_2]_2$  is indicated by its thermogram. Distillation of  $\text{OV}[\text{S}_2\text{P}(\text{OC}_2\text{H}_5)_2]_2$  from its melt in vacuo was always observed to leave a small residue of  $\text{V}[\text{S}_2\text{P}(\text{OC}_2\text{H}_5)_2]_3$ . The greater volatility of  $\text{OV}[\text{S}_2\text{PF}_2]_2$  and  $\text{OV}[\text{S}_2\text{P}(\text{CF}_3)_2]_2$  permitted sublimation of these complexes at 70°C without apparent decomposition but heating in evacuated and sealed tubes at 90-100°C resulted in extensive formation of the V(III) complexes<sup>55</sup>. The reason for the apparently facile thermally induced reductions of the vanadyl complexes with electronegative substituents is not clear.

While none of the five V(III) complexes studied herein could be kept in air, solid  $\text{V}[\text{S}_2\text{P}(\text{C}_6\text{H}_5)_2]_3$  appeared unchanged after exposures of several days although exposed halocarbon solutions rapidly turned from yellow to blue in color. Exposure of  $\text{V}[\text{S}_2\text{P}(\text{CH}_3)_2]_3$



TABLE 4.2

Thermal Data for the Complexes  $M[S_2PX_2]_n$ 

X	$M^{+n}$	Melting Point	T (°C)	% Weight Loss	Heating Rate (deg/min)	Thermogravimetric Data <sup>a</sup>	
$CH_3$	$OV^{+2}$	dec.	187 (sealed tube)	162	100	7.25	
V <sup>+3</sup>				144	100	4.34	
Cr <sup>+3</sup>				171	100	7.25	
Mn <sup>+2</sup>				185	100	7.25	
Fe <sup>+2</sup>				174	100	7.25	
Co <sup>+3</sup>				129	30.2	7.25	
				170	69.8		
Co <sup>+2</sup>				212	100	5.80	
Ni <sup>+2</sup>		dec. <sup>2</sup>		168	100	14.5	
Pd <sup>+2</sup>				208	100	14.5	
Pt <sup>+2</sup>				233	100	14.5	
Zn <sup>+2</sup>				197	100	7.25	
Cd <sup>+2</sup>				243	100	14.5	
Hg <sup>+2</sup>				203	100	14.5	
$CoOS_3P_2(CH_3)_4$				183	87.2	5.80	
$C_6H_5OV^{+2}$				250	~21.3	7.25	
				285	~38.4		



TABLE 4.2 (cont'd)

Thermal Data for the Complexes  $M[S_2PX_2]_n$ 

X	$M^{+n}$	Melting Point	Thermogravimetric Data <sup>a</sup>		
			T (°C)	% Weight Loss	Heating Rate (deg/min)
$C_6H_5$	OV <sup>+2</sup>		377 457	~10.4 ?	14.5
V <sup>+3</sup>			317	~90	14.5
Cr <sup>+3</sup>			329	100	14.5
Mn <sup>+2</sup>	250, dec.	14a	310	100	14.5
Fe <sup>+3</sup>			210 275	31.2 68.8	7.25
Fe <sup>+2</sup>			303	100	14.5
Co <sup>+3</sup>			183 242	31.0 69.0	7.25
Co <sup>+2</sup>	280	14b	274	100	14.5
Ni <sup>+2</sup>	>200	, dec.	14b	302	100
Pd <sup>+2</sup>				309	100
Pt <sup>+2</sup>				314	84
Zn <sup>+2</sup>	>200	<sup>2</sup>		291	100
Cd <sup>+2</sup>	>250	, dec.	14a	315	100
Hg <sup>+2</sup>				286	100



TABLE 4.2 (cont'd)

Thermal Data for the Complexes  $M[S_2PX_2]_n$ 

X	$M^{+n}$	Thermogravimetric Data <sup>a</sup>			
		Melting Point	T (°C)	% Weight Loss	Heating Rate (deg/min)
$OC_2H_5$	$OV^{+2}$	65°	107	98	7.25
	$V^{+3}$				
	$Cr^{+3}$		177	100	14.5
	$Co^{+3}$		156	100	14.5
	$Co^{+2}$		223	~82.5	7.25
	$Ni^{+2}$	105 <sup>35</sup>	119	100	14.5
	$Pd^{+2}$		132	100	14.5
	$Pt^{+2}$		139	100	14.5
	$Zn^{+2}$		231	~80	7.25
	$OV^{+2}$		≤25	100	7.25
	$V^{+3}$		≤42	100	7.25
	$Cr^{+3}$	53.0-53.5 <sup>18</sup>	≤34	100	7.25
	$Mn^{+2}$	168-170, dec. <sup>18</sup>	73	100	7.25
	$Fe^{+2}$	90-91 <sup>18</sup>	48	100	7.25
	$Co^{+3}$	34 <sup>18</sup>	≤25	100	
	$Co^{+2}$	44.0-44.5	≤25	100	
	$Ni^{+2}$	43-44 <sup>18</sup>	<<25	100	7.25



TABLE 4.2 (cont'd)

Thermal Data for the Complexes  $M[S_2^P X_2]_n$ 

X	$M^{+n}$	Melting Point	Thermogravimetric Data <sup>a</sup>		
			T (°C)	% Weight Loss	Heating Rate (deg/min)
F	Pd <sup>+2</sup>	56.5-57.18	<43	100	7.25
	Pt <sup>+2</sup>	53-54.18	<50	100	
	Zn <sup>+2</sup>	156-158.18	<100	100	
	Hg <sup>+2</sup>	163-164, dec. 18	<100	100	
	Ov <sup>+2</sup>		<52	100	7.25
CF <sub>3</sub>	V <sup>+3</sup>		59	100	7.25
	Cr <sup>+3</sup>		50	100	4.35
	Mn <sup>+2</sup>		58	100	7.25
	Fe <sup>+2</sup>		42	100	7.25
	Co <sup>+3</sup>		<100	100	
	Co <sup>+2</sup>		41	100	7.25
	Ni <sup>+2</sup>		<100	100	
	Pd <sup>+2</sup>		<44	100	
	Pt <sub>2</sub> S <sub>6</sub> P <sub>2</sub> (CF <sub>3</sub> ) <sub>8</sub>		<100	100	
	Zn <sup>+2</sup>		<100	100	
	Cd <sup>+2</sup>		<100	100	



TABLE 4.2 (cont'd)

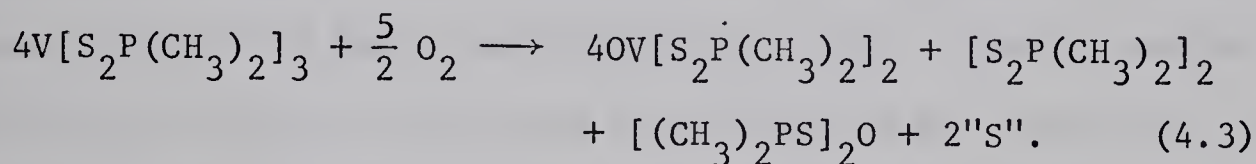
Thermal Data for the Complexes  $M[S_2PX_2]_n$ 

$X$	$M^{+n}$	Thermogravimetric Data <sup>a</sup>			
		Melting Point	T (°C)	% Weight Loss	Heating Rate (deg/min)
	Hg <sup>+2</sup>	<100	100		
	HS <sub>2</sub> P(CH <sub>3</sub> ) <sub>2</sub>	59 <sup>2</sup>			
	HS <sub>2</sub> P(C <sub>6</sub> H <sub>5</sub> ) <sub>2</sub>	54-56 <sup>2</sup>			
	HS <sub>2</sub> P(OC <sub>2</sub> H <sub>5</sub> ) <sub>2</sub>	oil at 25 <sup>o</sup> 1			
	HS <sub>2</sub> PF <sub>2</sub>	<-84 (b.p. 741at) <sup>16b</sup>			
	HS <sub>2</sub> P(CF <sub>3</sub> ) <sub>2</sub>	<-84 (b.p. 1021at) <sup>17b</sup>			

<sup>a</sup> The temperatures assigned to the weight-loss processes were obtained as described in Chapter II. The operating pressure was approximately  $10^{-2}$  torr. Thermogravimetric data listed without heating rates are estimates based on the amount of residue remaining after sublimation of a pure sample along a glass tube under vacuum and the approximate temperature required for the sublimation.



to air for 48 hours resulted in what appeared to be a pale blue mixture of solids. A thermogram of 10 mg of this material in conjunction with mass measurements of ions in the mass spectrum indicated that it contained at least  $OV[S_2P(CH_3)_2]_2$ ,  $[S_2P(CH_3)_2]_2$ , and  $[(CH_3)_2PS]_2O$  in the molar ratios 4:1:1, respectively. This stoichiometry is consistent with the equation



However, no elemental sulfur ( $\sim 4\%$  of the sample weight) could be accounted for in either the mass spectrum or thermogram of the mixture. It is possible that water enters into equation (4.3) such that the missing sulfur may have been carried away as  $H_2S$ , but the blue mixture yielded a milky suspension in chloroform whereas all the reaction products except elemental sulfur are soluble in that solvent. The behavior of the complexes in air with  $X = OC_2H_5$ , F, and  $CF_3$  did not appear simple and was probably complicated by hydrolysis, whereas the oxidation of  $V[S_2P(C_6H_5)_2]_3$  probably follows a course similar to that of equation (4.3). All the complexes sublime in vacuo with little decomposition.

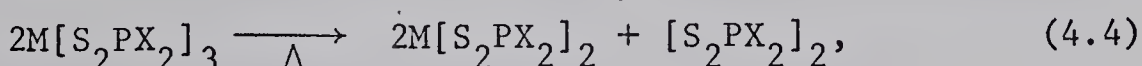
The complexes  $Cr[S_2PX_2]_3$ ,  $X = CH_3$ ,  $C_6H_5$ ,  $OC_2H_5$ , F, and  $CF_3$  are uniformly inert to molecular oxygen and sublime in vacuo without significant decomposition. The two fluorine containing compounds undergo slow hydrolysis.

While the complexes  $Mn[S_2PX_2]_2$  with  $X = CH_3$ ,  $C_6H_5$ , and  $F^{22}$  are quite stable to dry air in the solid state, solutions of



$\text{Mn}[\text{S}_2\text{P}(\text{CH}_3)_2]_2$  and  $\text{Mn}[\text{S}_2\text{PF}_2]_2^{18}$  in halocarbon solvents turn red irreversibly on exposure to air.  $\text{Mn}[\text{S}_2\text{PF}_2]_2$  and  $\text{Mn}[\text{S}_2\text{P}(\text{CF}_3)_2]_2$  are very hygroscopic solids. All these Mn(II) complexes sublime in vacuo without significant decomposition.

$\text{Fe}[\text{S}_2\text{P}(\text{CH}_3)_2]_3$  apparently has only a transitory existence in halocarbon solvent solutions obtained by extraction of concentrated aqueous mixtures of  $\text{FeCl}_3$  and  $\text{NaS}_2\text{P}(\text{CH}_3)_2 \cdot 2\text{H}_2\text{O}$ . These solutions are initially green in color but continuously fade depositing a tan colored material. A mass spectrum of this tan material was dominated by the parent ion molecules of  $\text{Fe}[\text{S}_2\text{P}(\text{CH}_3)_2]_2$ ,  $[\text{S}_2\text{P}(\text{CH}_3)_2]_2$ , and elemental sulfur.  $\text{Fe}[\text{S}_2\text{P}(\text{C}_2\text{H}_5)_2]_3$  is reported<sup>75</sup> to undergo a similar spontaneous decomposition over a period of days, even in vacuo. Hot ligroin solutions of this latter complex precipitated pale yellow  $\text{Fe}[\text{O}_2\text{P}(\text{C}_2\text{H}_5)_2]_3$  and elemental sulfur when exposed to air<sup>75</sup>. The black complex  $\text{Fe}[\text{S}_2\text{P}(\text{C}_6\text{H}_5)_2]_3$  appeared stable in air indefinitely but on heating decomposes according to the equation



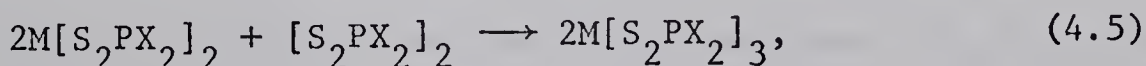
which parallels equation (4.1). Black crystals of  $\text{Fe}[\text{S}_2\text{P}(\text{OC}_2\text{H}_5)_2]_3$  are reported<sup>11</sup> to deliquesce in air and form brown hydrolysis products, while grayish-green ethanol solutions rapidly decolorize, presumably forming Fe(II). Both  $\text{Fe}[\text{S}_2\text{PF}_2]_3^{18,57}$  and  $\text{Fe}[\text{S}_2\text{P}(\text{CF}_3)_2]_3^{57}$  are dark materials formed by oxidation of the corresponding Fe(II) complex with molecular oxygen or the diligand, but purification posed unsurmounted difficulties.

Where  $\text{X} = \text{C}_6\text{H}_5$ ,  $\text{F}^{18,57}$ , and  $\text{CF}_3^{57}$ , the colors of the pure



complexes  $\text{Fe}[\text{S}_2\text{PX}_2]_2$  are very close to yellow, but on exposure to air the colors usually darken quickly to the near black of the Fe(III) complexes. The initially yellow complex  $\text{Fe}[\text{S}_2\text{P}(\text{CH}_3)_2]_2$  undergoes no apparent color changes in air, but samples kept in air for long periods (months to 3 years) no longer sublime, the only volatile component up to 200°C being elemental sulfur. This latter behavior is quite consistent with the formation of a yellow complex  $\text{Fe}[\text{O}_2\text{P}(\text{CH}_3)_2]_3$  by analogy with  $\text{Fe}[\text{S}_2\text{P}(\text{C}_2\text{H}_5)_2]_3^{75}$  as described above. Except for  $\text{Fe}[\text{S}_2\text{P}(\text{OC}_2\text{H}_5)_2]_2$  which was not prepared, the Fe(II) complexes with  $\text{X} = \text{CH}_3$ ,  $\text{C}_6\text{H}_5$ ,  $\text{F}^{18,57}$ , and  $\text{CF}_3^{57}$  are all sublimable in vacuo without significant decomposition.

Of the brown complexes  $\text{Co}[\text{S}_2\text{PX}_2]_3$  where  $\text{X} = \text{CH}_3$ ,  $\text{C}_6\text{H}_5$ ,  $\text{OC}_2\text{H}_5$ ,  $\text{F}^{18,57}$ , and  $\text{CF}_3^{52}$ , the latter three sublime in vacuo without significant decomposition, while the first two decompose according to equation (4.4). As with the Fe(III) complexes with  $\text{X} = \text{F}^{18,57}$  and  $\text{CF}_3^{57}$ , the Co(III) complexes with the same substituents have been prepared<sup>18,57</sup> by oxidation of the Co(II) complex with molecular oxygen or by the "diligand" according to the equation



which is the reverse of reaction (4.4). The ease of oxidation of  $\text{Co}[\text{S}_2\text{P}(\text{OC}_2\text{H}_5)_2]_2$  in solution by molecular oxygen suggests that it should also react according to equation (4.5) however this has not been done. While the solid complexes with  $\text{X} = \text{CH}_3$  and  $\text{C}_6\text{H}_5$  may be kept indefinitely under nitrogen or in vacuo, exposure to air resulted in a gradual transformation to a pasty mass containing the Co(II)



species. Solutions of the  $\text{CH}_3$  and  $\text{C}_6\text{H}_5$  substituted complexes are particularly susceptible to reduction (equation 4.4)) even with mild heating.  $\text{Co}[\text{S}_2\text{P}(\text{C}_2\text{H}_5)_2]_3$  is reported<sup>75</sup> to give a mixture containing the Co(II) complex and the trithiophosphorane  $(\text{C}_2\text{H}_5)_2\text{P}(\text{S})-\text{S}_3-\text{P}(\text{S})(\text{C}_2\text{H}_5)_2$  when exposed to air and to spontaneously decompose even in the absence of air.

In contrast to the ready oxidation reactions of the Co(II) complexes  $\text{Co}[\text{S}_2\text{PX}_2]_2$  with  $\text{X} = \text{OC}_2\text{H}_5$ ,  $\text{F}$ , and  $\text{CF}_3$ , the  $\text{CH}_3$  and  $\text{C}_6\text{H}_5$  substituted compounds are quite inert in air. If this inertness to molecular oxygen were the kinetic result of the crystal packing then it might be expected that solutions would be more susceptible, however, the complexes  $\text{Co}[\text{S}_2\text{P}(\text{CH}_3)_2]_2$  and  $\text{Co}[\text{S}_2\text{P}(\text{C}_6\text{H}_5)_2]_2$  are quite stable to oxidation by air in organic solvents. Except for  $\text{Co}[\text{S}_2\text{P}(\text{OC}_2\text{H}_5)_2]_2$ , these Co(II) complexes sublime in vacuo without significant decomposition. Whereas the alkoxy-substituted tris complexes apparently withstand sublimation in vacuo, olefin elimination is a significant process in the thermal decomposition of alkoxy-substituted bis dithiophosphinates<sup>25</sup>.

No redox reactions of the planar complexes  $\text{M}[\text{S}_2\text{PX}_2]_2$  have been observed where  $\text{M} = \text{Ni}, \text{Pd}, \text{Pt}; \text{X} = \text{CH}_3, \text{C}_6\text{H}_5, \text{OC}_2\text{H}_5, \text{F}$ , and  $\text{CF}_3$ . With the exceptions where  $\text{X} = \text{OC}_2\text{H}_5$  and possibly  $\text{Pt}[\text{S}_2\text{P}(\text{CF}_3)_2]_2$ , the complexes all sublime cleanly. Epr spectra<sup>39</sup> of Cu(II) complexes with  $\text{X} = \text{R}$  and  $\text{OR}$ , where  $\text{R}$  is an alkyl or aryl group, establish their existence as transitory intermediates in the formation of Cu(I) complexes. Prior to the recent report<sup>38</sup> of  $\text{Au}[\text{S}_2\text{P}(\text{C}_6\text{H}_5)_2]_3$  it was



thought<sup>18</sup> that only the univalent complexes of the coinage metals could be isolated. Where X is an alkyl group reduction of Ag(II) and Au(III) was observed to be the rule<sup>13</sup>. It is anticipated that the Au(III) complex should decompose when heated to produce the Au(I) complex and the diligand compound. No epr spectra have been observed for those coinage metal complexes where X = F<sup>18</sup> or CF<sub>3</sub><sup>57</sup>.

As expected, no reductions or oxidations of Zn or Cd complexes have been observed for any substituent. It might be anticipated that Hg(II) complexes would undergo reduction to the Hg(I) complex, but this has not been observed. Where X = CH<sub>3</sub>, F and CF<sub>3</sub>, the complexes of the three divalent metals all sublime with no significant decomposition.

#### 4.2 Reactions with Lewis Bases

##### Ligand Exchange

A change in chalcogen atoms from O to S transforms the conjugate bases of dichalcogen acids from "hard" to "soft" Lewis bases in the nomenclature of Pearson<sup>96</sup> with the attendant change in reactivity. From the relatively long M-S bond lengths and low M-S vibrational frequencies of dithiophosphinate complexes as compared with other dithioacid complexes it might be anticipated that the dithiophosphinate ligands are relatively labile. Livingstone<sup>97</sup> has discussed the order of formation constants of chalcogen containing complexes as a function of the metal ion and notes that the Mellor-Maley series (Mg < Mn < Fe < Cd < Zn < Co < Pb < Ni < Cu < Pd) generally holds except that Cd and Pb are out of sequence probably due



to ligand-metal  $\pi$  bonding. Shetty and Fernando<sup>41</sup> found a linear relationship between the logarithm of the formation constant and the inverse of the dielectric constant of ethanol-water solvent mixtures for the complexes  $M[S_2P(OC_2H_5)_2]_2$ ,  $M = Mn, Zn, Cd, \text{ and } Pb$ , and determined the formation constant order:  $Pb(II) > Cd(II) > Zn(II) > Mn(II)$ .

The latter authors conclude<sup>41</sup> that the M-S bonds are extremely labile in solvents of high dielectric constants and because of this the bonds are "ionic". Jorgensen<sup>54</sup> states quite emphatically that the correlation between lability and covalency cannot be maintained and this is corroborated in Chapter 6.

In the course of this work, but without quantitative support, it was observed that the rate of complex formation was strongly dependent upon the substituent with the partial and qualitative order



an order which does not correspond to the substituent order based on the M-S bond lengths or M-S infrared stretching frequencies in the Ni(II) complexes. Since the intermolecular forces determining precipitation, solvation (wettability), etc. are largely governed by the substituents, it is anticipated that the order of melting and/or boiling points of the acids  $HS_2PX_2$  (Table 4.2) should indicate the relative ease of solvolysis of the complexes. The thermal data available for the acids concurs with sequence (4.6). All the  $CH_3$  substituted complexes with the possible exception of  $V[S_2P(CH_3)_2]_3$  (not tested) dissolve in water with dissociation of the M-S bonds producing solution colors corresponding to the aquated metal ions.



The F and  $\text{CF}_3$  substituted compounds were notably more hygroscopic than their  $\text{CH}_3$  and  $\text{C}_6\text{H}_5$  substituted analogues where the tendency was not evident at all ( $M^{+n} = \text{OV}^{+2}$ ,  $\text{Mn}^{+2}$ ,  $\text{Co}^{+2}$ , and  $\text{Zn}^{+2}$ ).

Electronic spectral studies of  $\text{OV}[\text{S}_2\text{P}(\text{C}_6\text{H}_5)_2]_2^{55}$  and  $\text{M}[\text{S}_2\text{P}(\text{OC}_2\text{H}_5)_2]_2$  complexes where  $\text{M} = \text{Ni}^{11,98}$  or  $\text{Co}^{99}$  in solvent systems containing water indicate that the metal ion is either present in complexed or uncomplexed forms with no intermediate species being detected. Thus the introduction of one dithiophosphinate group into the first coordination sphere of the metal ion is probably the rate determining step in the complex formation by solvent molecule displacement.

Reaction of ammonia gas with  $\text{Co}[\text{S}_2\text{P}(\text{C}_2\text{H}_5)_2]_2$  and  $\text{Ni}[\text{S}_2\text{P}(\text{C}_2\text{H}_5)_2]_2$  is reported<sup>13,75</sup> to be reversible and yield respectively organic solvent insoluble, flesh colored  $[\text{Co}(\text{NH}_3)_6]^{+2}[\text{S}_2\text{P}(\text{C}_2\text{H}_5)_2]_2$  and lilac colored  $[\text{Ni}(\text{NH}_3)_6]^{+2}[\text{S}_2\text{P}(\text{C}_2\text{H}_5)_2]_2$ . Absence of metal-fluorine coupling in the  $^{19}\text{F}$  nmr spectra of  $\text{Cd}[\text{S}_2\text{PF}_2]_2$  and  $\text{Hg}[\text{S}_2\text{PF}_2]_2$  in acetonitrile solutions has been taken to imply rapid ligand exchange even at  $-50^\circ\text{C}$  although the free ion  $[\text{S}_2\text{PF}_2]^{18}$  was not detected in significant concentrations<sup>18</sup>. Addition of dimethyl sulfoxide or water to these latter solutions resulted in the observation of the  $^{19}\text{F}$  nmr spectrum of uncoordinated  $[\text{S}_2\text{PF}_2]^{18}$  ion. While metal-fluorine coupling has been detected<sup>18</sup> in the  $^{19}\text{F}$  nmr spectra of the diamagnetic complexes  $\text{Co}[\text{S}_2\text{PF}_2]_3$  and  $\text{Pt}[\text{S}_2\text{PF}_2]_2$ , such coupling has not been observed<sup>57,56</sup> in the  $^{19}\text{F}$  nmr spectra of any of the diamagnetic  $\text{M}[\text{S}_2\text{P}(\text{CF}_3)_2]_n$  complexes but in these cases the greater M-F separation



can readily account for this result without invoking ligand exchange.

The  $^{19}\text{F}$  nmr spectra of  $\text{Pt}[\text{S}_2\text{PF}_2]_2$  and  $\text{Pd}[\text{S}_2\text{PF}_2]_2$  contain additional fine structure<sup>18</sup> so it is difficult to define a spatial limit to M-F coupling.

The ligand substitution processes of the dithiophosphinate complexes confirms their "soft" classification. In fact the formation of more stable complexes with univalent coinage metals is quite consistent with the soft character of these metal ions. The inability to obtain the complexes  $\text{Mn}[\text{S}_2\text{P}(\text{CH}_3)_2]_2$  and  $\text{Cr}[\text{S}_2\text{P}(\text{CH}_3)_2]_3$  from water is also consistent with small formation constants and the "hard" nature of the metal ions.

#### Adduct Formation

It has been suggested<sup>100</sup> that chelates with small formation constants show the greatest tendency to form stable adducts. Thus an extensive adduct chemistry might be expected for the coordinatively unsaturated dithiophosphinates in view of their small formation constants.

Jorgensen<sup>39</sup> has shown that the electronic spectrum of  $\text{Co}[\text{S}_2\text{P}(\text{OC}_2\text{H}_5)_2]_2$  dissolved in ethanol is very different from that in carbon tetrachloride although the  $\text{Co}^{+2}$  ion is associated with two ligand groups in both solvents and the same complex is recovered from both solvents. Similar behavior has been observed in this work for  $\text{Co}[\text{S}_2\text{P}(\text{CH}_3)_2]_2$  in chlorocarbon solvents and alcohols (Chapter 6).

Jorgensen<sup>99</sup> postulates that a solvate  $\text{Co}[\text{S}_2\text{P}(\text{OC}_2\text{H}_5)_2]_2 \cdot 2\text{C}_2\text{H}_5\text{OH}$  of undetermined magnetism may exist in ethanolic solutions.

Dakternieks and Graddon report<sup>83</sup> that a stable mono-pyridine adduct



of  $Zn[S_2P(Oi-C_3H_7)_2]_2$  establishes an equilibrium with a bis-pyridine adduct in solution containing free pyridine. Kuchen et al.<sup>75,101</sup> claim an unstable bis-pyridine adduct of  $Co[S_2P(C_2H_5)_2]_2$  which reverts spontaneously to the original complex.

No adducts of  $Ni[S_2PX_2]_2$  complexes were isolated in this study although numerous five and six coordinated species have been claimed<sup>12,13,101,102</sup> or confirmed<sup>71,72,103</sup> in some of which the dithiophosphinate ligand is monodentate<sup>103</sup>. The common feature of these Ni(II) complex adducts is that they are unstable, spontaneously losing the non-dithiophosphinate ligands. Tebbe and Muetterties report<sup>18</sup> stable 1:1 and 2:1 phosphine and 1:1 arsine adducts of  $Pd[S_2PF_2]_2$  but it is not known whether the ligand is mono or bidentate.

The pyridine adduct of  $OV[S_2P(C_2H_5)_2]_2$  was recently reported<sup>37</sup>, although it was unstable to loss of pyridine. No adducts of  $OV[S_2PX_2]_2$  were isolated in this work rather pyridine and other bases were found<sup>104</sup> to decompose the vanadyl complexes where X =  $CH_3$  and  $C_6H_5$ . In addition, epr studies<sup>105</sup> of the exchange kinetics of the  $OV[S_2PX_2]_2$  complexes, (X =  $CH_3$ ,  $C_6H_5$  and  $OC_2H_5$ ) with non-destructive oxygen coordinating bases have produced puzzling and as yet unexplained results which may suggest transformation of the chelate dithiophosphinate to a monodentate ligand by the base. There is some evidence for a reversible reaction of the vanadyl complex with molecular oxygen.

Lewis bases are reported<sup>13,18</sup> to degrade the polymeric structures of univalent metal ion complexes.



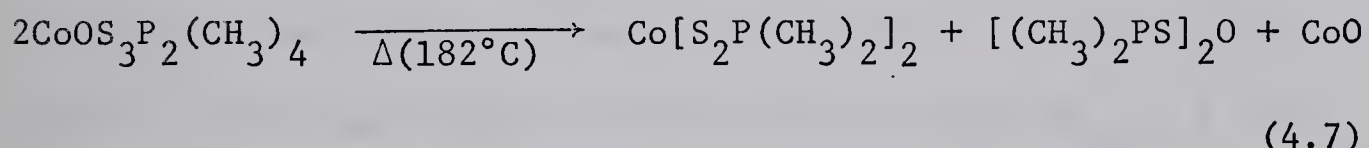
#### 4.3 Sulfur Replacement by Oxygen

As previously mentioned in Chapter 3, of the compounds investigated in this study, only the methyl substituted tetrahedral bis complexes showed significant replacement of sulfur atoms by oxygen. No sulfur atom replacement was detected in the volatile products of the molecular oxygen oxidations<sup>18,57</sup> of the complexes  $\text{Co}[\text{S}_2\text{PF}_2]_2$ ,  $\text{Co}[\text{S}_2\text{P}(\text{CF}_3)_2]_2$ ,  $\text{Fe}[\text{S}_2\text{PF}_2]_2$ , or  $\text{Fe}[\text{S}_2\text{P}(\text{CF}_3)_2]_2$ . Tebbe and Muetterties<sup>18</sup> report that green  $\text{Co}[\text{S}_2\text{PF}_2]_2$  reacts with water to give a blue sublimable solid which dissociated during attempted isolation and also that an <sup>19</sup>F nmr spectrum of  $\text{Pd}[\text{S}_2\text{PF}_2]_2$  in an acetonitrile-water solution indicated the presence of  $\text{F}_2\text{PS}_2^-$  and  $\text{F}_2\text{POS}^-$  but that some of the original dithiophosphinate was recovered by heating at 250°C in the liquid phase under nitrogen.

In the attempted preparations of  $\text{Co}[\text{S}_2\text{P}(\text{CH}_3)_2]_2$  from hydrated metal and ligand salts it was found that the extent of 0 for S replacement as measured by the infrared spectra of the products was dependent upon the total water concentration in the organic solvent used in the preparation. Thus, it was somewhat unexpected that aqueous solutions of 0.1 M in Co(II) halide salt and 0.2 M in  $^-\text{S}_2(\text{CH}_3)_2$  yielded the green tetrathio complex as a precipitate on standing as did mechanical mixing of the hydrated salts. The fate of the displaced sulfur in the organic solvent was undetermined since neither elemental sulfur nor gaseous sulfur compounds were detected in stoppered flask preparations of the blue complex  $\text{CoOS}_3\text{P}(\text{CH}_3)_4$ . Nevertheless, P-S bonds are well known<sup>68</sup> to be susceptible to hydrolysis with replacement of the sulfur atoms by oxygen and evolution of  $\text{H}_2\text{S}$ .



Fractional sublimation of blue  $\text{CoOS}_3\text{P}_2(\text{CH}_3)_4$  resulted in the separation of volatile green  $\text{Co}[\text{S}_2\text{P}(\text{CH}_3)_2]_2$  and white  $[(\text{CH}_3)_2\text{PS}]_2\text{O}$  from a black residue. The volatile products were identified by their infrared spectra, mass measurement of the parent ion-molecule in the mass spectra, and in the case of  $[(\text{CH}_3)_2\text{PS}]_2\text{O}$  by its  $^1\text{H}$  nmr spectrum which was characteristic of a symmetrical oxo bridged diphosphorus compound. The chemical analyses (C, H, and S) together with the thermogram (Table 4.2) indicate that the  $\text{CoOS}_3\text{P}_2(\text{CH}_3)_4$  complex decomposes according to the equation:



An analogous thermal decomposition must accompany the fractional sublimation of the other crude tetrahedral bis complexes  $\text{M}[\text{S}_2\text{P}(\text{CH}_3)_2]_2$  since  $[(\text{CH}_3)_2\text{PS}]_2\text{O}$  was always observed as a sublimable component.

#### 4.4 Mass Spectral Behavior

The ionization of the samples by electron impact in the production of mass spectra might be expected to yield fragments which reflect the thermal stability of the complexes. Since much of the spectral detail is not required for this discussion, the tabulated spectra are contained in Appendix B.

The most intense peak in the mass spectra of the complexes  $\text{OV}[\text{S}_2\text{PX}_2]_2$  with  $\text{X} = \text{CH}_3, \text{C}_6\text{H}_5, \text{OC}_2\text{H}_5, \text{F}$ , and  $\text{CF}_3$  was that of the parent ion-molecule. The simple loss of the O atom resulted in fairly intense peaks for all the substituents which is somewhat surprising in view of the usually robust nature<sup>106</sup> of the V-O bond,



but is consistent with the thermodynamic stability of V(III) with dithiophosphinate ligands. No diligand ions  $[S_2PX_2]_2^+$  were observed in the mass spectra where  $X = CH_3, C_6H_5$ , or F and the corresponding peaks where  $X = OC_2H_5$  and  $CF_3$  have ambiguous assignments in the absence of mass measurements and are of reduced intensity.

With the exceptions of the complexes  $M[S_2P(OC_2H_5)_2]_2$  and the Hg(II) compounds, the spectra of the bis complexes  $M[S_2PX_2]_2$  are dominated by the parent ions and those resulting from the loss of one ligand group with no diligand ion being observed. Where  $X = OC_2H_5$ , the spectra are complicated by the stepwise loss of  $C_2H_4$  units<sup>95</sup>. The mass spectra of the complexes  $Hg[S_2PX_2]_2$ ,  $X = CH_3, C_6H_5, F^{107}$ , and  $CF_3$  were dominated by the parent, diligand,  $Hg^+$ , and  $Hg^{++}$  ions. The mass spectrum of  $CoOS_3P_2(CH_3)_4$  was observed to be a composite of the spectra of  $Co[S_2P(CH_3)_2]_2$  and  $[(CH_3)_2PS]_2O$ .

Prominent ions observed in the spectra of the V(III) and Cr(III) complexes  $M[S_2PX_2]_3$ ,  $X = CH_3, C_6H_5, OC_2H_5, F$ , and  $CF_3$  were the parent ion-molecules and the parent minus one ligand group.

Peaks due to the ions  $SV[S_2PX_2]_2^+$  were weak but observable in the spectra of the V(III) compounds. In the spectra of the Fe(III) and Co(III) complexes, no parent peaks were observed with  $X = CH_3$  or  $C_6H_5$ , reduced parent peaks were observed with  $X = OC_2H_5, F$ , and  $CF_3$ , and in every case peaks corresponding to the M(II) complex were dominant. Excepted from the above generalizations is  $Fe[S_2P(OC_2H_5)_2]_3$  which was not included in this work, but it is not expected to behave differently. The observed spectra of the Co(III) and Fe(III) compounds also possess strong peaks attributable



to ligand ions  $[S_2PX_2]_2^+$  but again with an exception where X =  $C_6H_5$ . This latter exception is not understood as the thermograms of these phenyl substituted complexes clearly indicate that  $[S_2P(C_6H_5)_2]_2$  is a product of the thermal decomposition and the ion  $[S_2P(C_6H_5)_2]_2^+$  is observed in the spectrum of the Hg(II) complex where the source temperatures were comparable. The absence of diligand ions in the mass spectra of the V(III) and Cr(III) dithiophosphinates in conjunction with the voltammetric and thermal results render unlikely the eventual isolation of simple dithiophosphinate complexes of the divalent ions of these metals.

Consistent with the formulation  $Pt_2S_6P_4(CF_3)_8$ , the mass spectrum of this compound is dominated by a parent peak corresponding to the proposed<sup>45</sup> formulation and a fragment of half the dinuclear unit. All other ions (including one corresponding to  $Pt[S_2P(CF_3)_2]_2$ ) were not observed to contribute greatly to the total ionization. It is noted that the mass spectrum of a solid salt sample obtained from a cooled melt of  $K_2PtCl_4$  dissolved in  $[(CH_3)_3NH]^+[-S_2P(CF_3)_2]$  showed  $Pt[S_2P(CF_3)_2]_2^+$  as the most abundant ion with  $Pt_2S_6P_4(CF_3)_8^+$  present in nearly negligible amounts. Thus it may prove possible to isolate the complex  $Pt[S_2P(CF_3)_2]_2$  from molten salt reactions.

A brief and generalized summary of the fragmentations giving rise to metastable peaks is presented in Figure 4.1. It is also to be noted that  $M^{++}$  ions were generally observed only with the heavier metals Pt and Hg.



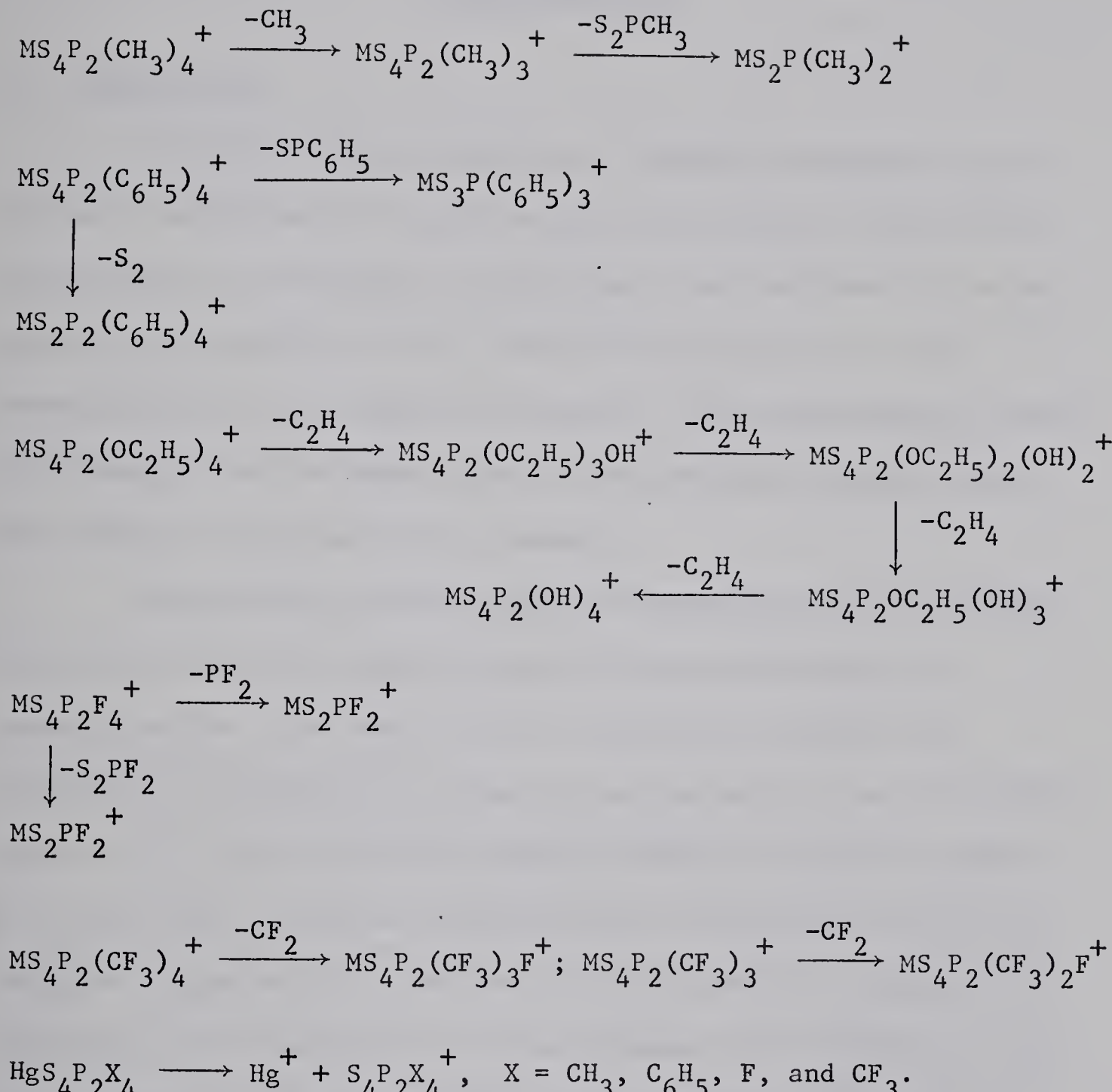


FIGURE 4.1: Mass spectral fragmentations usually resulting in metastable ions.



## CHAPTER 5

## MAGNETOCHEMISTRY

5.1 Introduction

Although both the electronic, spectral and magnetic properties of molecules are dependent upon the molecular energy level distributions the knowledge of the ground state obtainable from the magnetic properties provides a useful starting point for the interpretation of the electronic spectra. Hence the magnetic results are presented and discussed prior to the electronic spectral data with forward references where necessary.

Much of the present chapter is concerned with the results of static field bulk magnetic susceptibility measurements on powdered solids. The static field susceptibility results are presented most compactly in terms of the constants of the Curie-Weiss equation (2.6) and the derived magnetic moments contained in Table 5.1 so the more voluminous temperature-gram susceptibility data are relegated to Appendix C. The form of the Curie-Weiss equation used (equation (2.6)) results in the Weiss constant ( $\theta$ ) assuming the same sign as the coupling between the component magnetic dipoles of the compounds. However, ground state degeneracies and thermal population of higher term levels, among other possibilities, also affect the magnitude and even the sign of  $\theta^{62,63,108-110}$ . Thus the diagnostic value of  $\theta$  is dependent upon knowledge of its source. The three parameters A, B, and D of equation (2.7) are quite adequate to



describe (within experimental error) the temperature dependent magnetic behavior of most paramagnets at temperatures above -200°C. Failure of variations in A, B, and D to force the susceptibility data to yield a straight line is inferred to imply "magnetically concentrated" behavior<sup>62,63,108-113</sup>. For "normal" paramagnets, the effective magnetic moment is given by the equation<sup>62,63,108-113</sup>

$$\mu_{\text{eff}} = 2.828 \sqrt{\chi_M^{\text{corr}}(T-\theta)} \quad (5.1)$$

in units of Bohr magnetons where T is the temperature (°K) and  $\chi_M^{\text{corr}}$  is  $\chi_M$  corrected for the temperature independent susceptibility components.

The interpretation of the results is based upon the Ligand Field Theory as described in references 62, 63, 108-113.

## 5.2 Results and Discussion

### Zinc Group Complexes and Diamagnetic Corrections

As expected for a filled subshell configuration ( $d^{10}$ ), the complexes  $M[S_2PX_2]_2$ , where M = Zn, Cd, Hg, and X =  $CH_3$ ,  $C_6H_5$ ,  $OC_2H_5$ , F, and  $CF_3$  were found to be diamagnetic. Advantage was taken of the diamagnetism of the zinc complexes to estimate the diamagnetic susceptibilities of the ligand anions  $S_2^P(X_2^-)$ . The results are contained in Appendix C and are in reasonable agreement with values derived solely from Pascal's constants<sup>62,114</sup> with small differences of unknown origin in the cases of  $S_2^P(CH_3)_2$  and  $S_2^P(OC_2H_5)_2$ .

No separate account of the inherent diamagnetic component



of paramagnetic ions themselves were made. Thus the determinations of the temperature independent paramagnetism as  $TIP = D - \chi_M^D$  (equation (7), et seq.) result in TIP values that are inherently too small by the diamagnetism of the paramagnetic ion.

#### Oxovanadium(IV) Complexes

Vanadyl complexes usually possess a magnetic moment near the spin-only value of 1.73 BM consistent with a  $3d^1$  electronic configuration of the vanadium ion<sup>106</sup>. This "normal" behavior extends to the dithiocarbamates<sup>115</sup>. However, carboxylate complexes of the  $OV^{+2}$  ion<sup>84</sup> show distinct antiferromagnetic behavior which is different from that observed for the dinuclear Cu(II) carboxylates<sup>45</sup>. It has been suggested<sup>84</sup> that the vanadyl carboxylate magnetic behavior is the result of bridged polymeric chains compatible with  $V-O\cdots V-O\cdots$  interactions.

The respective normal magnetic moments of 1.77 BM (296°K) and 1.73 BM (298°K) recently reported for the blue complexes  $OV[S_2P(C_2H_5)_2]_2$ <sup>37</sup> and  $OV[S_2P(C_6H_5)_2]_2$ <sup>38</sup> are in agreement with the results of this work (Table 5.1) for the blue complexes where  $X = CH_3, C_6H_5$ , and  $OC_2H_5$ . The molecular packing observed<sup>15</sup> in the crystal structure of  $OV[S_2P(CH_3)_2]_2$  (Figure 3.2) suggests the absence of strong magnetic intermolecular interactions and is consistent with the small Weiss constants obtained for the blue compounds. The TIP values given in Table 5.1 for the compounds with  $X = CH_3, C_6H_5$ , and  $OC_2H_5$  are in rough agreement with the value  $100 \times 10^{-6}$  estimated by Ballhausen and Gray<sup>116</sup> for  $OVSO_4 \cdot 5H_2O$ .



TABLE 5.1

Static Field Magnetic Susceptibility Parameters for the Complexes  $M[S_2^{PX_2}]_n$ <sup>a</sup>

$M^{+n}$	$X$	$\mu_{eff}$ (B.M.)	$\theta$ ( $^{\circ}K$ )	A	B	TIP $\times 10^6$	
						Data fitting	Spectral analysis
$OV^{+2}$	$CH_3$	1.71(1.72)	- 0.98(-1.5)	2.72 (2.71)	2.7 (4.1)		6.3
	$C_6H_5$	1.71(1.76)	- 0.59(-5.1)	2.73 (2.59)	1.6 (13)		50
	$OC_2H_5$	1.64(1.66)	2.6 (0.7)	2.97 (2.91)	-7.6 (-2.1)		51
	F	2.49(2.25)	- 1.8 (17)	1.59 (1.29)	2.4 (-27)		-330
	$CF_3$	2.36(2.13)	- 7 (10)	1.44 (1.76)	10 (-18)		-329
	V <sup>+3</sup>	2.65(2.90)	- 3 (-20)	1.14 (0.950)	3.4 (18.8)		416
$V^{+3}$	$CH_3$	2.45(2.79)	- 1 (-26)	1.33 (1.02)	1.3 (27)		535
	$C_6H_5$	2.60(2.88)	- 1 (-21)	1.18 (0.962)	1.3 (20)		448
	$OC_2H_5$	2.65(2.87)	- 7 (-22)	1.14 (0.972)	8.6 (22)		373
	F	2.65(2.90)	- 1 (-20)	1.17 (0.954)	0.78(19)		454
	$CF_3$	3.84(3.93)	0 (-5)	0.542 (0.518)	0.18(2.3)		211
	Cr <sup>+3</sup>	3.87(3.93)	0 (-3)	0.535 (0.517)	0.09(1.6)		158
$Cr^{+3}$	$CH_3$	3.85(3.86)	1 (0.5)	0.541 (0.537)	-0.63(-0.29)		33
	$C_6H_5$	3.85(3.94)	0 (-4)	0.539 (0.515)	-0.16(1.9)		227
	$OC_2H_5$	3.84(3.93)	- 1 (-6)	0.543 (0.518)	0.80(3.0)		223
	F	5.86(6.06)	- 8 (-14)	0.233 (0.217)	1.8 (3.1)		737
	$CF_3$	5.92(5.89)	-21 (-20)	0.228 (0.230)	4.7 (4.6)		- 95
	Mn <sup>+2</sup>	6.03(5.93)	-38 (-35)	0.220 (0.227)	8.4 (7.8)		-317
		5.86(5.88)	- 5 (-6)	0.233 (0.231)	1.2 (1.3)		88



TABLE 5.1 (cont'd)

Static Field Magnetic Susceptibility Parameters for the Complexes  $M[S_2PX_2]_n$ <sup>a</sup>

$M^n$	X	$\mu_{eff}$ (B.M.)	$\theta$ ( $^{\circ}K$ )	A	B	TIP $\times 10^6$
				Data fitting		Spectral analysis
Fe <sup>+3</sup>	C <sub>6</sub> H <sub>5</sub>	5.91(5.98)	0 (-2)	0.229(0.224)	0.09(0.55)	252
Fe <sup>+2</sup>	CH <sub>3</sub>	5.01(5.11)	-8 (-12)	0.318(0.306)	2.7 (3.6)	294
	C <sub>6</sub> H <sub>5</sub>	5.40(5.51)	-31 (-35)	0.274(0.263)	8.5 (9.3)	334
F		5.74(5.52)	-45 (-37)	0.243(0.263)	11.0 (9.8)	-678
CF <sub>3</sub>		5.17(5.44)	-10 (-20)	0.300(0.270)	3.0 (5.4)	874
Co <sup>+2</sup>	CH <sub>3</sub>	4.38	-11	0.418	4.7	443 <sup>b</sup>
	C <sub>6</sub> H <sub>5</sub>	4.21	-9	0.451	4.2	443 <sup>b</sup>
OC <sub>2</sub> H <sub>5</sub>		5.49	-224	0.265	59	422 <sup>b</sup>
F		4.43	-17	0.407	7.1	-367
CF <sub>3</sub>		4.35	-22	0.422	9.4	874
CoOS <sub>3</sub> P <sub>2</sub> (CH <sub>3</sub> ) <sub>4</sub>		4.11	-8	0.474	3.6	734
HgCo(NCS) <sub>4</sub>		4.21	1	0.451	-0.38	1140
						501
						428 <sup>d</sup>

<sup>a</sup> Magnetic susceptibilities fitted to the Curie-Weiss equation,  $X_M = \frac{N\beta^2}{3k} \cdot \frac{\mu_{eff}^2}{T-\theta} + X_M^{Dia.} + TIP$  in the form  $1/X_M^{corr} = AT + B$  where  $X_M^{corr} = X_M - (X_M^{Dia.} + TIP)$  and  $\frac{N\beta^2 \mu_{eff}^2}{3k}$  is the Curie constant. Values in parentheses were derived without a TIP correction.

<sup>b</sup> TIP =  $8N\beta^2 / |10Dq|$

<sup>c</sup> TIP =  $4N\beta^2 / |10Dq|$

<sup>d</sup> Reference 126.



The solid state magnetic susceptibilities of the black complexes  $\text{OV}[\text{S}_2\text{PF}_2]_2$  and  $\text{OV}[\text{S}_2\text{P}(\text{CF}_3)_2]_2$  could not be fitted to the Curie-Weiss equation without assuming large "negative" TIP values (Table 5.1). When no TIP "correction" was applied to the susceptibility data the Weiss constants became quite large and positive (Table 5.1) possibly indicating ferromagnetic behavior. However on the basis of the simple Curie law (no TIP or  $\theta$  terms) a two-fold increase in the field parameter  $H \cdot \frac{\partial H}{\partial s}$  (equation 2.4) decreased the calculated magnetic moment by roughly 10% while a reduction in temperature increased the moments for both complexes. Such behavior is anomalous even for ferromagnets<sup>62,63,108-113</sup> and cannot be simply explained in terms of impurities since these would necessarily be volatile in order to co-sublime with the complexes during purification. Solution susceptibility measurements<sup>55</sup> by the Evans (nmr) method yielded magnetic moments of 1.75 BM ( $X = \text{F}$ ) and 1.77 BM ( $X = \text{CF}_3$ ) in 10% (v/v) toluene/benzene solutions where the paramagnetic susceptibilities were calculated from the relative chemical shifts of the methyl protons. Thus it appears that the interaction responsible for the anomalous solid state magnetic behavior of these complexes is disrupted upon dissolution.

Powdered  $\text{OV}[\text{S}_2\text{P}(\text{CF}_3)_2]_2$  gave<sup>55</sup> a broad epr spectrum centered at  $g \sim 2.3$  in support of the high moments determined from the Faraday method susceptibility measurements. The epr data obtained<sup>55</sup> from chloroform solutions at ambient temperatures and glasses formed from 3:1 (v/v) chloroform-isopropanol or pentane-isopropanol solutions at liquid nitrogen temperatures are collected



in Table 5.2 with data from other sources<sup>39</sup> for comparison. The spectra consisted of the expected 24 lines (octet of triplets) resulting from coupling of the uncompensated electron spin with the <sup>51</sup>V nuclear spin ( $I = 7/2$ ) and the two equivalent <sup>31</sup>P nuclear spins ( $I = 1/2$ ). In no case was super-hyperfine coupling to the substituents resolved.

Apart from the differing coupling constants, the spectra were further distinguished by significantly different line widths. While the lines of the complexes with  $X = \text{CH}_3$  and  $\text{CF}_3$  were narrow (~6 gauss) and well resolved, the spectra of the complexes with  $X = \text{C}_6\text{H}_5$ ,  $\text{OC}_2\text{H}_5$ , and F were complicated by line widths nearly twice as large causing extensive overlap of lines at the high field end of the spectra. It is notable that the line widths do not appear to be a strong function of molecular size and that the substituents which are classically thought capable of participation in the  $\pi$ -type bonding with the P atoms produce the widest lines. However, there appears to be no clear correlation between the line widths and the substituent electrical effects (Table 3.7).

The <sup>31</sup>P coupling constants  $A^P$  vary in accord with the frequency of the M-S vibrations (Chapter 3) suggesting that a shorter M-S bond length coincides with a shorter V-P separation resulting in an increased magnitude of  $A^P$ . While  $A^P$  appears to be isotropic within the accuracy of the measurements,  $A^V$  is anisotropic to the qualitative degree expected in view of the presumed molecular geometry in solutions.

The variation of  $A^V$  with substituent appears to support the



TABLE 5.2

EPR Parameters of  $\text{OV}[\text{S}_2\text{PX}_2]_2$  Systems<sup>a</sup>

$X =$	$\text{C}_6^{\text{H}}\text{S}$	$\text{OC}_2^{\text{H}}\text{S}$	$\text{OC}_2^{\text{H}}\text{S}^{\text{b}}$	$\text{OC}_2^{\text{H}}\text{S}$	$\text{C}_3^{\text{H}}\text{S}^{\text{b}}$	$\text{CH}_3$	F	$\text{CF}_3$
$g_{\text{av}}$	1.980	1.981	1.980	1.986	1.985	1.975	1.974	1.985
$g_{\perp}$	1.981	1.987	1.991	1.990	1.984	1.981		
$g_{  }$	1.960	1.967	1.971	1.970	1.960	1.963		
$A_{\text{av}}^V$ (gauss)	94.7	94.5	93.8	94	95	94.8	100.0	100.9
$A_{\perp}^V$ (gauss)	60	57.9	66.7	67	62	56.8		
$A_{  }^V$ (gauss)	169	167.8	161.9	162	167	167		
$A_{\text{av}}^P$ (gauss)	33.7	51.3	45.5	49	28	33.7	59.6	33.7
$A_{\perp}^P$ (gauss)	34.2	50.6	51.6	52	28	33		
$A_{  }^P$ (gauss)	34.2	52.6	53.2	52	28	34.7		

a  $A^V$  refers to hyperfine splitting of vanadium;  $A^P$  that of phosphorus. 55

b From reference 39.



concept of transduced substituent electrical effects by the following arguments. Defining a Cartesian coordinate system for the molecules  $\text{OV}[\text{S}_2\text{PX}_2]_2$  ( $C_{2v}$  symmetry) such that the OV and  $\text{PX}_2$  groups lie in the  $xz$  plane with the O-V bond on the  $z$  axis, then both the vanadium  $4s$  and  $3d_{x^2-y^2}$  orbitals are bases for  $A_1$  irreducible representations. Thus these orbitals will participate in the same MO's. The substituent dependence of  $A^P$  and electrostatic considerations support a principally vanadium  $3d_{x^2-y^2}$  character to the MO containing the odd electron<sup>39</sup>. Since the V  $3d_{x^2-y^2}$  orbital lies in the  $xy$  plane, the folding of the chelate rings away from the  $xy$  plane means that the "x" lobes of the  $d_{x^2-y^2}$  orbital project out and over the chelate rings. Hence this orbital is probably involved in bonding interactions affected by the  $\pi$ -type acidity of the ligands (although overlap is of the  $\sigma$  type). Qualitative MO considerations indicate that the fractional contribution by component orbitals to a MO is directly proportional to the component orbital overlap and inversely proportional to their energy difference. With reference to Figure 6.4 (the  $\pi$ -type label on the " $d_{x^2-y^2}$ " MO is arbitrary), a strong bonding interaction with the  $d_{x^2-y^2}$  atomic orbital is anticipated to raise the energy of the antibonding " $d_{x^2-y^2}$ " MO and thus increase the V  $4s$  orbital contribution and the magnitude of  $A^V$  (assuming a Fermi contact mechanism)<sup>110</sup>. Without a concurrent decrease in bond lengths (increased orbital overlap), the magnitude of  $A^P$  may be expected to be reduced by the same considerations. Transduction of the substituent electrical data given in Table 3.7 predicts that the ligands with  $X = F$  and  $\text{CF}_3$  should be the most  $\pi$  acidic and hence form complexes  $\text{OV}[\text{S}_2\text{PX}_2]_2$  with the largest vanadium couplings in



agreement with experiment (Table 5.2). The extent to which geometrical factors determine the magnitude of  $A^V$  is unknown and precludes speculation on the origin of smaller trends in the data.

### Vanadium(III) Complexes

The ion  $V^{+3}$  has  $3d^2$  electronic configuration for which the Orgel diagram predicts a  $^3T_{1g}$  ground term in an octahedral field<sup>74</sup>. The magnetic properties of a  $^3T_{1g}$  term under simultaneous perturbation by spin-orbit coupling and a trigonal ligand field component has been treated in theory by Figgis, et al.<sup>117</sup>. The splittings of the  $^3T_{1g}$  term are qualitatively indicated in Figure 5.1<sup>112</sup>. There is some uncertainty as to the relative ordering of the  $^3E$  and  $^3A_2$  terms although spectral studies<sup>31</sup> on single crystals (of  $V[S_2P(OC_2H_5)_2]_3$  diluted in the host lattice of  $In[S_2P(OC_2H_5)_2]_3$ ) support a  $^3A_2$  ground term. The magnetic susceptibility of guanidinium hexaquo-vanadium(III) sulfate is reported<sup>118</sup> to drop rapidly below 25°K in confirmation of a non-magnetic ground level. The values  $\delta_1 \sim 800K$  and  $\delta_2 \sim 7.2K$  were estimated<sup>118</sup> for this latter compound.

The complexes  $V[S_2PX_2]_3$  with  $X = CH_3, C_6H_5, OC_2H_5, F$ , and  $CF_3$  were found to obey the Curie-Weiss equation very closely in the temperature range 90 - 300°K with small Weiss constants (Table 5.1). When no TIP corrections were applied to the susceptibility data, large and negative Weiss constants indicating antiferromagnetic coupling resulted in contradiction with resultant magnetic moments which exceeded the spin-only value of 2.83 BM (except in the case of  $V[S_2P(C_6H_5)_2]_3$ ) (Table 5.1). However, point calculations from the susceptibility data, e.g. for  $V[S_2P(CF_3)_2]_3$ , assuming the simple



Curie law (to the neglect of  $\theta$  and TIP) yielded  $\mu_{313.3} = 2.82$  BM and  $\mu_{89.2} = 2.67$  BM. Therefore in apparent agreement with the predictions of the theory<sup>117</sup> the moment decreases with temperature, but the decrease is obtained at the expense of a TIP term contribution. If the value  $g_{av} = 1.87$  is assumed as found<sup>119</sup> for vanadium(III) corundum which is postulated to also possess a trigonally distorted ligand field about the vanadium atom, then the expression<sup>110</sup>

$$\mu_{eff} = g_{av} \sqrt{S(S+1)} \quad (5.1)$$

yields a moment of 2.64 BM ( $S=1$ ) in excellent agreement with the TIP corrected magnetic moments in Table 5.1.

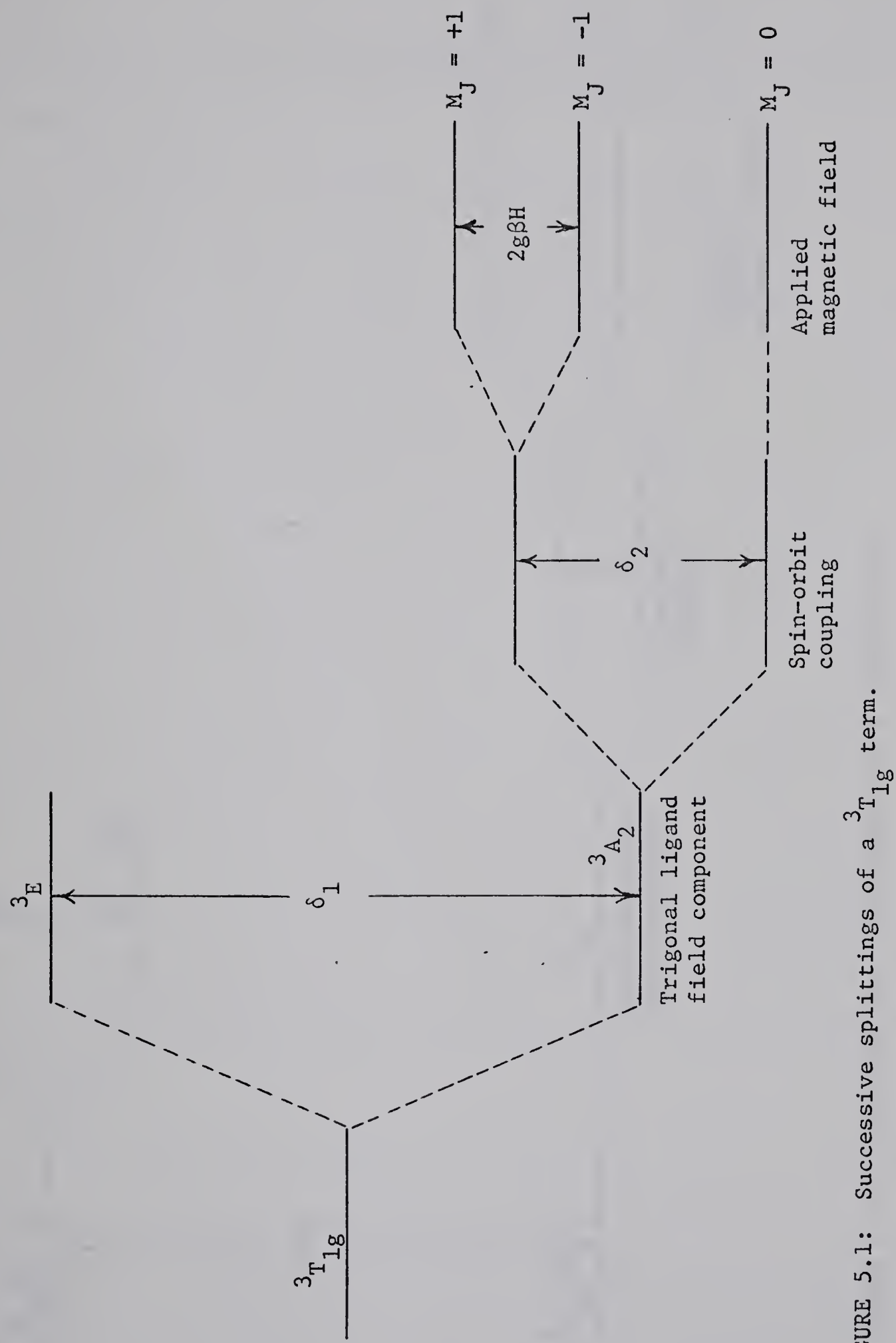
Clearly liquid helium temperature measurements are required to provide the definitive information on the ground states of these vanadium(III) dithiophosphinates. Unfortunately, short relaxation times and presumably a large value of  $\delta_1$  (Figure 5.1) have precluded the observation of epr spectra at ambient or liquid nitrogen temperatures<sup>28,54</sup>. Recently, the respective values  $\mu_{eff} = 2.7, 2.82$  and 2.84 BM at ambient temperatures were reported for the complexes  $V[S_2P(C_6H_5)_2]_3$ <sup>36</sup>,  $V[S_2P(C_2H_5)_2]_3$ <sup>37</sup>, and  $V[S_2P(C_3H_7)_2]_3$ <sup>37</sup> in agreement with the data in Table 5.1.

#### Chromium(III) Complexes

The Orgel diagram<sup>74</sup> for a  $3d^3$  electronic configuration in an octahedral ligand field predicts a  ${}^4A_{2g}(F)$  ground term. The term splittings induced by trigonal distortion, spin-orbit coupling, and an applied magnetic field are qualitatively depicted in Figure 5.2<sup>112</sup>.

The complexes  $Cr[S_2PX_2]_3$  with  $X = CH_3, C_6H_5, OC_2H_5, F$ , and  $CF_3$  were







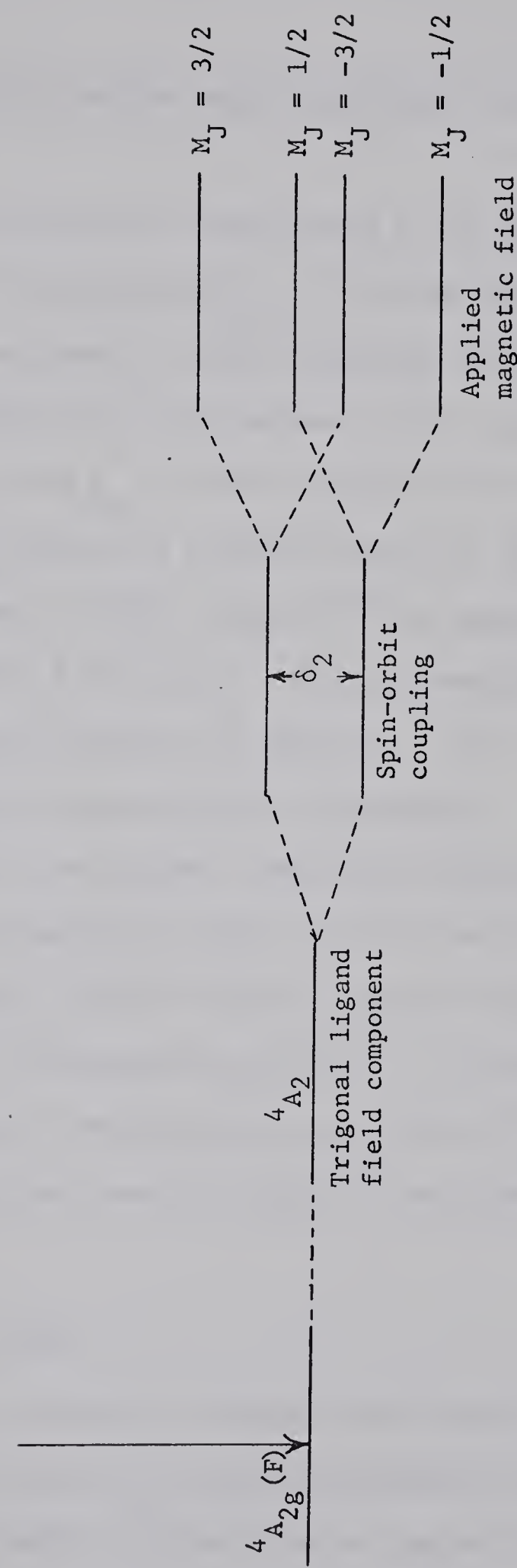
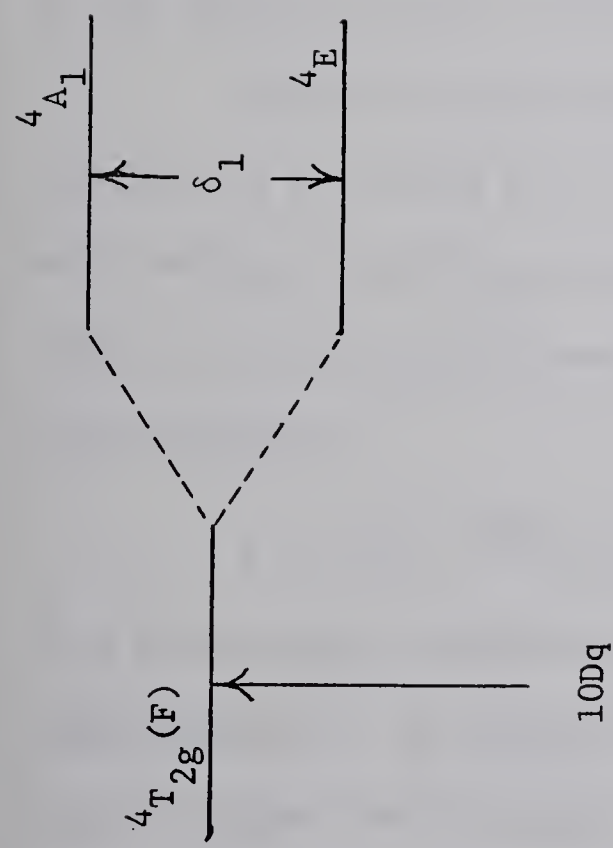


FIGURE 5.2: Successive term splittings for a Cr(III) ion.



found to obey the Curie-Weiss equation very closely with effectively zero  $\theta$ -values (Table 5.1).

Simple Curie law calculations (neglecting  $\theta$  and TIP) for  $\text{Cr}[\text{S}_2\text{P}(\text{CF}_3)_2]_3$  gave  $\mu_{303.3} = 3.90 \text{ BM}$  and  $\mu_{92.9} = 3.82 \text{ BM}$  which as with the V(III) complexes represents a slight reduction in moment with temperature. The latter values are to be compared with a spin-only moment of 3.87 BM. If the value  $g_{av} = 1.9905$  (obtained from the epr spectra of  $\text{Cr}[\text{S}_2\text{P}(\text{OC}_2\text{H}_5)_2]_3$  diluted in a single crystal of the isostructural<sup>31</sup> and diamagnetic Co(III) complex)<sup>120a</sup> is assumed, equation (5.1) gives a moment of 3.85 BM ( $S = 3/2$ ) in excellent agreement with the TIP corrected moments in Table 5.1. Once again inclusion of a TIP term in the expression for the magnetic susceptibility compensates for an apparent temperature dependence of the magnetic moment for temperatures above liquid nitrogen.

Mixing of the ground term with higher terms via spin-orbit coupling is accounted for in the measured g-values<sup>111</sup>. Considering only mixing of the  $^4A_{2g}$  ground term with the first excited  $^4T_{2g}$  term via the spin-orbit coupling operator, Figgis<sup>111</sup> has determined the expression

$$g = g_o (1 - 4k^2 \lambda_o / |10Dq|) \quad (5.2)$$

to a first order perturbation within the Crystal Field Theory approximations. In equation (5.2),  $g_o$  is the free electron value,  $\lambda_o$  is the free ion term spin-orbit coupling constant (as defined by Figgis<sup>111</sup>),  $k$  is the electron delocalization (orbital reduction) factor, and  $10Dq$  has its usual significance. For  $\text{Cr}[\text{S}_2\text{P}(\text{OC}_2\text{H}_5)_2]_3$



with  $g = 1.9905^{120a}$ ,  $\lambda_o = 91k^{111}$ ,  $10Dq = 14.4$  kK (Chapter 6), and  $g_o = 2.0023^{110}$ , the complexed ion spin-orbit coupling constant<sup>111</sup>  $\lambda = k\lambda_o \sim 44$  K, where  $k = 0.48$ .

Mixing of the ground  $^4A_{2g}$  term with the first excited  $^4T_{2g}$  term via the magnetic moment operator results in a TIP term for which Figgis<sup>111</sup> has determined the expression

$$\text{TIP} = 8k^2 N\beta^2 / |10Dq| \quad (5.3)$$

where  $N$  is the Avogadro number and  $\beta$  is 1 BM. As seen from the data in Table 5.1, there is only order of magnitude agreement between the "empirical" TIP values and those obtained from equation (5.3) using the spectral values of  $10Dq$  (Chapter 6) and assuming  $k = 1$ .

At a radiation frequency of 9320 MHz, Garif'yanov, et al.<sup>120b</sup> observed the epr spectra of  $\text{Cr}[\text{S}_2\text{P}(\text{C}_3\text{H}_7)_2]_3$  and  $\text{Cr}[\text{S}_2\text{P}(\text{OC}_2\text{H}_5)_2]_3$  in toluene solutions to consist of single broad lines ( $\Delta H \sim 300$  gauss) with  $g = 1.97$  at ambient temperatures. At an irradiating frequency of only 300 MHz a narrow ( $\Delta H \sim 40$  gauss) asymmetric line with  $g = 2.5$  at  $77^\circ\text{K}$  was found<sup>120b</sup>. Such a g-value is stated<sup>120b</sup> to be observable at low frequency only if  $\delta_2$  (Figure 5.2) is somewhat greater than the high frequency field quanta, i.e.  $\delta_2 > 0.01\text{K}$ . The epr studies<sup>120</sup> of the Cr(III) dithiophosphinates have revealed nearly isotropic g-values consistent with small distortions from cubic coordination of the metal atom. The line widths were too broad to observe hyperfine structure from the P atoms.

The magnetic moments of  $\text{Cr}[\text{S}_2\text{P}(\text{C}_2\text{H}_5)_2]_3^{121}$  and  $\text{Cr}[\text{S}_2\text{P}(\text{OR})_2]_3^{34}$  complexes where R is an alkyl group are reported to be close to the



spin-only value as determined by the Gouy method. Solution susceptibility measurements (Evans (nmr) method) on the latter complexes<sup>34</sup> and  $\text{Cr}[\text{S}_2\text{PF}_2]_3$ <sup>18</sup> similarly resulted in near spin-only values.

#### Manganese(II) and Iron(III) Complexes

The ions  $\text{Mn}^{+2}$  and  $\text{Fe}^{+3}$  have the common electronic configuration  $3d^5$  leading to a  ${}^6A_1$  ground term in ligand fields insufficiently strong to cause electron pairing<sup>111-112</sup>. Since no other sextet terms can arise from a  $d^5$  spin-free configuration, the TIP and orbital contributions are anticipated to be small<sup>111</sup>. The spin-only value for five unpaired electrons is 5.92 BM.

The magnetic moments of the "tetrahedral" manganese complexes (Table 5.1) are close to the spin-only value but range more widely than might have been expected for a magnetically simple system. The large  $\theta$ -values of the manganese compounds signify some degree of magnetically concentrated behavior, but the antiferromagnetism implied by the negative sign is not consistent with the large moment obtained for  $\text{Mn}[\text{S}_2\text{PF}_2]_2$ . The structural variation with substituents (Chapter 3) may account for the unexpectedly large differences in the Curie-Weiss equation parameters given in Table 5.1. Tebbe and Muettterties<sup>18</sup> found that  $\text{Mn}[\text{S}_2\text{PF}_2]_2$  in solution gave  $\mu_{293} = 5.9$  BM by the Evans (nmr) method. The results obtained for these Mn(II) dithiophosphinates agree quite well with values found<sup>122-123</sup> for tetrahedral complexes of Mn(II) with monodentate ligands.

$\text{Fe}[\text{S}_2\text{P}(\text{C}_6\text{H}_5)_2]_3$  was the only Fe(III) complex studied magnetically in the course of this work. The more effective magnetic



dilution in the tris complexes versus the bis complexes is demonstrated by the very small Weiss constant and more nearly spin-only value of the magnetic moment for  $\text{Fe}[\text{S}_2\text{P}(\text{C}_6\text{H}_5)_2]_3$  as compared with values for the  $\text{Mn}[\text{S}_2\text{PX}_2]_2$  complexes (Table 5.1). However, the moment 6.23 BM ( $\theta = -1$ ) reported by Kuchen and Judat<sup>75</sup> for  $\text{Fe}[\text{S}_2\text{P}(\text{C}_2\text{H}_5)_2]_3$  is unexpectedly large. Ewald, et al.<sup>61</sup>, found near spin-only moments decreasing slightly with temperature (96 - 300°K) and pressure (1 - 3000 atm.) for the complexes  $\text{Fe}[\text{S}_2\text{P}(\text{OR}_2)]_3$  with R =  $\text{CH}_3$ ,  $\text{C}_2\text{H}_5$ , n- $\text{C}_3\text{H}_7$  and i- $\text{C}_3\text{H}_7$ .

Thus the known magnetic data for the complexes  $\text{Fe}[\text{S}_2\text{PX}_2]_3$  clearly places them on the high-spin side of the ground state "cross-over" ( $^6\text{A}_1 \longleftrightarrow ^2\text{T}_2$ ) observed<sup>61</sup> in many other dithioacid ligand systems.

Garif'yanov, et al.<sup>124</sup>, observed the epr spectra of  $\text{Mn}[\text{O}_2\text{P}(\text{OC}_2\text{H}_5)_2]_2$  and  $\text{Fe}[\text{O}_2\text{P}(\text{OC}_2\text{H}_5)_2]_3$  in toluene solutions but were unable to obtain spectra of  $\text{Mn}[\text{S}_2\text{P}(\text{OC}_2\text{H}_5)_2]_2$  or  $\text{Fe}[\text{S}_2\text{P}(\text{OC}_2\text{H}_5)_2]_3$  between 4.2 and 350°K. For  $\text{Mn}[\text{O}_2\text{P}(\text{OC}_2\text{H}_5)_2]_2$  these latter authors<sup>124</sup> reported  $g_{\text{av}} = 2.000 \pm 0.002$  and  $A^{\text{Mn}} = 93 \pm 3$  gauss while for  $\text{Fe}[\text{O}_2\text{P}(\text{OC}_2\text{H}_5)_2]_3$  the value  $g_{\text{av}} = 2.001 \pm 0.002$  with line widths of 138.6 gauss at 295°K and 144 gauss at 77°K was found.

#### Iron(II) and Cobalt(III) Complexes

Although the free ions  $\text{Fe}^{+2}$  and  $\text{Co}^{+3}$  both have the electronic configuration  $3d^6$ , the ligand field is sufficiently large and the interelectronic repulsions sufficiently small to result in diamagnetic tris complexes  $\text{Co}[\text{S}_2\text{PX}_2]_3$  with X =  $\text{CH}_3$ ,  $\text{C}_6\text{H}_5$ ,  $\text{OC}_2\text{H}_5$ , F, and  $\text{CF}_3$  whereas the tetrahedral bis complexes  $\text{Fe}[\text{S}_2\text{PX}_2]_2$  complexes with X =  $\text{CH}_3$ ,  $\text{C}_6\text{H}_5$ , F, and  $\text{CF}_3$  are spin-free. The spin-only value for four unpaired electrons is 4.90 BM.



As generally found<sup>125</sup> for tetrahedral complexes of Fe(II), the magnetic moments of the complexes  $\text{Fe}[\text{S}_2\text{PX}_2]_2$  are higher than the spin-only value expected for six electrons restricted to five d orbitals (Table 5.1). The moment  $\mu_{303} = 5.2 \text{ BM}$  determined for  $\text{Fe}[\text{S}_2\text{PF}_2]_2$  in solution by Tebbe and Muetterties<sup>18</sup> is taken as evidence that the high moments are not due to some cooperative phenomenon characteristic of the solid state. However, as with the Mn(II) dithiophosphinates, the large negative Weiss constants are symptomatic of non-simple behavior as reinforced by the magnitudes and scatter of the empirical TIP values in Table 5.1. The structural variations with substituent (Chapter 3) must account for a large part of the magnetic variations.

The Orgel diagram<sup>74</sup> for a d<sup>6</sup> ion in a tetrahedral ligand field predicts that the free ion <sup>5</sup>D ground term should be split into a lower <sup>5</sup>E term and an upper <sup>5</sup>T<sub>2</sub> term. By consideration of spin-orbit coupling between these two terms, Figgis<sup>111</sup> arrived at the equation

$$\mu_{\text{eff}} = \mu_{\text{eff}}^{\text{so}} \frac{(1 - 2k^2 \lambda_o)}{|10Dq|}, \quad (5.4)$$

while coupling between the two terms via the magnetic moment operator gave

$$\text{TIP} = 4k^2 N\beta^2 / |10Dq|, \quad (5.5)$$

where the symbols have their previously defined significance (see equations 5.2 and 5.3). Taking  $|10Dq| \sim 7\text{kK}$  (Chapter 6) equations (5.4) and (5.5) lead to the impossible result that  $k$  is greater than unity. Thus the assumptions of the theory leading to equations (5.4) and (5.5) require re-evaluation. Nevertheless, TIP values estimated



from equation (5.5) with  $k = 1$  are included in Table 5.1.

Clark, et al.<sup>125</sup>, have attempted to account for the high moments obtained for tetrahedral Fe(II) halide complexes by inclusion of a contribution from the  $3d^5 4s^1$  configuration. Their calculations<sup>125</sup> indicated that by reduction of the positive charge at the  $\text{Fe}^{+2}$  ion, terms involving two more unpaired electrons could be brought into thermal range of the ground term. The free ion  $\text{Fe}^+$  configuration  $3d^6 4s^1$  has a ground term  $^6D$  with five unpaired electrons<sup>125</sup>. It is clear that consideration of a single electronic configuration is an oversimplification of the problem. Clark, et al.<sup>125</sup>, noted further than without TIP corrections, the magnetic moments of the Fe(II) halide complexes decreased monotonically with temperature. Point calculations (neglecting TIP and  $\theta$ ) for  $\text{Fe}[\text{S}_2\text{PF}_2]_2$  gave  $\mu_{303.3} = 5.20 \text{ BM}$  and  $\mu_{87.1} = 4.60 \text{ BM}$  in agreement with the behavior observed<sup>125</sup> for the tetrahedral halide complexes.

### Cobalt(II) Complexes

The Orgel diagram<sup>74</sup> for a  $3d^7$  electronic configuration in a tetrahedral ligand field predicts a  $^4A_2$  ground term. The magnetic moments of the complexes  $\text{Co}[\text{S}_2\text{PX}_2]_2$  with  $X = \text{CH}_3$ ,  $\text{C}_6\text{H}_5$ , F, and  $\text{CF}_3$  significantly exceed the spin-only value of 3.87 BM (Table 5.1). An explanation of the high moments can be developed parallel to that discussed for the Fe(II) complexes<sup>125</sup>. By consideration of spin-orbit and magnetic moment operator coupling between the ground  $^4A_2$  and first excited  $^4T_2$  terms, Figgis<sup>111</sup> derived the expressions

$$\mu_{\text{eff}} = \mu_{\text{eff}}^{\text{so}} \left( 1 - 4k^2 \lambda_o / |10Dq| \right) \quad (5.6)$$



and

$$\text{TIP} = 8k^2 N\beta^2 / |10Dq|. \quad (5.7)$$

From the spectral results of Chapter 6 and equation (5.6),  $k$  was calculated to be near unity. The TIP values calculated using  $k = 1$  in equation (5.7) are included in Table 5.1 for comparison with the empirical values.

Tebbe and Muetterties<sup>18</sup> present rather puzzling results for  $\text{Co}[\text{S}_2\text{PF}_2]_2$  in such solvents as heptane and 1,2-dichloroethane. Gouy method measurements gave  $\mu_{\text{eff}} = 5.1$  BM whereas Evans (nmr) method measurements gave  $5.9 - 6.2$  BM<sup>18</sup>. Both these latter sets of values are high in comparison with the solid state results given in Table 5.1. Mukherjee, et al.<sup>14a</sup>, found  $\mu_{298} = 4.37$  BM for  $\text{Co}[\text{S}_2\text{P}(\text{C}_6\text{H}_5)_2]_2$  in precise agreement with the TIP uncorrected value found in this study. Kuchen and Judat<sup>75</sup> report the values  $\mu_{\text{eff}} = 4.83 \pm 0.05$  BM ( $\theta = -49^\circ$ ) and  $\mu_{295} = 4.46$  BM (calculated from the simple Curie equation) for  $\text{Co}[\text{S}_2\text{P}(\text{C}_6\text{H}_5)_2]_2$ . No mention of TIP was made in this latter report<sup>75</sup> such that the large moments and  $\theta$ -value probably resulted from its neglect.

The poor analytical data obtained for  $\text{Co}[\text{S}_2\text{P}(\text{OC}_2\text{H}_5)_2]_2$  (Table 2.1) render unreliable the values included in Table 5.1, even though the electronic spectra of dissolved samples were in agreement with published spectra<sup>99</sup>. It is believed that these preliminary results establish  $\text{Co}[\text{S}_2\text{P}(\text{OC}_2\text{H}_5)_2]_2$  as a genuine anomaly in this series of Co(II) dithiophosphinates and worthy of further study.

The results obtained for  $\text{HgCo}(\text{NCS})_4$  (Table 5.1) are slightly different from the values  $\mu_{\text{eff}} = 4.32$  BM ( $\theta = -4$ ,  $\text{TIP} = 428 \times 10^{-6}$ )



previously reported<sup>126</sup>, although agreement is good for TIP uncorrected values at higher temperatures. The diamagnetic correction applied herein was obtained from the measured diamagnetic susceptibility of  $\text{HgZn}(\text{NCS})_4$ , corrected for the  $\text{Zn}^{++}$  ion<sup>114</sup> (Appendix C).

#### Divalent Nickel Group Complexes

The complexes  $\text{M}[\text{S}_2\text{PX}_2]_2$  with  $\text{M} = \text{Ni}, \text{Pd}, \text{Pt}$  and  $\text{X} = \text{CH}_3$ ,  $\text{C}_6\text{H}_5$ ,  $\text{OC}_2\text{H}_5$ ,  $\text{F}$ , and  $\text{CF}_3$  (except Pt) are uniformly diamagnetic in support of a general planar conformation.  $\text{Ni}[\text{S}_2\text{PF}_2]_2$  was shown<sup>18</sup> to be diamagnetic even in the molten state ( $\text{mp} \sim 43^\circ\text{C}$ ). The  $^{19}\text{F}$  nmr spectra of the complexes with  $\text{X} = \text{F}^{18}$  and  $\text{CF}_3^{56}$  are consistent with a diamagnetic species in solution.  $\text{Pt}_2\text{S}_6\text{P}_4(\text{CF}_3)_8$  was also determined to be diamagnetic in the solid state. The absence of planar  $\rightleftharpoons$  tetrahedral conformation equilibria<sup>30</sup> in this dithiophosphinate system is quite certain.

#### Copper(II) Complexes

No divalent metal ion complex  $\text{M}[\text{S}_2\text{PX}_2]_2$  has yet been isolated for any coinage metal (Cu, Ag, or Au). The sole reliable source of information concerning these Cu(II) complexes has been the epr spectra obtained from organic solvent solutions in which the Cu(II) complexes with  $\text{X} = \text{R}$  and  $\text{OR}$  ( $\text{R}$  is an alkyl or aryl group)<sup>39</sup> have a sufficiently long lifetime to allow observation of a spectrum before spontaneous reduction of the metal ion occurs (cf Table 4.1). Only the epr spectrum of  $\text{Cu}[\text{S}_2\text{P}(\text{C}_6\text{H}_5)_2]_2$  was observed in the course of this work and was found to be in agreement with a previously published spectrum<sup>39</sup>. Nevertheless, this system provides a further test of the substituent effect hypotheses developed herein.



relative to the R substituents. Since shorter bond lengths imply better overlap of atomic orbitals, the observed orders of both  $A_{\text{OR}}^{\text{Cu}}$  and  $A_{\text{R}}^{\text{P}}$ , i.e.  $A_{\text{OR}} > A_{\text{R}}$ , is accounted for by the substituent electrical effects. The small differences in coupling constants due to the changes in the R groups also appear ordered according to the Hammett-Taft parameters for the R groups (Table 3.7).

The compounds  $\text{CuS}_2\text{PX}_2$  with  $\text{X} = \text{CH}_3$ ,  $\text{C}_6\text{H}_5$ ,  $\text{OC}_2\text{H}_5^{39}$ ,  $\text{F}^{18}$  and  $\text{CF}_3$  were all diamagnetic as expected for a closed shell configuration ( $3d^{10}$ ). Other Cu(I), Ag(I) and Au(I) complexes bearing other substituents are undoubtedly also diamagnetic<sup>13,22,39</sup>.

### 5.3 Summary and Conclusions

It is quite clear that magnetic susceptibility measurements at and above liquid nitrogen temperatures are inadequate to unambiguously test the present theories of temperature dependent magnetism when applied to dithiophosphinates in particular. With the exceptions of  $\text{OV}[\text{S}_2\text{PF}_2]_2$ ,  $\text{OV}[\text{S}_2\text{P}(\text{CF}_3)_2]_2$ , and  $\text{Co}[\text{S}_2\text{P}(\text{OC}_2\text{H}_5)_2]_2$ , the magnetic behavior of dithiophosphinates quite generally parallels that of the corresponding metal ion complexes with monodentate ligands. The greater effective magnetic dilution afforded by tris coordination as opposed to bis coordination is manifested in the uniformly small Weiss constants for the tris complexes although part of this difference may be due to the smaller size of the trivalent ions. The negative sign of the Weiss constants for the tetrahedral bis complexes is indicative of antiferromagnetic coupling between the metal ions.

The significant influence of the substituents upon the



Unfortunately, no epr spectra have been obtained where  $X = F^{18}$  or  $CF_3^{127}$ , although attempts were made.

Tabulations by Wasson<sup>39</sup> give the isotropic solution epr parameters  $g_o = 2.054 \pm 0.001$ ,  $A^{Cu} = 73 \pm 2$  gauss,  $A^P = 9.2 \pm 0.3$  gauss for the complexes  $Cu[S_2P(OR_2)]_2$  and  $g_o = 2.047 \pm 0.002$ ,  $A^{Cu} = 69 \pm 1$  gauss,  $A^P = 5.6 \pm 0.3$  gauss for the complexes  $Cu[S_2PR_2]_2$ . If it is presumed that the Cu(II) complexes are planar with  $D_{2h}$  symmetry, then it might be further anticipated that the d-orbital energy orderings are similar to those of the Ni(II) complexes (*vide infra*, Figure 6.15). In a Cartesian coordinate system in which the plane of the molecule coincides with the xy plane and the metal and phosphorus atoms lie in the xz plane, the  $d_{xy}$  orbital with lobes directed at the sulfur atoms is expected to be of the highest energy. On the basis of Crystal Field Theory considerations, this is the orbital occupied by the odd electron and is a  $\sigma^*$  orbital in MO theory. Thus the order of couplings may well be considered to be determined by the  $\sigma$  bonding perturbations by the substituents.

Wasson<sup>39</sup> has noted that the degree of phosphorus 3s orbital involvement in molecular bonding is probably dependent upon the P-S bond lengths and SPS, XPX bond angles and partially rationalized the order of  $A^P$  values in these terms. However, he did not mention<sup>39</sup> the possible effects of M-S bond length variations with substituent which might be even more important. The electrical substituent effect arguments presented in Chapter 3 and applied to Ni(II) complexes are equally valid for planar Cu(II) complexes and predict simultaneous shortening of both the M-S and P-S linkages for the OR substituents



physical properties of dithiophosphinates is further emphasized by the three magnetically anomalous cases mentioned above. Except for the vanadyl complexes, the similarity in magnetic susceptibilities of the remaining compounds with  $X = \text{CH}_3$  and  $\text{CF}_3$  is notable and remarkable in view of the large difference in the substituent electrical effects (Table 3.7). A possible explanation for this latter regularity may be that the thermal population distributions of the complexes with  $X = \text{CH}_3$  and  $\text{CF}_3$  have the same statistical "shape"<sup>128</sup>. The sensitivity and precision of the epr results demonstrate that the  $\text{CH}_3$  and  $\text{CF}_3$  substituents affect the electronic environment of the vanadyl ion quite differently. In situations where the molecular environment is standardized (e.g. in solution), it appears that the Hammett-Taft parameters can be applied successfully to the interpretation of the differences in magnetic (electronic) properties resulting from variation of the substituents.



## CHAPTER 6

ELECTRONIC SPECTRA6.1 Introduction

In previous chapters attempts were made to analyze the known molecular structures, chemical reactions, and magnetic properties of dithiophosphinate complexes in terms of the specific contribution of the substituents on the phosphorus atoms. The potential sensitivity of electronic absorption spectra to small differences in chemical bonding is well established. While the electronic spectra of dithiophosphinates have been discussed in several recent papers and reviews<sup>11-13</sup>, no previous research involving dithiophosphinates has had the particular advantage of the wide range of substituents studied in this work. It is intended in this chapter to present and attempt an interpretation of the solution absorption and diffuse reflectance spectral results for OV(IV), V(III), Cr(III), Mn(II), Fe(III), Fe(II), Co(III), Co(II), Ni(II), Pd(II), Pt(II), Zn(II), Cd(II), Hg(II) dithiophosphinates and the dithiophosphinate anions with the phosphorus uniformly substituted by CH<sub>3</sub>, C<sub>6</sub>H<sub>5</sub>, OC<sub>2</sub>H<sub>5</sub>, F, and CF<sub>3</sub>. However, the matrix of compounds versus substituent was not completed for all five substituents in all cases (cf Table 2.1), but the absences are noted and in some cases were filled by other work.

The characteristics of electronic spectral absorption bands have been extensively discussed by many authorities<sup>64,74,111-113</sup> in terms of band origins, intensities, widths, fine structure, and asymmetries. From a phenomenological point of view absorption bands



of transition metal complexes in solution are usually broad compared with atomic absorptions and are of an approximately Gaussian shape when obtained as absorbance (A) or molar absorptivity ( $\epsilon$ ) versus exciting radiation frequency ( $\nu$ ). Thus it is possible to concentrate on only three parameters of each band: the position of the maximum ( $\nu_{\max}$ ), the half-width (width at half-height,  $\delta$ ), and the total intensity as measured by the area ( $\sqrt{\pi/\ln 2} \epsilon_0 \delta$ ) or some function of the area<sup>64</sup>. Asymmetry of bands may be accounted for in part by allowing different half-widths,  $\delta_-$  and  $\delta_+$ , for the low and high energy sides of each band such that<sup>64</sup>

$$\delta = (\delta_- + \delta_+)/2. \quad (6.1)$$

In concurrence with common practice, band intensities in solution spectra are presented in terms of the f-number or oscillator strength, which represents the ratio of the probability of radiation absorption or emission to the probability for the same process of an equivalent classical harmonic oscillator. Oscillator strengths have the interesting property that their sum over all transitions yields the number of electrons in the molecule<sup>129,130</sup>. For a Gaussian peak

$$f = \frac{10^3}{N} \frac{mc^2}{\pi e^2} \ln 10 \int \epsilon(\nu) d\nu = 9.20 \times 10^{-9} \epsilon_0 \delta \quad (6.2)$$

where  $m$  and  $e$  are the electron mass and charges,  $N$  is the Avogadro number, and  $c$  is the velocity of light<sup>130</sup>. For reasons most concisely presented by Lever<sup>74</sup>, a large indeterminacy is associated with diffuse reflectance spectral band intensities, although band positions are reliable. Comparisons of solution spectra and solid state reflectance



spectra can be used to indicate the presence of solid state effects or structural differences.

## 6.2 The Molecular Orbital Theory Applied to Dithiophosphinate Complexes

The hyperfine structure in the epr spectra of the OV(IV) and Cu(II) dithiophosphinates (Chapter 5) clearly indicates that covalency is significant in these complexes and that a unified molecular orbital (MO) treatment is most appropriate in a description of their electronic properties. Nevertheless, the historical distinction between weak bands attributable to Laporte forbidden electronic excitations within the metal ion d-orbital manifold (ligand field transitions) and the more intense bands at higher energy arising from transitions involving ligand orbitals (electron transfer transitions) will be retained for computational and classification purposes within established theory. In order to underline the most important MO energy differences, purely qualitative MO diagrams are produced for each idealized coordination geometry, assuming that the molecules are monomeric in solution. The MO diagrams are largely an extension of one published by Jorgensen<sup>131</sup> for the tris dithio- or diseleno-phosphinates  $M[S(e)_2P(OC_2H_5)_2]_3$  which was used herein as a model. An account of the bonding in structures  $X_2PA_2$  (e.g.  $R_2PO_2^-$ ) is given by Hudson<sup>132</sup>, while Ballhausen, et al.<sup>133</sup> have reviewed the limitations and pitfalls of simplified MO calculations in general.

Since the MO diagrams are only intended to be qualitative, a limited basis set of atomic orbitals has been used. Since the MSP bond angles in chelating ligands are close to  $90^\circ$ , only



the S 3p orbitals are included, along with the P 3s and 3p and the metal 3d, 4s, and 4p atomic orbitals. For the vanadyl complexes, only the 2p orbitals of the O atom were considered. Inclusion of the omitted orbitals is anticipated<sup>134</sup> to decrease the energies of the bonding MO's and add more high energy antibonding MO's, unnecessarily complicating a merely qualitative diagram. The relative energies of the atomic orbitals were estimated from their orbital ionization energies or the tetrahedral valence state ionization energy<sup>135</sup> in the case of the phosphorus atoms.

Since the metal atom M is presumed to be less electronegative than P, the predominantly  $\sigma_{SP}$  orbitals are placed below the  $\sigma_{SM}$  orbitals<sup>131</sup>. After all the  $\sigma_{SP}$  and  $\sigma_{SM}$  bonds are formed, there remains one  $\pi$ -type orbital per S atom. These will split up into a bonding and an antibonding MO set due to the presence of two closely adjacent S atoms in each  $S_2P$  unit<sup>131</sup>. The remaining MO orderings were qualitatively fixed on the bases that the extent of bonding is directly dependent on the atomic orbital overlap and inversely dependent upon the energy separation of the participating atomic orbitals<sup>133</sup>. It is realized that the actual MO's are linear combinations of all orbitals of appropriate symmetry but for simplicity only major atomic orbital components are connected to the respective MO by tie lines.

In these diagrams, shown in appropriate places in subsequent sections, the important energy separations to be determined by experiment are the highest bonding orbital-d-shell difference ( $\Delta_1$ ), the splittings within the metal d-shell (10Dq, etc.), and the



difference in energy between the metal d-shell and the higher antibonding levels ( $\Delta_2$ ). It is the d-orbital splittings of the metal ion which determine the character of the ligand field spectra while the relative magnitudes of  $\Delta_1$  and  $\Delta_2$  govern whether the lower electron transfer bands are of the metal-to-ligand ( $M \rightarrow L$ ) or ligand-to-metal ( $M \leftarrow L$ ) type.

The MO diagrams for the tris and tetrahedral bis complexes are given in Figures 6.1 and 6.2. In these and subsequent diagrams it is emphasized that qualitative considerations cannot give the relative orderings of orbitals within clustered sets. Furthermore, while there is some confidence in the gross ordering of the bonding orbital sets, the lowest lying antibonding orbitals above the metal d-orbitals are unknown.

The qualitative success of the point charge or dipole electrostatic Crystal Field Theory in accounting for the ligand field spectra and magnetic behavior of complexes with nearly octahedral or tetrahedral coordination geometries has led to its development as a semi-empirical MO theory, the Ligand Field Theory<sup>113</sup>. In the Ligand Field Theory, the d-orbital manifold of a transition metal ion in a complex is characterized electronically by three sets of semi-empirical parameters: (i) the Racah interelectronic repulsion parameters  $B'$  and  $C'$ , (ii) the orbital energy differences ( $10Dq$  in cubic symmetry, three values in tetragonal symmetry, and four in lower symmetries), and (iii) the ground term spin-orbit coupling constant  $\lambda^{113}$ .



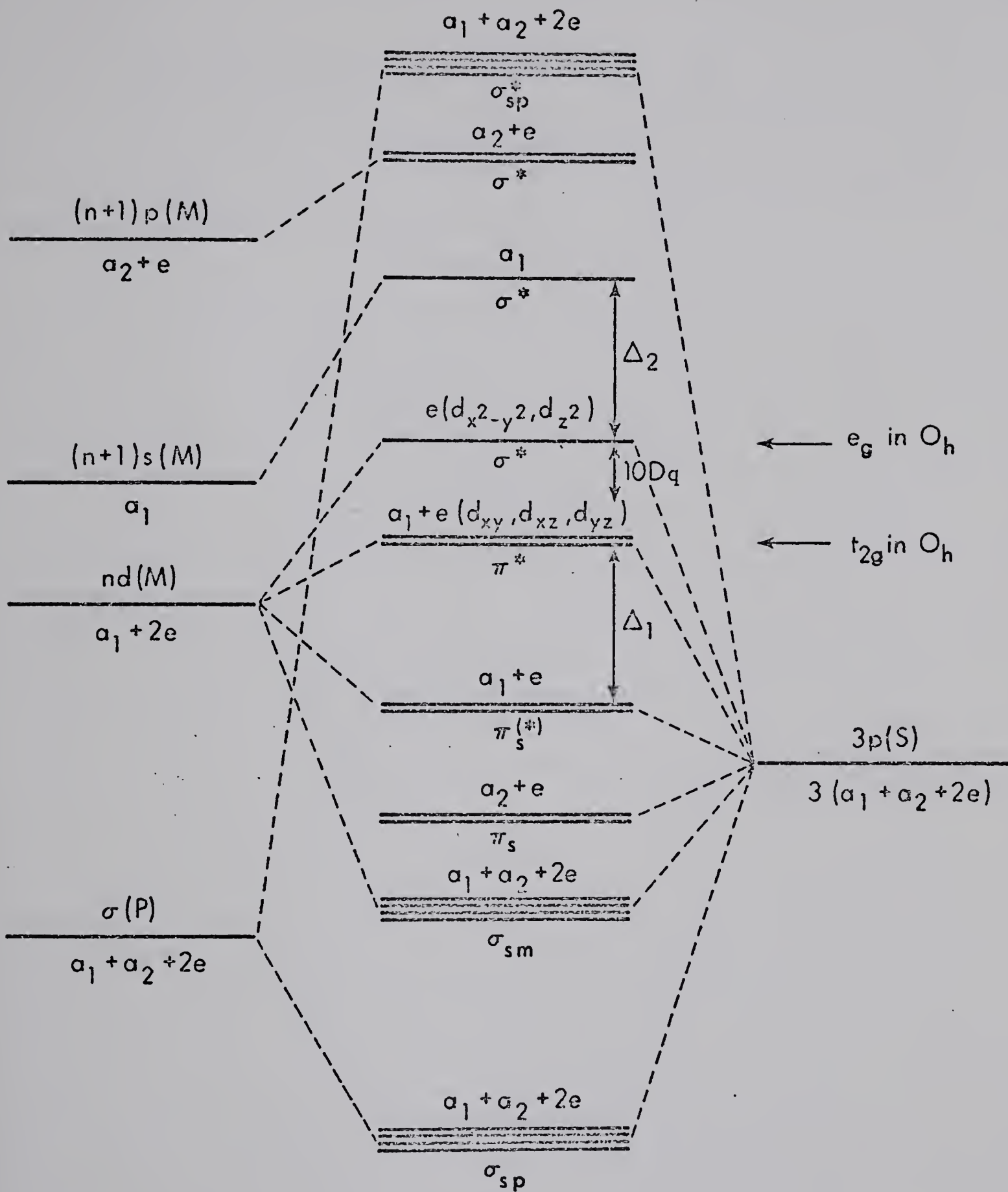


FIGURE 6.1: A qualitative MO diagram for a chromophore  $M(S_2P)_3$  of  $D_3$  symmetry (pseudo-octahedral).



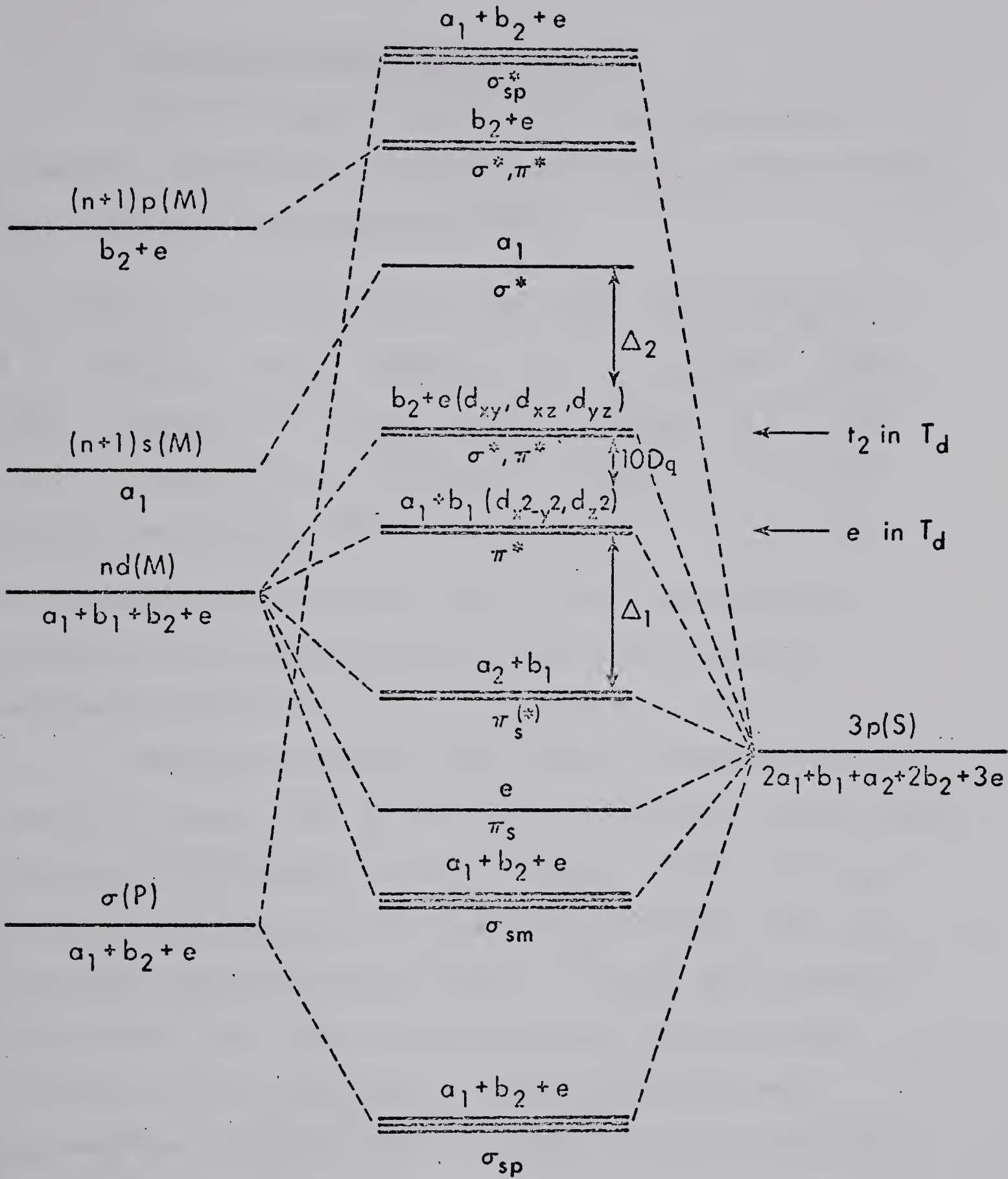
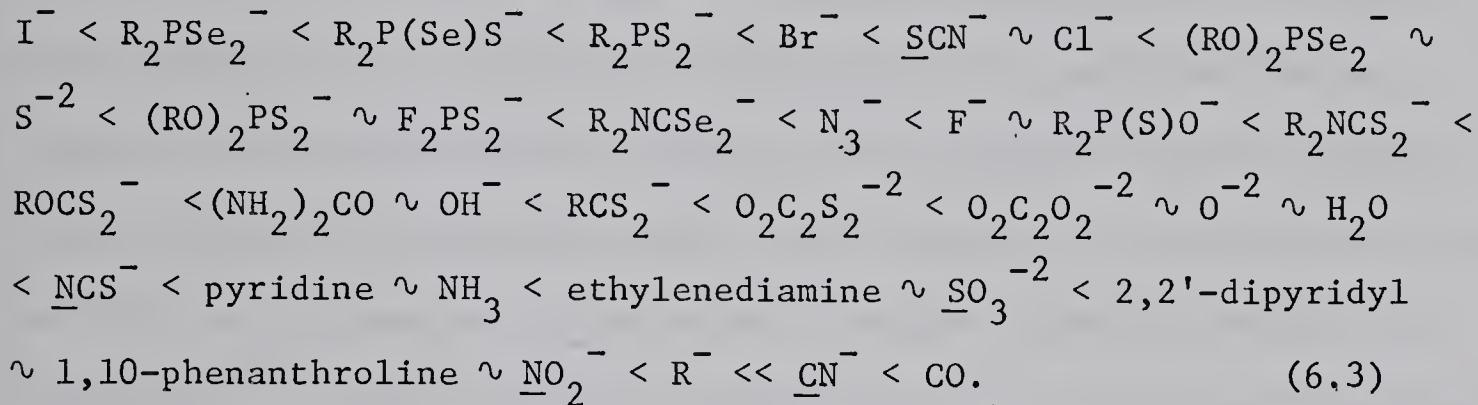


FIGURE 6.2: A qualitative MO diagram for a chromophore  $M(S_2P)_2$  of  $D_{2d}$  symmetry (pseudo-tetrahedral). The Cartesian axes with the  $M$  and  $P$  atoms on the  $z$  axis.



### The Spectrochemical Series of Ligands

Selected ligands of interest for comparison purposes are arranged in sequence (6.3) in order of increasing  $D_q$  values found for their transition metal complexes<sup>12,74,97</sup>.



In this spectrochemical series R is an alkyl or aryl group and ambiguity due to linkage isomerism is removed by underlining coordinating atom(s).

Referring to Figure 6.1 and assuming octahedral coordination by the ligands,  $10D_q$  is seen to be the difference between  $\sigma$ -anti-bonding and  $\pi$ -anti-bonding molecular orbitals. However, the  $t_{2g}$  set of d orbitals is anti-bonding with  $\pi$ -donor ligands ( $\pi(M \leftarrow L)$ ), non-bonding with non- $\pi$ -bonding ligands, or bonding with  $\pi$ -acceptor ligands ( $\pi(M \rightarrow L)$ ). Thus the spectrochemical order of ligands assumes the order of increasing  $\pi$  acidity in the Lewis sense.

Jorgensen<sup>64</sup> has considered  $10D_q$  for a complex of cubic coordination geometry to be the algebraic sum of at least four contributions

$$\begin{aligned} 10D_q \sim & \text{electrostatic first order perturbation} + \sigma(M \leftarrow L) + \pi(M \rightarrow L) \\ & - \pi(M \leftarrow L). \end{aligned} \quad (6.4)$$

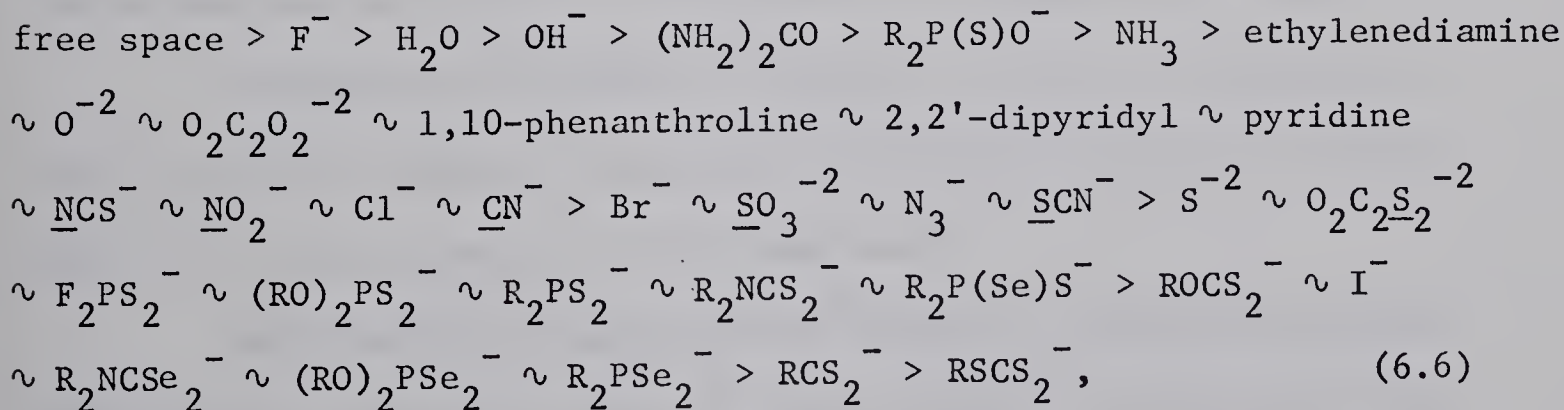


### The Nephelauxetic Series of Ligands

Where the  $B'$  values of the complexes are known, the ligands of sequence (6.3) may also be ordered according to increasing ability to reduce interelectron repulsions within the d-orbital manifold<sup>64,74</sup>. The generally observed reduction in repulsions has been attributed to two effects (i) an effective reduction in the metal ion nuclear charge by penetration of the d-shell by the ligand electrons (central field covalency) in accordance with the principle of electroneutrality, and (ii) delocalization of the metal electrons (symmetry restricted covalency)<sup>64,74</sup>. Both the above mechanisms ((i) and (ii)) imply an increase of the d-orbital radial functions with covalent bonding. For comparison of the relative reductions in electron repulsion within the d-orbital manifold between different complexes it is usual to compare the values of the nephelauxetic ratio<sup>64,74</sup>

$$\frac{B_{\text{complex}}}{B_{\text{free ion}}} = \frac{B'}{B} = \beta \quad (6.5)$$

In order of decreasing  $\beta^{64,74,97}$  the nephelauxetic series for most of the ligands of sequence (6.3) is



where R is an alkyl or aryl group and the coordinating atoms are underlined in cases of possible linkage isomerism.



The nephalauxetic ratio  $\beta$  is extremely sensitive to the method of determination of  $B'$  and  $B$ . The reported values of  $B'$  for the same complex can differ by  $\pm 50K$  which includes the whole range of diseleno- and dithioligands. Hence specific orderings are not very significant in sequence (6.6) but the overall trend is relatively firm. Furthermore  $B = F_2 - 5F_4$  in terms of the Slater-Condon electron repulsion integrals and thus contains at least two degrees of freedom hidden by the use of one parameter<sup>136</sup> (since  $C$  is often not known).

While the weak ligand field bands of transition metal complexes have been rationalized with some success within the limitations of the Ligand Field Theory, there are enormous difficulties associated with the interpretation of the Laporte-allowed bands. These latter bands are presumed to arise from four major classes of transitions: (i) electron transfer ( $M \leftarrow L$ ) from the ligands to partly filled shells of the central metal ion, (ii) electron transfer ( $M \rightarrow L$ ) from the metal to the ligands, (iii) transitions ( $L \rightarrow L$ ) between orbitals largely associated with the free ligands, and (iv) cooperative effects of polynuclear species which may result in transitions within the polynuclear structure not assignable to classes (i) - (iii)<sup>137</sup>.

Transitions belonging to classes (i) and (ii) change the formal oxidation number of the metal ion and hence should be indicative of the redox behavior of the complexes.

Qualitatively, bands arising from  $M \leftarrow L$  electron transfer mechanism are expected to occur at lower energy the more oxidizing the central metal ion and the more reducing the ligands (i.e. the smaller  $\Delta_2$  of Figures 6.1 and 6.2).



Jorgensen<sup>137</sup> has attempted to correlate optical electron transfer energies with an "optical electronegativity" ( $\chi_{\text{opt}}$ ) difference between the donor and acceptor orbitals through the equation

$$\Delta_1 = 30 (\chi_{\text{opt}_L} - \chi_{\text{opt}_M}) \text{ kK}, \quad (6.7)$$

where  $\Delta_1$  is the transition energy corrected for interelectronic repulsion differences between the ground and the excited MO's as well as  $10Dq$  if necessary. The factor  $30 \text{ kK}/\sqrt{\text{eV}}$  relates this optical electronegativity scale to the Pauling scale of electronegativities by arbitrarily setting  $\chi_{\text{opt}_F}$  at  $3.9\sqrt{\text{eV}}^{137}$ .

Since  $\chi_{\text{opt}_M}$  is known<sup>6</sup> for many metal ions in various coordination geometries and the interelectronic repulsion corrections are not simple, equation (6.7) may be rearranged to give  $\chi_{\text{opt}_L}$  explicitly

$$\chi_{\text{opt}_L} = \frac{1}{30} \nu'_{\text{ET}} + \alpha, \quad (6.8)$$

where  $\nu'_{\text{ET}}$  is the observed transition energy corrected only for  $10Dq$ , if necessary, and  $\alpha$  is a function of metal ion and molecular geometry only. Thus if  $\chi_{\text{opt}_L}$  is known for one of a homologous series of complexes,  $\alpha$  may be determined once and for all the ligands of the series. For this purpose  $\chi_{\text{opt}}$  of the group  $S_2P(OC_2H_5)_2$  is taken to be  $2.70^{11}$ .

Qualitatively bands arising from an  $M \rightarrow L$  electron transfer mechanism are expected to occur at higher energy the more oxidizing the central metal ion and the more reducing the ligands (i.e. the large  $\Delta_2$  of Figures 6.1 and 6.2). The optical electronegativity of



the ligands can now be obtained from the formula

$$\chi_{\text{opt}_L} = - \frac{1}{30} \sigma'_{ET} + \alpha \quad (6.9)$$

where the symbols have their previous significance (see sequence 6.8).

Bands assigned to  $L \leftarrow L$  transitions are usually those largely invariant to a change of metal ion and/or geometry<sup>64,74</sup>.

### 6.3 Results and Discussion

#### Spectra of the Ligand Salts and Filled d-Shell Complexes

Jorgensen<sup>11</sup> states that a usual condition for the occurrence of absorption bands at relatively low energies for compounds of elements outside the transition groups is the existence of bond-orders above unity. Thus it is of interest to determine the regions of the spectrum in which absorptions other than d-d transitions may be expected since the crystallographic data clearly indicated multiple bond character of the P-S linkages in both the salts and complexes.

Unfortunately, the electronic spectra of salts of the ions  $\text{S}_2^{\text{PF}_2}$  and  $\text{S}_2^{\text{P}(\text{CF}_3)_2}$  have not been obtained. However  $\text{NaS}_2^{\text{P}(\text{CH}_3)} \cdot 2\text{H}_2\text{O}$  and  $\text{NH}_4\text{S}_2^{\text{P}(\text{C}_6\text{H}_5)_2}$  in methanol were found to produce shoulders at 37.6 and 42.4 kK on very intense absorptions that increased until the solvent "cut-off". Jorgensen reported<sup>11</sup> that  $\text{NH}_4\text{S}_2^{\text{P}(\text{OC}_2\text{H}_5)_2}$  absorbs at 44.5 kK in ethanolic solution. It is noted that the phenyl group absorptions occurring at > 36 kK were very much weaker than the indicated shoulder for the anion  $\text{S}_2^{\text{P}(\text{C}_6\text{H}_5)_2}$ . Moreover,  $\text{NaS}_2^{\text{P}(\text{CH}_3)} \cdot 2\text{H}_2\text{O}$  in aqueous solution does not absorb until a shoulder occurs



at  $\sim 42.4$  kK with no bands near the shoulder at 37.6 kK observed in methanol. Thus a significant study of the ligand salt spectra requires that both the solvent and counter ion dependence of the spectra be determined.

In spite of the above limitations, it is possible to conclude with Jorgensen<sup>11,12</sup> that the first absorptions of the ligand anions are of remarkably high energy compared with other dithioanions but it is not valid to infer single bond character of the P-S bonds from these results. Jorgensen<sup>11,12</sup> assigns the band at 44.5 kK for  $\text{NH}_4\text{S}_2\text{P}(\text{OC}_2\text{H}_5)_2$  to some sort of Rydberg excitation  $3p \rightarrow 4s$  of the sulfur atoms.

A filled d-shell of the metal ion precludes  $M \leftarrow L$  transitions involving the metal nd-orbitals, although the relatively close metal (n+1)s orbital remains vacant in the ground state complex and may serve as an acceptor orbital. In order to put the assignments of the electron transfer spectra on a firm basis, it would have been exceedingly valuable to have been able to compare the spectra of the vacant d-shell complexes  $\text{Mg}[\text{S}_2\text{PX}_2]_2$  and  $\text{Ca}[\text{S}_2\text{PX}_2]_2$ ,  $\text{Al}[\text{S}_2\text{PX}_2]_3$  and (if possible)  $\text{Sc}[\text{S}_2\text{PX}_2]_3$  with those of their filled d-shell counterparts  $\text{Zn}[\text{S}_2\text{PX}_2]_2$  and  $\text{Ga}[\text{S}_2\text{PX}_2]_3$  for the series of substituents  $X = \text{CH}_3$ ,  $\text{C}_6\text{H}_5$ ,  $\text{OC}_2\text{H}_5$ , F, and  $\text{CF}_3$ . Lower row metals of the Periodic Table show spectra complicated by intermediate coupling effects.

Again unfortunately, the Zn group complexes with  $X = \text{CH}_3$  and  $\text{C}_6\text{H}_5$  proved insufficiently soluble in dichloromethane to obtain useful spectra and their reflectance spectra were singularly uninformative in the range (10-30 kK) accessible with the available



equipment. There was some indication of bands near 30 kK for the phenyl substituted complexes in dichloromethane solutions obtained by boiling the solvent with an excess of complex. However, Müller, et al.<sup>38</sup> report bands at 32.9 and 39.2 kK for  $\text{In}[\text{S}_2\text{P}(\text{C}_6\text{H}_5)_2]_3$  in chloroform solution while Jorgensen<sup>11,12</sup> found bands at 34.0 and 41.0 kK for  $\text{In}[\text{S}_2\text{P}(\text{OC}_2\text{H}_5)_2]_3$  in ethanol solutions. Jorgensen<sup>12</sup> speculates that the band at 34 kK may represent a transition from the highest occupied MO of the ligands to a Rydberg orbital consisting of a mixture of indium 5s and sulfur 4s orbitals. This latter assignment implies that the transition energy includes  $\Delta_1 + 10Dq + \Delta_2$  minus the gain in reduced interelectronic repulsion (cf Figure 6.1).

While severely limited by the lack of the relevant data suggested above, some progress can be made in the interpretation of the electron transfer bands by the variations in bond energies with change of substituent as illustrated by the indium complexes. If the sum  $10Dq + \Delta_2$  (Figure 6.1) is largely determined by the metal atom while  $\Delta_1$  is largely determined by the ligand (i.e. substituent) then Jorgensen's<sup>11,12</sup> assignment of the  $\sim 34$  kK band of the indium complexes is consistent with a greater ligand electronegativity (i.e.  $\Delta_1$ ) for  $\text{X} = \text{OC}_2\text{H}_5$  than for  $\text{X} = \text{C}_6\text{H}_5$ .

#### Spectra of Oxovanadium(IV) Complexes

Considerable controversy still surrounds the interpretation of the electronic spectra of complexes formed by the cation  $\text{OV}^{+2}$  ( $3d^1$ ). All semi-quantitative attempts<sup>116,138</sup> to describe the bonding in these complexes have thus far ignored  $\pi$  bonding between atoms other than the V-O linkage and arrive at essentially the same ordering of d



orbitals, i.e.  $d_{z^2} > d_{xy} > d_{xz} \sim d_{yz} > d_{x^2-y^2}$ . Selbin<sup>106</sup> has pointed out that the primary effect of equatorial bonding may be to invert the order of the  $d_{xy}$  and  $d_{xz}$ ,  $d_{yz}$  orbital sets which is the order supported by McCormick<sup>115</sup> from a study of the dithiocarbamate complexes. It is impossible to obtain this order from the Crystal Field approach so that if the order is correct then calculations based on electrostatic models must be abandoned.

The electronic spectra of vanadyl complexes consistently show at least three bands below 30 kK of intensity much lower than those above 30 kK<sup>82,115,139</sup>. The solution spectra of the vanadyl dithiophosphinates studied herein are illustrated in Figure 6.3 while the resolved band parameters and derived quantities are collected in Table 6.1. In compliance with previous practice<sup>82,115,139</sup> the apparently Laporte forbidden bands are respectively labelled I, II, and III, in order of increasing energy.

Band II of  $\text{OV}[\text{S}_2\text{P}(\text{CF}_3)_2]_2$  shows a distinct asymmetry at the maximum and a definite shoulder on the high energy side suggesting that band II in this case at least is actually the envelope of three components. The unique resolution observed in the spectrum of  $\text{OV}[\text{S}_2\text{P}(\text{CF}_3)_2]_2$  is believed to result from the wider separation of bands I and II allowing a clearer resolution of band II in this complex. Close scrutiny of the high energy slope of band II in the complexes where  $X = \text{C}_6\text{H}_5$ ,  $\text{OC}_2\text{H}_5$ , and F reveals a possible inflection or noticeable tailing to high energy indicative of a submerged band, but band II with  $X = \text{CH}_3$  appears simple. The apparent four bands contained in bands I and II in the spectrum of  $\text{OV}[\text{S}_2\text{P}(\text{CF}_3)_2]_2$



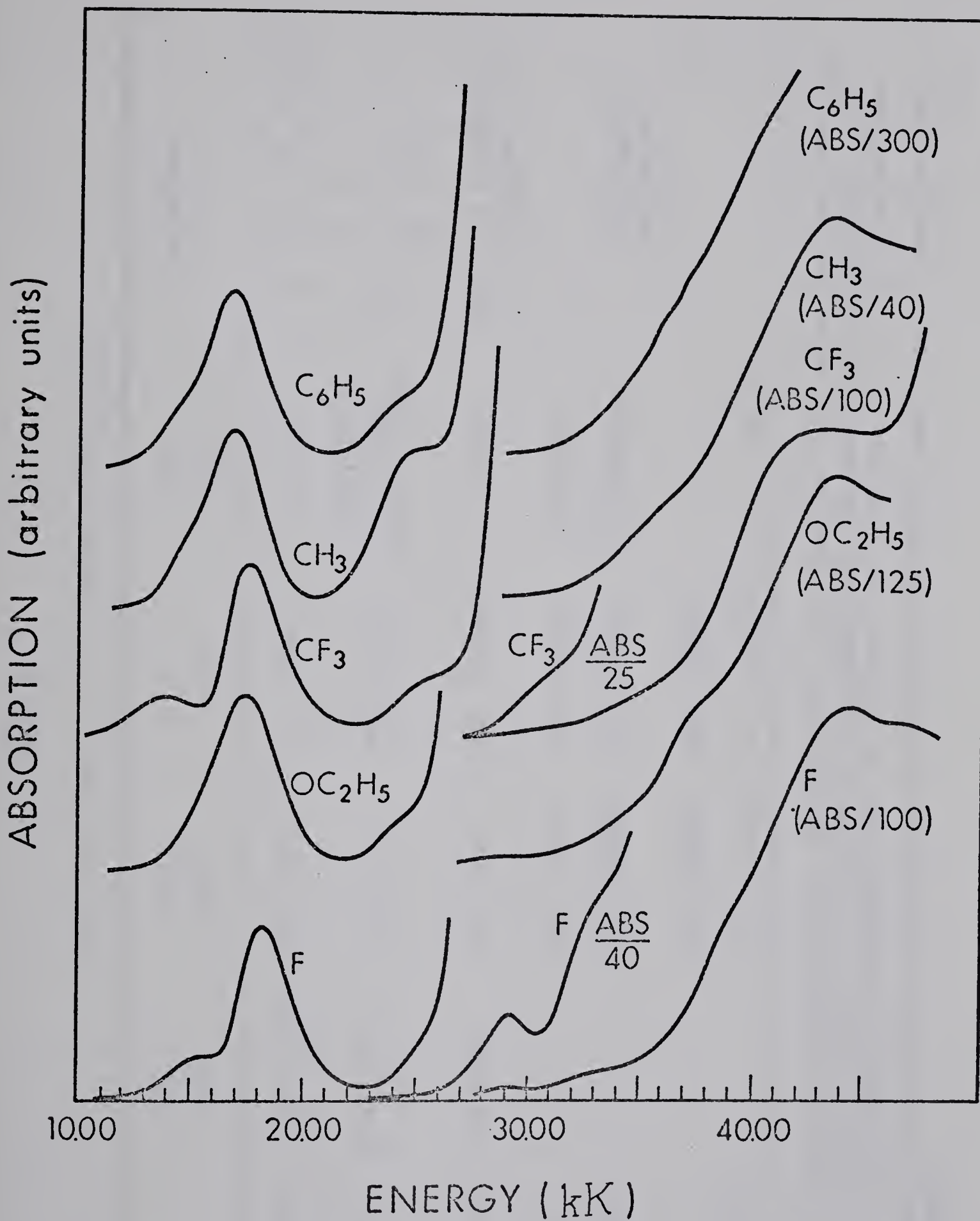


FIGURE 6.3: Electronic absorption spectra of  $OV[S_2^{P\bar{X}_2}]_2$  complexes in  $CH_2Cl_2$  solution.



TABLE 6.1

Electronic Spectra of the Complexes  $\text{OV}[\text{S}_2\text{PX}_2]_2^a$ 

$X = \text{CH}_3$	$\text{C}_6\text{H}_5$	$\text{OC}_2\text{H}_5$	F	$\text{CF}_3$	Assignment
$\nu(\kappa\text{K})$	$\nu(\kappa\text{K})$	$\nu(\kappa\text{K})$	$\nu(\kappa\text{K})$	$\nu(\kappa\text{K})$	
14.5 (0.4)sh	14.4 (0.7)sh	15.1 (1)sh	15.1 (1)sh	14.0(1)sh	I: $2_{\text{A}_2} \leftarrow 2_{\text{A}_1}$ "10Dq"
16.86(4.55)	16.89(5.92)	17.51(16.0)	18.21(5.40)	16.8(0.2)sh 17.7(4.60) $\sim$ 18.8( $\sim$ 0.2)sh	II: $2_{\text{B}_1}, 2_{\text{B}_2} \leftarrow 2_{\text{A}_1}$ $2_{\text{A}_1} \leftarrow 2_{\text{A}_1}$
24.4 (3.5)sh	24.2 (2)sh	24.2 (2)sh	24.7 (0.8)sh	25.7 ( $\sim$ 2)sh	III: M $\leftarrow$ L electron transfer
30.4 (80)sh		29.0 (31)sh	29.0 (29)sh	30.4 (20)sh	
34.7 (200)sh		34.3 (200)sh	32.5 (30)sh	35.2 (200)sh	Intraligand excitation
	?	b	37.2 (800)sh	38.7 (500)sh	?
43.3 (1.0x10 <sup>3</sup> )			43.9 (1.2x10 <sup>3</sup> )	44.1 (3.0x10 <sup>3</sup> )	41.2 (2x10 <sup>3</sup> )sh

a The table entries are the positions (kilokayser) of the resolved band maxima obtained from the spectra of  $\text{CH}_2\text{Cl}_2$  solutions. The values in parentheses are the oscillator strengths (f)  $\times 10^4$  and "sh" implies that the unresolved band was observed as a shoulder, or "i" as an inflection.

b An unresolved monotonically increasing absorption upon which the phenyl group transitions are superimposed.



suggests that all ligand field transitions in these complexes occur below 20 kK, as proposed<sup>140</sup> for vanadyl acetylacetone.

It is noted that band I is shifted with X with reference to Table 6.1, Figure 6.3 and equation (6.4), precisely as would be predicted by the difference between a lower anti-bonding  $\pi$  MO and an upper anti-bonding  $\sigma$  MO, where the metal experiences the transduced substituent effects (Table 3.1). The low intensity and tailing properties of band I are consistent with a vibronically allowed transition (cf Figure 6.3). Hence band I is assigned to the  $^2A_2 \leftarrow ^2A_1$  transition (and thus is  $10Dq$  in terms of the electrostatic model<sup>116</sup>). Since it is anticipated that the energies of the  $b_1$ ,  $b_2$  ( $\pi^*$ ) orbitals should be strongly affected by the  $\pi$  acidity of the ligands, becoming more anti-bonding the stronger the  $\pi$  bonding between metal and ligand, the higher energy positions of band II where X = OC<sub>2</sub>H<sub>5</sub>, F, and CF<sub>3</sub> suggests its assignment to the  $^2B_1$ ,  $^2B_2 \leftarrow ^2A_1$  transitions. If the OVS<sub>4</sub> chromophore is subject to C<sub>4v</sub> selection rules, both the transitions  $^2A_2$ ,  $^2A_1 \leftarrow ^2A_1$  are forbidden as electric dipole transitions and are expected to be at least weak relative to the E (i.e.,  $^2B_1 + ^2B_2 \leftarrow ^2A_1$ ) allowed electric dipole transitions. Therefore the weak band (where discernable) on the high energy slope of band II is assigned to the  $^2A_1 \leftarrow ^2A_1$  transition. Finally, with all ligand field transitions accounted for, band III is assigned to a spin or symmetry forbidden M  $\leftarrow$  L electron transfer. In fact the position of band III varies as expected for a variation in  $\Delta$  (Figure 6.4) with the electronegativity of the substituents.



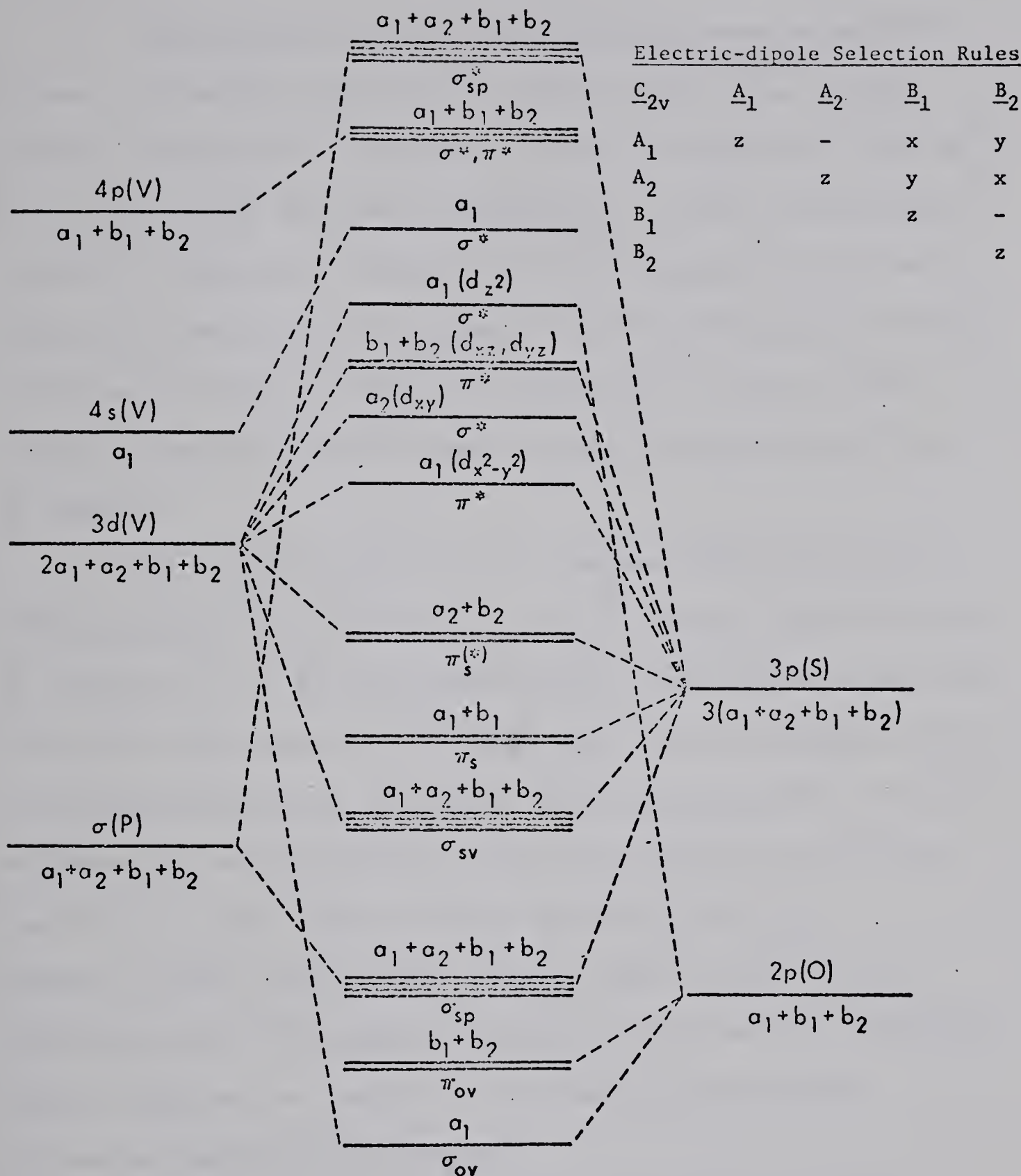


FIGURE 6.4: A qualitative MO diagram for the chromophore  $OV(S_2^P)_2$  of  $C_{2v}$  symmetry. The Cartesian coordinate system is oriented such that the z axis coincides with the 2-fold rotation axis and the O, V, and P atoms lie in the xz plane.



Although the tentative spectral assignments below 20 kK present a reasonable explanation of the available data, clearly further confirmation is required. A variable temperature study of the single crystal spectrum of  $\text{OV}[\text{S}_2\text{P}(\text{CH}_3)_2]_2$  would be potentially capable of testing the validity of all the assignments made herein. Transition symmetries as determined<sup>33</sup> for  $\text{Ni}[\text{S}_2\text{P}(\text{OC}_2\text{H}_5)_2]_2$  indicate a similar inversion of orbitals as postulated for these vanadyl complexes where  $\pi^*$  orbitals assume a higher energy position than  $\sigma^*$  orbitals.

Both recent reports on the complexes  $\text{OV}[\text{S}_2\text{P}(\text{C}_6\text{H}_5)_2]_2$ ,<sup>36</sup>  $\text{OV}[\text{S}_2\text{P}(\text{C}_2\text{H}_5)_2]_2$ ,<sup>37</sup> and  $\text{OV}[\text{S}(\text{Se})\text{P}(\text{C}_2\text{H}_5)_2]_2$ <sup>37</sup> include a band at  $\sim 10$  kK in the spectra. It has been demonstrated in the course of this work that such a band appears on bubbling oxygen into the sample solution. The reflectance spectra of powdered  $\text{OV}[\text{S}_2\text{P}(\text{C}_6\text{H}_5)_2]_2$  (this work and reference 36) and  $\text{OV}[\text{S}_2\text{P}(\text{CH}_3)_2]_2$  are very similar to the solution spectra of the pure complexes while solid  $\text{OV}[\text{S}_2\text{P}(\text{CF}_3)_2]_2$  absorbs strongly over the whole visible range as expected of a black material. The intense coloration of the F and  $\text{CF}_3$  substituted vanadyl complexes is consistent with some (as yet unknown) cooperative solid state phenomenon.

Finally, it is to be noted that the order of "10Dq" parameters arranged by substituent is very close to what would have been predicted by sequence (3.11) of the M-S vibrational frequencies



Spectra of Vanadium(III) Complexes

Reported<sup>31</sup> single crystal studies of  $V[S_2P(OC_2H_5)_2]_3$  in the host lattice of  $In[S_2P(OC_2H_5)_2]_3$  at ambient and reduced temperatures while of somewhat uncertain interpretation nevertheless indicate that the complex obeys  $D_3$  symmetry selection rules and that the term splittings ( $\sim 130K$ ) are largely due to the trigonal component in the ligand field and not to spin-orbit coupling. Since the effects of these small splittings are not observed in the solution spectra, the spectra are analyzed to a good approximation in terms of  $O_h$  symmetry. The strong field expressions for the relative energies of the triplet levels were used:<sup>74</sup>

$$\begin{aligned} E(^3T_{1g}(F)) &= 7.5B - 3Dq - \frac{1}{2}(225B^2 + 100(Dq)^2 + 180DqB)^{\frac{1}{2}} \\ E(^3T_{2g}(F)) &= 2Dq \\ E(^3T_{1g}(P)) &= 7.5B - 3Dq + \frac{1}{2}(225B^2 + 100(Dq)^2 + 180DqB)^{\frac{1}{2}} \end{aligned} \quad (6.10)$$

and  $E(^3A_{2g}(F)) = 12Dq$

The spectra are illustrated in Figure 6.5 while the band parameters, assignments, and derived values are collected in Table 6.2.

When the values of  $Dq$  and  $B'$  are determined from the assignments of the first two transitions and equations (6.10), the third spin allowed (sa) transition is predicted by equations (6.10) to occur near 25 kK, where perhaps fortuitously a band is observed in a trough between two Laporte-allowed transitions. This  $v_3(^3A_{2g}) \leftarrow ^3T_{1g}$  band is generally not observed in other complexes of V(III)



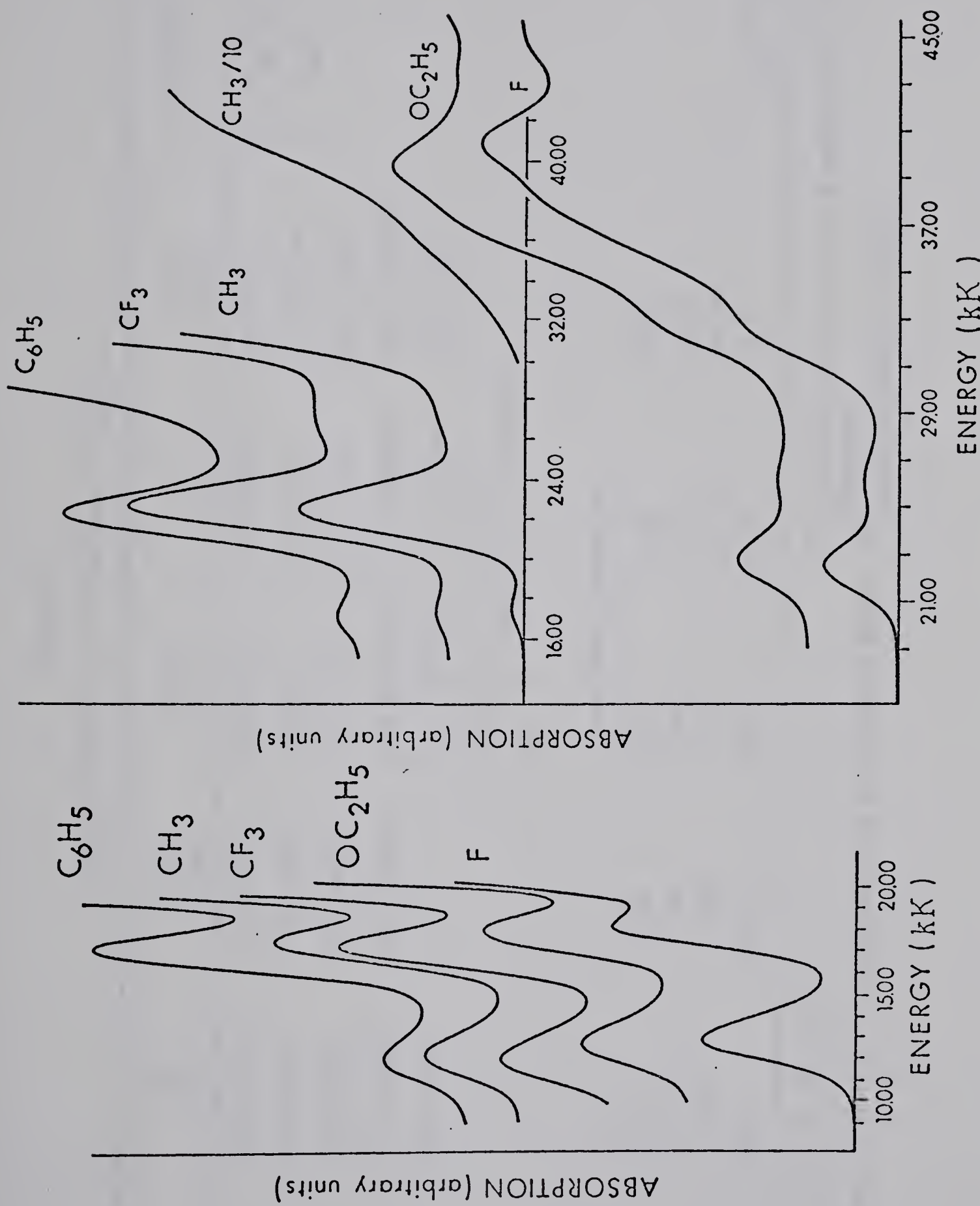


FIGURE 6.5: Electronic absorption spectra of  $V[S_2PX_2]_3$  complexes in  $CH_2Cl_2$  solution.



TABLE 6.2

Electronic Spectra of the Complexes  $V[S_2PX_2]_3^a$ 

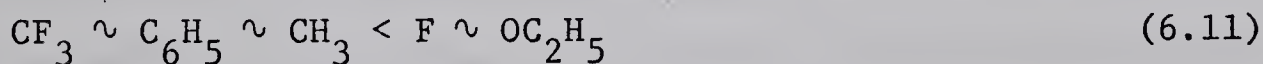
$X =$	$CH_3$	$C_6H_5$	$OC_2H_5$	F	$CF_3$	Assignment <sup>b</sup>
	$\nu(kK)$	$\nu(kK)$	$\nu(kK)$	$\nu(kK)$	$\nu(kK)$	
	12.18(4.01)	12.06(2.88)	12.82(6.6)	12.90(8.12)	12.03(5.0)	$v_1: {}^3T_{2g}(F) \leftarrow {}^3T_{1g}(F)$
	17.45(9.4)	17.21(10.8)	18.08(11)	17.95(5.1)	17.27(10.6)	$v_2: {}^3T_{1g}(P) \leftarrow {}^3T_{1g}(F)$
22.39(225)	22.23(128)	22.7 (260)	22.5 (180)	22.6 (280)		
$\sim 27.1$ (180)sh	$\sim 25.0$ (30)sh	$\sim 26.4$ ( $\sim 250$ )sh	$\sim 26.1$ ( $\sim 250$ )sh	$\sim 26.6$ ( $\sim 160$ )sh		
$\sim 33.0$ (?)sh	c	$\sim 33.1$ ( $\sim 10^3$ )sh	32.3 (450)sh	$\sim 33.0$ (?)sh		
		$37.5sh \left\{ \begin{array}{l} (4.0 \times 10^3) \\ 29.4 \end{array} \right.$	$38.5sh \left\{ \begin{array}{l} (4.4 \times 10^3) \\ 40.5 \end{array} \right.$			
Ligand Field Parameters						
$10Dq$	12.97	12.83	13.58	13.38	12.81	
$B'$	0.404	0.394	0.404	0.411	0.401	
$\beta_{35}^d$	0.470	0.458	0.470	0.478	0.466	
$\nu_3^{(calc.)}$	25.29	24.89	26.38	26.10	24.84	${}^3A_{2g} \leftarrow {}^3T_{1g}(F)$

<sup>a</sup> See footnote (a) of Table 6.1.<sup>c</sup> No discernible structure on a monotonically increasing absorption.<sup>b</sup> The ligand field bands are assigned using an octahedral model. <sup>d</sup> Calculated using  $B = 861$  K.<sup>74</sup>.



and is forbidden as a two electron transition ( $e_g^2 \leftarrow t_{2g}^2$ ) in the strong field approximation. The unusually high intensity of the  $\nu_3$  band may arise by intensity borrowing from the Laporte allowed neighboring bands. There is also the distinct possibility that the  $\nu_3$  band is completely masked by electron transfer bands. In fact the polarization of the band near 25 kK could not be explained in the crystal studies of  $V[S_2P(OC_2H_5)_3]^{31}$ , thus reinforcing its assignment as other than due to a d-d transition.

From the results of Table 6.2, the spectrochemical series of ligands by X is



in agreement with the infrared spectra (sequence 3.11). In order of increasing  $\beta$ , the nephelauxetic series of ligands by X is



This is not the order that would have been predicted by increasing covalency as measured by the order of increasing M-S stretching frequencies. If the ir band assignments and methods of calculation of  $\beta$  are correct then a re-evaluation of the interpretation of symmetry restricted covalency and central field covalency is necessary as both have been stated<sup>74</sup> to predict a reduced  $\beta$  with increasing covalency.

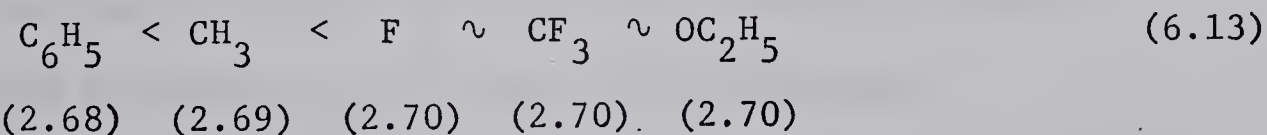
Clark, et al.<sup>125</sup> note that if there is charge release to the metal ion by the ligands the distinction between bonding and non-bonding electrons inside a shell of defined radius disappear. Furthermore, it is difficult to imagine how an increase in electron density within a defined volume should result in reduced



interelectronic repulsions. More consistent with the results presented here is that increased covalency in the tris complexes of V(III) and Cr(III) (*vide infra*) increases interelectronic repulsions. Since the  $\beta$  values are still less than unity, it is inferred that interelectronic repulsions within the  $\pi^*(t_{2g})$  subshell are the net result of a largely symmetry restricted covalent reduction together with a smaller central field covalent increase. This interpretation (i.e. a synergic effect) is consistent with the accepted explanation of the bonding in transition metal carbonyl complexes<sup>3</sup>.

However, the above qualitative arguments do not provide a quantitative basis for separating the magnitudes of the central field and symmetry restricted covalency effects. The nephelauxetic series (6.12) is taken to imply that the interelectronic repulsions increase within the metal d-shell faster as a function of M-S bond length than they are relieved by delocalization effects.

If the first high intensity (Laporte allowed) band is assigned to an  $M \leftarrow L$  electron transfer, then the order of  $\chi_{opt_L}$  values by substituent, X, is



While the gross ordering between the sets  $\{C_6H_5, CH_3\}$  and  $\{F, CF_3, OC_2H_5\}$  of sequence (6.13) is in agreement with the group electronegativities listed in Table 3.7, the ordering within these two sets is exactly opposite. If it is assumed that  $\chi_{opt_L}$  is determined by  $\Delta_1$  (Figure 6.1), then the factors influencing the relative energies



of the levels  $\pi_s^{(*)}$  and  $\pi^*(t_{2g})$  must be exposed in order to explain sequence (6.13). Stronger bonding (shorter P-S bond lengths) within the  $P \begin{array}{c} S \\ \diagup \\ \diagdown \\ S \end{array} \pi$  system is anticipated to raise the energies of the  $\pi_s^{(*)}$  orbitals and consequently reduce  $\Delta_1$ . Since the  $PS_2$  group vibrational frequencies (see sequence (3.9)) are more sensitive to variation of the substituents than metal atom, it might be inferred that the differences in  $\chi_{opt_L}$  values should be dominated by the shifts of the  $\pi_s^{(*)}$  orbitals. Furthermore, the  $\pi^*(t_{2g})$  orbitals are anticipated to be more strongly anti-bonding the greater the  $\pi$ -acidity of the ligand, thus shifting in energy in the same sense as the  $\pi_s^{(*)}$  orbitals. Electron repulsion considerations are ignored in the above discussion but the small differences in  $\chi_{opt_L}$  values do not justify further elaboration.

With respect to band positions and ligand field parameters, the results obtained herein are in agreement with those found<sup>37</sup> for  $V[S_2P(C_2H_5)_2]_3$  and  $V[S_2P(C_3H_7)_2]_3$  in carbon tetrachloride solution. Band positions observed for  $V[S_2P(C_6H_5)_2]_3$  in benzene solution<sup>36</sup> and  $V[S_2P(OC_2H_5)_2]_3$  in toluene solution<sup>28</sup> are some 0.3 - 0.4 kK higher than observed herein in halocarbon solvents and with commensurate increases in the ligand field parameters.

### Spectra of Chromium(III) Complexes

Reports on all the complexes  $Cr[S_2PX_2]_3$  studied herein, except  $Cr[S_2P(CF_3)_2]_3$ <sup>53</sup>, have been published by other workers with varying degrees of completeness (cf. Table 1.1). However, few have taken adequate note of the conspicuous fine structure in the first two ligand field bands in the spectra of these  $d^3$  systems. The



solution spectra are illustrated in Figure 6.6 while the band parameters and derived quantities are collected in Table 6.3. The relative energies of the quartet and singlet levels resulting from the free ion terms ( $^4F$ ,  $^4P$ ,  $^2G$ ) upon application of a strong crystal field of octahedral symmetry are given by the expressions (including configuration interaction, with the assumption that  $C = 4B$ )<sup>74,141</sup>:

$$\begin{aligned}
 E(^4A_{2g}(F)) &= -12Dq \\
 E(^2E_g(G)) &= -12Dq + 9B + 3C - 90\beta_{35}^2/(10Dq) \\
 E(^4T_{2g}(F)) &= -2Dq \\
 E(^2T_{1g}(G)) &= -12Dq + 9B + 3C - 24\beta_{35}^2/(10Dq) \quad (6.14) \\
 E(^4T_{1g}(F)) &= 3Dq + 7.5B - \frac{1}{2}[(15B)^2 + (10Dq)^2 - 180DqB]^{\frac{1}{2}} \\
 E(^2T_{2g}(G)) &= -12Dq + 15B + 5C - 176\beta_{35}^2/(10Dq) \\
 E(^4T_{1g}(P)) &= 3Dq + 7.5B + \frac{1}{2}[(15B)^2 + (10Dq)^2 - 180DqB]^{\frac{1}{2}}
 \end{aligned}$$

Algebraic solution of the equations (6.14) shows that for the first two spin allowed (sa) transitions,  $\nu_1 = E(^4T_{2g}) - E(^4A_{2g})$  and  $\nu_2 = E(^4T_{1g}) - E(^4A_{2g})$ :

$$10Dq = \nu_2 - \nu_1 \text{ and } B' = (2\nu_1 - \nu_2)(\nu_2 - \nu_1)/(27\nu_1 - 15\nu_2) \quad (6.14)$$

In common with the spectra of other Cr(III) compounds<sup>74</sup>, the solution spectra of the complexes  $\text{Cr}[\text{S}_2\text{PX}_2]_3$ ,  $\text{X} = \text{CH}_3$ ,  $\text{C}_6\text{H}_5$ ,  $\text{OC}_2\text{H}_5$ ,  $\text{F}$ , and  $\text{CF}_3$ , show two weak (Laporte forbidden) band systems in the visible region, generally assigned<sup>131</sup> as  $\nu_1$  and  $\nu_2$ . If the visible spectra (with a common energy scale) of all five complexes are superimposed, it is apparent that the fine structure components of the  $\nu_1$  and  $\nu_2$  bands occur at relatively constant positions independent of the substituent, i.e.  $10Dq$ . For example, the shoulders



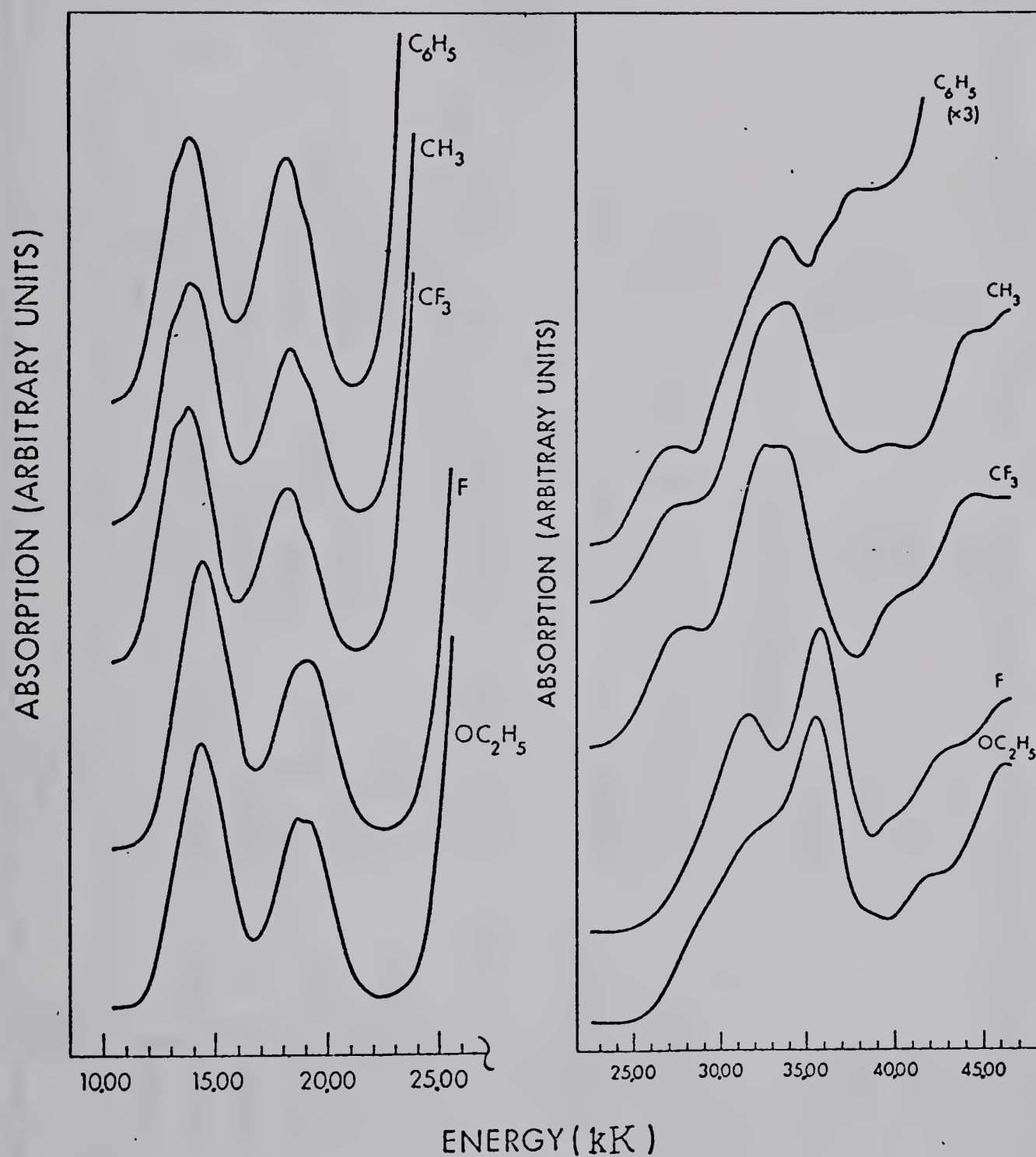


FIGURE 6.6: Electronic spectra of  $\text{Cr}[\text{S}_2\text{PX}_2]_3$  complexes in  $\text{CH}_2\text{Cl}_2$  solution.



TABLE 6.3

Electronic Spectra of the Complexes  $\text{Cr}[\text{S}_2\text{PX}_2]_3^a$ 

$\text{CH}_3$ $\nu(\text{kk})$	$\text{C}_6\text{H}_5$ $\nu(\text{kk})$	$\text{OC}_2\text{H}_5$ $\nu(\text{kk})$	$\text{F}$ $\nu(\text{kk})$	$\text{CF}_3$ $\nu(\text{kk})$	Assignment <sup>b</sup>
13.1sh	13.0sh	13.1sh	13.1sh	13.1sh	$2_E(G) \leftarrow {}^4A_{2g}(F)$
13.73	(39.3)	13.70	(36.9)	14.38	$v_1: {}^4T_{2g}(F) \leftarrow {}^4A_{2g}(F)$
14.1sh	14.0sh	14.1sh	14.1sh	14.1sh	${}^2T_{1g}(G) \leftarrow {}^4A_{2g}(F)$
18.26	18.12	18.95	18.95	18.10	$v_2: {}^4T_{1g}(F) \leftarrow {}^4A_{2g}(F)$
19.2sh	(27.8)	(35.7)	(33.9)	(23.6)	${}^2T_{2g}(G) \leftarrow {}^4A_{2g}(F)$
27.4(730)sh	27.0(1.0x10 <sup>3</sup> )sh	28.7(690)sh	~28.7(sh)	27.4(940)sh	
32.6sh	{(4.1x10 <sup>3</sup> )}	~31.2sh	31.9(1.6x10 <sup>3</sup> )sh	31.5	$(2.08 \times 10^3)$
34.0	{(4.1x10 <sup>3</sup> )}	33.6	35.62(2.60x10 <sup>3</sup> )	35.83(2.04x10 <sup>3</sup> )	$32.4\text{sh}$ $v_{33.6}$ $(3.7 \times 10^3)$
39.5(920)sh	36.0sh	37.1sh	(3x110 <sup>3</sup> )	38.5(290)sh	Intraligand excitation phenyl group transitions
43.6sh	{(6.5x10 <sup>3</sup> )}	41.6(1x10 <sup>3</sup> )	41.6sh	42.5sh	$39.6(310)\text{sh}$
46.6	{~46.7(?)}		46.4	46.6	$(3.9 \times 10^3)$ $44.5(7 \times 10^3)$
Ligand Field Parameters					
$10D_q$	13.73	13.70	14.38	14.39	13.70
$\beta_{35}^c$	0.468	0.455	0.466	0.466	0.453
$\beta_{55}^d$	0.733	0.730	0.730	0.730	0.729
$v_3(\text{calc.})$	29.4	29.2	30.6	30.6	29.2
					${}^4T_{1g}(P) \leftarrow {}^4A_{2g}(F)$

<sup>a</sup> See footnote (a) of Table 6.1.<sup>b</sup> The ligand field bands are assigned using an octahedral model.<sup>c</sup> Calculated using  $B = 918 \text{ K}$ .<sup>d</sup> Calculated using  $9B + 3C = 19.812 \text{ kk}$ .



on either side of the  $\nu_1$  band of  $\text{Cr}[\text{S}_2\text{P}(\text{CH}_3)_2]_3$  occur as inflections on the low energy slope of the  $\nu_1$  band of  $\text{Cr}[\text{S}_2\text{PF}_2]_3$ . Thus there is little doubt that the three "extra" discernable components are due to the three spin-forbidden (sf) transitions predicted by equations (6.14) and are not the result of spin-orbit coupling or low symmetry splitting of the orbitally degenerate  $^4T$  terms. The intensity of these sf transitions is probably a result of their proximity to the sa transitions  $\nu_1$  and  $\nu_2$  allowing intensity borrowing. Resolution of the sf bands by the computer program BIGAUSS was inadequate due to an insufficiently fine energy grid so that the sf band positions were estimated by visual inspection while the total intensity was given to the sa bands.

In the strong crystal field approximation, two kinds of electronic transitions are expected within the d-orbital manifold of an octahedral  $d^3$  system: (i) those sf transitions within the  $t_{2g}$  subshell, i.e. between  $\pi$  anti-bonding orbitals, and (ii) those sa transitions between the  $\pi^*(t_{2g})$  and the  $\sigma^*(e_g)$  sets. The difference in electronic repulsion energies that must exist between the two types (sa and sf) transitions is quantitatively accounted for by defining two nephelauxetic parameters<sup>74</sup>:

$$\beta_{35} = B'_{\text{sa}}/B = \beta \quad (6.16)$$

and  $\beta_{55} = B'_{\text{sf}}/B$

$$= \frac{(3B+C)'}{3B+C}, \text{ provided that } C \propto B. \quad (6.17)$$

The subscripts derive from the nomenclature  $\gamma_3 \equiv e_g$  and  $\gamma_5 \equiv t_{2g}$ <sup>141</sup>.

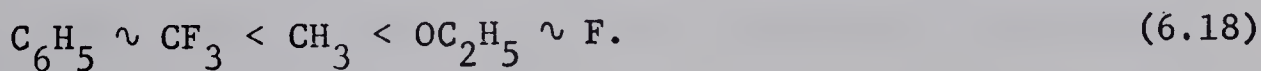
From equations (6.14) it is seen that, to second order perturbation,



sub-shell configuration intermixing introduces small terms in multiples of  $\beta_{35}^2 / (10Dq)$  to the energies of the sf transitions and hence a slight dependence upon  $10Dq^{141}$ . A large difference between  $\beta_{35}$  and  $\beta_{55}$  is interpreted to indicate little interaction between the  $\sigma^*(e_g)$  and  $\pi^*(t_{2g})$  subshells (cf. Figure 6.1)<sup>74</sup>.

The calculated values of  $B'_{sa}$ ,  $\beta_{35}$ , and  $\beta_{55}$  are included in Table 6.3. It is clear that  $\beta_{35} \ll \beta_{55}$  indicating, according to Lever<sup>74</sup>, extensive electron delocalization onto the sulfur atoms in the  $\sigma^*(e_g)$  orbitals. A simpler explanation more consistent with the discussion of the  $\beta$ -values observed for the  $V[S_2PX_2]_3$  complexes is that the occupation of a more distant and previously unoccupied MO subshell relieves electron repulsions. Moreover, the  $\beta_{55}$  values are in agreement with the extent of symmetry restricted covalency predicted by the  $\pi$ -acidity of the ligands when the electrical substituent effects in Table 3.7 are considered to be transduced by the P atoms. Large values of  $\beta_{55}$  relative to  $\beta_{35}$  may indicate less electron delocalization in the  $\pi^*(t_{2g})$  orbitals than in the  $\sigma^*$  orbitals of the complexes  $Cr[S_2PX_2]_3$  in accordance with the expected differences in M-S bond lengths. The  $\beta_{55}$  values listed in Table 6.3 were calculated from the  $^2E_g \leftarrow ^4A_{2g}$  transition energy but are also very close to the average value obtained by using all three sf transitions, e.g.  $(0.733 + 0.733 + 0.698)/3 = 0.72$  for  $Cr[S_2P(CH_3)_2]_3$ .

In agreement with the ir spectra (i.e. sequence (3.11),) the spectrochemical series of ligands, by X, is





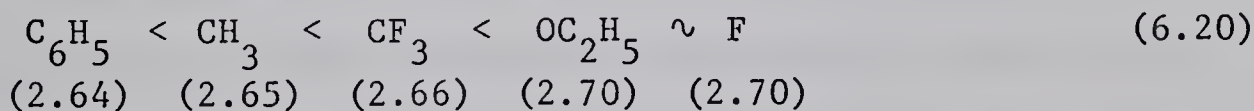
Also the nephelauxetic series of ligands, by X, is



where the high positions of  $\text{CH}_3$  might be attributed to its  $\pi$  donor effect on the  $\pi^*(t_{2g})$  subshell with all orbitals singly occupied.

This nephelauxetic series provides further support that the symmetry restricted covalency is a dominant effect as the M-S vibrational frequencies (Chapter 3) would indicate a larger central field covalency for either  $X = \text{OC}_2\text{H}_5$  or F than with  $X = \text{CH}_3$ .

Assuming with Jorgensen<sup>131</sup> that the first weak bands in the uv spectra of the complexes  $\text{Cr}[\text{S}_2\text{PX}_2]_3$  are due to the transitions  $\pi^*(t_{2g}) \leftarrow \pi_s^{(*)}$  (Figure 6.1), then the order of ligand optical electronegativities, by X is



This sequence is similar to that found for the V(III) complexes and a similar explanation is believed valid (*vide supra*).

Single crystal studies<sup>31</sup> of  $\text{Cr}[\text{S}_2\text{P}(\text{OC}_2\text{H}_5)_2]_3$  show that the transition intensities obey the electron dipole selection rules for  $D_3$  symmetry and confirm the assignments of  $\nu_1$  and  $\nu_2$ . Moreover, the excited  ${}^4T_{2g}(F)$  term was found<sup>31</sup> to be split into a lower  ${}^4A_1$  level and an upper  ${}^4E$  level separated by 0.150 kK. Finally, these crystal studies demonstrated that the intensity behavior of the first uv band in polarized light was inconsistent with its assignment to the  $\nu_3$  (d-d) transition. The expected positions of the  $\nu_3$  band calculated from  $10Dq$  and  $B'$  values are included in Table 6.3, but reference to Figure 6.6 shows this spectral region to be masked by high intensity



Laporte-allowed bands.

Cancellieri, et al.<sup>142</sup> found both  $\text{Cr}[\text{S}_2\text{P}(\text{C}_6\text{H}_5)_2]_3$  and  $\text{Cr}[\text{S}_2\text{P}(\text{OC}_2\text{H}_5)_2]_3$  to be inactive in emission, giving no detectable luminescence (fluorescence or phosphorescence) bands in either the visible or near-ir regions. These authors attribute<sup>142</sup> the absence of luminescence to the small separation between the ground state, the potentially phosphorescent spin doublet states and the potentially fluorescent  $^4\text{T}_{2g}$  state, allowing nonradiative decay. This is the probable explanation for the failure in this study to obtain Raman spectra either from crystals or  $\text{CH}_2\text{Cl}_2$  solutions due to strong internal absorption by the complexes  $\text{Cr}[\text{S}_2\text{PX}_2]_3$ , X =  $\text{CH}_3$ ,  $\text{C}_6\text{H}_5$ ,  $\text{OC}_2\text{H}_5$ , F, and  $\text{CF}_3$ .

In conclusion of this discussion of the complexes  $\text{Cr}[\text{S}_2\text{PX}_2]_3$  it is noted that the spectra and band assignments from this work are in agreement with other studies within small solvent shifts (Table 1.1). A parallel investigation of the spectral dependence upon the alkyl (R) groups in the complexes  $\text{Cr}[\text{S}_2\text{P}(\text{OR})_2]_3$  revealed a small red-shift of  $\nu_1$  with increasing mass of R accompanied by a corresponding increase in band intensities<sup>12</sup>. A more recent and possibly less careful study<sup>34</sup> of the same effect indicated no such dependence.

#### Spectra of Manganese(II) and Iron(III) Complexes

The tetrahedral bis complexes  $\text{Mn}[\text{S}_2\text{PX}_2]_2$  and the octahedral tris complexes  $\text{Fe}[\text{S}_2\text{PX}_2]_3$  are both 3d high spin systems (Chapter 5). Therefore, by the "hole formalism"<sup>74</sup> their ligand field spectra should be analyzable in terms of the same energy level



expressions. The ground terms are  $^6A_{1(g)}$ . The absence of any other sextet terms requires that all ligand field transitions including the ground state be both spin and Laporte forbidden. Hence the d-d bands are anticipated to be very weak. The solid Mn(II) dithiophosphinates range in color from very pale green ( $X = C_6H_5, CF_3$ ) to very pale pink ( $X = F$ ) while the solid Fe(III) dithiophosphinates appear intensely black.

Of the four complexes of Mn(II),  $X = CH_3, C_6H_5, CF_3$ , and F prepared for this study, reflectance spectra were obtained for only the first three compounds. These spectra were sufficient to indicate a very low absorption profile preceding the onset of electron transfer bonds. However, as often found with Mn(II) complexes with organic ligands, too much of the ligand field spectrum was obscured by Laporte-allowed bands for a meaningful analysis<sup>11</sup>.

Unlike  $Fe[S_2P(OC_2H_5)_2]_3$  which is reported<sup>11</sup> to be unstable in solution,  $Fe[S_2P(C_6H_5)_2]_3$  could be kept in halocarbon solutions indefinitely provided it was protected from air. The electronic spectra of these two Fe(III) dithiophosphinate complexes are the only ones known to date. The solution spectrum of  $Fe[S_2P(C_6H_5)_2]_3$  is illustrated in Figure 6.7 while the band positions of both the  $X = OC_2H_5$  and  $C_6H_5$  complexes are collected in Table 6.4.

From the oxidizing nature of Fe(III), the intensity and breadth of the absorption bands, Jorgensen<sup>11</sup> has inferred that all the observed bands are Laporte allowed and mask the ligand field bands. Bands have been reported<sup>61</sup> for  $Fe[S_2P(OC_2H_5)_2]_3$  as shoulders at 7.5 and 10.8 kK, but the presence of bands at such low energy are



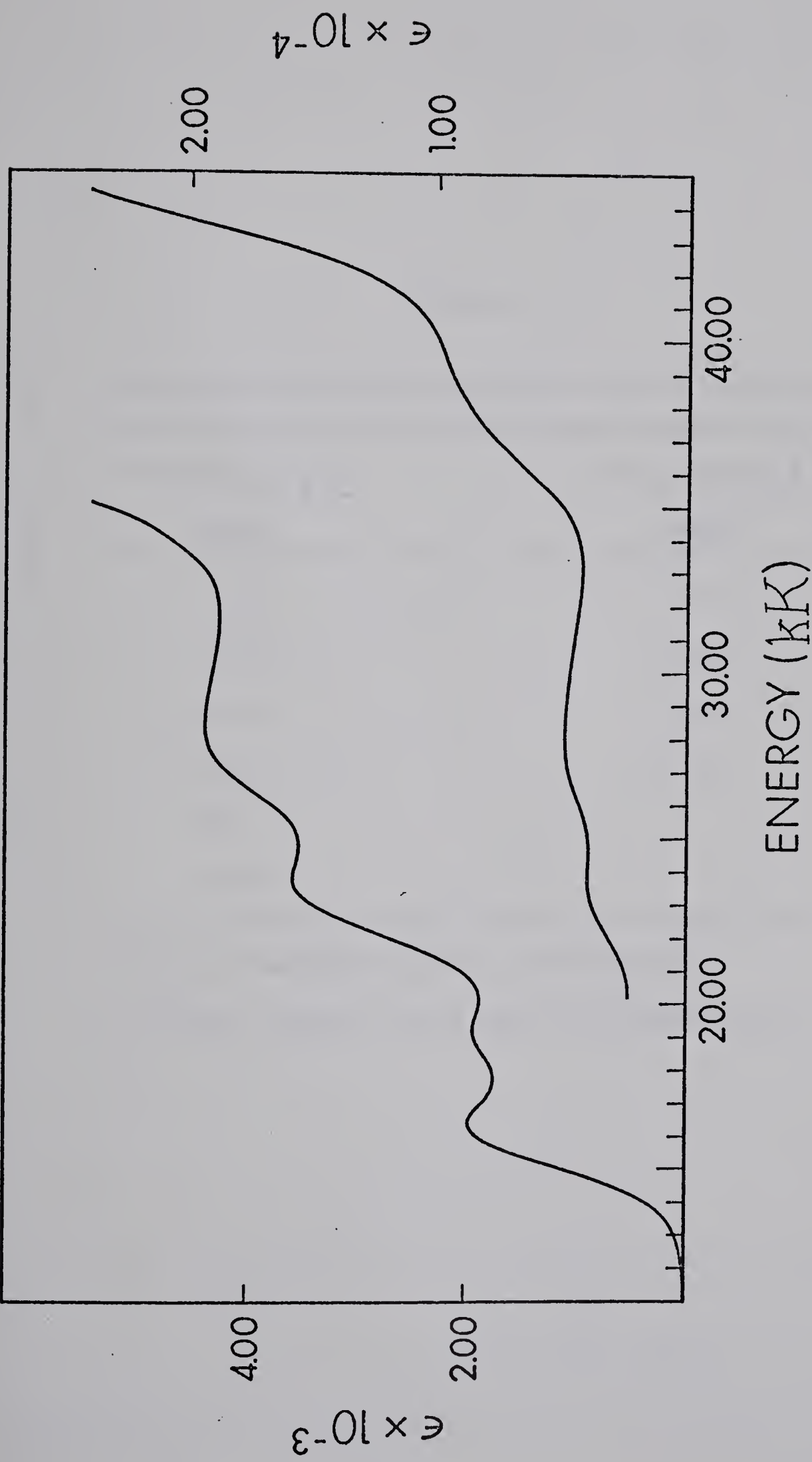


FIGURE 6.7: Electronic spectra of  $\text{Fe}[\text{S}_2\text{P}(\text{C}_6\text{H}_5)_2]_3$  in  $\text{CH}_2\text{Cl}_2$  solution.



TABLE 6.4

## Electronic Absorption Spectra of Fe(III) Complexes

$\text{Fe}[\text{S}_2\text{P}(\text{C}_6\text{H}_5)_2]_3^{\text{a}}$	$\text{Fe}[\text{S}_2\text{P}(\text{OC}_2\text{H}_5)_2]_3^{\text{b}}$
$\nu$ (kK)	$\nu$ (kK)
16.3	16.7
19.2	20.1
22.8	25.5
27.4	28.3
~31	
38.5	

<sup>a</sup> Dichloromethane solution, see Figure 6.7.

<sup>b</sup> Ethanol solution, data taken from Reference 11.



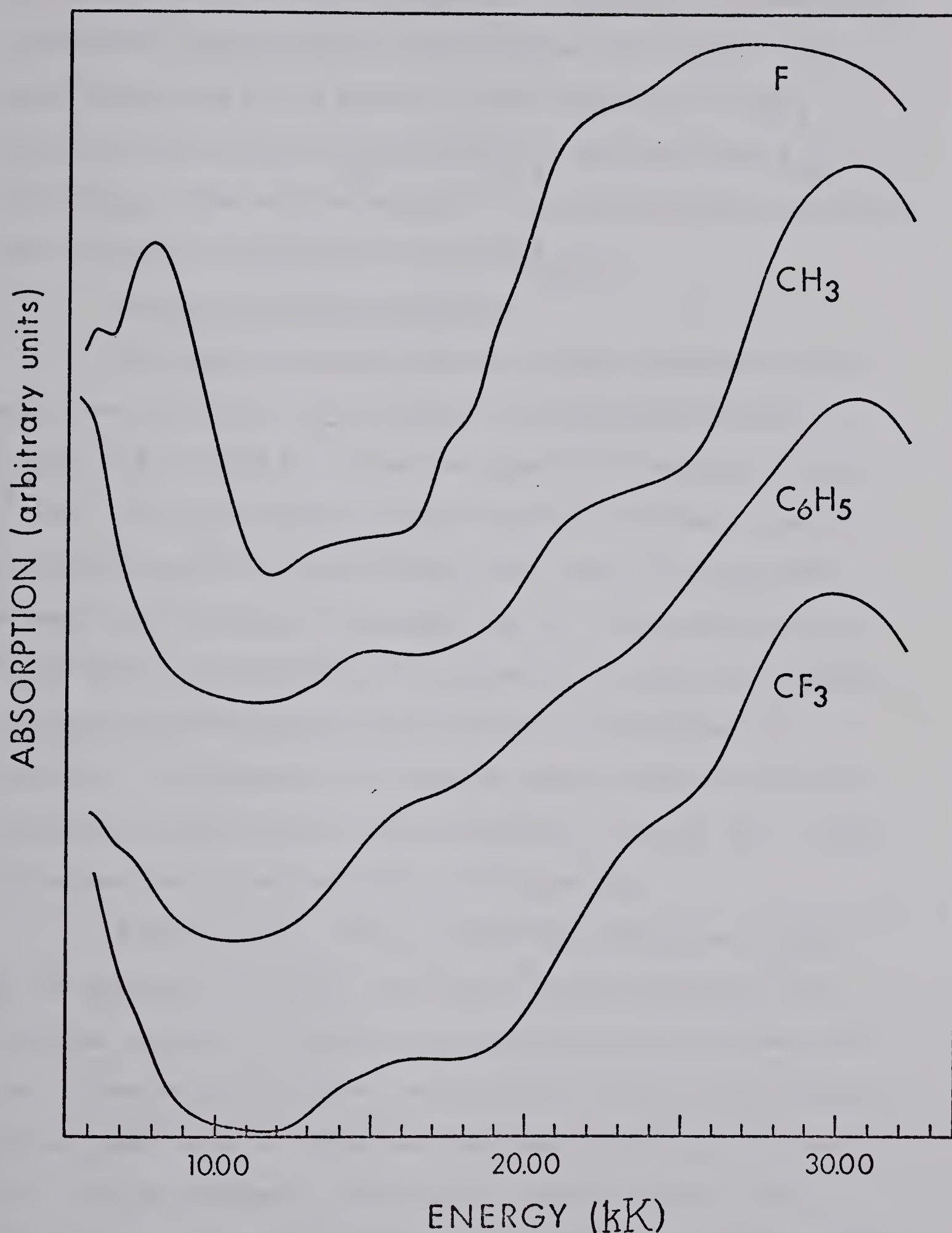


FIGURE 6.8: Diffuse reflectance spectra of  $\text{Fe}[\text{S}_2\text{PX}_2]_2$  complexes .



not supported by this work or Jorgensen<sup>11</sup>. However,  $\text{Fe}[\text{S}_2\text{P}(\text{OC}_2\text{H}_5)_2]_2$  is expected to absorb near the latter regions (*vide infra*). The higher energy bias of the Laporte allowed bands with  $X = \text{OC}_2\text{H}_5$  (Table 6.4) indicate that  $\chi_{\text{opt}}(\text{S}_2\text{P}(\text{OC}_2\text{H}_5)_2)$  is greater than  $\chi_{\text{opt}}(\text{S}_2\text{P}(\text{C}_6\text{H}_5)_2)$ . The very low energies of the first bands are consistent with the thermal instability of  $\text{Fe}[\text{S}_2\text{P}(\text{C}_6\text{H}_5)_2]_3$ .

#### Spectra of Iron(II) Complexes

The magnetic results (Chapter 5) have established a high spin ground state for these tetrahedral bis complexes  $\text{Fe}[\text{S}_2\text{PX}_2]_2$ ,  $X = \text{CH}_3$ ,  $\text{C}_6\text{H}_5$ , F, and  $\text{CF}_3$ . Thus the ligand field spectra of these  $d^6$  metal ion compounds should parallel those of a  $d^1$  metal ion with the added potential of spin-forbidden (sf) bands. Only one spin-allowed (sa) transition is expected, the  $^5\text{T}_2 \leftarrow ^5\text{E}$  transition. Due to the extreme sensitivity of the complexes to oxidation in solution, only the reflectance spectra were obtained as illustrated in Figure 6.8. Unfortunately, the spectral range accessible with the available equipment was not quite sufficient to observe the 3 - 6 kK region expected to contain the  $^5\text{T}_2 \leftarrow ^5\text{E}$  transition.

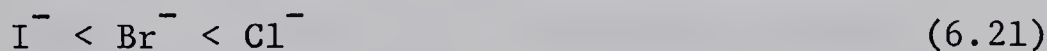
However, a well defined maximum was observed at 8.05 kK in the spectrum of  $\text{Fe}[\text{S}_2\text{PF}_2]_2$  and partial peaks observed for the remaining complexes of Figure 6.8 indicate extrapolated maxima near 6 kK. Since no other bands are anticipated to occur in this spectral region, these bands are tentatively assigned to the  $^5\text{T}_2 \leftarrow ^5\text{E}$  transition. Such an assignment results in the highest values of  $10Dq$  thus far observed for four coordinate Fe(II) complexes. The structure apparent in the low energy band is probably the spin-forbidden band



arising from the  $^3T_1 \leftarrow ^5E$  transition, but splitting due to Jahn-Teller distortion<sup>111</sup> or spin-orbit coupling<sup>125,143</sup> cannot yet be ruled out.

Analysis of the substituent effects within this system is complicated both by the incomplete spectra and the probable structural variations in the solid state. The MSP bond angles in  $\text{Fe}[\text{S}_2\text{P}(\text{CH}_3)_2]_2$  are certain to be close to  $109^\circ$  similarly to  $\text{Co}[\text{S}_2\text{P}(\text{CH}_3)_2]_2$ , (Table 3.1) and so the transmission of substituent effects may be quite different for bridging ligands as compared with chelating ones. Nevertheless, the indicated spectrochemical order of ligands by X group is  $\{\text{CF}_3, \text{C}_6\text{H}_5, \text{CH}_3\} < \text{F}$ .

It is implicit in the band assignments of the tris complexes that the MO energy separations illustrated in Figure 6.1 are in the order  $\Delta_2 > \Delta_1 > 10D_q$  in agreement with results obtained<sup>74,141</sup> for the hexahalide complexes  $\text{MY}_6^{-3}$ ,  $\text{Y} = \text{I}^-, \text{Br}^-, \text{and Cl}^-$ . Similarly, the electron transfer band energies of the tetrahedral complexes  $\text{FeY}_4^{-2}$  are in the order by Y<sup>143</sup>:



indicating  $\text{M} \leftarrow \text{L}$  transfer and the same order of MO energy separations. (Figure 6.2). Figure 6.8 clearly shows that the electron transfer band energies of the complexes  $\text{Fe}[\text{S}_2\text{PX}_2]_2$  shift in an opposite sense to the anticipated magnitudes of  $10D_q$ . The parameter expected to decrease with increasing  $10D_q$  is  $\Delta_2$  (Figure 6.2), and thus the lower energy bands in the near-uv spectral region are assumed to be  $\text{M} \rightarrow \text{L}$  transfer bands implying that the order  $\Delta_1 > \Delta_2 > 10D_q$  may be characteristic of these tetrahedral bis complexes.



Two kinds of  $M \rightarrow L$  electron transfer may occur in a high spin tetrahedral  $d^6$  complex. Since two of the electrons in the  $e$  subshell (Figure 6.2) must be paired, the transition energies are approximately<sup>74</sup>

$$\begin{aligned} E(L^* \leftarrow t_2) &\sim \Delta_2 \\ \text{or} \quad E(L^* \leftarrow e) &\sim \Delta_2 + 10Dq - P, \end{aligned} \quad (6.22)$$

where  $L^*$  is some undefined MO lying above the  $t_2$  set, and  $P$  is a mean pairing energy within the  $e^3$  configuration. For a high-spin complex  $P$  must be greater than  $10Dq$  and hence the lower energy electron transfer bands are assigned to the  $L^* \leftarrow e$  type transitions.

#### Spectra of Cobalt(III) Complexes

Both the Fe(II) complexes of the preceding section and these Co(III) complexes are formally  $d^6$  metal ion systems, but the larger ligand field generated by coordination of three bidentate dithiophosphinate groups to a trivalent metal ion is sufficient to force electron pairing and a  ${}^1A_{1g}$  ground state in the pseudo-octahedral Co(III) compounds (Chapter 5). The solution spectra are illustrated in Figure 6.9 while the band parameters and derived quantities are collected in Table 6.5. It proved exceedingly difficult to produce the Co(III),  $X = \text{CH}_3$ ,  $\text{C}_6\text{H}_5$ , and F compounds completely free of the Co(II) species, hence the spectra in Figure 6.9 include arrows marking the contributions from these impurities. Furthermore, the positions of the  $v_2$  bands which appear as definite shoulders with  $X = \text{OC}_2\text{H}_5$  and F were extracted with large uncertainty from the spectra where  $X = \text{CH}_3$ ,  $\text{C}_6\text{H}_5$ , and  $\text{CF}_3$ . Therefore, the



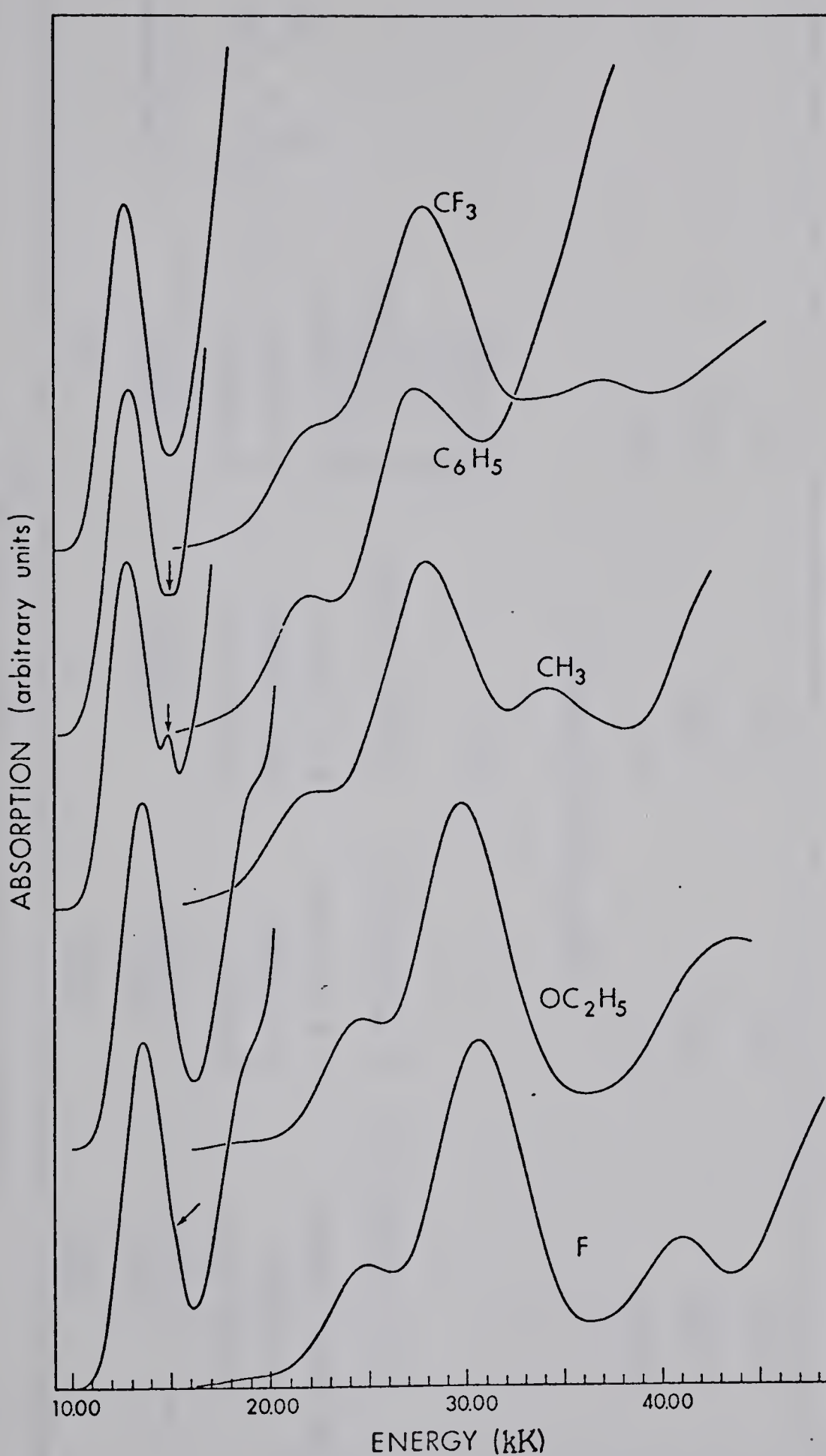


FIGURE 6.9: Electronic spectra of  $\text{Co}[\text{S}_2\text{PX}_2]_3$  complexes in  $\text{CH}_2\text{Cl}_2$  solution. Arrows mark positions of Co(II) species absorptions. Relative absorption scale factors, UV/Vis, according to X:  $\text{CH}_3$  33.6,  $\text{C}_6\text{H}_5$  37.5,  $\text{OC}_2\text{H}_5$  101.4, F 51.3,  $\text{CF}_3$  62.3.



TABLE 6.5  
Electronic Spectra of the Complexes  $\text{Co}[\text{S}_2\text{PX}_2]_3^a$

$X = \text{CH}_3$	$C_6\text{H}_5$	$\text{OC}_2\text{H}_5$	F	$\text{CF}_3$	Assignments <sup>b</sup>
	$\mathcal{V}(k \bar{k})$	$\mathcal{V}(k \bar{k})$	$\mathcal{V}(k \bar{k})$	$\mathcal{V}(k \bar{k})$	
12.76(53.7)	12.68(35.8)	13.56(45.3)	13.58(30.7)	12.59(32.8)	$v_1: 1T_{1g} \leftarrow 1A_{1g}$
17.66( $\sim$ 20)i	17.56(?)i	18.47(20)sh	18.49(120)sh	17.45( $\sim$ 30)i	$v_2: 1T_{2g} \leftarrow 1A_{1g}$
21.8 ( $1.12 \times 10^3$ )sh	21.6 (884)sh	24.2 (958)sh	24.6 (790)	22.0 (820)sh	
27.9 ( $3.8 \times 10^3$ )	27.2 ( $3.53 \times 10^3$ )sh	29.77( $3.93 \times 10^3$ )	30.69( $3.75 \times 10^3$ )	24.8 (30)i	
			$\sim$ 30 (?)i	27.7 ( $3.11 \times 10^3$ )	
			33.8 (?)i		
			41.0	36.8 (?)sh	
Ligand Field Parameters					
10Dq	13.370	13.28	14.22	14.24	13.19
B'	0.356	0.355	0.353	0.353	0.353
$\beta_{35}^c$	0.33	0.33	0.33	0.33	0.33

<sup>a</sup> See footnote (a) of Table 6.1.

<sup>b</sup> The ligand field bands are assigned using an octahedral model.

<sup>c</sup> Calculated using  $B = 1100\text{K}$ .



numbers listed in Table 6.5 for the  $\nu_2$  band of those latter complexes represent a very optimistic accuracy.

Diamagnetic, six-coordinate Co(III) derivatives are anticipated to exhibit two spin-allowed and two spin-forbidden transitions of which it is necessary to observe three in order to calculate  $10Dq$ ,  $B'$ , and  $C'$ <sup>74</sup>. The spin-forbidden bands, expected to occur at lower energy than the spin-allowed bands, were not observed in this investigation and were not reported by Jorgensen<sup>99</sup> in his study of  $\text{Co}[\text{S}_2\text{P}(\text{OC}_2\text{H}_5)_2]_3$  but Lever<sup>74</sup> quotes the values 1620 K for  $C'$  and 4.05 for the ratio  $C'/B'$ . The strong crystal field energy expressions for the singlet terms arising from the free ion term  $^3D$  are<sup>74</sup>

$$\begin{aligned} E(^1A_{1g}) &= -24Dq + 37B - 120B^2/(10Dq) \\ E(^1T_{1g}) &= -14Dq + 33B - 34B^2/(10Dq) \\ E(^1T_{2g}) &= -14Dq + 49B - 118B^2/(10Dq) \end{aligned} \quad (6.23)$$

where it is assumed that  $C = 4B$  and multiples of  $B^2/(10Dq)$  account for configurational interaction. It is unclear in equations (6.23) whether  $B'$  or  $\beta_{35}$  should be used in the configurational interaction terms, but fortuitously, the magnitudes of these two quantities are similar and the alternate usages produce negligible differences ( $B'$  was used for the results listed in Table 6.5).

The spectrochemical series of ligands in order by X is



in agreement with the order predicted by the ir measurements.

The nephelauxetic series of ligands might be anticipated to be an even stronger function of the  $\pi$  acidity of the ligands in

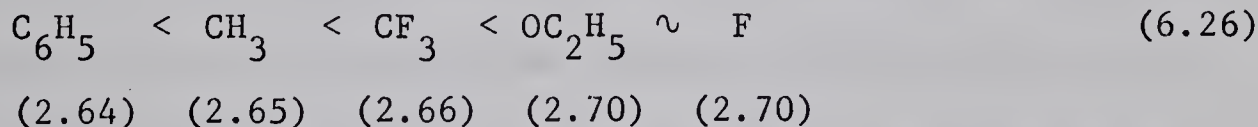


cases where the  $\pi^*(t_{2g})$  subshell is filled than in cases such as the Cr(III) complexes where the  $\pi^*(t_{2g})$  subshell is half-filled. While the differences are somewhat smaller than expected, the order by substituent, X



is indeed in the reverse order of increasing  $\pi$ -acidity.

The distribution of bands in the uv spectra of these Co(III) complexes (Figure 6.9) is again consistent with  $M \leftarrow L$  electron transfer and hence the order  $\Delta_1 > \Delta_2 > 10Dq$  (Figure 6.1). Assuming that the first uv band arises from a  $\sigma^*(t_{2g}) \leftarrow \pi_s^{(*)}$  transition, the optical electronegativities of the ligands fall in the order, by X



The qualitative explanation of this order is assumed to be the same as that given for the V(III) complexes.

The oriented single crystal spectra of  $\text{Co}[\text{S}_2\text{P}(\text{OC}_2\text{H}_5)_2]_3^{31}$  using polarized light and variable temperature conditions confirms the assignments of the spin-allowed transitions. The ligand field band intensities were observed<sup>31</sup> to obey the electric-dipole selection rules for  $D_3$  symmetry. Furthermore, the  $^1T_{1g}$  term was shown to be split by  $\sim 0.15$  kK into a lower  $^1A_2$  and upper  $^1E$  term<sup>31</sup>. Allowing for solvent shifts the results found herein are in agreement with those reported by Jorgensen<sup>99</sup> for  $\text{Co}[\text{S}_2\text{P}(\text{OC}_2\text{H}_5)_2]_3$  and recently by Müller, et al.<sup>38</sup> for  $\text{Co}[\text{S}_2\text{P}(\text{C}_6\text{H}_5)_2]_3$ .



### Spectra of Cobalt(II) Complexes

By the "hole formalism" the ligand field term energies of the high spin  $d^7$  tetrahedral bis complexes  $\text{Co}[\text{S}_2\text{PX}_2]_2$  should be described by the same expressions used for the  $d^3$  octahedral tris complexes  $\text{Cr}[\text{S}_2\text{PX}_2]_3$ , i.e. equations (6.14). The spectra illustrated in Figure 6.10 for the substituents  $X = \text{CH}_3, \text{C}_6\text{H}_5, \text{OC}_2\text{H}_5, \text{F}$ , and  $\text{CF}_3$ , clearly indicate the difficulty of the analysis problem. However, the spectra of tetrahedrally coordinated Co(II) have been extensively investigated<sup>74</sup> so that there is a broad base of both theory and experiment to aid in the interpretations. The band parameters and derived quantities are collected in Table 6.6.

Weakliem<sup>144</sup> performed a detailed analysis of the crystal spectra of  $\text{Co}^{+2}$  ions in ZnS and CdS (both of the Wurtzite structure) and calculated the band patterns and intensity distributions among spin-orbit components for a  $\text{Co}^{+2}$  ion tetrahedrally coordinated by sulfur atoms. Ferguson<sup>145</sup> subsequently demonstrated that the splittings of the orbitally degenerate excited electronic states are dominated by the low symmetry components of the ligand field, that the assumption of cubic symmetry is valid only for the determination of the approximate band positions, and further that fine structure may not be wholly spin-orbit in origin. The large band widths observed for regular tetrahedral  $\text{CoY}_4^{-2}$  ions in solution have been attributed to the cumulative effects of vibrational structure, spin-orbit coupling, and a possible dynamic Jahn-Teller distortion in the excited states<sup>74</sup>.



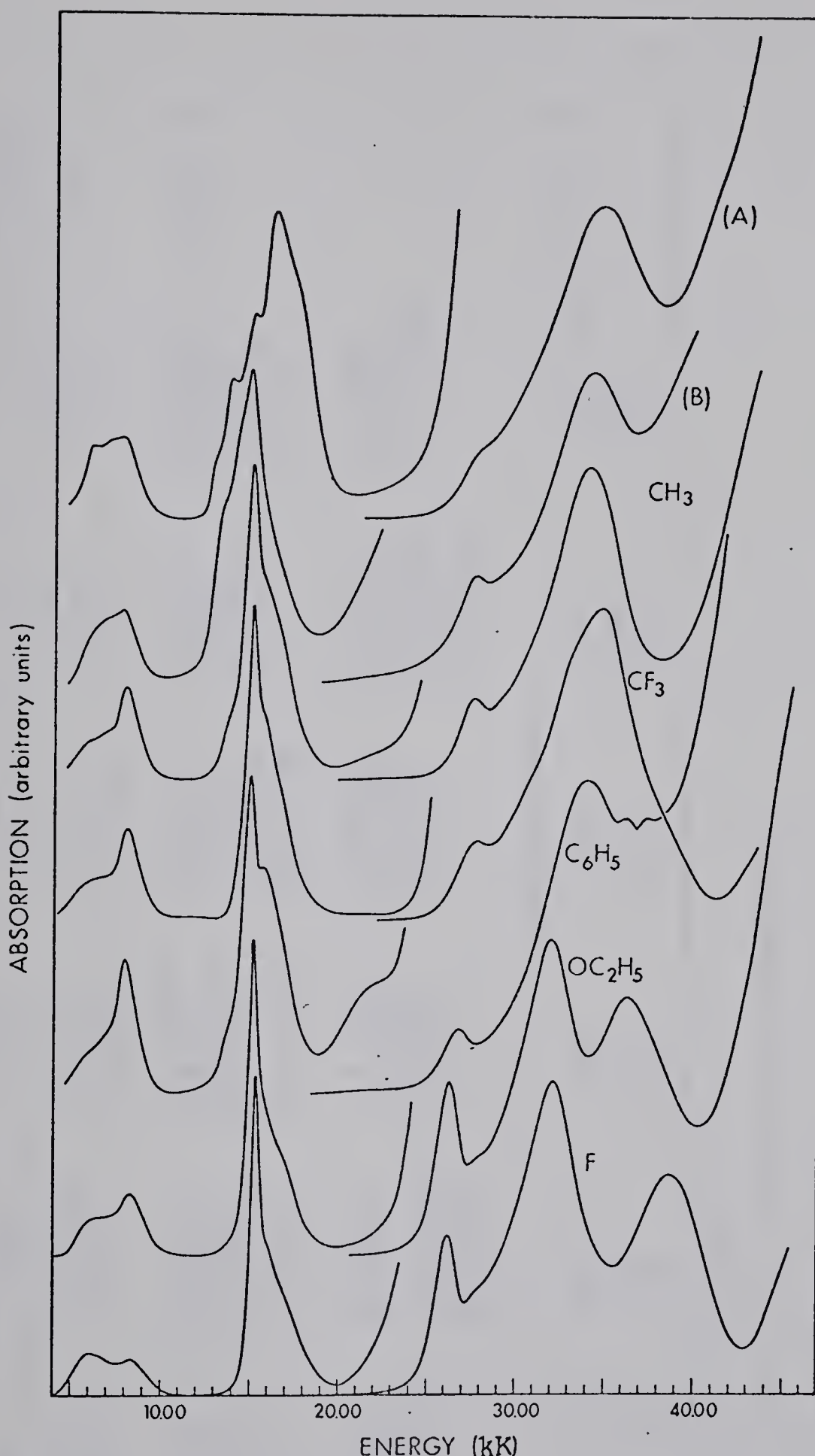


FIGURE 6.10: Electronic spectra of  $\text{Co}[\text{S}_2\text{PX}_2]_2$  complexes in  $\text{CH}_2\text{Cl}_2$  solutions.  $\text{CoOS}_3\text{P}_2(\text{CH}_3)_4$  in  $\text{CH}_2\text{Cl}_2$  produced spectrum (A) but in  $\text{CCl}_4$  produced spectrum (B). Relative absorption scale factors, UV/Vis, according to X: (A) 11.6, (B), 13.8,  $\text{CH}_3$  19.7,  $\text{C}_6\text{H}_5$  42.6,  $\text{OC}_2\text{H}_5$  16.8, F 17.0,  $\text{CF}_3$  13.7.



TABLE 6.6

Electronic Spectra of the Complexes  $\text{Co}[\text{S}_2\text{PX}_2]_2^a$ 

$X = \text{CH}_3$	$\text{C}_6\text{H}_5$	$\text{OC}_2\text{H}_5$	$\text{F}$	$\text{CF}_3$	$\text{CoOS}_3\text{F}_2(\text{CH}_3)_4$
$\nu(\text{KK})$	$\nu(\text{KK})$	$\nu(\text{KK})$	$\nu(\text{KK})$	$\nu(\text{KK})$	$\nu(\text{KK})$
5.9 ( $\sim 2$ ) sh	5.8 ( $\sim 2$ ) sh	6.2 (2.4) sh	6.0 (3)	5.8 (3) sh	5.84 (5.3) sh
6.8 ( $\sim 0.4$ ) sh	6.8 ( $\sim 0.4$ ) sh	$\sim 7$ ( $\sim 0.1$ )?	$\sim 7$ ( $\sim 0.1$ ) sh	6.7 (0.1)?	6.81 (1.2) sh
7.93 (5.2)	7.93 (6.3)	8.27 (3.2)	8.41 (2.7)	8.01 (4.0)	7.74 (9.8)
		9.3 ( $\sim 0.1$ ) sh	9.3 ( $\sim 0.1$ ) sh		
13.8 (3) sh	13.8 (3) sh	13.6 ( $\sim 0.1$ ) sh	14.9 ( $\sim 1.5$ )?	14.2 (1.2) i	12.74 (1.3) sh
14.87 (8.85)	14.85 (9.7)	15.11 ( $\sim 9$ )	15.31 (5.5)	14.99 (9.5)	13.67 (12) sh
16.0 ( $\sim 3$ ) sh	15.6 ( $\sim 2$ ) sh	$\sim 16.0$ ( $\sim 0.2$ ) sh	16.0 (6) sh	15.8 (8) sh	14.80 (6.4) sh
17.1 (9) sh	16.9 ( $\sim 5$ ) sh	17.0 (3.7) sh	17.2 (3) sh	16.9 (3) sh	16.07 (37)
			$\sim 18.6$ ( $\sim 1$ )?	18.0 (2) sh	17.8 (13) sh
21.7 (5) sh	21.7 (10) sh	20.7 ( $\sim 0.1$ ) sh	20.8 ( $\sim 0.1$ ) sh	?	22.0 ( $\sim 2$ )?
?	?	?	?	?	?
27.5 (130)	26.6 (190)	26.2 (160)	26.15 (150)	27.5 (81)	27.5 (110)
28.9 ( $\sim 10$ ) sh	28.9 (160)?	27.7 (40) sh	27.7 ( $\sim 30$ ) sh	29.5 (40) sh	29.0 (40) sh
30.2 (130) i	?	29.5 ( $\sim 50$ )?	$\sim 29.0$ ( $\sim 50$ )?	30.5 ( $\sim 10$ ) sh	30.8 (40) i
$34.01(1.21 \times 10^3)$	$33.85(2.43 \times 10^3)$	31.85 (480)	32.15 (730)	$\sim 32.8$ ( $\sim 40$ ) sh	$34.3 (1.53 \times 10^3)$
	36.1 (?) sh <sup>c</sup>	36.3 (730)	38.7 (700)	34.7 (800)	
	36.3 (?) sh <sup>cc</sup>	?	?	38.1 (150) sh	

## Ligand Field Parameters

$-10Dq$	4.715	4.716	4.944	$\nu_1$ (calc): ${}^4T_2(F) + {}^4A_2$
$B'$	0.577	0.575	0.570	$\nu_1$ (calc): ${}^4T_2(F) + {}^4A_2$
$\beta_{35}^d$	0.59	0.59	0.59	$\nu_1$ (calc): ${}^4T_2(F) + {}^4A_2$

<sup>a</sup> See footnote (a) of Table 6.1.<sup>b</sup> The ligand field bands are assigned using a tetrahedral model.<sup>c</sup> Phenyl group transition.<sup>d</sup> Calculated using  $B = 971\text{K}$ .<sup>e</sup> Calculated using centers of gravity of the  $\nu_2$  and  $\nu_3$  multiplets.



Of the three sa ligand field transitions predicted by equations (6.14) for tetrahedral Co(II) compounds, the  $\nu_1(^4T_2(F) \leftarrow ^4A_2)$  transition is forbidden by electric-dipole selection rules in  $T_d$  symmetry and is very weak when discernible at all, occurring near 3 kK in the infrared spectral region<sup>74,144</sup>. The weak ligand field generated on tetrahedral coordination allows both the  $\nu_2(^4T_1(F) \leftarrow ^4A_2)$  and  $\nu_3(^4T_1(P) \leftarrow ^4A_2)$  transitions to be observed in the visible region of the spectrum<sup>74,144</sup>. In the strict  $D_{2d}$  point group symmetry of a free molecule  $\text{Co}[\text{S}_2\text{PX}_2]_2$ , all three sa ligand field transitions are electric-dipole allowed, but the  $\nu_1$  band has not been observed in either this investigation or by Jorgensen<sup>99</sup> for  $\text{Co}[\text{S}_2\text{P}(\text{OC}_2\text{H}_5)_2]_2$ .

The most prominent features in the visible and near-ir spectra (Figure 6.10) of the  $\text{Co}[\text{S}_2\text{PX}_2]_2$  complexes is the "spike" at 15 kK and the component of the lower  $\nu_2$  band system at ~8 kK. It is believed herein that whatever the source of the fine structure in bands  $\nu_2$  and  $\nu_3$ , use of these distinctive and ligand field dependent features as measures of  $\nu_2$  and  $\nu_3$  in calculations should allow a sensitive comparison of substituent effects. The more common practice of determining centers of gravity for the  $\nu_2$  and  $\nu_3$  band systems is possibly even less accurate<sup>145</sup> and more laborious.

The spectrochemical series of ligands by X is

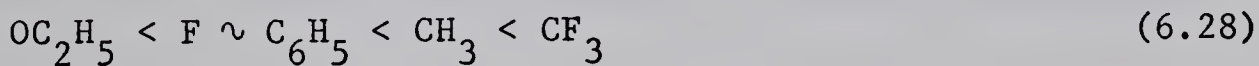


as shown by the data in Table 6.6. This order is believed to reflect the effect of  $\pi^*$  character in the upper occupied  $t_2$  subshell



(Figure 6.2) of the metal ion d shell. The stronger  $\pi$ -acid ligands are now positioned to the right in sequence (6.27).

These Co(II) complexes are both the first tetrahedral dithiophosphinate system as well as the first dithiophosphinate system in which both subshells of the split d-orbital manifold of the metal ion are occupied in the ground state for which  $\beta_{35}$  values have been calculated. If, as Lever<sup>74</sup> maintains, the large difference between  $\beta_{35}$  and  $\beta_{55}$  observed in the tris Cr(III) compounds is due to a large degree of electron delocalization in the  $e_g(\sigma^*)$  orbitals in octahedral molecules, then it might be anticipated that  $\beta_{35}$  should be even smaller in these bis Co(II) complexes in which  $\sigma^*$  orbitals are occupied in the ground state. By comparison of the data in Tables 6.3 and 6.6 this is seen not to be the case nor is it true of halide complexes<sup>74</sup>, i.e.  $\text{CrY}_6^{-3}$  vs  $\text{CoY}_4^{-2}$  complexes. However, the nephelauxetic series of ligands in order of increasing  $\beta$ , by X, i.e.

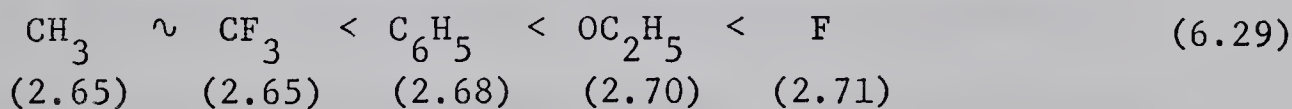


would indicate the dominance of the  $\pi$ -acid effect of the ligands in relieving electron repulsions in both the e and  $t_2$  levels (Figure 6.2) were it not for the position of  $\text{CF}_3$ . Since the  $\text{CF}_3$  substituted ligand appears to be the weakest coordinating ligand of the series, at least in the tris complexes, the high position of  $\text{CF}_3$  in sequence (6.28) is in partial support of Lever's contention that  $\sigma^*$ -type delocalization may be significant, but is not necessarily the cause of large differences between  $\beta_{55}$  and  $\beta_{35}$ . It is noted (Table 3.4)



that the M-S stretching frequencies of  $\text{Co}[\text{S}_2\text{P}(\text{CF}_3)_2]_2$  are the lowest of the series although such comparisons are tenuous when the solid state structures are not known.

As with the complexes  $\text{Fe}[\text{S}_2\text{PX}_2]_2$ , Figure 6.10 shows that the uv bands of the complexes  $\text{Co}[\text{S}_2\text{PX}_2]_2$  are shifted with X in an opposite sense to the shifts of  $10Dq$ . Thus once again electron transfer appears to be of the  $M \rightarrow L$  type. Similar arguments as proposed for the Fe(II) complexes suggest that the lowest energy electron transfers are to be assigned to  $L^* \leftarrow e$  transitions, where  $L^*$  is some undefined MO. Thus using equation (6.9) the order of  $\chi_{\text{opt}}^L$  values by substituent are



The small value of  $\chi_{\text{opt}}^L(\text{S}_2\text{P}(\text{CF}_3)_2)$  is probably the result of weak M-S bonding resulting in a smaller value of  $\Delta_1$  in Figure 6.2 (see the previous V(III) section for discussion of factors determining  $\Delta_1$ ).

Included in Figure 6.10 are the spectra of  $\text{CoOS}_3[\text{S}_2\text{P}(\text{CH}_3)_4]$  in dichloromethane and carbon tetrachloride. The dichloromethane solution was deep blue in color as were chloroform solutions which gave superimposable spectra. For lack of alternatives, the centers of gravity of the  $\nu_2$  and  $\nu_3$  multiplets were used to estimate the ligand field parameters given in Table 6.6. The carbon tetrachloride solutions were deep green and gave solution spectra distinctly more similar to those of the complex  $\text{Co}[\text{S}_2\text{P}(\text{CH}_3)_2]_2$ , indicating selective



dissolution of the "tetrathio component" of the blue complex  $\text{CoOS}_3\text{P}(\text{CH}_3)_4$  in nonpolar solvent.

Comparison of Figures 6.10 and 6.11 illustrates the spectral changes that occur upon dissolution of both  $\text{Co}[\text{S}_2\text{P}(\text{CH}_3)_2]_2$  and  $\text{CoOS}_3\text{P}(\text{CH}_3)_4$  in alcohol. Jorgensen<sup>99</sup> postulates that the spectral changes observed for  $\text{Co}[\text{S}_2\text{P}(\text{OC}_2\text{H}_5)_2]_2$  in ethanol are due to a six coordinate disolvate, however, the dentateness of the dithiophosphinate ligands in these species is unknown. All complexes were recovered unchanged from the alcohols.

#### Spectra of Planar Nickel Group Complexes

An enormous volume of literature exists describing attempts to rationalize the bonding of the planar complexes of Ni(II), Pd(II), and Pt(II) in terms of their electronic spectra with no single set of experimental results appearing to provide a definite solution to the problem. In the assignment of the ligand field spectra the major uncertainty seems to revolve about the positions of the lower three metal ion d orbitals and nearly all permutations have been reported with support claimed from some piece of evidence or other. Chatt, et al.<sup>146</sup> proposed that in square planar,  $d^8$  complexes, the d orbitals increase in energy in the order  $d_{z^2} < d_{xz}, d_{yz} < d_{x^2-y^2} < d_{xy}$  referred to the coordinate system of Figure 6.12. Tomlinson and Furlani<sup>32a</sup> studied the oriented crystal

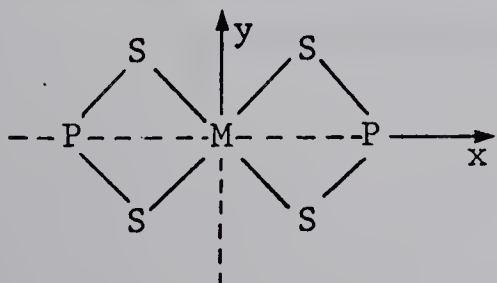


Figure 6.12. Molecular coordinate system (xy plane).



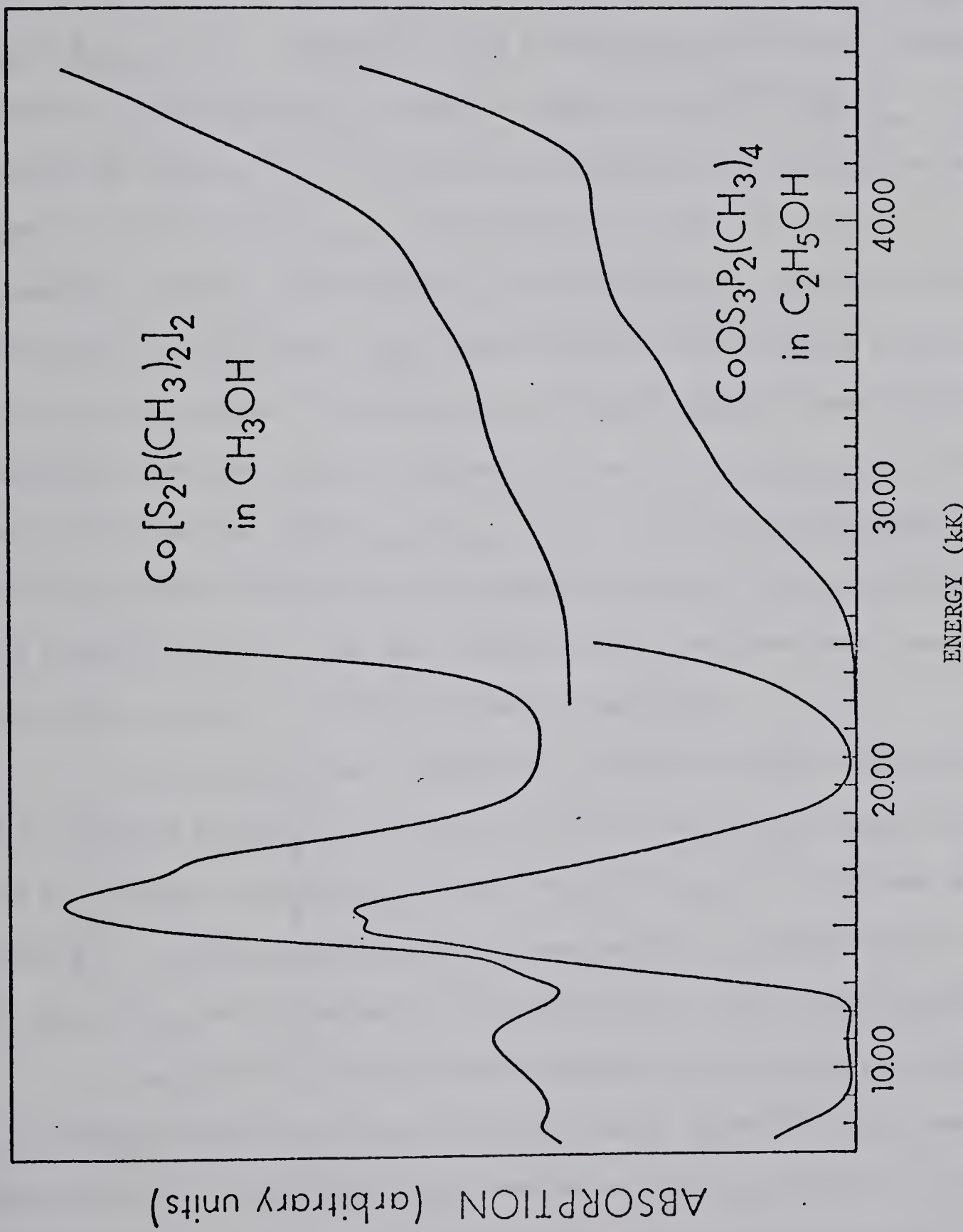


FIGURE 6.11: Electronic spectra of the  $\text{CoS}_4\text{P}_2(\text{CH}_3)_4$  and  $\text{CoOS}_3\text{P}_2(\text{CH}_3)_4$  complexes in alcohol solutions. Relative absorption scale factors, UV/Vis: 60 and 237, respectively.



spectra of  $\text{Ni}[\text{S}_2\text{P}(\text{C}_6\text{H}_5)_2]_2$ ,  $\text{Ni}[\text{S}_2\text{P}(\text{OC}_2\text{H}_5)_2]_2$ , and  $\text{Ni}[\text{S}_2\text{CNR}_2]_2$ , where

$\text{R} = \text{H}$ ,  $\text{C}_2\text{H}_5$ ,  $n\text{-C}_3\text{H}_7$ , and  $i\text{-C}_4\text{H}_9$ , but found the results inconclusive.

Nevertheless these latter authors<sup>32a</sup> support the order  $d_{xz} < d_{yz} < d_{z^2} < d_{x^2-y^2} < d_{xy}$ . Dingle<sup>32b</sup>, in a re-examination of the crystal spectra of  $\text{Ni}[\text{S}_2\text{CN}(\text{C}_2\text{H}_5)_2]_2$  supports Chatt's order<sup>146</sup> with  $d_{xz} < d_{yz}$ .

Looney and Douglas<sup>33</sup>, in a study of the magnetic circular dichroism

spectra of  $\text{Ni}[\text{S}_2\text{P}(\text{OC}_2\text{H}_5)_2]_2$ ,  $\text{Ni}[\text{S}_2\text{CN}(\text{C}_2\text{H}_5)_2]_2$  and other less

symmetric complexes observed that the lowest energy transition was

degenerate in all cases. The ramifications of this latter result are

- (i) the out-of-plane  $\pi$  bonding is so strong in these planar Ni(II) complexes that the  $d_{xz}$ ,  $d_{yz}$  orbitals lie above the  $d_{x^2-y^2}$ ,  $d_{z^2}$  orbitals,
- and (ii) since the order  $d_{xz}, d_{yz} > d_{x^2-y^2}, d_{z^2}$  is not obtainable from an electrostatic model, the real meaning of Crystal Field calculations and results obtained from this starting point are even more questionable when applied to dithiophosphinate complexes.

The spectral band parameters obtained in this study for the complexes  $\text{M}[\text{S}_2\text{PX}_2]_2$ ,  $\text{M} = \text{Ni}, \text{Pd}, \text{Pt}$ ,  $\text{X} = \text{CH}_3, \text{C}_6\text{H}_5, \text{OC}_2\text{H}_5, \text{F}$ , and  $\text{CF}_3$  (except  $\text{Pt}[\text{S}_2\text{P}(\text{CF}_3)_2]_2$ ) and  $\text{Pt}_2\text{S}_6\text{P}_4(\text{CF}_3)_8$  are contained in Table 6.7. Representative spectra from the Ni, Pd, and Pt series and  $\text{Pt}_2\text{S}_6\text{P}_4(\text{CF}_3)_8$  are illustrated in Figures 6.13 - 6.16, respectively.

Jorgensen<sup>12</sup> has expressed surprise that the energy of the  $d_{z^2}$  orbital should be so low in Chatt's order (above)<sup>146</sup> as it was expected to be a third as  $\pi$ -anti-bonding as the  $d_{xy}$  orbital. In compliance with Jorgensen's expectation<sup>12</sup>, and the MCD results<sup>33</sup>, another MO diagram is drawn in Figure 6.17 for these planar complexes which moves the  $d_{x^2-y^2}$  orbital from second highest in the



TABLE 6.7

Electronic Spectra of Planar  $M[S_2PX_{2-2}]_2$  Complexes<sup>a</sup>

$X =$	$CH_3$	$C_6H_5$	$OC_2H_5$	F	$CF_3$
Ni	13.77(8.22) 17.90(12.6)	13.58(11.1) 17.75(15.8)	14.54(8.42) 19.10(13.5)	14.08(7.72) 18.91(9.12)	12.65(5.65) 17.33(3.25)
	$\sim 25.6$ (130) sh $\sim 30.18$ (3280) $\sim 34.1$ (210)? $\sim 39.5$ (200)i $\sim 43.2$ (4000)	24.9 (190) sh 29.75 (4270) $\sim 32.8$ (390)? 37.1 (1410) 43.6 (?)	25.9 (132) sh 31.27 (4580) 35.6 (1010) sh 40 (?) 43.2 (4000)	25.49 (59.8) sh 32.00 (2360) 36.4 (610) sh 40.0 (470) sh ?	24.3 (25) sh 30.55 (2130) $\sim 34.8$ (120)? 39.3 (100) sh 43.6 (500)
Pd	20.48(43.5) 28.1 (380) sh 32.82(4610) $\sim 36.4$ (550)? ?	20.02(62.3) 27.4 (580) sh 32.00(5690) 36.2 (2600) sh 43.6 (510) sh $\sim 19.8$ (1.7)? 22.93(21.2) $\sim 31.4$ (54)?	23.2 (3.3) sh 29.3 (450) sh 33.90 (4160) 38.7 (1100) sh $\sim 44.4$ (604)? $\sim 20.6$ (2.3)? 22.43 (34.3) $\sim 28.7$ (140)? 33.0 (550) sh 36.8 (2800) sh 43.34 (5000)	22.31 (33.7) 29.0 (250) sh 34.49 (4020) 39.2 ((1130) sh 45.8 (1700) $\sim 20.3$ (1) 23.16 (13.3) $\sim 31.0$ (280)? 35.4 (490) sh 39.3 (835) sh 42.5 (5000)	20.20 (37.5) 27.4 (270) sh 32.87 (4570) 37.3 (580) sh 44.8 (880) 25.0b (150) sh 29.2b (480) sh 31.6b (150) sh
Pt				29.7 (80) sh 35.10 (254) 40.6 (2700) 46.0 (?)	34.8b (?) sh 39.1b (?) 41.2b (?)

<sup>a</sup> See footnote (a) of Table 6.1.<sup>b</sup> Spectrum of  $Pt_2S_6P_4(CF_3)_8$ .



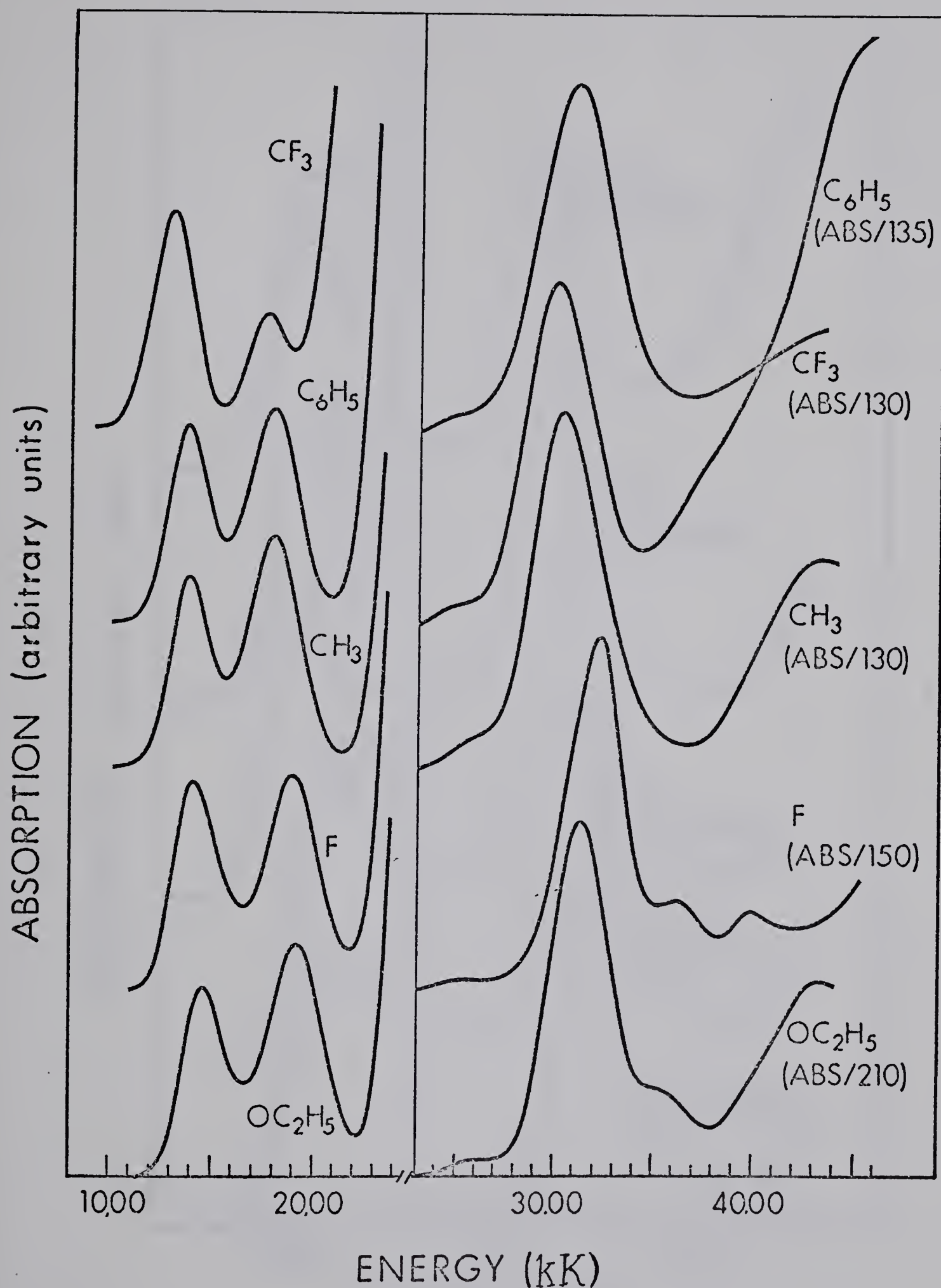


FIGURE 6.13: Electronic spectra of the  $\text{Ni}[\text{S}_2\text{PX}_2]_2$  complexes in  $\text{CH}_2\text{Cl}_2$  solution.



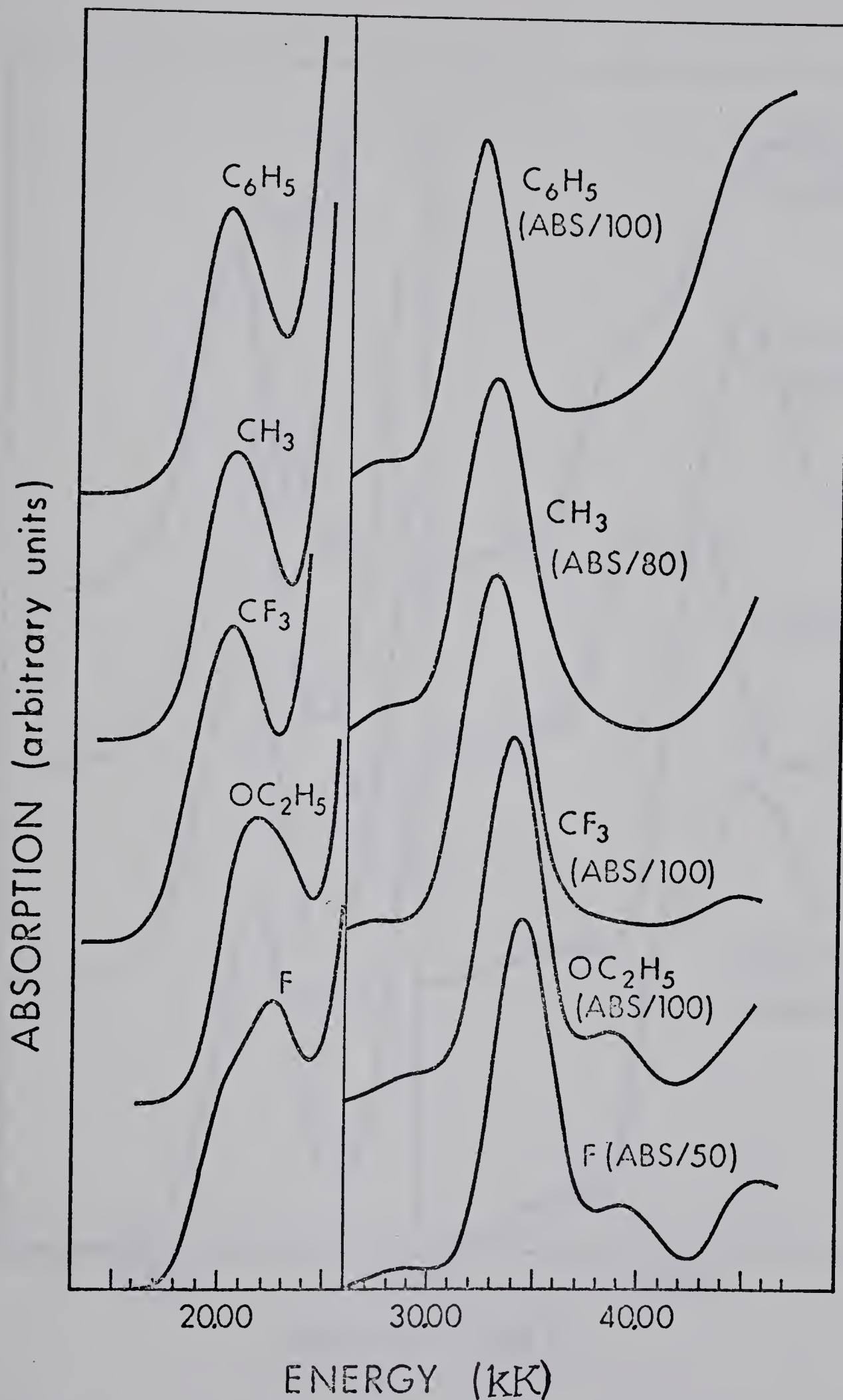


FIGURE 6.14: Electronic spectra of the  $Pd[S_2PX_2]_2$  complexes in  $CH_2Cl_2$  solution.



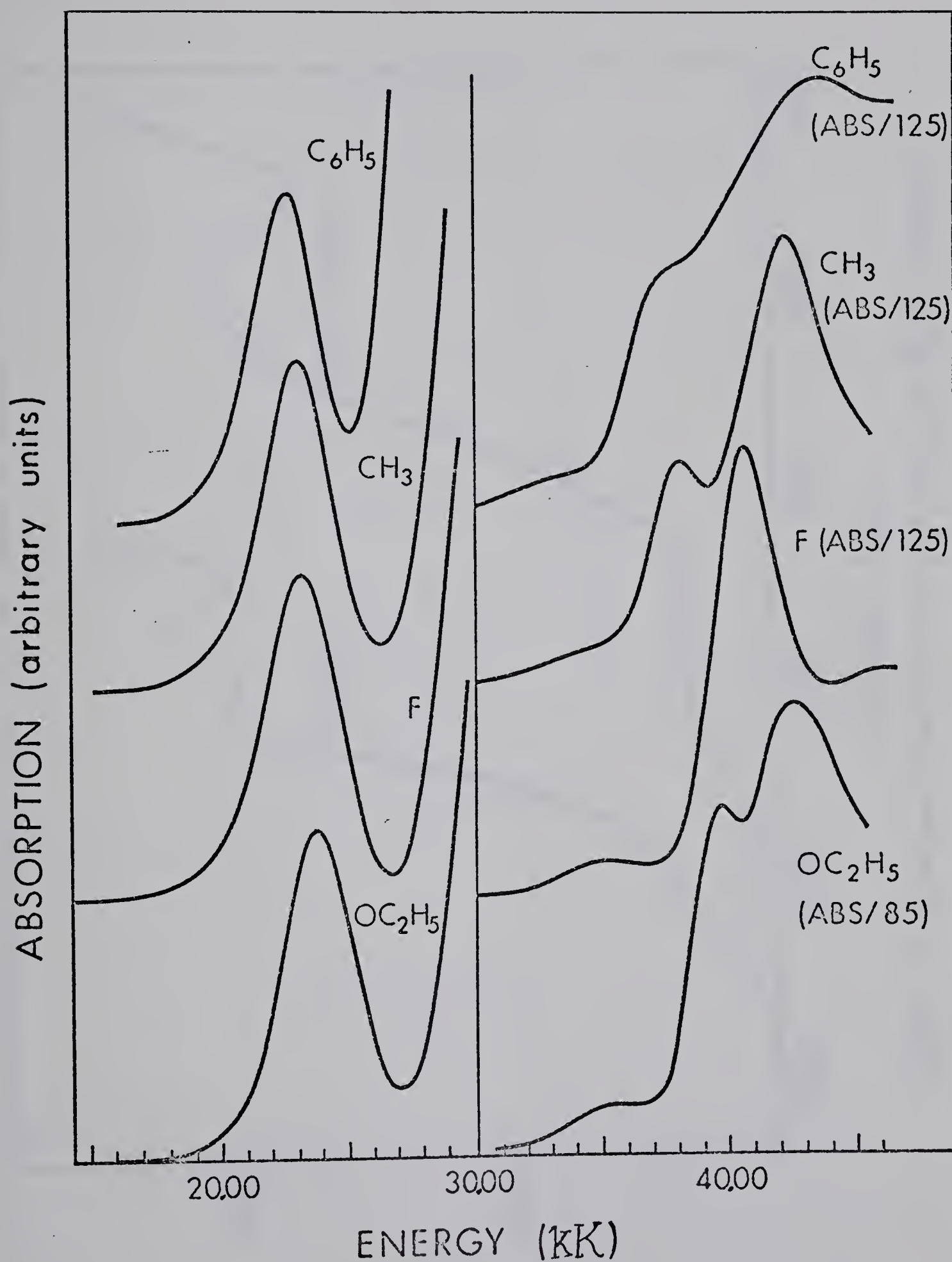


FIGURE 6.15: Electronic spectra of the  $\text{Pt}[\text{S}_2\text{PX}_2]_2$  complexes in  $\text{CH}_2\text{Cl}_2$  solution.



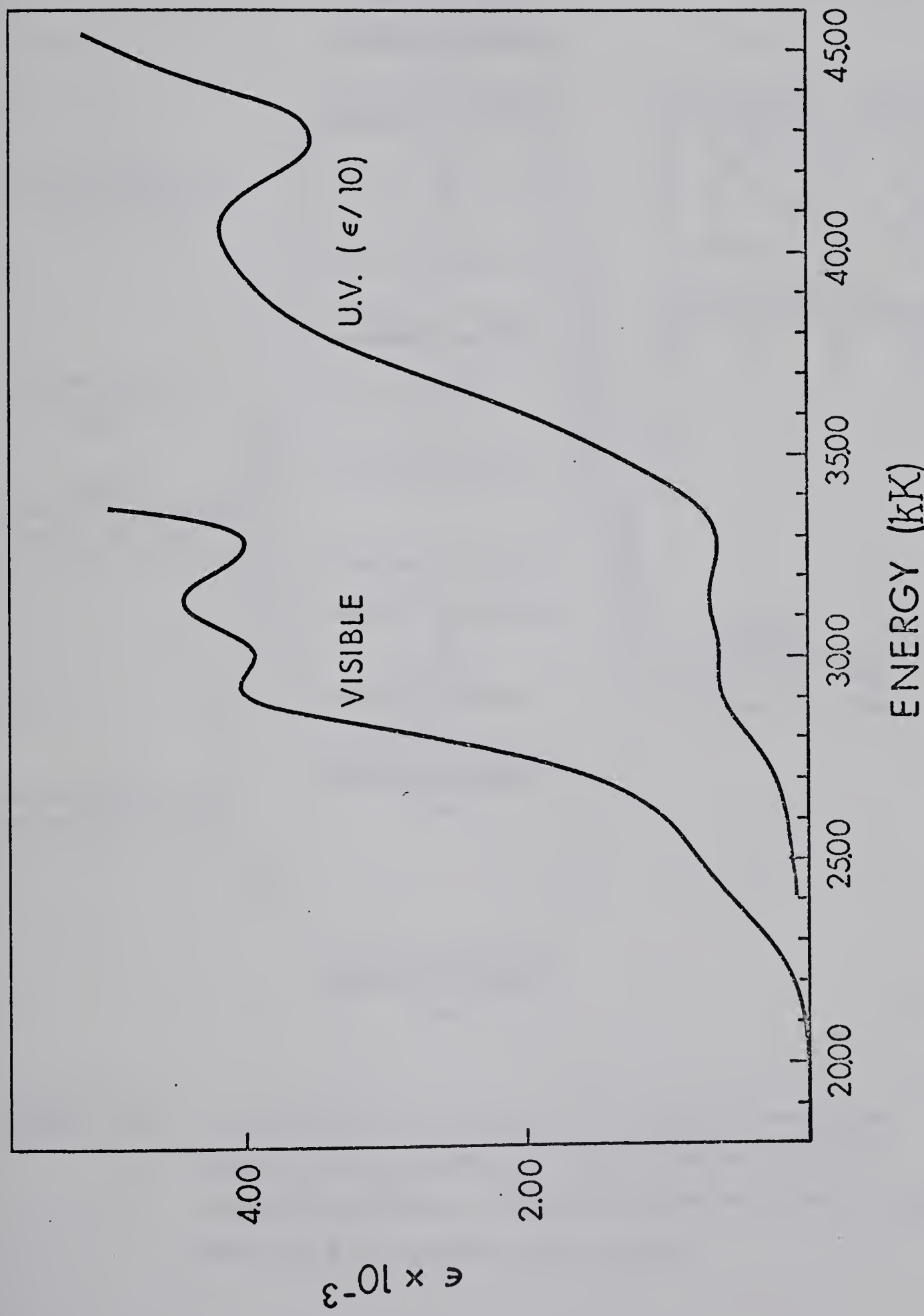
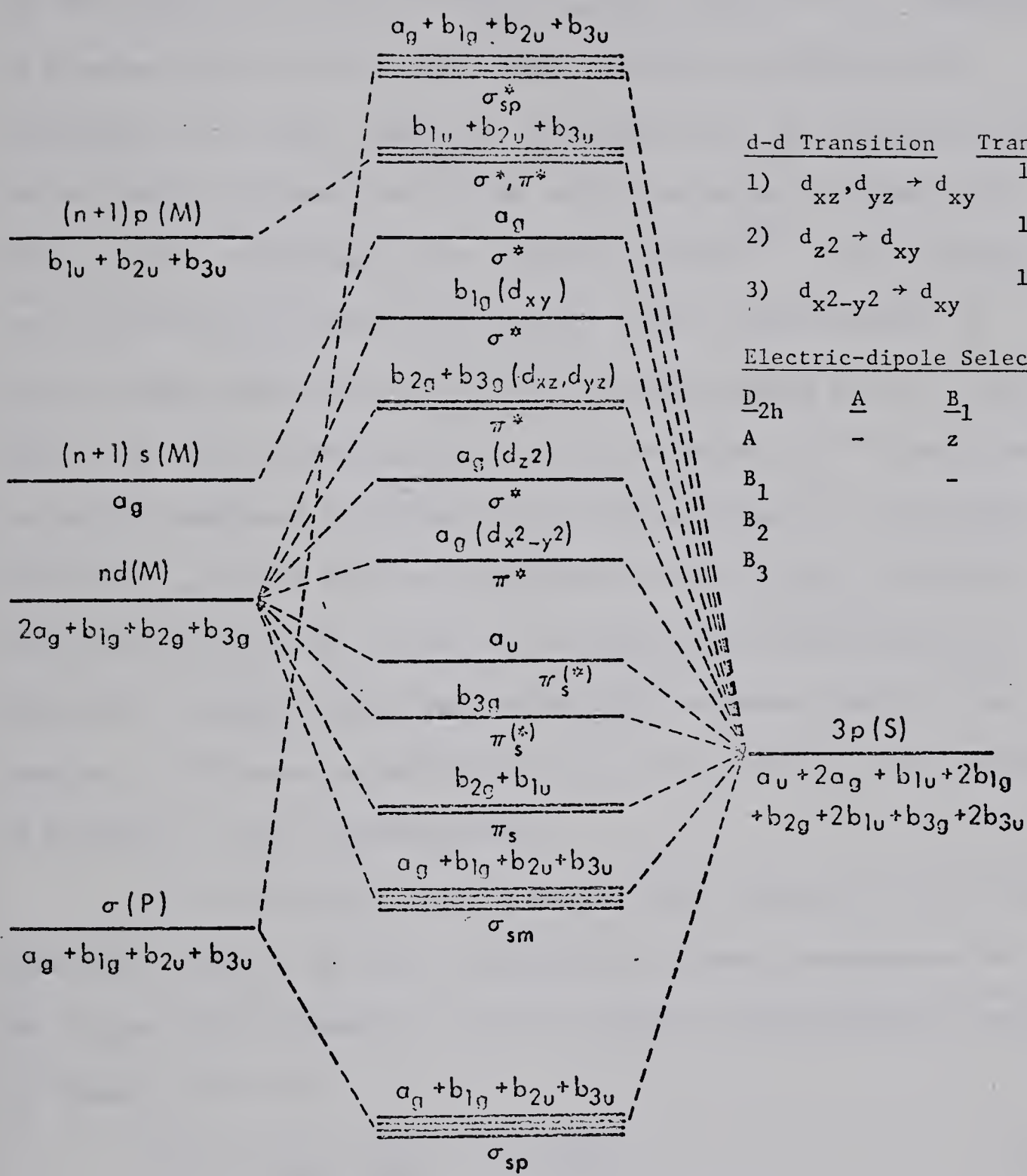


FIGURE 6.16: Electronic Spectrum of  $\text{Pt}_2\text{S}_6\text{P}_4(\text{CF}_3)_8$  in  $\text{CH}_2\text{Cl}_2$  Solution





d-d Transition		Transition Symmetry		
1)	$d_{xz}, d_{yz} \rightarrow d_{xy}$	$1_A g$	$\rightarrow 1_B 3g, 1_B 2g$	
2)	$d_{z2} \rightarrow d_{xy}$	$1_A g$	$\rightarrow 1_B 1g$	
3)	$d_{x^2-y^2} \rightarrow d_{xy}$	$1_A g$	$\rightarrow 1_B 1g$	

#### Electric-dipole Selection Rules

$D_{2h}$	$A$	$B_1$	$B_2$	$B_3$
A	-	$z$	$y$	$x$
$B_1$		-	$x$	$y$
$B_2$			-	$z$
$B_3$				-

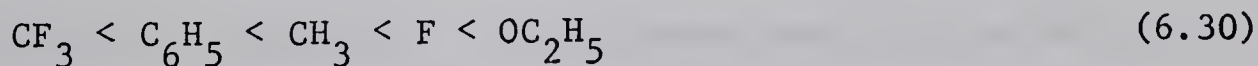
FIGURE 6.17: A qualitative MO diagram for a planar chromophore  $M(S_2P)_2$  of  $D_{2h}$  symmetry. The Cartesian axes are oriented such that the molecular and  $xy$  planes coincide with the  $M + P$  atoms on the  $x$  axis.



Chatt order to the lowest level. In the cases of the nickel complexes the MCD results<sup>33</sup> and the crystal spectral studies<sup>32</sup> are consistent in showing that the first and second observed transitions are forbidden or at least reduced in intensity in z and xy-polarization respectively, as predicted by the selection rules included with Figure 6.15. Furthermore, the crystal spectra<sup>32a</sup> of  $\text{Ni}[\text{S}_2\text{P}(\text{C}_6\text{H}_5)_2]_2$  and  $\text{Ni}[\text{S}_2\text{P}(\text{OC}_2\text{H}_5)_2]_2$  show extra bands in the visible region to higher energy than the two observable in the liquid solution spectra. Thus it is quite possible that all the so-called "d-d" transitions in the Ni complexes lie below 20 kK as postulated for the vanadyl complexes and found for the tetrahedral bis  $\text{Co}[\text{S}_2\text{PX}_2]_2$  complexes.

The peak occurring at 21.2 kK in the spectrum of  $\text{Ni}[\text{S}_2\text{P}(\text{CF}_3)_2]_2$  possesses a maximum which was reproducible between spectra from samples of different preparations, but by its position and intensity is possibly a spin forbidden band.

If either the first or second band positions in the solution electronic spectra of the Ni complexes are taken as measures of the ligand field strength, then the apparent spectrochemical series of ligands, by X, is



in agreement with the infrared data and known crystallographic results ( $X = \text{CH}_3$ ,  $\text{C}_6\text{H}_5$  and  $\text{OC}_2\text{H}_5$ ). In view of the uncertainty concerning the applicability of electrostatic models to this system, no attempt is made to determine Crystal Field parameters of orbital energy separations or interelectronic repulsions. Furthermore,



uncertainty as to the assignment of bands attributable to electron transfer precludes determination of a new series of  $\chi_{\text{opt}}^L$  values.

For the palladium complexes, evidence obtained from  $\text{Pd}(\text{NH}_3)_4^{+2}$  and related species<sup>11,12</sup> indicates that the three expected "d-d" transitions coincide within twice the half-width of the band observed. Both  $\text{Pd}[\text{S}_2\text{P}(\text{OC}_2\text{H}_5)_2]_2$  and  $\text{Pd}[\text{S}_2\text{PF}_2]_2$  show structure in the first observed electronic band not observed for the other Pd complexes. Superposition of the spectra of these two Pd complexes ( $X = \text{OC}_2\text{H}_5$  and F) indicates that the structure may be due to a spin-forbidden transition revealed only because of the high energy shift of the spin-allowed transition induced by the substituents  $\text{OC}_2\text{H}_5$  and F. The extent to which hidden components alter the apparent band positions is unknown, but the overall order of band positions is close to that observed for the Ni-series as a function of X and hence a similar spectrochemical series of ligands pertains.

For the platinum complexes the regular increase in orbital splittings down the Periodic Table continues. The pronounced tailing to lower energies of the first band is general for all the substituents (except possibly  $\text{CF}_3$ ) and is the probable result of a vibronic excitation mechanism. A temperature study is necessary to settle this point. Thus the bands extracted from the low energy side of this first transition are spurious in all probability. It is somewhat surprising that spin-forbidden bands are not more evident in the spectra of the Pt complexes due to the increase in spin-orbit coupling down the Periodic Table<sup>64,94</sup>. The large shift in the most intense uv absorption from that observed in the complexes of other



metals is unexpected, since this band is anticipated to result from an intraligand transition of much less sensitivity to changes of metal ion. However, a large perturbation of the ligand bonding by Pt may be suggested by the formation of the dinuclear complex

$\text{Pt}_2\text{S}_6\text{P}_4(\text{CF}_3)_8$  unique among the dithiophosphinate complexes isolated thus far. It is notable that such a complex should form with the ligand forming the weakest M-S bonds in most other systems (see Chapter 3). It would prove exceedingly interesting to determine whether the probable  $\text{Pt}-\text{S}-\text{P}-\text{S}-\text{Pt}$  ring in this dinuclear compound is planar or puckered as a plane ring would indicate a most unusual aromatic heterocycle. The spectrum illustrated in Figure 6.16 clearly indicates that the electronic properties of this complex are very different from those of the expected but as yet unisolated mononuclear compound  $\text{Pt}[\text{S}_2\text{P}(\text{CF}_3)_2]_2$  (cf Figure 6.16).

Relative band intensities were not discussed previously and no explanations are attempted but it is noted that the band intensities observed for the tris complexes are much higher than those of the same metal ion with monodentate ligands, while those of the tetrahedral bis complexes are lower<sup>74</sup>. Within the set of five substituents employed in this study the general trend in intensities, by X, was observed to be



#### 6.4 Summary and Conclusions

Subject to further verification the successes in the spectral assignments for the complexes  $\text{Ni}[\text{S}_2\text{PX}_2]_2$  and  $\text{OV}[\text{S}_2\text{PX}_2]_2$



render highly uncertain the analyses of spectra of dithiophosphate complexes using electrostatic models when metal-ligand  $\pi$ -bonding is suspected or known to be significant.

The Ligand Field Theory approximations<sup>113</sup> do seem to yield reasonable results comparable over a wide range of ligands provided that the coordination geometry is close to tetrahedral or octahedral. In the tris dithiophosphinate complexes it appears that if there are vacant  $\pi^*$  orbitals, then  $\text{OC}_2\text{H}_5$  assumes a lower spectrochemical position than F, but the order is reversed when the  $\pi^*$  levels are filled. This latter effect is possibly the result of the greater  $\pi$ -donor property of the ligand induced by  $\text{OC}_2\text{H}_5$  (Table 3.7).

A definite correlation exists between the M-S vibrational frequencies observed in the infrared spectra and the magnitude of the "d-d" transition energies observed in the electronic spectra. The higher the M-S vibrational frequency, the higher the "d-d" electronic transition energy. This correlation breaks down somewhat if the degree of polymerization is not the same between the two physical measurements.

Electron transfer bands in the tris and vanadyl complexes appear uniformly to be of the  $L \rightarrow M$  type while in the tetrahedral bis complexes, transfer appears to be of the  $M \rightarrow L$  type. By the direction of uv band shifts with substituent it would appear that electron transfer (if it occurs at all in the region observed) is of the  $L \rightarrow M$  type. Also, as is to be expected, the  $\chi_{\text{opt},L}$  values of the ligands reflect more upon the strength of the metal-ligand bonding



than on the group electronegativity of the substituent.

The postulate that the electrical  $\sigma, \pi$  effects of the substituents are transduced by the phosphorus atoms provides a plausible and in some cases possibly a semi-quantitative explanation of the differences in the electronic spectra of complexes where the substituent is the only atomic variable. In their electronic spectral properties, the dithiophosphinate complexes appear quite "normal", except that  $\pi$ -bonding effects in the planar and vanadyl complexes are much greater than might have been predicted on the basis of the "odd" character of the ligands<sup>47</sup>.



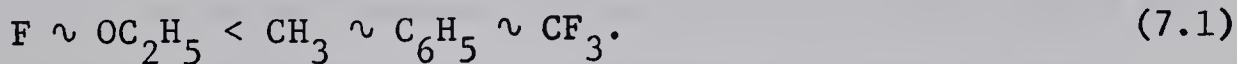
## CHAPTER 7

## CORRELATIONS AND CONCLUSIONS

7.1 Substituent Dependence in Dithiophosphinates and Related Compounds

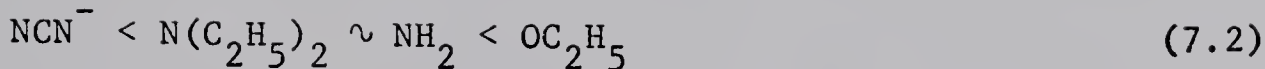
In the previous chapters the dithiophosphinates have been largely discussed in isolation from other 1,1-dithioacid systems of complexes. The recently reported<sup>147</sup> dithioarsinate complexes  $M[S_2As(CH_3)_2]_n$  appear to be very similar to their phosphorus analogues and the nuclear spin of the arsenic atoms ( $I = 3/2$ ) should also provide an interesting intramolecular probe for epr studies. For the dithiocarboxylate complexes  $M[S_2CX]_n^{+m}$  the geometry of the ligands is such that the directional transmission of the substituent electrical effects to the  $MS_4$  chromophore may be anticipated to be quite different from the cases where the substituents are "tetrahedrally" opposed to the sulfur atoms.

As indicated in Chapter 3 (Table 3.1), the bond length data is the most complete at present for the divalent nickel complexes. For the dithiophosphinates  $Ni[S_2PX_2]_2$ , the infrared spectral and crystallographic results together suggest that the M-S bond lengths lie in the order by X



Unfortunately for comparison purposes, crystal structures of the complexes  $Ni[S_2C-X]_2$  with a parallel series of substituents have not been reported. The published structures for the complexes  $Ni[S_2CX]_2$  indicate that the M-S bond lengths lie in the order by X<sup>29,30</sup>





The coordination geometry of the carbon atom to which the substituent is bound is trigonal in both the dithiocarboxylates and the benzene system from which the Hammett-Taft parameters were determined<sup>86</sup>. The relative order of substituents in sequence (7.2) is consistent with a "direct" transmission of substituent electrical properties (Table 3.7) as opposed to the "inverted" transmission indicated by sequence (7.1). Sequences (7.1) and (7.2) are both consistent with a synergic interpretation of metal-ligand bonding.

Porta, et al.<sup>21</sup>, noted a monotonic (but not linear) relationship between the M-S bond lengths and the energy of the first band ( $\nu_{1el}$ ) in the electronic spectra of 1,1-dithioacid complexes of divalent nickel. Tomlinson and Furlani<sup>32a</sup> further showed that the correlation also held for the second electronic spectral band of these complexes. Lever and Mantovani<sup>148</sup> anticipated that a larger ligand field would be reflected in higher metal-ligand vibrational frequencies ( $\nu_{ML}$ ) and found  $\nu_{\text{Cu-N}}^2$  to be a reasonably linear function of  $\nu_{1el}$  for a series of planar, N-coordinated copper complexes. A similar correlation is illustrated in Figure 7.1 for the complexes  $\text{Ni}[\text{S}_2\text{PX}_2]_2$  with X =  $\text{CH}_3$ ,  $\text{C}_6\text{H}_5$ ,  $\text{OC}_2\text{H}_5$ , F, and  $\text{CF}_3$ . Dichloromethane presents a window in its ir spectrum between 300 and 450 K in which region M-S vibrations may be observed. Since the electronic spectra were obtained from dichloromethane solutions, the molecular environment was standardized between the vibrational and electronic spectral measurements by use of dichloromethane solutions for the ir spectral measurements as well. The linearity of the results depicted in Figure 7.1 is somewhat



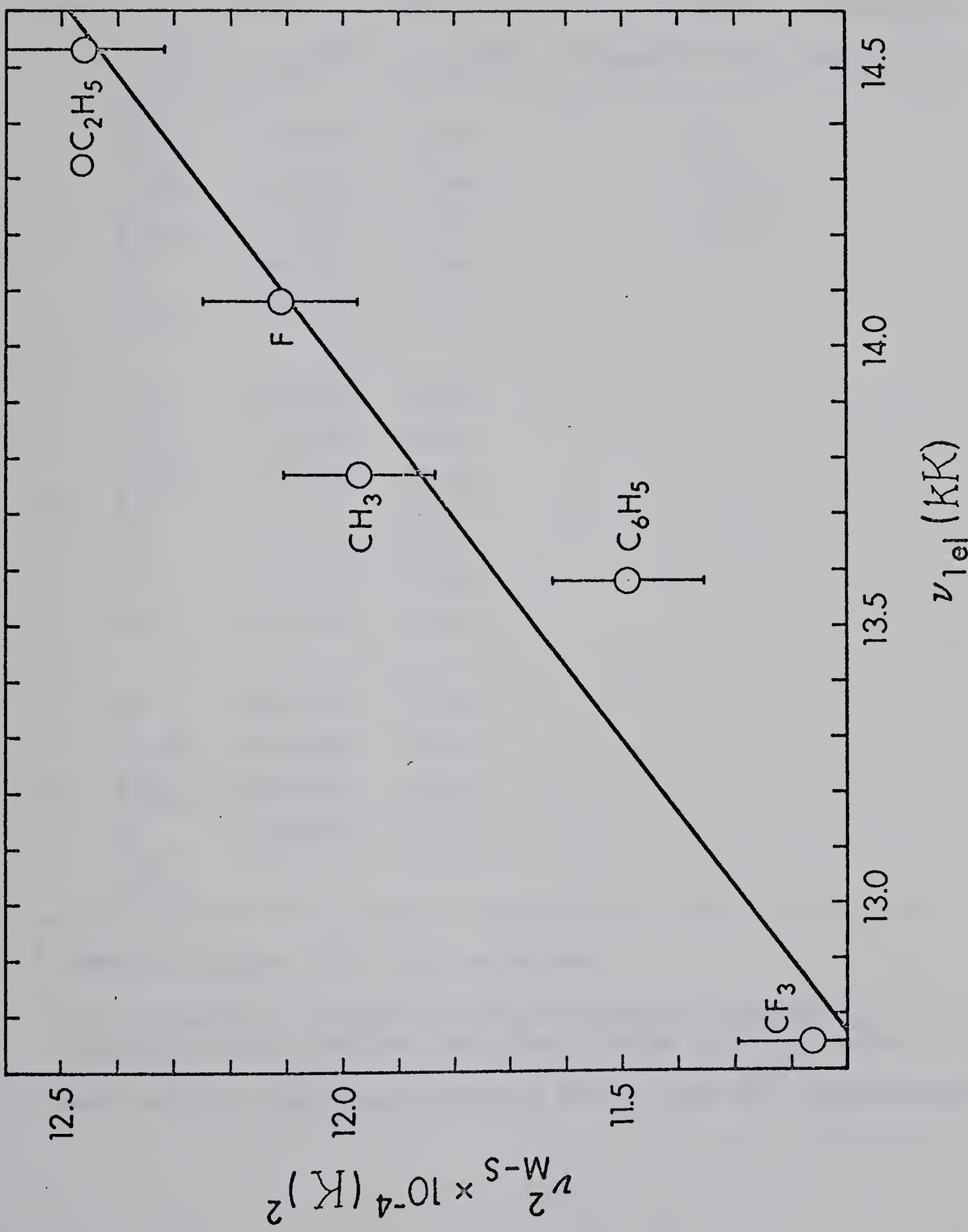


FIGURE 7.1:  $\nu_{\text{M-S}}^2 - \nu_1^2$  correlation for  $\text{Ni}[\text{S}_2\text{PX}_2]_2$  complexes. The vertical error lines represent an uncertainty of  $\pm 2 \text{ K}$  in  $\nu_{\text{M-S}}$ .



TABLE 7.1

Ligand Field-Metal-Sulfur Vibrational Frequency Correlation<sup>a</sup>

M	X	$\nu_{M-S}$ (K) <sup>b</sup>	$\nu_{1\text{ el}}$ (kK)	Average M-S bond length ( $\text{\AA}$ ) <sup>c</sup>
Ni	$\text{CH}_3$	346(347)	13.77	2.238
	$\text{C}_6\text{H}_5$	339(339)	13.58	2.236(7)
	$\text{OC}_2\text{H}_5$	353(354)	14.53	2.233(4)
	F	348(349)	14.08	
	$\text{CF}_3$	334(334)	12.65	
Pd	$\text{CH}_3$	307(309)	20.48	
	$\text{C}_6\text{H}_5$	306(308)	20.02	
	$\text{OC}_2\text{H}_5$	309(311)	21.28	
			23.2	
	F	309(311)	19.7	
Pt			22.31	
	$\text{CH}_3$	299(300)	22.93	
	$\text{C}_6\text{H}_5$	295(299)	22.43	
	$\text{OC}_2\text{H}_5$	304(304)	23.86	
	F	298(304)	23.16	
$\text{CF}_3$		-	-	

<sup>a</sup> Spectra obtained from  $\text{CH}_2\text{Cl}_2$  solutions.

<sup>b</sup> Bands observed in "window" of  $\text{CH}_2\text{Cl}_2$  spectrum, 300-450 K, bracketed values are band positions observed in Nujol mulls.

<sup>c</sup> Bond lengths taken from references 20, 21, and 23a, respectively.



unexpected as no allowance was made for the widely varying substituent masses. The small spread in  $\nu_{MS}$  values for the Pd and Pt series of complexes makes parallel correlations less meaningful (Table 7.1).

Similar vibrational-electronic correlations appear to hold for the vanadyl and tris complexes. No such readily apparent relationship was found for the tetrahedral bis complexes probably due to the variation in ligand function between the solid state mulls from which the ir spectra were obtained and the dichloromethane solutions from which the electronic spectra were obtained.

In comparing the dithiophosphinate complexes with their dithiocarboxylate analogues<sup>12,51</sup>, it is notable that the ligand fields are generally higher and the electron repulsion parameters are generally lower for the dithiocarboxylates. Nevertheless, the Co(II) and Mn(II) dithiocarboxylates are unstable with respect to formation of the trivalent metal ion complex<sup>51</sup> in contrast to the reverse instability observed for Fe(III) and Co(III) dithiophosphinates. Such divergent behavior is attributable in part to the different manner of transmission of substituent effects to the  $MS_4$  chromophore but much of the difference must be due to the change from carbon to phosphorus as the subtending atom.

Where the solid state of the dithiophosphinate complexes is not complicated by ligand bridging, the relative crystal lattice energies as functions of substituent were inferred from sublimation and fusion temperatures as well as apparent solubilities to lie in the order by X





Sequence (7.3) represents an order of intermolecular interactions which is quite different from the sequences presented in previous chapters giving the relative orders of intramolecular interactions and is clearly not simply related to the electrical effects of the substituents given in Table 3.7.

## 7.2 The Application of Hammett-Taft Parameters in Inorganic Chemistry

That atoms and groups of atoms have transferable properties (e.g. electronegativities, group vibrational frequencies, formal oxidation numbers, "hard" and "soft" Lewis acid or base behavior, etc.) is not a new concept but is well recognized to be of tremendous predictive value. The results of this investigation provide further support for a synergic interpretation of chemical bonding in transition metal complexes. No other physical constants are known to the author which provide such intimate insight into the "give-and-take" nature of charge transfer in the formation of chemical bonds as the Hammett-Taft parameters<sup>86</sup>. Graham, et al.<sup>149</sup>, have demonstrated that vibrational force constants and nmr data for organometallic complexes can be correlated with  $\sigma, \pi$  electron polarizations which are not inconsistent with the Hammett-Taft substituent constants. Furthermore, Olsen, et al.<sup>150</sup>, found a linear relationship between polarographic half-wave reduction potentials ( $E_{1/2}$ ) of transition metal 1,2-dithiolene complexes and the inductive constants ( $\sigma^*$ ) of the ligand substituents.

The specific utility of the Hammett-Taft substituent constants as opposed to less quantitative classification schemes will be developed for the ion  $\text{CoF}_6^{-3}$ . In spite of the fact that the



ions  $\text{Co}^{+3}$  and  $\text{F}^-$  are both "hard" in Pearson's kinetic classification<sup>96</sup>, the complex ion  $\text{CoF}_6^{-3}$  is high-spin<sup>151</sup> whereas all other known compounds of Co(III) are low-spin<sup>74</sup>. With reference to Figure 6.1 it may be seen that for an octahedral complex with a low-spin  $d^6$  metal-ion configuration that the  $\pi^*(t_{2g})$  orbitals are filled. This is probably of little consequence to ligands with small  $\pi$ -donor tendencies. The data in Table 3.7 clearly indicate that the fluorine atom has a large  $\pi$ -donor tendency. Thus the high-spin ions  $\text{CoF}_6^{-3}$  quite possibly represent the compromise of the loss of some  $\sigma$ -type bonding (through occupation of  $\sigma^*$  orbitals) with the gain in some  $\pi$ -type bonding. It is also noteworthy that the ions  $\text{F}^-$  and  $\text{S}_2\text{PX}_2^-$  generate very similar magnitudes of  $10Dq$  in their octahedral Cr(III) complexes<sup>74</sup>. Therefore, the low-spin ground states of the complexes  $\text{Co}[\text{S}_2\text{PX}_2]_3$  is the probable result of the smaller inter-electronic repulsions in the complexes afforded by the  $\pi$ -acid ligand ions  $\text{S}_2\text{PX}_2^-$  versus the  $\pi$ -base  $\text{F}^-$  ions.

While the interpretation that charge polarization effects of tetrahedrally opposed substituents may be considered inverted (transduced) on transmission through the subtending atom is subject to further confirmation, it has provided a consistent interim rationalization of the results presented herein. As quantitative measures of the substituent charge polarization tendencies the Hammett-Taft parameters have proven very useful.

### 7.3 Indicated Further Work

Should a preparative route to the complexes  $\text{M}[\text{S}_2\text{PH}_2]_n$  be found the properties of these compounds are anticipated to convincingly



settle the question of the importance of substituent steric effects. Thorough normal coordinate analyses for representative members of each coordination geometry should allow firm vibrational band assignments and a quantitative evaluation of the vibrational electronic band correlations taking substituent mass effects into account. The unambiguous identification of the excited electronic states as well as the mechanisms of excitation of transition metal dithiophosphinates still requires extensive single crystal, MCD, and low temperature solution spectral studies. Further spectral analyses of the salts and non-transition metal dithiophosphinates are required to assign the electron transfer and ligand spectra.

Low temperature (liquid helium) static field susceptibility and epr investigations still remain to be carried out. The epr spectra of the dithioarsinate complexes  $M[S_2AsX_2]_n$  should prove exceedingly interesting in comparison with those of their phosphorus analogues ( $I_{As} = 3/2$ ).

Very little quantitative and systematic thermodynamic data is yet available for dithiophosphinate complexes. A differential thermal analysis of these complexes should provide some insight into the energetics of the thermally induced redox reactions and provide some indication of the energy of the polymer-monomer transformations.

It is hoped that the results of this investigation will lead to a greater general understanding of chemical bonding.



## REFERENCES

1. G. M. Kosolapoff, "Organophosphorus Compounds", John Wiley & Sons, Inc., New York (1950).
2. L. Maier, *Topics in Phosphorus Chemistry*, 2, 43 (1965).
3. F. A. Cotton and G. Wilkinson, "Advanced Inorganic Chemistry", Second Edition, John Wiley & Sons, Inc., New York (1969).
4. A. W. v. Hofmann, *Ber.*, 4, 430 (1871); A. W. v. Hofmann and F. Mahla, *Ber. Dtsch. Chem. Ges.*, 25, 2436 (1892).
5. P. S. Pistschimuka, *Ber.*, 41, 3854 (1908).
6. L. Malatesta and R. Pizzotti, *Chim. Ind. (Milan)*, 27, 6 (1945).
7. L. Malatesta, *Gazz. Chim. Ital.*, 77, 509 and 518 (1947).
8. M. M. Rauhut, H. A. Currier, and V. P. Wystrach, *J. Org. Chem.*, 26, 5133 (1961).
9. P. E. Newallis, J. P. Chupp, and L. C. D. Groenweghe, *J. Org. Chem.*, 27, 3829 (1962).
10. J. P. Chupp and P. E. Newallis, *J. Org. Chem.*, 27, 3832 (1962).
11. C. K. Jorgensen, *J. Inorg. Nucl. Chem.*, 24, 1571 (1962).
12. C. K. Jorgensen, *Inorg. Chim. Acta*, 2, 65 (1968).
13. W. Kuchen and H. Hertel, *Angew. Chem.*, 81, 127 (1969).
14. (a) R. N. Mukherjee, V. V. Krishna Rao, and J. Gupta, *Indian J. Chem.*, 4, 209 (1966).  
(b) R. N. Mukherjee, A. Y. Sonsale and J. Gupta, *ibid.*, 4, 500 (1966).
15. M. J. Bennett and R. H. Sumner, personal communication.
16. (a) H. W. Roesky, F. N. Tebbe, and E. L. Muettterties, *J. Am. Chem. Soc.*, 89, 1272 (1967).



- (b) R. W. Mitchell, M. Lustig, F. A. Hartman, J. K. Ruff, and J. A. Merritt, *J. Am. Chem. Soc.*, 90, 6329 (1968).
- (c) T. L. Charlton and R. G. Cavell, *Inorg. Chem.*, 8, 281 (1969).
- (d) H. W. Roesky, F. N. Tebbe, and E. L. Muetterties, *Inorg. Chem.*, 9, 831 (1970).
17. (a) K. Gosling and A. B. Burg, *J. Am. Chem. Soc.*, 90, 2011 (1968).
- (b) R. C. Dobbie, L. F. Doty, and R. G. Cavell, *J. Am. Chem. Soc.*, 90, 2015 (1968).
- (c) A. A. Pinkerton and R. G. Cavell, *J. Am. Chem. Soc.*, 93, 2384 (1971).
18. F. N. Tebbe and E. L. Muetterties, *Inorg. Chem.*, 9, 629 (1970).
19. H. W. Roesky, *Angew. Chemie*, 80, 844 (1968).
20. P. E. Jones, G. B. Ansell, and L. Katz, *Acta Cryst.*, B25, 1939 (1969).
21. P. Porta, A. Sgamellotti, and N. Vinciguerra, *Inorg. Chem.*, 7, 2625 (1968).
22. V. Kastalsky, and J. F. McConnell, *Acta Cryst.*, B25, 909 (1969).
23. (a) J. F. McConnell and V. Kastalsky, *Acta Cryst.*, 22, 853 (1967).
- (b) Q. Fernando and C. D. Green, *J. Inorg. Nucl. Chem.*, 29, 647 (1967).
24. S. L. Lawton and G. T. Kokotailo, *Inorg. Chem.*, 8, 2410 (1969).
25. S. L. Lawton, *Inorg. Chem.*, 10, 328 (1971).
26. M. Calligaris, G. Nardin, and A. Ripamonti, *J. Chem. Soc. (A)*, 714 (1970).
27. T. Ito, T. Igarashi, and H. Hagihara, *Acta Cryst.*, B25, 2303 (1969).



28. C. Furlani, A. A. G. Tomlinson, P. Porta, and A. Sgamellotti, *J. Chem. Soc. (A)*, 2929 (1970).
29. R. E. Eisenberg, *Prog. Inorg. Chem.*, 12, 295 (1970).
30. R. H. Holm and M. J. O'Connor, *Progr. Inorg. Chem.*, 14, 241 (1971).
31. (a) A. A. G. Tomlinson, *J. Chem. Soc. (A)*, 1409 (1971).  
(b) J. D. Lebedda and R. A. Palmer, *Inorg. Chem.*, 10, 2704 (1971).
32. (a) A. A. G. Tomlinson and C. Furlani, *Inorg. Chim. Acta*, 3, 487 (1969).  
(b) R. Dingle, *Inorg. Chem.*, 10, 1141 (1971).
33. Q. Looney and B. E. Douglas, *Inorg. Chem.*, 9, 1955 (1970).
34. J. R. Wasson, S. J. Wasson, and G. M. Woltermann, *Inorg. Chem.*, 9, 1576 (1970).
35. S. E. Livingstone and E. Mikhelson, *Inorg. Chem.*, 9, 2545 (1970).
36. A. Müller, V. V. K. Rao, and E. Diemann, *Chem. Ber.*, 104, 461 (1971).
37. H. Hertel and W. Kuchen, *Chem. Ber.*, 104, 1740 (1971).
38. A. Müller, V. V. K. Rao, and G. Klinksiek, *Chem. Ber.*, 104, 1892 (1971).
39. J. R. Wasson, *Inorg. Chem.*, 10, 1531 (1971), and references therein.
40. S. L. Lawton, *Inorg. Chem.*, 9, 2269 (1970).
41. (a) P. S. Shetty and Q. Fernando, *J. Inorg. Nucl. Chem.*, 28, 2873 (1966).  
(b) P. S. Shetty and Q. Fernando, *ibid.*, 29, 1921 (1967).
42. "Chelating Agents and Metal Chelates", Edited by F. P. Dwyer and D. P. Mellor, Academic Press, New York (1964).
43. M. Calligaris, A. Ciana, S. Meriani, G. Nardin, L. Randaccio, and A. Ripamonti, *J. Chem. Soc. (A)*, 3386 (1970).



44. B. P. Block, *Coord. Chem.*, *Proc.*, 248 (1969); K. Dehnicke and R. Schmitt, *Z. Anorg. Allg. Chem.*, 358, 1 (1968); J. Weidlein, *ibid.*, 358, 13 (1968); J. J. Pitts, M. A. Robinson, and S. I. Trotz, *J. Inorg. Nucl. Chem.*, 31, 3685 (1969).
45. C. Oldham, *Progr. Inorg. Chem.*, 10, 223 (1968); F. A. Cotton, B. G. De Boer, M. D. La Prade, J. R. Pipal, D. A. Ucko, *J. Am. Chem. Soc.*, 92, 2926 (1970).
46. J. A. McCleverty, *Progr. Inorg. Chem.*, 10, 49 (1968).
47. G. N. Schrauzer, *Acc. Chem. Res.*, 2, 72 (1969).
48. A. Davison and E. S. Switkes, *Inorg. Chem.*, 10, 837 (1971); M. R. Churchill, J. Cooke, J. P. Fennessey, and J. Wormald, *Inorg. Chem.*, 5, 103 (1971).
49. O. Siemann and J. Fresco, *J. Am. Chem. Soc.*, 92, 2652 (1970); G. A. Heath and R. L. Martin, *Aust. J. Chem.*, 23, 1721 (1970).
50. D. Coucovanis, R. E. Coffmann, and D. Piltingsrud, *J. Am. Chem. Soc.*, 92, 5004 (1970); A. R. Latham, V. C. Hascall, and H. B. Gray, *Inorg. Chem.*, 4, 788 (1965).
51. D. Coucovanis, *Prog. Inorg. Chem.*, 11, 233 (1970).
52. B. N. Figgis and R. S. Nyholm, *J. Chem. Soc.*, 4190 (1958).
53. R. G. Cavell, W. Byers, and E. D. Day, *Inorg. Chem.*, 10, 2710 (1971).
54. R. G. Cavell, E. D. Day, W. Byers, and P. M. Watkins, *Inorg. Chem.*, 10, 2716 (1971).
55. R. G. Cavell, E. D. Day, W. Byers, and P. M. Watkins, *Inorg. Chem.*, in press.
56. R. G. Cavell, W. Byers, E. D. Day, and P. M. Watkins, *Inorg. Chem.*, in press.



57. R. G. Cavell, E. D. Day, W. Byers, and P. M. Watkins, *Inorg. Chem.*, in press.
58. W. Kuchen, W. Strolenberg, and J. Metten, *Chem. Ber.*, 96, 1733 (1963).
59. D. E. Coldberry, W. C. Fernelius, and M. Shamma, *Inorg. Syntheses*, 6, 142 (1960).
60. S. E. Livingstone, L. F. Lindoy, and T. N. Lockyer, *Aust. J. Chem.*, 18, 1545 (1965); R. N. Jowitt and P. C. H. Mitchell, *J. Chem. Soc. (A)*, 2632 (1969).
61. A. H. Ewald, R. L. Martin, E. Sinn, and A. H. White, *Inorg. Chem.*, 8, 1837 (1969).
62. P. W. Selwood, "Magnetochemistry", Interscience, New York (1956).
63. L. F. Bates, "Modern Magnetism", Fourth Edition, Cambridge University Press, London (1961).
64. C. K. Jorgensen, "Absorption Spectra and Chemical Bonding in Complexes", Addison-Wesley Publishing Company, Inc., Reading, Mass. (1962).
65. L. Pauling, "The Nature of the Chemical Bond", Third Edition, Cornell University Press, Ithaca, New York (1960); Table 7.2.
66. F. W. B. Einstein, B. R. Penfold, and Q. T. Tapsell, *Inorg. Chem.*, 4, 186 (1965).
67. P. Coppens, C. H. MacGillavry, S. G. Hovenkamp, and H. Downes, *Acta Cryst.*, 15, 765 (1962).
68. D. E. Rogers and G. Nickless, "Inorganic Sulphur Chemistry", Elsevier, Amsterdam (1968), Chapter 9.
69. R. M. Tuggle and M. J. Bennett, personal communication.



70. D. M. Adams and J. B. Cornell, *J. Chem. Soc. (A)*, 1299 (1968).
71. P. Porta, A. Sgamellotti, and N. Vinciguerra, *Inorg. Chem.*, 10, 541 (1971).
72. S. Ooi and Q. Fernando, *Inorg. Chem.*, 6, 1558 (1967).
73. W. Kuchen and H. Mayatepek, *Chem. Ber.*, 101, 3454 (1968).
74. A. B. P. Lever, "*Inorganic Electronic Spectroscopy*", Elsevier, Amsterdam (1968).
75. W. Kuchen and A. Judat, *Chem. Ber.*, 100, 991 (1967).
76. K. Nakamoto, "*Infrared Spectra of Inorganic and Coordination Compounds*", Second Edition, Wiley-Interscience (1970).
77. D. E. C. Corbridge, *Topics in Phosphorus Chemistry*, 6, 235 (1969).
78. R. A. Nyquist, *Spectrochim. Acta*, 25, 47 (1969).
79. G. E. Coates and R. N. Mukherjee, *J. Chem. Soc.*, 1295 (1964).
80. J. Goubeau, *Angew. Chem.*, 81, 343 (1969).
81. D. W. James and M. J. Nolan, *Progr. Inorg. Chem.*, 9, 195 (1968).
82. P. R. Wells, *Progr. Phys. Org. Chem.*, 6, 111 (1968) and references therein.
83. D. R. Dakternieks and D. P. Graddon, *Aust. J. Chem.*, 23, 1989 (1970).
84. D. R. Dakternieks, C. M. Harris, P. J. Milham, B. S. Morris, and E. Sinn, *Inorg. Nucl. Chem. Lett.*, 5, 97 (1969); A. T. Casey and J. R. Thackeray, *Aust. J. Chem.*, 22, 2549 (1969).
85. M. Charton, *J. Am. Chem. Soc.*, 91, 615 (1969).
86. P. R. Wells, S. Ehrensen, and R. W. Taft, *Progr. Phys. Org. Chem.*, 6, 147 (1968).



87. M. I. Kabachnik, T. A. Mastrukova, A. E. Shipov, and T. A. Melentyeva, *Tetrahedron*, 9, 10 (1960).
88. M. Charton, *J. Org. Chem.*, 34, 1877 (1969).
89. W. A. G. Graham, *Inorg. Chem.*, 7, 315 (1968).
90. R. G. Cavell and A. R. Sanger, submitted to *Inorg. Chem.* for publication.
91. (a) R. G. Cavell and A. R. Sanger, submitted to *Inorg. Chem.* for publication.  
(b) R. G. Cavell and A. R. Sanger, unpublished observations.
92. A. A. Pinkerton and R. G. Cavell, *J. Am. Chem. Soc.*, 93, 2384 (1971).
93. D. A. Buckingham and A. M. Sargeson, "Chelating Agents and Metal Chelates", Edited by F. P. Dwyer and D. P. Mellor, Academic Press, New York (1964), Chapter 6.
94. B. Kratochvil, personal communication.
95. J. J. Dickert and C. N. Rowe, *J. Org. Chem.*, 32, 647 (1967); J. P. Fackler, W. C. Siedel, and M. Myron, *Chem. Comm.*, 1133 (1969).
96. R. G. Pearson, *Survey of Progr. in Chem.*, 5, 1 (1969).
97. S. E. Livingstone, *Quart. Revs.*, 19, 386 (1965).
98. R. Ripon and C. Mirel, *Rev. Roum. Chim.*, 9, 567 (1964).
99. C. K. Jorgensen, *Acta Chem. Scand.*, 16, 2017 (1962).
100. W. R. Walker and N. C. Li, *J. Inorg. Nucl. Chem.*, 27, 2255 (1965).
101. K. Diemert and W. Kuchen, *Chem. Ber.*, 104, 2592 (1971).
102. J. R. Angus, G. M. Woltermann, and J. R. Wasson, *J. Inorg. Nucl. Chem.*, 33, 3967 (1971).
103. P. S. Shetty and Q. Fernando, *J. Am. Chem. Soc.*, 92, 3964 (1970).



104. W. Byers and R. G. Cavell, unpublished results.
105. G. Miller and R. E. D. McClung, personal communication.
106. J. Selbin, *Chem. Rev.s*, 65, 153 (1965); J. Selbin, *Coord. Chem. Rev.s*, 1, 293 (1966).
107. L. F. Doty and R. G. Cavell, unpublished results.
108. J. H. Van Vleck, "Theory of Electric and Magnetic Susceptibilities", Oxford University Press, London (1932).
109. A. Earnshaw, "Introduction to Magnetochemistry", Academic Press Inc., (London) Ltd., London (1968).
110. A. H. Morrish, "The Physical Principles of Magnetism", John Wiley & Sons, Inc., New York (1965).
111. B. N. Figgis, "Introduction to Ligand Fields", John Wiley & Sons, New York (1966).
112. C. J. Ballhausen, "Introduction to Ligand Field Theory", McGraw-Hill Book Company, Inc., New York (1962).
113. J. S. Griffith, "The Theory of Transition-Metal Ions", Cambridge University Press, London (1961).
114. G. Foëx, C. J. Gorter, and L. J. Smits, "Constantes Selectionées 7, Diamagnetisme et Paramagnétisme relaxation paramagnétique", Masson, Paris (1957).
115. B. J. McCormick, *Inorg. Chem.*, 7, 1965 (1968); *ibid*, 9, 1779 (1970).
116. C. J. Ballhausen and H. B. Gray, *Inorg. Chem.*, 1, 111 (1962).
117. B. N. Figgis, J. Lewis, F. E. Mabbs, and G. A. Webb, *J. Chem. Soc. (A)*, 1411 (1966).
118. R. L. Carlin and E. G. Terezakis, *J. Chem. Phys.*, 47, 4901 (1967).
119. R. M. MacFarlane, *J. Chem. Phys.*, 40, 373 (1964).



120. (a) S. Gregorio, J. Weber, and R. Lacroix, *Helv. Phys. Acta*, 38, 172 (1965);  
(b) N. S. Garif'yanov, B. M. Kozyrev, and S. A. Luchkina, *Zh. Strukt. Khim.*, 9, 901 (1968).
121. H. Hertel and W. Kuchen, *Chem. Ber.*, 104, 1735 (1971).
122. N. S. Gill and R. S. Nyholm, *J. Chem. Soc.*, 3997 (1959).
123. D. Forster and D. M. L. Goodgame, *J. Chem. Soc.*, 268 and 454 (1965)
124. N. S. Garif'yanov, S. E. Kamenev, B. M. Kozyrev, and I. V. Obchinnikov, *Dokl. Akad. Nauk SSSR*, 177, 880 (1967).
125. R. J. H. Clark, R. S. Nyholm, and F. B. Taylor, *J. Chem. Soc. (A)*, 1802 (1967).
126. F. A. Cotton, D. M. L. Goodgame, M. Goodgame, and A. Sacco, *J. Am. Chem. Soc.*, 83, 4157 (1961).
127. R. G. Cavell and P. M. Watkins, personal communication.
128. R. W. Gurney, "Introduction to Statistical Mechanics", Dover Publications, Inc., New York (1966).
129. A. D. Liehr, *Advan. Chem. Phys.*, V, 241 (1963); G. Herzberg, "Molecular Spectra and Molecular Structure", Van Nostrand, New York (1966); E. V. Condon & G. H. Shortly, "The Theory of Atomic Spectra", Cambridge University Press, Cambridge (1967).
130. C. K. Jorgensen, *Progr. Inorg. Chem.*, 12, 101 (1970).
131. C. K. Jorgensen, *Mol. Phys.*, 5, 485 (1962).
132. R. F. Hudson, "Structure and Mechanism in Organo-Phosphorus Chemistry", Academic Press, New York (1965).
133. C. J. Ballhausen and H. B. Gray, "Molecular Orbital Theory", W. A. Benjamin, Inc., New York (1965); J. P. Dahl and C. J.



- Ballhausen, *Advan. Quant. Chem.*, 4, 170 (1968).
134. K. A. R. Mitchell, *Chem. Revs.*, 69, 157 (1969); D. W. J. Cruickshank and B. C. Webster, "Inorganic Sulphur Chemistry", Ed. G. Nickless, Elsevier, Amsterdam, Chapter 2, page 7.
135. J. Hinze and H. H. Jaffé, *J. Am. Chem. Soc.*, 84, 540 (1962).
136. J. Ferguson, *Progr. Inorg. Chem.*, 12, 159 (1970).
137. C. K. Jorgensen, *Progr. Inorg. Chem.*, 12, 101 (1970).
138. L. G. Vanquickenborne and S. P. McGlynn, *Theor. Chim. Acta*, 9, 390 (1968).
139. G. Vigee and J. Selbin, *J. Inorg. Nucl. Chem.*, 31, 3187 (1969).
140. J. Selbin, T. R. Ortolano, and F. J. Smith, *Inorg. Chem.*, 2, 1315 (1963).
141. C. K. Jorgensen, *Advan. Chem. Phys.*, 5, 33 (1963).
142. P. Cancellieri, E. Cervone, C. Furlani, and G. Sartori, *Z. Phys. Chem., Neue Folge*, 62, 35 (1968).
143. C. D. Burbridge and D. M. L. Goodgame, *J. Chem. Soc. (A)*, 1074 (1968).
144. H. A. Weakliem, *J. Chem. Phys.*, 36, 2117 (1962).
145. J. Ferguson, *J. Chem. Phys.*, 39, 116 (1963).
146. J. Chatt, G. A. Gamlen, and L. E. Orgel, *J. Chem. Soc.*, 486 (1958).
147. M. Forster, H. Hertel, and W. Kuchen, *Angew. Chem.*, 82, 842 (1970); A. T. Casey, N. S. Ham, D. J. Mackey, and R. L. Martin, *Aust. J. Chem.*, 23, 1117 (1970); A. T. Casey, D. J. Mackey, and R. L. Martin, *Aust. J. Chem.*, 24, 1587 (1971).
148. A. P. B. Lever and E. Mantovani, *Inorg. Chem.*, 10, 817 (1971).



149. W. A. G. Graham, *Inorg. Chem.*, 7, 315 (1968); M. G. Hogben and W. A. G. Graham, *J. Am. Chem. Soc.*, 91, 283 (1969); M. G. Hogben, R. A. Gay, A. J. Oliver, J. A. J. Thompson, and W. A. G. Graham, *ibid*, 91, 291 (1969).
150. D. C. Olsen, V. P. Mayweg, and G. N. Schrauzer, *J. Am. Chem. Soc.*, 88, 4876 (1966).
151. F. A. Cotton and M. D. Meyers, *J. Am. Chem. Soc.*, 82, 5023 (1960).



**APPENDIX A**



## APPENDIX A

TABLE A1

Infrared Spectral Bands of the  $PX_2$  Group in the Complexes  $M[S_2PX_2]_n$ 

$\nu^{+3}$	$Cr^{+3}$ b	$Co^{+3}$	$Mn^{+2}$	$Fe^{+2}$	$Co^{+2}$	$Zn^{+2}$	$Cd^{+2}$	$Hg^{+2}$	$Ni^{+2}$	$Pd^{+2}$	$Pt^{+2}$	$Ov^{+2}$	Assignment <sup>c</sup>
1422w	1421w	1423wsh	1420w	1422w	1422wsh	1421w	1415w	1416w	1415w	1414w	1412m	1411w	$\nu_{P-CH_3}$
1412w	1412w	1414w	1415w	1404wsh	1405wsh	1405w	1405w	1403wsh	1403wsh	1403wsh	1403wsh	1403wsh	$\nu_{P-CH_3}$
1402wsh	1401wsh	1405wsh	1404wsh	1395m	1395m	1400w	1400w	1399w	1399w	1395w	1394m	1395w	$\nu_{P-CH_3}$
1397m	1396m	1397m	1395m	1394w	1394w	1394w	1394w	1394w	1394w	1395w	1381m	1382m	$\nu_{P-CH_3}$
1286w	1283w	1285wsh	1295m	1295m	1295m	1296w	1296w	1297w	1297w	1295w	1291w	1291w	$\nu_{P-CH_3}$
1276m	1271s	1275s	1282s	1283m	1282m	1283m	1283m	1283m	1283m	1282m	1279m	1279m	$\nu_{P-CH_3}$
951s	950s	950s	946m	946m	946m	948m	947m	947m	945s	940s	940s	940s	$\nu_{P-CH_3}$
940s	947s	940s	946s	942m	942m	943m	943m	943m	934s	934s	935ssh	936s	$\rho_{CH_3}$
909s	905s	900s	912ssh	903ssh	905ssh	908ssh	908ssh	910ssh	900m	900m	898m	897m	$\rho_{CH_3}$
901m	900s	897ssh	904s	901s	901s	900s	900s	900s	890m	890m	888m	887m	$\rho_{CH_3}$
856w	855m	855m	855s	853m	855m	855m	855m	855m	857m	848m	847m	846m	$\rho_{CH_3}$
852wsh	850w	848wsh	849s	847m	847m	847m	847m	849m	848m	844m	844m	844m	$\rho_{CH_3}$
844m	840m	840m	840m	840m	840m	840m	840m	840m	837w	837w	837w	837w	$\rho_{CH_3}$
738m	740msh	742m	741m	744m	742m	742m	742m	742m	743m	736s	736s	732s	$\nu_{P-C}$
726s	730s	719s	719s	717s	718s	718s	718s	719s	719s	716s	720msh	720msh	$\nu_{P-C}$
													$\nu_{P-C}$

<sup>a</sup> Spectra obtained from Nujol mulls. Frequencies of band maxima in units of kaysers. Spectral range: 1500-360K.<sup>b</sup> Bands due to C-H stretching in a halo oil null of the complex  $Cr[S_2P(CH_3)_2]_3$ : 2989w, 2968w, 2896w.<sup>c</sup>  $\nu$  implies a stretching mode,  $\rho$  implies a rocking mode.



TABLE A2

 $\chi = C_6H_5^a$ 

	$V^{+3}$	$Cr^{+3} b$	$Fe^{+3}$	$Co^{+3}$	$Mn^{+2}$	$Fe^{+2}$	$Co^{+2}$	$Zn^{+2}$	$Cd^{+2}$	$Hg^{+2}$	$Ni^{+2}$	$Pd^{+2}$	$Pt^{+2}$	$Ov^{+2}$
1434s	1434s	1434s	1434s	1431s	1430s	1432s	1431s	1430s	1433s	1432s	1433s	1434s		
1304w	1305m	1304w	1304w	1303w	1304w	1304w	1304w	1303w	1305w	1304w	1303w	1304w		
1180w	1181w	1182w	1181w	1184w	1181w	1180w	1183w	1181w	1180w	1178w	1178w	1180w		
1153w	1155w	1155w	1156w	1155w	1151w	1151w	1153w	1153w	1157w	1156w	1156w	1157w		
1125w			1128w											
1095s	1095s	1097s	1097s	1097s	1097s	1095s	1095s	1095s	1097ssh	1097ssh	1100s	1103s	1102s	1102ssh
1065w	1065w	1066w	1066w	1066w	1066w	1066w	1066w	1066w	1096ssh	1096ssh	1093s	1095s	1095s	1096s
1023w	1025w	1025w	1025w	1024w	1022w	1024w	1022w	1020w	1023w	1021w	1023w	1063w	1063w	1062w
996w	996w	997w	997w	997w	996w	996w	995w	995w	996w	994w	994w	1022w	1022w	1022w
920vw	921vw	921vw	920vw	842w	842w	841w	841w	841w	843w	840w	841s	994w	994w	995wsh
842w	845w	845w	842w	750msh	745msh	740m	742m	742s	745s	745s	744s	746s	746s	840vw
750msh	744msh	744msh	740m											
740m														
705s	705s	704s	706s	703s	704s	704s	704s	704s	705s	704s	704s	704s	704s	704s
686s	684s	685s	686s	686s	686s	686s	686s	689s	689s	689s	689s	687s	687s	687s
612m	610s	609m	607w	608m	610m	609m	611s	610s	608s	608s	609m	603m	603m	612m
488m	488s	488m	489m	491s	492m	554s	553s	554s	552s	550s	545s			
480wsh	480msh	480msh	480msh	479wsh	475w	475w	475w	473w	476m	474m	471w	465w	465w	484m
472wsh	474msh	476wsh	470wsh	444w	449m	449m	448w	447m	448m	446m	446m	454w	453w	455m
448w	448w	450w	358m	351m	359m	360m	360m	360m	366m	362m	361m	360wsh	356	361m
358m	353m													

a Spectra obtained from Nujol mulls. Frequencies of band maxima in units of keymers. Spectral range: 1460-350K.

b Spectrum of halo oil mull showed bands at: 3068wsh, 3050w, 2920w, 2850w, 1580wsh, 1570w, 1480w, 1473wsh.



TABLE A3

 $X = OC_2H_5$ <sup>a</sup>

V <sup>+3</sup>	Cr <sup>+3</sup> b	Co <sup>+3</sup>	Co <sup>+2</sup>	Zn <sup>+2</sup>	Ni <sup>+2</sup>	Pd <sup>+2</sup>	Pt <sup>+2</sup>	OV <sup>+2</sup>
1288w	1287w	1276w	1263w	1263w	1278w	1278w	1278w	1281mw
1161m	1160w	1162wsh	1154w	1154w	1158m	1157m	1155m	1152m
1106m	1105w	1101w			1101m	1101w	1101w	1095msh
1060ssh	1060ssh	1058msh			1036ssh	1044ssh	1049ssh	1048s
1043ssh	1040ssh	1032msh	1016s	1016s	1017s	1000s	1010s	1008s
1015s	1015s	1007s	966s	966s	968ssh	963s	967s	965s
973s	970s	960s			955s	956s		960s
819s	812s	812s			817ssh	812s	812s	812s
803ssh	800s	795ssh	787msh	788msh	805s	800ssh	799ssh	
789ssh	785ssh		774m	775m	782msh	777msh		777msh
			734wsh	735wsh	723wsh	721msh	721msh	720s
			495m	486m				498w
397w	400w	396w	377w	380w	394w	396w	400w	400w
363m	358w	347w			354s	353w	350w	367s

<sup>a</sup> Spectra obtained from Nujol mulls. Frequencies of band maxima in units of keyssers.  
Spectral range: 1300-340.

<sup>b</sup> Spectrum of a halo oil mull showed bands at: 2985w, 2962w, 2936w, 2895w, 2863w,  
1473w, 1453w, 1435w, 1421wsh, 1389w,  
1342w.



TABLE A4

 $X = F^a$ 

$\nu^{+3}$	$Cr^{+3}$	$Co^{+3}$	$Mn^{+2}$	$Fe^{+2}$	$Co^{+2}$	$Zn^{+2}$	$Ni^{+2}$	$Pd^{+2}$	$Pt^{+2}$	$Ov^{+2}$	Assignments
905s,br	925ssh		917s,br				905s	902s	905ssh	905s	
895s		880s,br	887vs	885vs	889w	887vs	889s	895ssh	896s	899vs,br	$\nu_{PF_2}$
855ssh		821m,br		868vs			864msh	854wsh	886ssh		
806m		835vs		835vs	840s				860s		
720msh		720s	718ssh	718ssh	806s		722w	722w	720m	720ssh	
714s	712s		785s	715vs	704s				712ssh	712ssh	
				785s	675s					600w	
404s	405s	403m	401m	399m	390m	398m	432wsh	431wsh	421wsh		
360m	358s	357m		367msh	369m	368s	403s	402s	402s	406ms	
352m	352s			355m	358msh		355msh	349m	349m	377msh	
										370m	
										355m	
										335mw	

<sup>a</sup> Spectra obtained from Nujol mulls. Frequencies of band maxima in units of kaysers. Spectral range: 1000-330K.



TABLE A5  
 $X = CF_3^a$

$V^{+3}$	$Cr^{+3}$	$Fe^{+3}$	$Co^{+3}$	$Mn^{+2}$	$Fe^{+2}$	$Co^{+2}$	$Zn^{+2}$	$Cd^{+2}$	$Hg^{+2}$	$Ni^{+2}$	$Pd^{+2}$	$Pt^{+2}$	$b$	$OV^{+2}$
1294w	1295w	1295w	1291w	1289w	1290w	1291w	1292w	1290w	1287w	1303w	1302w	1294wsh	1300w	
1210msh	1205s	1210msh	1208s	1211ssh	1209s	1218ssh				1202s	1204s	1210ssh	1222s	
1194ssh	1185ssh	1200s	1186ssh	1186s	1186ssh	1193ssh	1200s	1191s	1184ssh	1182s	1184s	1187s	1200vs,br	
1180s	1175s		1170ssh		1179ssh				1172s	1174w	1174w	1171s	1175vs	
1165s	1160s	1164s	1163s	1158s	1161s	1162s	1160s	1160ssh	1162s					
1135msh	1150s	1135msh	1150ssh	1138s	1144s	1144ssh	1140s	1146s	1150s	1145m	1140s	1140s		
		1130ssh						1078m						
755w		753w	751w	750w	751w	754w	745w	750w		884m	885m	892m	870ms	
722wsh		720m	720w	721msh	712wsh	712wsh		723m	722w	756m	756w	756w	722w	720w
										721w				
628ssh				605s	611s	607s	611s	597s	602m	632ssh	628msh	622ssh	676m	
				600msh	602ssh	595s	600s	589s	589s	626s	620s	614s		
										608msh	602wsh	603msh		
												538m		
477s	475s	470m	472m	478s	480m	477m	480s	472m	480m	474s	473m	473m	490m	
383s	380s		372m	382m	383m	384m	381msh		377w	422w	418w	418w	476ms	
										378ssh	380m	380m		

a Spectra obtained from Nujol mulls. Frequencies of band maxima in units of kaysers. Spectral range: 1350-370K.

b Spectrum of  $Pt_2S_6P_4(CF_3)_8$ . Bands below 370K: 326w, 306w, 282wsh, 271w.



## APPENDIX B



TABLE B1

Mass Spectral Data for the Tris Complexes  $M[S_2PX_2]_3^a$ 

Assignment	$CH_3$				$C_6H_5$				$OC_2H_5$				$F$				$CF_3$			
	V	Cr	Fe <sup>b</sup>	Co	V	Cr	Fe	Co	V	Cr	Co	V	Cr	Co	V	Cr	Fe	Co		
$MS_6P_3X_6$	426(73)	427(61)	-	-	798(103)	799(33)	-	-	606(100)	607(61)	614(0)	450(138)	451(85)	458(26)	750(230)	751(101)	755(12)	758(1)		
$MS_6P_3X_2$	-	-	-	-	490(17)	-	-	-	-	-	-	-	-	382(1)	-	-	479(0)	-		
$MS_6P_3$	-	-	-	-	-	-	341(9)	-	-	-	-	336(43)	-	-	-	-	-	-	-	
$MS_6P_2X_4$	-	-	-	-	-	-	-	-	-	-	-	381(1)	-	-	581(13)	-	586(0)	-		
$MS_6PX_3$	-	-	-	-	-	-	-	-	409(44)	-	-	-	-	-	-	-	-	-		
$MS_6$	-	-	-	-	-	-	-	-	243(156)	-	-	-	-	251(13)	-	-	-	251(1)		
$MS_5P_3X_6$	-	395(0)	-	-	766(7)	-	-	-	-	-	-	-	426(19)	-	-	-	-	-		
$MS_5P_3$	-	-	-	-	304(18)	305(5)	-	-	-	-	-	-	-	-	-	-	-	-		
$MS_5P_2X_4$	333(16)	334(2)	-	-	581(163)	582(2)	-	-	453(44)	-	-	349(1)	-	-	549(20)	550(3)	554(0)	-		
$MS_5P_2X_2$	-	-	-	-	427(3)	-	-	-	363(33)	-	-	-	-	411(3)	412(0)	416(0)	-			
$MS_4P_2X_2$	301(100)	302(100)	306(100)	309(100)	549(100)	550(100)	554(100)	557(100)	421(100)	422(100)	429(100)	317(100)	318(100)	325(100)	517(100)	518(100)	522(100)	525(100)		
$MS_4P_2X_3$	286(20)	287(7)	291(19)	294(16)	472(3)	-	477(0)	480(0)	-	377(1)	384(5)	298(0)	-	306(10)	-	449(2)	453(2)	456(2)		
$MS_4P_2X_2$	271(17)	-	276(2)	-	-	-	400(0)	-	-	332(1)	-	-	-	287(1)	379(4)	380(7)	384(5)	387(3)		
$MS_4P_4$	-	242(1)	-	249(11)	-	-	-	249(1)	241(322)	242(1)	249(4)	-	-	249(7)	-	242(1)	246(1)	249(0)		
$MS_4PX_3$	-	-	-	-	441(13)	-	-	-	345(156)	-	-	267(12)	-	-	417(3)	418(1)	-	425(3)		
$MS_4PX_2$	-	-	-	-	364(5)	365(1)	369(0)	372(0)	300(167)	301(2)	308(5)	248(5)	249(18)	256(352)	348(5)	349(26)	353(6)	356(22)		
$MS_4F$	-	-	-	-	-	-	-	-	210(256)	-	-	-	-	-	210(12)	211(3)	215(1)	218(4)		
$MS_4X$	-	-	-	-	-	-	-	-	-	225(1)	-	198(6)	-	-	248(15)	-	-	256(0)		
$MS_4$	-	-	-	187(28)	-	-	-	-	179(367)	180(2)	-	179(6)	-	187(11)	-	180(2)	184(1)	187(1)		
$MS_3P_2X_4$	269(17)	270(12)	-	-	517(35)	518(5)	522(0)	525(0)	-	-	-	286(2)	293(2)	-	486(0)	490(0)	493(0)			
$MS_3PX_3$	-	-	-	-	409(82)	410(5)	414(4)	417(5)	313(411)	-	-	235(63)	236(3)	-	385(9)	386(2)	390(0)	393(1)		
$MS_3PX_2$	-	-	-	-	332(26)	-	337(1)	340(1)	-	-	276(4)	216(3)	217(2)	224(26)	-	317(0)	321(1)	324(5)		
$MS_3PX$	193(24)	194(1)	-	-	255(21)	-	-	-	223(244)	224(1)	-	197(0)	-	-	-	248(0)	252(1)	255(0)		
$MS_3P$	178(9)	-	-	186(327)	-	-	183(8)	-	178(633)	179(1)	186(14)	-	-	186(4)	178(16)	179(2)	183(4)	186(6)		
$MS_3X$	162(10)	-	167(4)	-	-	-	-	-	-	-	-	166(11)	167(2)	174(5)	216(18)	217(2)	221(0)	224(2)		
$MS_3$	147(4)	-	-	155(16)	-	-	-	-	147(222)	148(1)	-	147(7)	-	155(22)	-	-	152(3)	155(2)		
$MS_2P_2X_4$	237(2)	238(1)	242(5)	245(16)	-	-	490(1)	493(0)	-	-	-	-	-	-	-	-	-	461(0)		
$MS_2P_2X_3$	-	-	227(4)	230(13)	-	-	416(0)	-	-	-	-	-	-	-	-	-	-	-		
$MS_2P_2X$	192(32)	-	-	-	254(20)	-	-	262(13)	-	-	-	-	-	-	-	-	251(0)	-		
$MS_2P_2$	-	-	-	185(79)	-	-	185(15)	-	-	185(7)	-	178(515)	-	-	-	-	182(0)	185(1)		
$MS_2PX_3$	-	-	-	-	377(14)	378(6)	382(2)	385(10)	-	282(3)	-	203(11)	204(27)	211(4)	353(1)	-	-	-		
$MS_2PX_2$	-	-	-	-	-	301(20)	305(17)	308(18)	236(200)	237(5)	244(14)	184(6)	185(23)	192(303)	-	285(17)	289(18)	292(45)		
$MS_2PX$	-	162(4)	166(5)	169(20)	-	-	228(2)	-	-	192(1)	-	165(1)	-	173(2)	-	-	220(1)	223(1)		
$MS_2P$	-	147(5)	151(11)	154(11)	-	147(3)	151(3)	154(3)	146(322)	147(1)	154(6)	146(9)	-	154(3)	-	147(15)	151(10)	154(11)		
$MS_2X_2$	-	-	-	-	269(22)	270(1)	-	-	-	-	-	153(13)	-	-	253(66)	254(5)	258(4)	-		
$MS_2X$	130(8)	131(2)	-	-	192(202)	-	-	-	-	-	-	134(14)	135(8)	142(28)	184(42)	185(6)	189(6)	192(7)		
$MS_2$	115(5)	-	-	-	115(10)	-	-	-	116(2)	-	115(10)	116(9)	123(78)	-	116(22)	120(7)	123(8)			
$MS_2P_2$	145(2)	-	-	153(13)	-	-	-	-	-	153(16)	-	-	-	145(33)	-	150(1)	-			
$MS_2PX_2$	-	-	-	-	-	273(1)	-	-	-	-	-	-	160(29)	-	-	-	-			
$MS_2P$	114(2)	115(1)	119(28)	122(13)	-	-	119(1)	122(3)	114(400)	115(1)	-	114(3)	-	-	-	119(14)	122(8)			
$MSX$	-	-	-	-	160(202)	161(12)	165(3)	168(4)	-	129(2)	-	102(6)	-	-	-	153(7)	157(8)	160(8)		
$MS$	83(3)	84(1)	-	-	-	-	88(0)	-	-	-	-	83(11)	84(6)	91(57)	83(76)	84(4)	88(5)	91(3)		
$XP_2X_2$	-	-	-	-	-	268(1)	272(1)	275(3)	-	-	-	-	152(34)	-	251(16)	-	-			
$XP_2X$	128(4)	129(3)	133(4)	-	-	191(3)	195(1)	-	158(167)	-	-	-	-	-	182(27)	-	187(0)			
$MP_2$	-	-	-	-	-	-	-	-	113(344)	114(1)	121(25)	-	114(7)	-	113(139)	-	118(0)			
$MP_2X_2$	-	-	117(21)	-	236(15)	237(1)	241(1)	244(3)	-	-	-	120(1)	-	128(10)	220(41)	-	-			
$MX$	-	-	-	-	128(147)	-	133(2)	136(2)	-	97(10)	-	70(8)	71(5)	78(16)	-	-	125(1)	128(1)		
$M$	51(1)	52(5)	-	59(149)	51(15)	52(12)	56(1)	59(2)	-	-	59(2)	51(45)	-	59(47)	51(22)	52(9)	56(6)	59(3)		
$S_4P_2X_4$	-	-	250(207)	250(451)	-	-	-	-	-	370(12)	-	-	266(41)	-	-	466(6)	466(21)			
$S_3P_2X_4$	-	-	218(33)	218(285)	466(14)	466(1)	466(0)	-	338(6)	-	-	-	-	-	-	434(0)	-			
Source Temp. (°C)	200	150	150	125	245	240	245	310	160	150	150	15	30	60	100	30	80	100		

<sup>a</sup> The data is presented as an array of m/e values for uni-positive, metal containing ions followed by the relative intensities of the corresponding peaks scaled such that the intensities of the ions  $MS_2P_2X_2^+$  were set at 100. Only peaks assignable without fragmentation of the X group are included (the omitted peaks are an appreciable fraction of the total ionization where  $X = C_6H_5$ ,  $CF_3$  and  $OC_2H_5$  where the step-wise loss of  $C_2H_4$  units dominates the spectrum<sup>26</sup>). Only peaks are included where there are at least two entries in a row and at least one of which has an intensity greater than 10.

<sup>b</sup> This data was obtained from the mass spectrum of the residue of a green dichloromethane solution, after removal of the solvent.



TABLE B2  
Mass Spectral Data for the Tetrahedral Bis Complexes  $M[S_2PP'_2]_2$ <sup>a</sup>

		Assignments												
$\Sigma$	$M$	Source	$T_{\text{exp.}} (\text{°C})$	$\underline{\text{MS}_4P_2X_4}$	$\underline{\text{MS}_4P_2X_3}$	$\underline{\text{MS}_4P_2X_2}$	$\underline{\text{MS}_4P}$	$\underline{\text{MS}_3P_2X_3}$	$\underline{\text{MS}_3P_2X_2}$	$\underline{\text{MS}_3P}$	$\underline{\text{MS}_2P_2X_2}$	$\underline{\text{MS}_2P}$	$\underline{\text{MS}_2X}$	$\underline{\text{MS}}$
$\text{CH}_3$	Mn	200	305(100)	290(19)	244(1)	-	258(1)	227(0)	212(2)	-	180(100)	165(6)	150(12)	119(3)
	Fe	260	305(100)	291(20)	245(4)	-	259(2)	-	213(2)	-	181(71)	166(5)	151(12)	-
	Co	110	309(100)	294(15)	248(2)	-	262(2)	231(2)	216(2)	-	184(53)	169(5)	154(8)	-
	Zn	195	314(100)	299(42)	253(3)	-	267(3)	-	221(6)	-	189(77)	-	159(6)	-
	Cd	220	364(100)	349(37)	-	-	271(3)	-	239(53)	-	209(1)	-	-	146(1)
	Hg	200	452(100)	437(1)	-	361(25)	-	-	-	-	-	-	-	114(4)
														202(292)
$\text{C}_6\text{H}_5$	Mn	250	553(100)	476(0)	-	-	413(8)	336(1)	-	304(63)	-	150(5)	119(0)	195(2)
	Fe	225	554(100)	477(0)	-	-	445(1)	414(9)	-	183(20)	305(27)	228(3)	151(5)	119(1)
	Co	290	557(100)	480(0)	372(0)	-	448(1)	417(5)	340(5)	186(9)	303(22)	231(14)	154(14)	-
	Zn	255	562(100)	485(1)	-	-	453(57)	422(79)	345(3)	-	313(71)	-	-	-
	Cd	250	612(100)	535(1)	-	-	503(38)	472(53)	395(1)	-	363(20)	-	-	-
	Hg	250	700(100)	-	-	-	-	-	-	-	-	-	-	-
														136(13)
$\text{OC}_2\text{H}_5$	Co	200	429(100)	384(4)	308(6)	218(5)	-	276(4)	166(15)	244(17)	-	154(9)	123(9)	122(15)
	Zn	240	434(100)	-	313(3)	-	357(82)	-	281(8)	191(5)	249(21)	-	128(8)	91(2)
	Fe	40	321(100)	302(1)	252(7)	-	-	239(0)	220(1)	-	188(62)	-	-	-
	Co	50	322(100)	303(1)	253(21)	-	-	240(2)	221(1)	-	189(22)	170(1)	-	119(5)
	P	40	325(100)	306(1)	256(33)	-	-	224(2)	186(0)	192(29)	173(0)	154(0)	120(12)	141(0)
	Zn	90	330(100)	311(1)	261(1)	-	279(0)	248(0)	229(5)	-	197(37)	178(0)	159(0)	123(8)
	Hg	150	468(100)	449(1)	-	-	-	-	367(6)	329(17)	335(4)	316(1)	-	146(0)
$\text{CP}_3$	Mn	60	521(100)	452(4)	352(3)	214(0)	420(6)	389(3)	320(1)	182(2)	288(38)	-	150(7)	119(4)
	Fe	50	522(100)	-	353(2)	215(1)	421(7)	-	321(1)	183(1)	239(1)	220(5)	151(6)	120(2)
	Co	70	525(100)	456(4)	356(18)	218(4)	424(8)	393(1)	324(6)	186(8)	292(41)	-	154(14)	123(11)
	Zn	135	530(100)	461(37)	-	-	429(3)	-	-	191(16)	297(54)	159(13)	-	91(6)
	Cd	60	580(100)	-	411(0)	-	479(3)	-	379(3)	241(1)	347(15)	278(0)	177(1)	146(1)
	Hg	100	668(100)	599(15)	-	-	567(3)	-	467(15)	-	435(9)	-	266(15)	-
												-	234(45)	-

<sup>a</sup> See footnote (a) of Table B1, reading "columns" for "rows". The relative intensities were obtained considering only the component peaks of the major isotopic species, i.e.  $^{64}\text{Zn}$ ,  $^{114}\text{Cd}$ , and  $^{202}\text{Hg}$ .



TABLE B3  
Mass Spectral Data for Planar  $M[S_2PX_2]_2$  Complexes<sup>a</sup>

X -	$CH_3$			$C_6H_5$			P			$CF_3$	
	Ni	Pd	Pt	Ni	Pd	Pt	Ni	Pd	Pt	Ni	Pd
$MS_4P_2X_4$	308(100)	356(100)	445(100)	556(100)	604(100)	693(100)	324(100)	372(100)	461(100)	524(100)	572(100)
$MS_4P_2X_3$	293(4)	341(11)	430(10)	-	-	616(0)	305(0)	353(1)	442(1)	455(3)	-
$MS_4PX_2$	-	-	384(9)	-	-	-	255(29)	303(2)	392(33)	355(22)	403(0)
$MS_4PX$	-	-	-	-	-	-	236(8)	-	373(5)	286(3)	-
$MS_4$	-	-	-	-	234(4)	-	186(3)	284(10)	323(9)	186(5)	-
$MS_3P_2X_4$	276(1)	324(1)	-	524(7)	572(3)	661(1)	-	-	-	492(0)	540(0)
$MS_3P_2X_3$	261(3)	309(3)	398(4)	447(0)	495(8)	584(5)	-	-	-	423(6)	471(6)
$MS_3P_2X$	-	-	-	293(22)	-	-	-	-	-	-	333(1)
$MS_3PX_3$	-	-	-	416(12)	-	-	-	-	-	-	-
$MS_3PX_2$	215(3)	-	-	-	-	476(1)	223(3)	271(0)	360(3)	323(9)	371(1)
$MS_3P$	-	-	322(4)	-	-	-	-	-	-	185(11)	233(5)
$MS_3$	-	-	291(6)	-	-	-	154(5)	202(3)	291(6)	154(3)	-
$MS_2P_2X_4$	244(34)	292(36)	381(25)	492(7)	540(27)	629(23)	-	308(1)	-	460(1)	508(1)
$MS_2P_2X_3$	229(26)	277(28)	366(29)	415(8)	463(4)	552(6)	-	-	378(1)	-	-
$MS_2PX_3$	198(1)	-	335(5)	384(18)	-	-	-	-	-	-	-
$MS_2PX_2$	183(20)	231(26)	320(8)	307(3)	355(3)	191(36)	-	239(32)	328(13)	291(25)	339(36)
$MS_2PX$	168(2)	216(2)	-	230(5)	-	367(3)	-	220(0)	309(3)	222(5)	270(1)
$MS_2P$	-	-	-	-	-	290(1)	-	-	-	153(21)	201(24)
$MS_2$	122(3)	-	-	-	-	-	122(20)	170(18)	259(12)	122(26)	170(33)
$MSP_2X_3$	197(0)	245(1)	334(4)	-	431(23)	520(12)	-	-	-	-	-
$MSP_2X$	-	215(2)	304(4)	229(12)	277(1)	-	-	-	-	-	-
$MSPX_3$	166(4)	-	-	352(32)	400(16)	-	-	-	-	-	-
$MSPX_2$	151(6)	199(39)	288(4)	275(2)	323(24)	159(6)	-	207(8)	296(7)	259(1)	307(11)
$MSPX$	136(3)	184(7)	-	198(18)	-	-	-	-	-	190(2)	-
$MSP$	-	169(26)	258(7)	-	169(66)	258(7)	-	-	-	121(31)	169(90)
$MS$	-	138(1)	227(1)	-	-	-	90(7)	138(4)	227(6)	90(10)	138(4)
$MP_2X$	135(1)	183(7)	272(1)	197(3)	245(6)	334(8)	-	-	-	-	-
$MP_2$	-	-	-	-	-	-	120(7)	-	-	-	-
$MPX_3$	-	-	-	-	368(8)	-	-	-	-	-	-
$MPX_2$	-	-	-	243(11)	291(24)	-	-	175(8)	263(3)	-	-
$MP$	-	-	-	-	-	-	-	-	-	89(1)	137(6)
$M$	-	106(3)	195(0)	58(10)	106(1)	-	58(11)	106(9)	-	58(23)	106(14)
Source Temp. (°C)	150	200	200	270	260	260	60	80	25	50	80

<sup>a</sup>See footnote<sup>a</sup> of Table B1, reading 4 in place of 10 for the intensity restriction. Peaks listed all contain the metal isotopic pattern. The intensities, in parentheses following the m/e values, were obtained from the component of the major isotopic species ( $Ni^{58}$ ,  $Pd^{106}$ ,  $Pt^{195}$ ). Spectra were scaled such that parent ion intensity is set at 100 and peaks are included only if at least one entry in a row has an intensity >4 on this intensity scale.



TABLE B4  
Mass Spectral Data for the Complexes  $\text{OV}[\text{S}_2\text{PX}_2]_2^{\text{a}}$

Assignment	X				
	$\text{CH}_3$	$\text{C}_6\text{H}_5$	$\text{OC}_2\text{H}_5$	F	$\text{CF}_3$
$\text{OVS}_4\text{P}_2\text{X}_4$	317(100)	565(100)	437(100)	333(100)	533(100)
$\text{VS}_4\text{P}_2\text{X}_4$	301(4)	549(74)	421(2)	317(83)	517(27)
$\text{VS}_4\text{PX}_3$	-	-	345(7)	267(68)	-
$\text{VS}_4\text{PX}_2$	-	-	300(7)	248(7)	348(24)
$\text{OVS}_3\text{P}_2\text{X}_4$	285(1)	533(18)	-	-	-
$\text{VS}_3\text{PX}_3$	-	409(18)	313(19)	235(80)	385(2)
$\text{VS}_3\text{P}$	-	-	178(14)	-	178(13)
$\text{VS}_3\text{X}$	-	-	-	166(18)	-
$\text{OVS}_3$	163(2)	-	163(5)	163(3)	163(60)
$\text{VS}_3$	147(2)	-	147(4)	147(10)	147(14)
$\text{OVS}_2\text{P}_2\text{X}_4$	253(50)	501(13)	-	-	-
$\text{OVS}_2\text{P}_2\text{X}$	208(14)	-	-	-	-
$\text{OVS}_2\text{P}_2$	193(16)	-	-	-	-
$\text{OVS}_2\text{PX}_3$	-	393(41)	297(62)	219(29)	369(5)
$\text{VS}_2\text{PX}_3$	-	377(4)	-	203(13)	-
$\text{OVS}_2\text{PX}_2$	192(26)	316(13)	-	200(13)	-
$\text{OVS}_2\text{P}$	162(7)	162(5)	162(4)	-	162(14)
$\text{VS}_2\text{P}$	-	146(6)	146(6)	-	146(14)
$\text{VS}_2\text{X}_2$	-	269(4)	-	153(34)	253(18)
$\text{VS}_2\text{X}$	-	-	-	134(43)	184(71)
$\text{VS}_2$	115(3)	-	-	115(14)	-
$\text{OVSPX}_2$	160(12)	284(3)	-	-	-
$\text{OVSP}$	130(6)	130(12)	-	-	130(14)
$\text{VSX}$	-	160(4)	-	102(10)	152(13)
$\text{VS}$	83(3)	-	-	83(18)	83(35)
$\text{VP}_2$	-	-	-	-	113(209)
$\text{VP}$	-	-	-	82(5)	82(16)
$\text{OV}$	67(3)	67(6)	-	67(8)	67(25)
$\text{V}$	51(1)	51(16)	-	51(11)	51(15)
$\text{S}_4\text{P}_2\text{X}_4$	-	-	370(23)	-	466(1)
Source Temp. ( $^{\circ}\text{C}$ )	200	230	105	10	50

<sup>a</sup> See footnote (a) of Table B1.



TABLE C1

## Static Field Magnetic Susceptibility Data

OV[S <sub>2</sub> PX <sub>2</sub> ] <sub>2</sub> Complexes									
X =	CH <sub>3</sub>	C <sub>6</sub> H <sub>5</sub>	OC <sub>2</sub> H <sub>5</sub>	F	CF <sub>3</sub>				
T(°K)	X <sub>g</sub> × 10 <sup>6</sup>	X <sub>g</sub> × 10 <sup>6</sup>	X <sub>g</sub> × 10 <sup>6</sup>	T(°K)	X <sub>g</sub> × 10 <sup>6</sup>	T(°K)	X <sub>g</sub> × 10 <sup>6</sup>	T(°K)	X <sub>g</sub> × 10 <sup>6</sup>
95.0	11.71	94.6	6.294	90.1	8.497			89.9	12.50
103.2	10.73	103.4	5.798	103.3	7.361				
113.9	9.741	113.8	5.250	113.6	6.645	113.8	18.60	113.6	9.808
123.3	8.982	123.4	4.791	123.3	6.095				
133.3	8.278	133.3	4.388	133.3	5.607	133.3	15.74	131.9	8.286
143.2	7.689	143.2	4.080	143.2	5.187				
153.4	7.165	153.4	3.771	153.4	4.812	153.4	13.54	153.4	7.113
163.1	6.706	163.1	3.529	163.1	4.511				
173.2	6.298	173.2	3.278	173.2	4.225	173.2	11.85	173.1	6.214
183.2	5.949	183.2	3.083	183.2	3.980				
193.2	5.631	193.2	2.874	193.3	3.756	193.2	10.49	193.2	5.494
203.4	5.315	204.0	2.716	203.4	3.551				
213.3	5.073	213.3	2.573	213.3	3.382	213.3	9.358	213.3	4.898
223.2	4.820	223.2	2.433	223.2	3.211				
233.0	4.604	233.0	2.314	233.0	3.055	233.0	8.446	233.0	4.413
243.1	4.395	243.2	2.217	243.1	2.918				
253.0	4.198	253.0	2.108	253.0	2.788	253.0	7.662	253.0	3.992
263.2	4.040	263.2	2.002	263.2	2.677				
273.3	3.891	273.3	1.897	273.3	2.560	273.3	6.997	273.3	3.634
283.3	3.744	283.3	1.843	283.3	2.459				
293.3	3.600	293.3	1.755	293.3	2.367	293.3	6.433	293.3	3.333
303.3	3.465	303.3	1.689	303.3	2.282				
						313.2	5.942	313.2	3.034



## APPENDIX C



TABLE C2

## Static Field Magnetic Susceptibility Data

V[S <sub>2</sub> PX <sub>2</sub> ] <sub>3</sub> Complexes													
X =	CH <sub>3</sub>	C <sub>6</sub> H <sub>5</sub>			OC <sub>2</sub> H <sub>5</sub>			F			CF <sub>3</sub>		
T(°K)	X <sub>g</sub> × 10 <sup>-6</sup>	T(°K)	X <sub>g</sub> × 10 <sup>-6</sup>	T(°K)	X <sub>g</sub> × 10 <sup>-6</sup>	T(°K)	X <sub>g</sub> × 10 <sup>-6</sup>	T(°K)	X <sub>g</sub> × 10 <sup>-6</sup>	T(°K)	X <sub>g</sub> × 10 <sup>-6</sup>	T(°K)	X <sub>g</sub> × 10 <sup>-6</sup>
89.0	22.93	86.2	10.84	85.9	16.21	86.0	21.26	89.2	12.89				
		103.4	9.087	107.7	13.12	103.7	17.84						
		114.3	8.243			114.4	16.29	113.7	10.18				
123.3	16.84	123.2	7.644	123.2	11.48	123.2	15.29						
		133.3	7.059	133.3	10.63	132.1	14.32	133.3	8.714				
		143.2	6.606	143.2	9.916	143.2	13.29						
153.4	13.70	153.3	6.182	153.4	9.269	153.3	12.46	153.4	7.595				
		163.1	5.819	163.1	8.734	163.0	11.78						
		173.1	5.507	173.2	8.252	173.2	11.12	173.2	6.747				
		183.2	5.207	183.2	7.811	183.2	10.57						
		193.1	4.942	193.2	7.416	193.1	10.06	193.2	6.078				
203.5	10.53	203.4	4.677	203.4	7.069	203.4	9.610						
		213.3	4.463	213.4	6.745	213.3	9.188	213.3	5.524				
		223.1	4.292	223.2	6.462	223.1	8.856						
		233.0	4.124	233.0	6.195	233.0	8.477	233.0	5.074				
		243.1	3.949	243.2	5.952	243.1	8.160						
		253.0	3.816	253.0	5.732	253.0	7.841	253.0	4.690				
		263.2	3.648	263.2	5.519	263.2	7.567						
		263.3	3.524	273.3	5.326	273.3	7.301	273.3	4.357				
283.3	7.755	283.3	3.400	283.3	5.137	283.3	7.076						
		293.3	3.300	293.3	4.977	293.3	6.853	293.3	4.072				
		303.3	3.197	303.3	4.826	303.3	6.636						
312.6	7.082							313.3	3.824				



## Static Field Magnetic Susceptibility Data

$\text{Cr}[\text{S}_2\text{PX}_2]_3$ Complexes									
$X =$	$\text{CH}_3$			$\text{OC}_2\text{H}_5$			$\text{CF}_3$		
	$T(^{\circ}\text{K})$	$\chi_g \times 10^6$	$T(^{\circ}\text{K})$	$\chi_g \times 10^6$	$T(^{\circ}\text{K})$	$\chi_g \times 10^6$	$T(^{\circ}\text{K})$	$\chi_g \times 10^6$	$T(^{\circ}\text{K})$
95.9	44.86	92.9	24.72	96.0	31.57	87.7	47.13	92.9	25.86
103.3	41.73	103.3	22.22	103.3	29.32	103.4	39.93	104.7	23.04
113.7	37.96	113.6	20.18	113.6	26.61	113.8	36.31	113.6	21.43
123.4	35.08	123.3	18.57	123.3	24.49	123.3	33.50	123.4	19.77
133.4	32.43	133.4	17.16	133.3	22.58	133.3	30.97	133.3	18.23
143.2	30.21	143.2	15.92	143.1	20.98	143.2	28.81	143.2	16.96
153.5	28.21	153.4	14.88	153.4	19.53	153.4	15.88	153.4	15.88
162.8	26.57	163.1	13.96	163.1	18.33	163.1	25.28	163.1	14.92
173.2	24.98	173.2	13.13	173.2	17.23	173.2	23.83	173.2	14.07
183.3	23.62	183.2	12.38	183.2	16.26	183.2	22.56	183.2	13.25
193.2	22.40	193.2	11.74	193.2	15.41	193.1	21.40	193.2	12.59
203.5	21.27	203.4	11.14	203.4	14.59	203.4	20.31	203.4	11.99
213.4	20.29	213.4	10.59	213.3	13.89	213.3	19.36	213.3	11.48
223.2	19.40	223.2	10.09	223.2	13.25	223.2	18.53	223.2	10.95
233.0	18.60	233.0	9.649	233.0	12.66	233.0	17.73	233.1	10.47
243.1	17.82	242.0	9.276	243.1	12.11	243.1	16.99	243.2	10.04
253.0	17.15	253.0	8.847	253.0	11.62	253.0	16.33	253.1	9.629
263.3	16.49	263.2	8.486	263.2	11.15	263.2	15.70	263.3	9.290
273.3	15.87	273.3	8.171	273.3	10.72	273.3	15.12		
283.2	15.34	283.3	7.890	283.3	10.34	283.3	14.59	283.3	8.582
293.3	14.81	293.3	7.593	293.3	9.961	293.3	14.09	293.3	8.370
303.2	14.32	303.2	7.352	303.3	9.623	303.3	13.64	303.3	8.079



TABLE C4

## Static Field Magnetic Susceptibility Data

Mn[X <sub>2</sub> PX <sub>2</sub> ] <sub>2</sub> Complexes					
X =	CH <sub>3</sub>	C <sub>6</sub> H <sub>5</sub>	F	CF <sub>3</sub>	
T(°K)	X <sub>g</sub> x10 <sup>6</sup>	T(°K)	X <sub>g</sub> x10 <sup>6</sup>	T(°K)	X <sub>g</sub> x10 <sup>6</sup>
94.8	138.8	88.5	71.64	88.5	110.4
103.4	128.6				
113.7	117.5	123.4	54.33	88.5	110.4
123.3	109.3				
133.3	101.6				
143.2	95.07				
153.4	89.19	153.4	44.79	123.2	86.54
163.1	84.28				
173.2	79.62				
183.2	75.53	183.2	38.14	123.3	86.54
193.2	71.95				
203.4	68.53				
213.3	65.59	213.3	33.12	123.3	86.54
223.2	62.86				
233.0	60.36				
243.2	58.06	243.2	29.25	123.3	86.54
253.0	55.91				
263.2	53.88				
273.3	52.02	273.4	26.21	123.3	86.54
283.3	50.27				
293.3	48.68				
303.3	47.22	303.3	23.74	123.3	86.54



TABLE C5

## Static Field Magnetic Susceptibility Data

 $\text{Fe}[\text{S}_2\text{P}]_2 \text{ Complexes}$ 

$\text{Fe}[\text{S}_2\text{P}(\text{C}_6\text{H}_5)_2]_3$	X = CH <sub>3</sub>	C <sub>6</sub> H <sub>5</sub>	F	CF <sub>3</sub>
T(°K)	$\chi_g \times 10^6$	T(°K)	$\chi_g \times 10^6$	T(°K)
87.4	61.76	87.3	107.8	88.9
113.6	47.46	123.2	78.72	54.77
133.2	40.40	123.3	42.75	87.1
153.3	35.18	153.4	64.07	94.00
173.1	31.10	153.4	64.07	133.3
183.2	183.2	153.4	35.75	69.25
193.2	27.81	183.3	30.74	133.2
213.4	25.19	213.3	46.91	56.09
233.0	23.05	213.3	26.94	173.2
243.2	243.2	243.1	24.01	56.09
253.0	21.23	243.1	24.01	36.15
263.1	20.35	243.1	24.01	213.3
273.3	19.63	273.4	37.04	46.88
293.3	18.26	303.3	33.53	303.3
313.2	17.08	303.3	19.73	34.21
				303.3
				21.67



TABLE C6

## Static Field Magnetic Susceptibility Data

Co[S <sub>2</sub> PX <sub>2</sub> ] <sub>2</sub> Complexes									
X =	CH <sub>3</sub>	C <sub>6</sub> H <sub>5</sub>	OCH <sub>2</sub> H <sub>5</sub>	F	CF <sub>3</sub>				
T(°K)	X <sub>g</sub> × 10 <sup>6</sup>	T(°K)	X <sub>g</sub> × 10 <sup>6</sup>	T(°K)	X <sub>g</sub> × 10 <sup>6</sup>	T(°K)	X <sub>g</sub> × 10 <sup>6</sup>	T(°K)	X <sub>g</sub> × 10 <sup>6</sup>
94.8	75.12	94.7	38.69	88.9	26.93	88.3	73.54	88.4	41.70
112.8	64.56	103.4	35.28	113.7	24.81				
122.5	59.96	113.8	32.34						
132.6	55.50	135.1	27.66	133.4	23.46	133.3	52.65	133.1	30.14
142.5	51.96	143.3	26.22						
142.7	48.72	153.4	24.65	153.4	22.20				
162.7	46.01	162.8	23.30						
172.9	43.53	173.2	21.98	173.2	20.99	173.2	41.93	173.2	24.11
182.9	41.35	183.2	20.85						
192.9	39.37	193.2	19.85	193.2	19.91				
202.9	37.63	203.4	18.92						
212.8	36.03	213.3	18.04	213.3	18.88	213.3	35.00	213.3	20.14
223.0	34.47	223.2	17.28						
232.7	33.18	233.0	16.58	233.0	17.97				
243.2	31.87	243.2	15.90						
253.1	30.72	253.1	15.30	253.0	17.21				
263.0	29.70	263.2	14.75						
273.2	28.68	273.3	14.22	273.3	16.47				
283.5	27.71	283.3	13.75						
293.5	26.90	293.3	13.30	293.3	15.81				
303.3	26.07	303.3	12.89						
				303.3	25.88	303.3	14.87		
				313.3	15.22				



TABLE C7

## Static Field Magnetic Susceptibility Data

CoOS <sub>3</sub> P <sub>2</sub> (CH <sub>3</sub> ) <sub>4</sub>		HgCo(NCS) <sub>4</sub>		Zn[S <sub>2</sub> PX <sub>2</sub> ] <sub>2</sub> Complexes	
T (°K)	X <sub>g</sub> x10 <sup>6</sup>	T (°K)	X <sub>g</sub> x10 <sup>6</sup>	X	X <sub>M</sub> x10 <sup>6</sup> (complex) <sup>a</sup>
89.5	77.60	95.6	49.11	CH <sub>3</sub>	-127
		103.3	45.50		- 57
113.5	62.81	113.8	41.32	C <sub>6</sub> H <sub>5</sub>	-316
		123.4	38.16		-151
133.2	54.52	133.3	35.35	OC <sub>2</sub> H <sub>5</sub>	-154
		143.3	32.92		- 70
153.4	48.17	153.4	30.78	F	-145
		162.8	29.00		- 66
173.1	43.29	173.2	27.28	CF <sub>3</sub>	-222
		183.2	25.84		-104
193.2	39.33	193.2	24.54		
		203.4	23.32		
213.3	36.06	213.7	22.27		
		223.2	21.33		
233.0	33.41	233.1	20.45		
		243.2	19.60		
253.0	31.10	253.0	18.85		
		263.2	18.13		
273.3	29.11	273.3	17.53		
		283.3	16.92		
293.3	27.42	293.3	16.36		
		303.3	15.87		
313.3	25.92				

<sup>a</sup> Measured at 25°C.<sup>b</sup> Ligand ion susceptibilities were calculated using

$$\chi_A(Zn^{++}) = -13.5 \times 10^{-6}$$



**APPENDIX D**



## APPENDIX D

Description of the Faraday Balance Assembly

Detailed accounts of the Faraday method for determining the magnetic susceptibilities of materials are given in references 62 and 63. The basic operational principle of the Faraday technique is that a constant product of the magnetic field and field gradient  $\left(H \cdot \frac{\partial H}{\partial s}\right)$  over a sample reduces the dimensional restrictions and removes the uniform packing requirements for the sample<sup>62,63</sup>. The magnet tracks, balance table, and cryostat tube with auxiliary apparatus were designed by Dr. R. G. Cavell, who also assembled the remaining components. The system was made operational by the author.

The magnetic field was generated by a Varian model V-4004 four-inch electromagnet system (V-2300A power supply and V-2301 current regulator) using specially tapered pole caps. The magnet was mounted on a wheeled carriage riding on rails leading under a table bearing the Cahn electrobalance (model G) used to measure the forces induced by the application of the magnetic field to the sample. The "field-on" and "field-off" conditions were achieved by moving the electromagnet "in" and "out" along the rails.

The electrobalance was modified for remote operation such that the balance chamber was relocated under a bell jar resting on an aluminum adapter plate bolted down onto a pump plate. Holes were drilled through the base of the balance chamber housing below the beam loops each of which were alignable with the central hole of the pump plate via the adapter plate. A brass tube fitted with a



tapered joint was bolted to the bottom of the pump plate. Samples were suspended from the balance beam by a fine quartz fiber leading through the brass tube and into either a glass envelope for ambient temperature measurements or the cryostat tube both fitted with tapered joints mating with the brass joint.

Temperatures were varied by immersing the cryostat tube in liquid nitrogen and varying the heating current applied to wires wrapped about an inner copper tube in which the sample is suspended. A "proportional heating" system maintained a given heating rate and temperature. Variable temperature measurements were carried out under an atmosphere of helium. The liquid nitrogen level in the dewer containing the cryostat tube was maintained by an automatic feed system.

In the initial stages of this work, air stable samples were loaded into open quartz buckets while air sensitive materials were sealed into quartz bulbs (~5 mm in diameter). The latter technique suffered the disadvantages of extreme heating near the sample and a large uncertainty in the diamagnetic correction to be applied to the sample container. Subsequently it was discovered that medical polyethylene tubing (Intramedic Cat. No. PE 240 (7451), i.d. 0.066 inches, o.d. 0.095 inches) would snugly (air tightly) fit over 2 mm quartz tubing. Thus, the necks of bulbs blown from 2 mm quartz tubing could be cut quite short (~2 mm) and the polyethylene tubing could be worked to give caps with suspension hooks pulled to length. Samples of even extreme air sensitivity were found to keep without apparent change for periods up to several days in such containers.



Diamagnetic corrections for the polyethylene capped bulbs were obtained prior to loading and the robustness of the containers proved a distinct advantage for handling in glove bags.

During the course of variable temperature magnetic measurements, temperatures were obtained from the voltages generated by a copper-constantan thermocouple junction placed a few millimeters below the sample in the cryostat tube and referenced to a junction in an ice-water slurry.



**APPENDIX E**



APPENDIX E  
COMPUTER PROGRAM LISTINGS

```

C.....***** MAINLINE MASPEC *****
C
C      PROGRAMMED BY E.D. DAY, JUNE 15, 1971
C
C      MASPEC IS WRITTEN SPECIFICALLY FOR THE ANALYSIS OF THE MASS SPECTRA
C      OF DITHIOPHOSPHINIC ACID DERIVATIVES WITH HOMOGENEOUS SUBSTITUENT
C      GROUPS.  THE INPUT PEAK MASSES ARE ASSIGNED ACCORDING TO THE CONSTI-
C      TUENT METAL, SULFER, PHOSPHORUS, AND SUBSTITUENT GROUPS FOUND TO BE
C      IN MASS AGREEMENT.  THE INPUT SPECTRUM IS SCALED SUCH THAT ANY ARBI-
C      TRARY PEAK IS SET TO 100.  FRAGMENTATION OF THE SUBSTITUENT GROUP IS
C      ALLOWED ONLY FOR CF3.
C
C....INPUT AND FORMATS
C
C      ALL NUMBERS ARE TO BE INTEGERS AND RIGHT JUSTIFIED IN THEIR FIELD.
C      ALL MASSES ARE TO BE EXPRESSED IN ATOMIC MASS UNITS (A.M.U.).
C
C      CARD 1
C
C      TITLE (9A4, COLS. 1-36) = SAMPLE FORMULA, SOURCE TEMP., ETC,
C      TMETAL (1A4, COLS. 37-40) = LEFT JUSTIFIED LETTERS OF METAL SYM-
C          BOL (IF ANY) ALWAYS FOLLOWED IMMEDIATELY BY AN APOSTROPHE.
C      MW    (15, COLS. 41-45) = MOLECULAR MASS.
C      MM    (15, COLS. 46-50) = MASS OF METAL GROUP.
C      MX    (15, COLS. 51-55) = MASS OF SINGLE SUBSTITUENT GROUP.
C      NP    (15, COLS. 56-60) = NUMBER OF INPUT PEAK MASSES.
C      IMAX (15, COLS. 61-65) = PEAK HEIGHT TO BE SCALED TO 100.
C      NP    (13, COLS. 66-68) = NUMBER OF PHOSPHORUS ATOMS/MOLECULE.
C      NS    (13, COLS. 69-71) = NUMBER OF SULFUR ATOMS/MOLECULE.
C      NX    (13, COLS. 72-74) = NUMBER OF SUBSTITUENT GROUPS/MOLECULE
C      METAL (13, COLS. 75-77) = OXO-MOLECULE/LIGAND CHECK PARAMETER
C          (BLANK IMPLIES METAL PRESENT, ASSIGNS PEAKS UNASSIGNED TO
C          METAL CONTAINING SPECIES TO LIGAND PEAKS; NUMBER<0 IMPLIES
C          NO METAL IN MOLECULE; NUMBER>0 IMPLIES MONO-OXO-MOLECULE).
C
C      CARDS 2 ON: N=0,1,...,9
C      TYPE   (1A1, COL. 10*N+1) = BLANK IMPLIES USUAL PEAK; '*' IMPLIES
C          METASTABLE PEAK, NO ASSIGNMENT; 'N' IMPLIES PEAK NOT OF EX-
C          PECTED ISOTOPIC PATTERN, PEAK ASSIGNED TO LIGAND SPECIES.
C      PEAK   (14, COLS. 10*N+2-10*N+5) = PEAK MASS.
C      INTENS (15, COLS. 10*N+6-10*(N+1)) = PEAK INTENSITY.
C
C.....***** DECLARATION STATEMENTS.
C
C      IMPLICIT INTEGER*2 (I-N)
C      LOGICAL*1 PATERN(150), ASSIGN(150), TM(150), F(150), CF2(150), OV(150),
C      IVO, FM, CM, SS, PS, XS, SX, PX, SO, PG, XO, TO, CHECK
C      DIMENSION TYPE(150), FMT(14), PART(11), TITLE(9)
C      DATA FMT(1)/'(1X,'/,FMT(2)/'A1,I')/,FMT(3)/'4,19'/,FMT(4)/',8X,'/,
C      1PART/'  '' ','  ''0'',','''S''',','''P''',','''Y''',',''11 ''',''  ''',
C      2'  '' ','''CF'',''2'') ''','''F'''/,B/IN//,A/1 ''/,C/*'/
C      INTEGER*2 PEAK(150), INTENS(150), P(200), S(150), X(150), FRAG
C      READ INPUT.  START OF EACH DATA SET.

```



```

1 READ(5,900)TITLE,TMETAL,MW,MM,MX,NPEAK,I MAX,NP,NS,NX,METAL,
  I(TYPE(I),PEAK(I),INTENS(I),I=1,NPEAK)
C WRITE CARD 1.
  WRITE(6,901) TITLE,MW,MM,MX,NPEAK,I MAX,NP,NS,NX,METAL
C INITIALIZE PARAMETERS.
  MASS = MW
  Q = A
  CHECK = METAL.LT.0
  VO = METAL.GT.0
  FM = .FALSE.
  CM = FM
  II = 1
  IF(MX.EQ.69) II=II+2
  IF(VO) II=II+1
  IF(II.EQ.4) II=6
  D = 100.0/I MAX
C SCALE SPECTRUM.
  DO 2 I=1,NPEAK
    ASSIGN(I) = .FALSE.
  2 INTENS(I) = D*INTENS(I)+0.5
  NPP = NP+1
  NSP = NS+1
  NXp = NX+1
C ENTER FRAGMENTATION LCCPS.
  3 II = II-1
C CHECK PEAK TYPE.
  DO 4 I=1,NPEAK
    4 PATERN(I) = TYPE(I).EQ.Q
C ADD PHOSPHORUS ATOMS TO FRAGMENT LOST.
  N = -31
  DO 9 I=1,NPP
C ADD SULFUR ATOMS TO FRAGMENT LOST.
  N = N+31
  M = N-32
  DO 8 J=1,NSP
C ADD SUBSTITUENT GROUPS TO FRAGMENT LOST.
  M = M+32
  FRAG = M-MX
  DO 7 K=1,NXP
    FRAG = FRAG+MX
    ICN = MASS-FRAG
C SEARCH SPECTRUM FOR RESIDUAL FRAGMENT.
  DO 6 L=1,NPEAK
    IF(ION-PEAK(L)) 6,5,7
  5 IF(.NOT.PATFRN(L).AND..NOT.CHECK.OR.TYPE(L).EQ.C.OR.ASSIGN(L))
    GO TO 7
    X(L) = NXp-K
    IF(FM.AND.X(L).EQ.C.OR.CM.AND.X(L).EQ.NX) GO TO 7
    P(L) = NPP-I
    S(L) = NSP-J
    OV(L) = VO
    TM(L) = .NOT.CHECK
    CF2(L) = CM
    F(L) = FM
    ASSIGN(L) = .TRUE.

```



```

IF(.NOT.FM.OR.P(L).EQ.NP.OR.X(L)+1.LE.2*P(L)) GO TO 7
P(L) = P(L)+1
CF2(L) = .TRUE.
F(L) = .FALSE.
GO TO 7
6 CONTINUE
7 CONTINUE
8 CONTINUE
9 CONTINUE
IF(II.GT.0) GO TO 10
IF(CHFCK) GO TO 13
C CHECK UNASSIGNED PEAKS FOR LIGAND (DI-LIGAND) FRAGMENTS.
CHECK = .TRUE.
FM = .FALSE.
IF(MX.EQ.69) II=3
MW = 2*(MW-MM)/NP
MASS = MW
NSP = (NS+NS)/NP+1
NXP = (NX+NX)/NP+1
NPP = NXP/2+1
Q = B
GO TO 3
10 IF(II.EQ.5.CR.II.EQ.2) GO TO 11
IF(II.EQ.4.CR.CM.AND.II.EQ.1) GO TO 12
C SUBTRACT OXYGEN ATOM FROM OXO-MOLECULE.
MW = MW-16
MASS = MW
VO = .FALSE.
FM = .FALSE.
GO TO 3
C SUBTRACT CF2 GROUP FROM CF3 SUBSTITUTED MOLECULE.
11 MASS = MW+19
CM = .TRUE.
GO TO 3
C SUBTRACT FLUORINE ATOM FROM CF3 SUBSTITUTED MOLECULE.
12 MASS = MW-19
FM = .TRUE.
CM = .FALSE.
GO TO 3
C WRITE ASSIGNMENTS.
13 DO 19 I=1,NPEAK
IF(ASSIGN(I)) GO TO 14
WRITE(6,9C2) TYPE(I),PEAK(I),INTENS(I)
GO TO 19
14 FMT(5) = PART(1)
IF(OV(I)) FMT(5)=PART(2)
FMT(6) = PART(1)
IF(TM(I)) FMT(6)=TMETAL
FMT(7) = PART(3)
FMT(8) = PART(6)
FMT(9) = PART(4)
FMT(10) = PART(6)
FMT(11) = PART(5)
FMT(12) = PART(6)
FMT(13) = PART(8)

```



```

FMT(14) = PART(7)
IF(.NOT.F(I)) GO TO 15
X(I) = X(I)-1
FMT(13) = PART(9)
FMT(14) = PART(10)
15 IF(CF2(I)) FMT(13)=PART(11)
SS = S(I).GT.0
PS = P(I).GT.0
XS = X(I).GT.0
IF(SS.AND.PS.AND.XS) GO TO 18
SX = SS.AND.XS.AND..NOT.PS
PX = PS.AND.XS.AND..NOT.SS
SO = SS.AND..NOT.PS.AND..NOT.XS
PC = PS.AND..NOT.SS.AND..NOT.XS
XC = XS.AND..NOT.SS.AND..NOT.PS
TO = .NOT.SS.AND..NOT.PS.AND..NOT.XS
IF(SX.OR.XO) GO TO 16
IF(PX) GO TO 17
FMT(11) = PART(8)
FMT(12) = PART(8)
IF(SO.OR.TO) GO TO 16
IF(PO) GO TO 17
WRITE(6,FMT) TYPE(I),PEAK(I),INTENS(I),S(I),P(I)
GO TO 19
16 FMT(9) = PART(8)
FMT(10) = PART(8)
IF(SO) WRITE(6,FMT) TYPE(I),PEAK(I),INTENS(I),S(I)
IF(SX) WRITE(6,FMT) TYPE(I),PEAK(I),INTENS(I),S(I),X(I)
IF(SO.OR.SX) GO TO 19
17 FMT(7) = PART(8)
FMT(8) = PART(8)
IF(TO) WRITE(6,FMT) TYPE(I),PEAK(I),INTENS(I)
IF(XO) WRITE(6,FMT) TYPE(I),PEAK(I),INTENS(I),X(I)
IF(PO) WRITE(6,FMT) TYPE(I),PEAK(I),INTENS(I),P(I)
IF(PX) WRITE(6,FMT) TYPE(I),PEAK(I),INTENS(I),P(I),X(I)
GO TO 19
18 WRITE(6,FMT) TYPE(I),PEAK(I),INTENS(I),S(I),P(I),X(I)
19 CONTINUE
GO TO 1
20 WRITE(6,903)
STOP
900 FORMAT(10A4,5I5,4I3/(8(A1,I4,I5)))
901 FORMAT('1',5X,'MASS SPECTRAL ASSIGNMENTS'//',5X,'-----
1-----'//1X,9A4//' MOLECULAR MASS =',I5,' A.M.U.'//' MASS OF MET
2AL GROUP PER MOLECULE =',I5,' A.M.U.'//' MASS OF SUBSTITUENT GROUP
3IN MOLECULE =', I5,' A.M.U.'//' NUMBER OF PEAKS INPUT FOR ANALYSIS
4=',I5//' PEAK INTENSITY SCALED TO 100 =',I5//' NUMBER OF PHOSPHORUS
5ATOMS PER MOLECULE =',I3//' NUMBER OF SULFER ATOMS PER MOLECULE =',
6I3//' NUMBER OF SUBSTITUENT GROUPS =',I3//' OXO-MOLECULE/LIGAND PEAK
7 CHECK PARAMETER =',I3//' M/E      INTENSITY      ASSIGNMENT'
8' (A.M.U.) (SCALED)'//')
902 FORMAT(1X,A1,I4,I9,10X,'---')
903 FORMAT('1',6X,'**** END OF EXECUTION ****')
END

```



C MAINLINE MAGSUS C  
C MAGNETIC SUSCEPTIBILITY MARK III (MAGSUS - D)

C PROGRAM IS WRITTEN FOR A CARRIAGE LENGTH OF 120 CHARACTERS, HENCE,  
C MAY EITHER BE SUBMITTED TO COMPUTER AS A DECK OR USED AT A TERMINAL.

C BASICALLY, PROGRAM CALCULATES GRAM, MOLAR AND RECIPROCAL MOLAR SUS-  
C CEPTIBILITIES, AND SUBJECTS RESULTS OF RECIPROCAL MOLAR SUSCEPTIBIL-  
C ITY, AS A FUNCTION OF KELVIN TEMPERATURE, TO A LINEAR LEAST SQUARES  
C ANALYSIS.

C A GRAPH OF RECIPROCAL MOLAR SUSCEPTIBILITY VERSUS KELVIN TEMPERATURE  
C IS PLCTTED, INCLUDING THE OBSERVED POINTS AND LEAST SQUARES LINE  
C (FROM WHICH THE WEISS CONSTANT IS EVALUATED). PLOTS ARE DONE ON AN  
C 11.0 X 8.5 INCH AREA WITH CENTIMETER SCALE, I.E., 2.54 DIVISIONS/IN.

C PROGRAMMED BY E.D.DAY, R.G.CAVELL, AND L.F.DOTY.

C LATEST RFVISION: 26 AUGUST 1970

C...NOTE:

- (1) A MAXIMUM OF 40 DATA POINTS CAN BE PROCESSED WITHOUT REDIMEN-  
C SIONING ARRAYS, HOWEVER, ANY NUMBER OF DATA SETS MAY BE PROCESSED  
C BY STACKING DATA DECKS. ABOUT 0.05 MINUTES AND 70 LINES ARE REQU-  
C IRED PER DATA SET.
- (2) PLOTTER REQUIREMENTS ARE 6 MINUTES AND 30 FEET OF TAPE PER  
C DATA SET, UNLESS A DUMMY TAPE CARD IS USED AND PLOTTING FOREGONE.
- (3) SAMPLE FORCE DATA ARE EXPECTED TO BE OBTAINED IN HELIUM  
C ATMOSPHERE.

C...DEFINITION OF SYMBOLS:

(WEIGHTS IN MILLIGRAMS, FORCES IN UNIFORM ARBITRARY UNITS, THERMO-  
C COUPLE VOLTAGES (REFERENCE JUNCTION AT ICE-POINT) IN MILLIVOLTS,  
C TEMPERATURES IN KELVINS, AND SUSCEPTIBILITIES IN CGS UNITS)

C INPLT QUANTITIES:

NAME	= NAME OF SAMPLE COMPOUND, S, OF UNKNOWN SUSCEPTIBILITY (LEFT JUSTIFIED, SINCE WILL APPEAR ON PLOT.)
FW	= FORMULA WEIGHT OF S.
DICOR	= DIAMAGNETIC COMPONENT OF MOLAR SUSCEPTIBILITY OF S.
WS	= WEIGHT OF S.
WBS	= WEIGHT OF CONTAINER (BUCKET OR BULB) OF S.
LF(I)	= CBS. FORCE (UNCORRECTED FOR CONTAINER COMPONENT) ON S
V(I)	= VOLTAGE GENERATED BY THERMOCOUPLE WITH PROBE JUNCTION AT TEMPERATURE OF POINT 0.6 CM BELOW S, UNDER OPERAT- ING CONDITIONS(LIQUID NITROGEN COOLING).
WSTC	= WEIGHT OF STANDARD SAMPLE, STD, USED TO DETERMINE THE FIELD.
WBSTD	= WEIGHT OF CONTAINER (BUCKET OR BULB) OF STD.
UFSTD	= FORCE ON STANDARD IN AIR, CORRECTED FOR CONTAINER.
VSTD	= VOLTAGE GENERATED BY THERMOCOUPLE WITH PROBE JUNCTION AT TEMPERATURE OF STD UNDER ROOM CONDITIONS.
N	= NUMBER OF DATA POINTS.
C1	= FORCE ON SAMPLE CONTAINER IN AIR AT ROOM TEMPERATURE. C1 IS LATER MODIFIED INTERNALLY.
C2	= COEFFICIENT OF TEMPERATURE DEPENDENT TERM IN EXPRES- SION FOR CONTAINER FORCE COMPONENT.



```
C      FB = C1+C2*WB*FSTD/(WSTD*XGSTD)*T
```

```
C INPUT DATA FORMATS:
```

```
C CARD 1
C      NAME    (12A4, COLS. 1-48)
C      FW      (F12.0, COLS. 49-60)
C      DICOR   (E15.0, COLS. 66-75)
C      N       (15,   COLS. 76-80)
C CARD 2
C      WSTD    (F10.0, COLS. 1-10)
C      WBSTD   (F10.0, COLS. 11-20)
C      VSTD    (F10.0, COLS. 31-40)
C      UFSTD   (F10.0, COLS. 21-30)
C      WS      (F10.0, COLS. 41-50)
C      WBS     (F10.0, COLS. 51-60)
C      C1      (F10.0, COLS. 61-70)
C      C2      (E10.0, COLS. 71-80)
C CARDS 3 TO (N+2)
C      V(I)    (F10.0, COLS. 1-10)
C      UF(I)   (F10.0, COLS. 11-20)
```

```
C CALCULATED QUANTITIES:
```

```
C      TSTD     = KELVIN TEMPERATURE OF STD.
C      XGSTD   = GRAM SUSCEPTIBILITY OF STD AT TEMPERATURE OF STD.
C      T(I)     = KELVIN TEMPERATURE OF S.
C      CF(I)    = CORRECTED FORCE ON S.
C      XG(I)    = GRAM SUSCEPTIBILITY OF S.
C      XM(I)    = CORRECTED MOLAR SUSCEPTIBILITY OF S.
C      Z(I)     = RECIPROCAL OF XM(I).
C      XMLSC   = LEAST SQUARES MOLAR SUSCEPTIBILITY.
C      DEV     = DEVIATION OF XM(I) FROM LEAST SQUARES VALUE.
C      DEVINV  = DEVIATION OF Z(I) FROM LEAST SQUARES LINE.
C      A       = SLOPE OF LEAST SQUARES LINE IN PLOT OF Z(I) VERSUS T.
C      B       = ABSCISSAL INTERCEPT OF ABOVE LEAST SQUARES LINE.
C      BM     = EFFECTIVE MAGNETIC MOMENT IN BOHR MAGNETONS.
C      WEISS   = WEISS CONSTANT OF S.
C      SDX     = STANDARD DEVIATION OF POINTS.
C      SDA     = STANDARD DEVIATION OF A.
C      SDB     = STANDARD DEVIATION OF B.
C      SDW     = STANDARD DEVIATION OF WEISS CONSTANT.
```

```
C.....REAL DATA(2048),T(42),Z(42),UF(40),V(40),CF(40),XG(40),XM(40),
1NAME(12)
```

```
TST(V) = 273.1566+V*(25.68936-V*6.474187E-01)
XGST(T) = 5.385363E-05+T*(-2.028206E-07+T*2.564732E-10)
```

```
TS(V) = 272.7185+V*(25.95607+V*(-7.512920E-1+V*(-1.655135E-2+V*
1(-3.249633E-2+V*(1.051523E-2+V*(4.735817E-3+V*9.258457E-4))))))
```

```
C TST(V), XGST(T), AND TS(V) ARE VALID FOR TEMPERATURE RANGES 279-317 K,
C 253-303 K, AND 85-323 K, RESPECTIVELY.
```

```
C INITIALIZE PLOTS.
```

```
FUN(K) = ((K/3)*3)/K
CALL FLOTS(DATA(1),8192)
NPLCT = 0
```



```

C ***** START OF EACH PROBLEM *****
C
1 READ(5,900,END=8) NAME,FW,DICOR,N,WSTD,WBSTD,VSTD,UFSTD,WS,WBS,C1,
1C2,(V(I),UF(I),I=1,N)
C CALCULATE KELVIN TEMPERATURE OF STANDARD SAMPLE.
TSTD = TST(VSTD+0.009)
C CALCULATE GRAM-SUSCEPTIBILITY OF STANDARD SAMPLE.
XGSTD = XGST(TSTD)
C WRITE INPUT CONSTANTS.
WRITE(6,901) NAME,WSTD,FW,WBSTD,DICOR,UFSTD,WS,VSTD,WBS,TSTD,C1,
1XGSTD,C2
C CALCULATE KELVIN TEMPERATURES, SUSCEPTIBILITIES, AND LEAST SQUARES
C LINEAR PARAMETERS.
P = WSTD*XGSTD/(1.0018*UFSTD)
C2 = C2*WBS/P
C1 = C.957*C1-C2*TSTD
R = P/WS
SUMX = 0.0
SUMY = 0.0
SUMX2 = 0.0
SUMXY = 0.0
TMIN = 1.0E50
TMAX = 0.0
YMIN = 1.0E50
YMAX = 0.0
DO 2 I=1,N
X = TS(V(I))
IF(X.LT.TMIN) TMIN=X
IF(X.GT.TMAX) TMAX=X
CF(I) = UF(I)-(C1+C2*X)
XG(I) = CF(I)*R
XM(I) = XG(I)*FW-DICOR
Y = 1.0/XM(I)
IF(Y.LT.YMIN) YMIN=Y
IF(Y.GT.YMAX) YMAX=Y
SUMX = SUMX+X
SUMY = SUMY+Y
SUMX2 = SUMX2+X*X
SUMXY = SUMXY+X*Y
T(I) = X
2 Z(I) = Y
D = N*SUMX2-SUMX*SUMX
A = (N*SUMXY-SUMX*SUMY)/D
E = (SUMX2*SUMY-SUMX*SUMXY)/D
C CALCULATE WEISS CONSTANT.
WEISS = -B/A
C CALCULATE MAGNETIC MOMENT.
BM = 2.828/SQRT(A)
C CALCULATE RESIDUALS AND SUM OF SQUARED RESIDUALS.
SUM = 0.0
DO 3 I=1,N
Y = A*T(I)+B
XMLSG = 1.0/Y
DEV = XMLSG-XM(I)
DEINV = Y-Z(I)
SUM = SUM+DEINV*DEINV
3 WRITE(6,902) I,T(I),Y,Z(I),DEINV,XMLSG,XM(I),DEV,XG(I),CF(I),
1UF(I),V(I)
C CALCULATE STANDARD DEVIATIONS.
SDX = SQRT(SUM/(N-2))

```



```

      SDA = SDX*SQRT(N/D)
      SDB = SDX*SQRT(SUMX2/D)
      SCW = APS(WFISS*(ABS(SCB/B)+SDA/A))
      SCM = BM*SDA/A
      WRITE(6,903) A,SDA,B,SDB,SDX,WFISS,SCW,BM,SCM
C
C ***** PLOT DATA *****
C
C DRAW BOUNDING RECTANGLE ABCUT PLOT.
      CALL PLOT(0.0,8.5,2)
      CALL PLOT(11.0,8.5,2)
      CALL PLOT(11.0,0.0,2)
      CALL PLOT(0.0,0.0,2)
C DRAW X-AXIS.
      CALL SCALE(1.05*(TMAX-TMIN),7.5,UPD,SCT,D,TMIN,NT)
      CALL PLOT(0.75,0.25,3)
      DC = 7.75-NT*D
      CALL SYMBOL(0.75,DC,0.06,13,90.0,-2)
      DO 4 I=1,NT
      4 CALL SYMBOL(0.75,DC+I*D,0.06,13,90.0,-2)
      CALL PLCT(0.75,7.75,-3)
      CALL PLCT(0.00,0.03,2)
C LABEL X-AXIS.
      CALL SYMBOL(-0.55,-2.70,0.15,'TEMPERATURE ( K )',-90.0,16)
      CALL NUMBER(-0.45,-4.40,0.08,0.0,-90.0,-1)
C NUMBER X-AXIS.
      DO 5 I=1,NT,2
      X = I*UPD+TMIN
      ND = ALOG10(X)+1.0
      5 CALL NUMBER(-0.18,0.05*ND-0.02-I*D,0.12,X,-90.0,-1)
C DRAW MAGNETIC PARAMETERS.
      CALL SYMBOL(1.25,-4.00,0.25,34,-90.0,-1)
      CALL SYMBOL(1.17,-4.14,0.09,'EFF',-90.0,3)
      CALL SYMBOL(1.25,-4.32,0.14,' = ',-90.0,3)
      CALL NUMBER(1.25,-4.68,0.14,BM,-90.0,2)
      CALL SYMBOL(1.25,-5.28,0.14,23,-90.0,-1)
      CALL NUMBER(1.25,-5.40,0.14,SDM,-90.0,3)
      CALL SYMBOL(1.25,-6.12,0.15,'B.M.',-90.0,4)
      CALL SYMBOL(2.00,-4.00,0.18,112,-90.0,-1)
      CALL SYMBOL(2.09,-4.05,0.07,13,0.0,-1)
      CALL SYMBOL(2.00,-4.12,0.14,' = ',-90.0,3)
      CALL NUMBER(2.00,-4.42,0.14,WFISS,-90.0,1)
      D = -4.42-0.12*(INT(ALOG10(ABS(WFISS)))+3.0+(WFISS-ABS(WFISS))/1(WFISS+WFISS))
      CALL SYMBOL(2.00,D-.14,0.14,23,-90.0,-1)
      CALL NUMBER(2.00,D-.26,0.14,SDW,-90.0,1)
      D = D-0.12*(INT(ALOG10(SDW))+3.0)-0.25
      CALL SYMBOL(2.00,D-.21,0.15,'K',-90.0,1)
      CALL NUMBER(2.10,D-.11,0.08,0.0,-90.0,-1)
C DRAW LEAST SQUARES LINE.
      FMIN = A*TMIN+B
      YMIN = AMIN1(YMIN,FMIN)
      CALL SCALE(1.05*(YMAX-YMIN),9.0,UPD,SCY,D,YMIN,NT)
      CALL PLOT((A*TMAX+B-YMIN)/SCY,(TMIN-TMAX)/SCT,3)
      CALL PLOT((FMIN-YMIN)/SCY,0.0,2)
C DRAW Y-AXIS.
      CALL PLOT(0.0,0.0,3)
      DC 6 I=1,NT
      6 CALL SYMBOL(I*D,0.0,0.06,13,0.0,-2)
      CALL PLOT(9.0,0.0,2)

```



```

C NUMBER Y-AXIS.
DO 7 I=1,NT,2
Y = I*UPD+YMIN
ND = 2-INT(ALCG10(Y))
7 CALL NUMBER(I*D-0.06,0.34-0.10*ND,0.12,Y,-90.0,-1)
C LABEL Y-AXIS.
DD = (D+D)*INT(0.25*NT+0.5)
CALL SYMBOL(DD+0.10,0.67,0.16,113,-90.0,-1)
CALL SYMBOL(DD+0.02,0.63,0.17,97,-90.0,-1)
CALL SYMBOL(DD-0.13,0.56,0.40,39,-90.0,-1)
CALL SYMBOL(DD+0.10,0.37,0.09,'CORR',-90.0,4)
CALL SYMBOL(DD-0.21,0.29,0.12,84,-90.0,-1)
C DRAW TITLE.
CALL SYMBOL(9.50,0.25,0.184,NAME,-90.0,48)
C DRAW EMPIRICAL POINTS.
N1 = N+1
N2 = N+2
T(N1) = TMIN
T(N2) = -SCT
Z(N1) = YMIN
Z(N2) = SCY
CALL LINE(Z,T,N,1,-1,3)
C SET ORIGIN OF NEXT PLOT.
NPLOT = NPLOT+1
CALL PLOT(12.0*FUN(NPLOT)-0.75,9.5*(MOD(NPLOT,3)-FUN(NPLOT+1))
1*(-1)**(NPLOT/3)-7.75,-3)
GC TO 1
C
C ***** END OF DATA SET PROCESSING *****
C
C CLOSE TAPE.
8 CALL FLUT(0.0,0.0,999)
C WRITE TOTAL PLOT COUNT.
WRITE(6,904) NPLOT
STOP
900 FORMAT(12A4,F12.0,E15.0,15/7F10.0,E10.0/(2F10.0))
901 FORMAT('1',16X,'TEMPERATURE DEPENDENT MAGNETIC DATA FOR ',12A4/
1'CONSTANTS:'//13X,'WEIGHT OF STANDARD      = ',F6.3,' MG',16X,
2'FORMULA WT. OF SAMPLE   = ',F7.3,' GM/MOLE'//'0',12X,'WT. OF STD.
3CONTAINER = ',F6.3,' MG',16X,'MOLAR DIAMAGNETIC SUSC. = ',3PE10.1
4,' (CGS UNITS)'//'0',12X,'OBSERVED FORCE ON STD. = ',0PF6.4,
5,' (ARE. UNITS)      WEIGHT OF SAMPLE',8X,'= ',F6.3,' MG'//'0',12X,
6'VSTD',19X,'= ',F5.3,' MV',17X,'WT. OF SAMPLE CONTAINER = ',F6.3,
7' MG'//'0',12X,'TEMPERATURE OF STD.     = ',F5.1,' K',18X,'C1 =',
8FE.4// 13X, 'GRAM SUSC. OF STD     = ',2PE9.2,' (CGS UNITS) C2
9 =',1PE11.3//'0 N   T(K) 1.0/XM(LSQ) 1.0/XM(OBS) DEVIATION X
AM(LSQ)    XM(OBS)    DEVIATION XG(OBS)    SAMPLE SAMPLE V(M
BV)'//38X,'(LSQ-CBS)',27X,'(LSQ-CBS)',16X,'FCRCE FORCE'//98X,'COR.')
C (UNCOR.)')
902 FORMAT(I3,F8.1,2(1PE12.3),E12.2,2E12.3,E12.2,E12.3,0PF9.4,F8.4,
1F8.3)
903 FCRMAT(/'ODATA FIT TO EQUATION: 1.0/XM = ('',F7.4,'+',F6.4,'')*T +
1 ('',F8.4,'+',F6.4,'') :      STD. DEV. OF 1.0/XM(LSQ) = ',F6.3//'+',
24IX,'+',22X,'+',//'CHEISS CCNSTANT = ',F8.3,'+',F5.3,' K ;      EFFE
3CTIVE MAGNETIC MOMENT = ',F4.2,'+',F5.3,' B.M. ;',14X,'.....DATA
4FLGTTED.'//'+',26X,'+',47X,'+')
904 FORMAT('TOTAL NUMBER OF GRAPHS PLOTTED IN THIS RUN IS:',I4)
END

```



```
SUBROUTINE SCALE(RANGE,DIM,UPD,UPI,D,ORIGIN,NT)
D = ALOG10(RANGE/(2.5*DIM))
ID = D
IF(D.LT.0.0) ID = ID-1
D = 10.0**(D-ID)
UPD = 1.0
IF(D.LE.1.0) GO TO 1
UPD = 2.0
IF(D.LE.2.0) GO TO 1
UPD = 4.0
IF(D.LE.4.0) GO TO 1
UPD = 5
IF(D.LE.5.0) GO TO 1
UPD = 8.0
IF(D.LE.8.0) GO TO 1
UPD = 10.0
1 DPI = 2.5*D/UPD
UPD = UPD*10.0**ID
UPI = DPI*UPD
D = UPD/UPI
NT = DIM*DPI
P = 10.0*INT(CRIGIN/10.0)
ORIGIN = P+UPD*INT((ORIGIN-P)/UPD)
RETURN
END
```



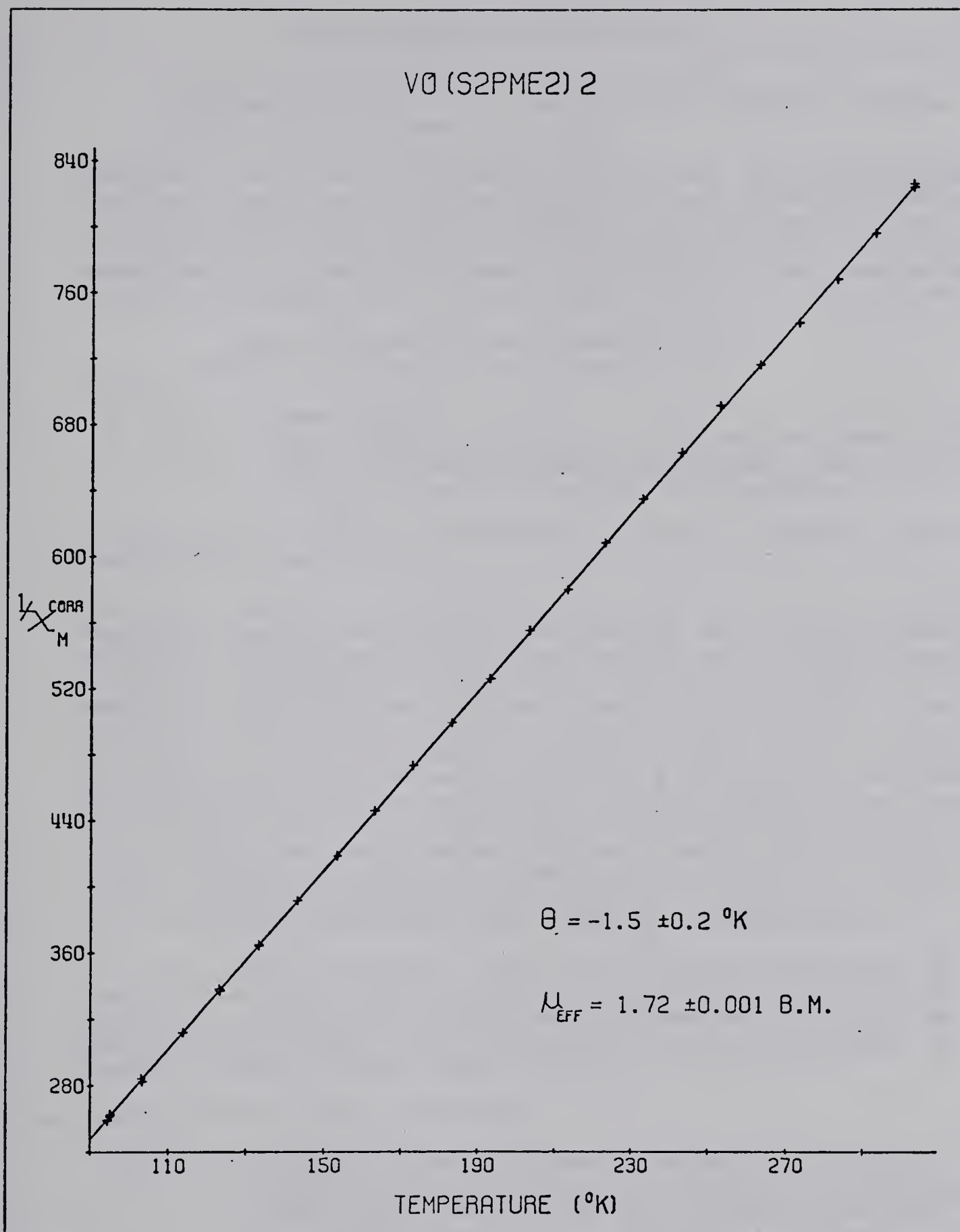


FIGURE E1: Sample Calcomp plot from MAGSUS.



## \*\*\*\*\* MAINLINE BIGAUSS \*\*\*\*\*

PROGRAMMED BY E.D. DAY, D.R. MCTAVISH, AND R.G. CAVELL.  
LATEST REVISION: APRIL 20, 1970

PROGRAM IS WRITTEN SPECIFICALLY FOR ANALYSIS OF ELECTRONIC SPECTRA WITH WAVELENGTH AND ABSORPANCE SCALES, USING A GAUSSIAN APPROXIMATION TO RESOLVE THE SPECTRAL ENVELOPE INTO COMPONENT PEAKS. TO ALLOW FOR ASYMMETRY, DIFFERENT WIDTH PARAMETERS ARE DETERMINED FOR EACH SIDE OF A COMPONENT PEAK, THE RESULTANT PEAKS HERE BEING CALLED 'BI-GAUSSIANS'. THE FUNCTIONAL FORM OF A BI-GAUSSIAN IS

$$Y(X) = A * \exp(-B(-)*(X-C)^2), X < C,$$

$$\text{AND } Y(X) = A * \exp(-B(+)*(X-C)^2), X > C,$$

WHERE

A = PEAK HEIGHT.  
B(+), B(-) = PEAK WIDTH PARAMETERS OF HIGH AND LOW ENERGY SIDES OF PEAK. DISTANCE BETWEEN INFLECTION POINTS =  $\sqrt{2/B}$ .  
C = POSITION (ENERGY SCALE) OF PEAK MAXIMUM.

(SEE: C.K. JOERGENSEN, 'ABSORPTION SPECTRA AND CHEMICAL BONDING IN COMPLEXES', CHAPTER 6.)

THE INPUT SPECTRUM (A DISCRETE FUNCTION OF WAVELENGTH) IS FIRST BASELINE ADJUSTED AND THEN IS TRANSFORMED TO A DISCRETE FUNCTION OF ENERGY (WAVENUMBERS), INTERPOLATING VALUES AT 0.1 KILOKAYSER (1000/CM) INTERVALS BY FINDING THE INTERPOLATED POINTS ON A CUBIC SEGMENT PASSING THROUGH THE FOUR NEAREST INPUT POINTS. ANALYSIS PROCEEDS ITERATIVELY, RESOLVING THE SPECTRUM INTO THE INPUT NUMBER OF PEAKS. AFTER A PRELIMINARY SEARCH IN WHICH INITIAL PARAMETERS ARE OBTAINED FOR THE PEAKS AND THE PEAKS CALCULATED FROM THESE PARAMETERS SUCCESSIVELY SUBTRACTED FROM THE SPECTRUM, AN ITERATION NOW CONSISTS OF ADDING, SEARCHING FOR, AND SUBTRACTING EACH CALCULATED PEAK FROM THE RESIDUAL SPECTRUM. AFTER EACH ITERATION, THE SUM OF SQUARED RESIDUALS IS COMPARED WITH A TOLERANCE FACTOR. IF, AFTER A REASONABLE NUMBER OF ITERATIONS, THE SUM HAS NOT APPROACHED A MINIMUM, PROCESSING OF THE DATA SET IS TERMINATED.

ALL INPUT DATA IS OUTPUT AS WELL AS CALCULATED PARAMETERS OF COMPONENTS, INCLUDING THE OSCILLATOR STRENGTHS OF THE RESPECTIVE TRANSITIONS. PLOTTING INFORMATION (CALCOMP PLOTTER) FOR THE INPUT SPECTRUM, THE FINAL SET OF COMPONENTS AND THEIR ENVELOPE, IS OPTIONALLY CALCULATED AND STORED ON TAPE.

## .....DEFINITION OF INPUT QUANTITIES:

NAME = SPECTRUM IDENTIFICATION (COMPOUND NAME, ETC.).  
M = GUESS AS TO NUMBER OF PEAKS COMPOSING THE SPECTRUM.  
COUNT SHOULD INCLUDE ANY TAIL RISING TO THE UV. IF M  
IS NEGATIVE, SPECTRUM IS ANALYZED IN TERMS OF SIMPLE  
GAUSSIAN PEAKS. IF FIELD LEFT BLANK, ANALYSIS IS  
FOREGONE BUT RESCALED INPUT SPECTRUM MAY BE PLOTTED.  
IBASLN = -1, BASELINE DATA MUST BE SUPPLIED JUST AFTER THE



C FIRST SPECTRUM DATA SET FOR WHICH IT IS TO BE USED.  
 C = 0 (FIELD LEFT BLANK), BASELINE IS ASSUMED TO BE CON-  
 C STANT WITH VALUE STORED IN 'ZERO'.  
 C = +1, BASELINE PREVIOUSLY DEFINED WILL BE USED TO ADJUST  
 C SPECTRUM.  
 C ISEE = 1, THE RESULTS OF EACH ITERATION ARE DISPLAYED. IF  
 C FIELD LEFT BLANK, ONLY FINAL RESULTS ARE PRESENTED.  
 C = -1, IN INITIAL SEARCH FOR BI-GAUSSIAN PEAKS, PEAK'S  
 C NARROWEST SIDE IS REFLECTED ACROSS LINE OF MAXIMUM.  
 C = 2, RESULTS IN REFLECTION AND DISPLAY.  
 C IPLOT = 1, PLOTTING DATA ARE CALCULATED FOR BOTH 'OBSERVED'  
 C (I.E. RESCALED INPUT SPECTRUM) AND CALCULATED SPECTRA.  
 C = 2, PLOTTING DATA ARE CALCULATED FOR OBSERVED SPECTRUM.  
 C = 3, PLOTTING DATA FOR CALCULATED SPECTRUM ARE CALCULAT-  
 C ED. AN ENERGY SCALE OF 1.0 KK/CM IS USED UNLESS ANY  
 C OF THE ABOVE PARAMETERS ARE NEGATIVE, WHEREWITH AN  
 C ENERGY SCALE OF 0.5 KK/CM IS USED. IF ABS(IPLOT) > 3,  
 C THEN THE NUMBER OF ITERATIONS = ABS(IPLOT).  
 C WMIN,WMAX = LOWEST AND HIGHEST WAVELENGTH READINGS ON SPECTRUM,  
 C RESPECTIVELY. DEFINE WAVELENGTH RANGE (ANGSTROMS).  
 C WINT = CONSTANT WAVELENGTH INTERVAL AT WHICH ABSORPTION VAL-  
 C UES ARE TAKEN. NO. OF DATA POINTS=(WMAX-WMIN)/WINT+1.  
 C ZERO = BASELINE READING AT WMAX. IF NOT SPECIFIED (I.E.,  
 C FIELD LEFT BLANK) OR SET TO 0.0, R.H.S. ABSORBANCE  
 C READING TAKEN AS ZERO OF SPECTRUM.  
 C ERR = ESTIMATED UNCERTAINTY ASSOCIATED WITH ABSORBANCE READ-  
 C INGS FROM THE CHART SPECTRUM (ABOUT 0.002). ERR MAY  
 C BE USED CAUTIOUSLY AS A 'RESOLUTION' PARAMETER AS IT  
 C DETERMINES THE AMOUNT OF 'RIPPLE' IGNORED.  
 C TAU = RELATIVE TOLERANCE TEST VALUE FOR DIFFERENCE BETWEEN  
 C SUCESSIVE SUMS OF SQUARED RESIDUALS. A REASONABLE  
 C VALUE IS BETWEEN 0.001 AND 0.0001.  
 C PATH = PATH LENGTH OF CELL (CENTIMETERS), OTHERWISE SET TO 1.  
 C CONC = MOLARITY OF SOLUTION, OR 1.0E0 IF NOT KNOWN.  
 C AP(I) = I-TH ABSORBANCE READING (INITIALLY).  
 C BNAME = BASELINE IDENTIFICATION, DATE, ETC.  
 C BMIN = LOWEST WAVELENGTH READING ON BASELINE.  
 C NB = NUMBER OF BASELINE DATA POINTS (SEE CALCULATION IN  
 C DEFINITION OF WINT).  
 C B(I) = I-TH BASELINE ABSORBANCE READING. RANGE (ANGSTROMS)  
 C MUST INCLUDE ALL RANGES FOR WHICH BASELINE IS TO BE  
 C USED, AND ALSO, 'WINT' MUST BE THE SAME.

## C.....INPUT FORMATS:

## C CARD 1

C NAME (15A4, COLS. 1-60)  
 C M,IEASLN,ISEE,IPLOT  
 C (4I5, COLS. N- N+4, N=61,...,76, RESPECTIVELY)

## C CARD 2

C WMIN,WMAX,WINT,ZERO,ERR,TAU,PATH  
 C (7F10.0, COLS. N- N+9, N=1,11,...,61, RESPECTIVELY)  
 C CONC (E10.0, COLS. 71-80)



C  
C        CARDS 3 TO END OF DATA SET (IN ORDER OF INCREASING WAVELENGTH)  
C  
C        AP(I)    (8F10.0, COLS. N- N+9, N=1,11,...,71, RESPECTIVELY)  
C  
C        BASELINE DATA (IMMEDIATELY FOLLOWING FIRST APPLICABLE DATA SET):  
C  
C        CARD 1  
C  
C        BNAME    (15A4,    COLS. 1-60)  
C        BMIN     (F10.0,    COLS. 61-70)  
C        NB       (15,      COLS. 71-75)  
C  
C        CARDS 2 TO END OF BASELINE (IN ORDER OF INCREASING WAVELENGTH)  
C  
C        B(I)     (8F10.0, COLS. N- N+9, N=1,11,...,71, RESPECTIVELY)  
C  
C.....NOTE: (1) UP TO 500 DATA POINTS AND 10 PEAKS PER DATA SET CAN BE  
C        ACCOMMODATED WITHOUT REDIMENSIONING ARRAYS. ANY NUMBER OF  
C        DATA SETS CAN BE PROCESSED BY STACKING DATA DECKS. APPROX-  
C        IMATELY, 0.2 MINUTES, 200 LINES (OR 300\*M LINES, IF ISEE=1),  
C        PER DATA SET ANALYZED, AND 15 FEET OF TAPE, AND 0.07 HOURS  
C        PLOTTING TIME PER GRAPH, ARE REQUIRED. LAST BLOCK ADDRESS  
C        ON TAPE IS 2\*(NUMBER OF GRAPHS)+1.  
C        (2) 'RESCALED SPECTRUM' OUTPUT HAS BEEN BASELINE ADJUSTED.  
C        (3) PEAKS ARE SEARCHED FOR IN ORDER OF DECREASING HEIGHT.  
C        THERE MUST BE NO PARTIAL PEAKS ON IR SIDE OF SPECTRUM.  
C        (4) HALF WIDTH (H.W.) OF ANY PEAK = (H.W.(-) + H.W.(+))/2.  
C        PARAMETERS CALCULATED FOR PEAKS LACKING A MAXIMUM IN THE  
C        GIVEN SPECTRAL RANGE ARE NOT TO BE BELIEVED, THEY HAVE BEEN  
C        CALCULATED TO OBTAIN A GOOD FIT IN THE EXPLICIT RANGE ONLY.  
C        (5) ALL GRAPHS ARE 8.5 INCHES HIGH WITH A 7.0 INCH ORDINATE.  
C        THE WIDTH IS SET TO THE LARGER OF 11.0 INCHES AND ABSISSA  
C        PLUS 0.8 INCHES. FOR CONVENIENT COMPARISON OF SPECTRA,  
C        TWO FIXED ENERGY SCALES (IPLOT) ARE PROVIDED. HOWEVER, THE  
C        ABSORPTIVITY SCALE IS DATA DEPENDENT. GRAPHS ARE PLOTTED IN  
C        COLUMNS OF 3, ACROSS THE WIDTH OF PLOTTER CHART PAPER. TAPE  
C        CONTROL CARDS (SEE CALCOMP USER'S MANUAL, PAGE 37) MAY BE  
C        OMITTED ONLY IF NO PLOTTING IS REQUESTED FOR ANY DATA SET.  
C  
C.....  
C  
COMMON A(500),X(500),N,N1,PH(10),PML(10),PWR(10),PC(10),MAX(10),  
1T(10),ERR,ASYN,REFINE,BACK,TCL,RFLECT  
REAL SPACE(2048),A\*8,XP(1000),AP(1000),B(500),NAME(15),BNAME(15),  
1YDIM/7.0/,WIDEST/0.0/  
LOGICAL BASLN,T,ASYM,NOSEE,NOPLT,TWICE,TAI1,REFINE,BACK,RFLECT  
FUN(K) = ((K/3)\*3)/K  
XPLOT(W,K) = (W+1.0)\*FUN(K)-0.5  
YPLOT(K) = 9.5\*(MOD(K,3)-FUN(K+1))\*(-1)\*\*(K/3)-0.5  
CALL PLOTS(SPACE(1),8192)  
NPLT = 0  
C  
C.....START OF EACH PROBLEM.....  
C  
1 READ(5,900,END=25) NAME,M,IBASLN,ISEE,IPLOT,WMIN,WMAX,WINT,ZERO.



```

1FRR,TAU,PATH,CCNC
  NO = (WMAX-WMIN)/WINT+1.5
  READ(5,901) (AP(I+500),I=1,NO)
C CALCULATION OF WAVELENGTHS AND CORRESPONDING KK VALUES.
  IF(ZERO.EQ.0.0) ZERO=AP(NO+500)
  NB = NO
  BMIN = WMIN
  BASLN = IBASLN.NE.0
  IF(IBASLN.LT.0) READ(5,902) BNAME,BMIN,NB,(B(I),I=1,NB)
  K = (WMIN-BMIN)/WINT+0.5
  D = ZERO
  IF(BASLN) D=D-B(NO+K)
  DO 2 I=1,NB
  P = (I-1)*WINT
  IF(I.GT.NO) GO TO 2
  IP = I+500
  XP(I) = WMIN+P
  XP(IP) = 100000.0/XP(I)
C BASELINE ADJUST SPECTRUM.
  AP(I) = AP(IP)-D
  IF(BASLN) AP(I)=AP(I)-B(I+K)
  2 X(I) = BMIN+P
C WRITE BASELINE SPECTRUM.
  IF(IBASLN.LT.0)CALL WRYTE(BNAME,NB,170,X,B,' BASELINE SPECTRUM ')
C WRITE INPUT SPECTRUM.
  CALL WRYTE(NAME,NO,130,XP,AF,' INPUT SPECTRUM ')
C FIT SPFCTRM TO WAVENUMBER SCALE WITH POINTS AT 0.1 KK INTERVALS.
  LMT = 10.0*XP(501)
  XO = LMT/10.0
  N = LMT-INT(10.0*XP(NO+499))
  N1 = N-1
  YMAX = AP(1)
  DO 5 I=1,N
  XI = XO-0.1*(I-1)
  WI = 100000.0/XI
  J = (WI-XP(1))/WINT+1.5
  IF(ABS(XP(500+J)-XI).LT.0.0001) GO TO 3
  K = 2
  IF(WI-XP(J).GT.0.0) K=1
  K = J-K
  IF(K.LT.1) K=1
  KP = K+1
  A1 = AP(K)
  A2 = AP(KP)
  D21 = A2-A1
  D32 = AP(K+2)-A2
  DX = WI-XP(KP)
  TERM = AP(K+3)-3.0*D32-A1
C USE QUADRATIC SEGMENT BETWEEN FIRST TWO POINTS.
  CUBIC = 0.0
  IF(ABS(TERM).GT.1.0E-6.AND.WI.GT.XP(2)) CUBIC=((DX-WINT)/(3.0*WINT
  1))*TERM
  AI = A1+((DX+WINT)/WINT)*(D21+(DX/(WINT+WINT))*(D32-D21+CUBIC))
  GO TO 4
  3 AI = AP(J)
  4 IF(AI.GT.YMAX) YMAX=AI

```



```

AP(500+I) = AI
5 X(I) = XI
C WRITE POINTS ON RESCALED SPECTRUM.
CALL WRYTE(NAME,N,160,X,AP,' RESCALED SPECTRUM ')
C WRITE CONTROL CONSTANTS.
WRITE(6,903) NAME,WMIN,WMAX,N,WINT,CONC,NO,PATH,N,ZERO,ISEE,ERR,
IIPLOT,TAU,[BASLN,X(1),X(N)
C CONVERT ABSORBEDANCES TO ABSORPTIVITIES.
C = PATH*CONC
IY = -ALOG10(YMAX/C)
IY2 = IY+IY
C = 10.0**IY/C
YMAX = C*YMAX
TOL = ERR*YMAX*10.0**(-INT(ALOG10(ERR))-2)
ERR = C*ERR
DO 6 I=1,N
6 A(I) = C*AP(500+I)
C CALCULATE PLOT CONTROL PARAMETERS.
NOPLLOT = IPLOT.EQ.0
IF(NOPLLOT) GO TO 8
XMAX = INT(XP(501))+1
XMIN = INT(XP(NO+500))
SCX = 2.54
TWICE = IPLOT.LT.0
IF(TWICE) SCX=1.27
IPLOT = IAES(IPLOT)
XDIM = (XMAX-XMIN)/SCX
WIDE = AMAX1(XDIM+0.8,11.0)
XD = XDIM/2.0
C SET VERTICAL SCALE FOR PLOTS.
YD = 2.54
DY = ALOG10(YMAX/(YD*YDIM))
IDY = DY
IF(DY.LT.0.0) IDY=IDY-1
DYP = 10.0**((DY-FLOAT(IDY)))
YM = 1.0
IF(DYP.LE.1.0) GO TO 7
YM = 2.0
IF(DYP.LE.2.0) GO TO 7
YM = 4.0
IF(DYP.LE.4.0) GO TO 7
YM = 5.0
IF(DYP.LE.5.0) GO TO 7
YM = 8.0
IF(DYP.LE.8.0) GO TO 7
YM = 10.0
7 YD = YD*DYP/YM
SCY = YD*YM*10.0**IDY
C WRITE PLOT PARAMETERS.
WRITE(6,904) SCX,YD,XDIM,YDIM
C PLOT RESCALED INPUT SPECTRUM.
CALL INTRP(XP,AP,NP,0,0.0,0)
NP1 = NP+1
NP2 = NP1+1
XP(NP1) = XMIN
XP(NP2) = SCX

```



```

AP(NP1) = 0.0
AP(NP2) = SCY
IF(IPLOT.GT.2) GO TO 8
CALL AXES(NAME,WIDE,XDIM,XMIN,SCY,YD,IY,TWICE)
CALL SYMBOL(XD-1.50,7.1,0.2,'OBSERVED SPECTRUM',0.0,17)
CALL LINE(XP,AP,NP,1,0,0)
NPLOT = NPLOT+1
IF(WIDE.GT.WIDEST.OR.MOD(NPLOT,3).EQ.1) WIDEST=WIDE
CALL PLOT(XPLOT(WIDEST,NPLCT),YPLCT(NPLOT),-3)
IF(IPLOT.EQ.2.OR.M.EQ.0) GO TO 24
C
C.....GAUSSIAN ANALYSIS.....
C
C FIND PEAKS.
8 NOSEE = ISEE.LE.0
ASYM = M.GT.0
REFINE = .FALSE.
RFLECT = ISEE.LT.0.OR.ISEE.GT.1
M = IAABS(M)
DO 10 I=1,M
CALL PKFD(I)
IF(.NOT.T(I).OR..NOT.BACK) GO TO 10
AA = PH(I)
BB = PWL(I)
CC = PC(I)
C = 0.0
K = 4
DO 9 J=5,N1
D = -BB*(X(J)-CC)**2
IF(D.LT.-40.0) GO TO 9
D = SNGL(A(J))-AA*EXP(D)
IF(D.GT.C) GO TO 9
C = D
K = J
9 CONTINUE
IF(C.GT.-TOL) GO TO 10
D = CC-X(1)
PWL(I) = ALOG(SNGL(DABS(A(1)/A(K))))/((X(1)-X(K))*(CC-X(K)+D))
PWR(I) = PWL(I)
PH(I) = SNGL(A(1))*EXP(PWL(I)*D*D)
10 CALL PKOP(I,-1)
C REFINE FIT OF PEAKS.
REFINE = .TRUE.
RFLECT = .FALSE.
SS = 1.0E50
ITER = IPLOT
IF(IPLOT.LE.3) ITER=10*M
DO 14 I=1,ITER
K = I
DO 11 J=1,M
CALL PKOP(J,1)
CALL PKFD(J)
11 CALL PKOP(J,-1)
C CALCULATE SUM OF SQUARED RESIDUALS.
S = 0.0
DO 12 J=1,N

```



```

12 S = S+(SNGL(A(J)))**2
    IF(NOUSEE) GO TO 13
    WRITE(6,905) I,IY2,S,IY,(J,PH(J),PWR(J),PWL(J),PC(J),J=1,M)
    WRITE(6,906) IY,(A(J),J=1,N)
13 IF(ABS(S-SS)/S.LT.TAU.AND.I.GT.M) GO TO 15
14 SS = S
    WRITE(6,907)
15 WRITE(6,908) K,IY2,S,IY,(A(J),J=1,N)
C PLOT PEAKS, THEIR ENVELOPE, AND RECORD PARAMETERS.
    IF(NOPLOT.OR.IPLOT.EQ.2) GO TO 20
    DO 16 I=1,N
16 A(I) = 0.000
    DO 17 I=1,M
17 CALL PKOP(I,1)
    CALL INTRP(XP,AP,NP,0,0.0,0)
    CALL AXES(NAME,WIDE,XDIM,XMIN,SCY,YD,IY,TWICE)
    CALL SYMBOL(XD-1.6,7.3,0.2,'CALCULATED SPECTRUM',0.0,19)
    XX = 1.25
    IF(ASYM) GO TO 18
    CALL SYMBCL(XD-1.23,7.1,0.12,'( GAUSSIAN COMPONENTS)',0.0,24)
    XX = 1.10
    GO TO 19
18 CALL SYMBOL(XD-1.38,7.1,0.12,'( BI-GAUSSIAN COMPONENTS)',0.0,27)
19 CALL NUMBER(XD-XX,7.1,0.12,FLOAT(M),0.0,-1)
    CALL LINE(XP,AP,NP,1,0,0)
20 WRITE(6,909) IY
    DO 23 I=1,M
        H = PH(I)
        C = PC(I)
C CONVERT WIDTH PARAMETERS TO HALF-WIDTHS.
        BL = SQRT(0.693147/PWL(I))
        BR = SQRT(0.693147/PWR(I))
C PLOT COMPONENTS.
        IF(NOPLOT.OR.IPLOT.EQ.2) GO TO 22
        DO 21 J=1,N
21 A(J) = 0.000
        CALL PKOP(I,1)
        CALL INTRP(XP,AP,NP,MAX(I),BL,1)
        NP1 = NP+1
        NP2 = NP1+1
        XP(NP1) = XMIN
        XP(NP2) = SCX
        AP(NP1) = 0.0
        AP(NP2) = SCY
        CALL LINE(XP,AP,NP,1,0,0)
C CALCULATE OSCILLATOR STRENGTHS.
22 STRNTH = 4.59745*10.0**(-6-IY)*H*(BL+BR)
23 WRITE(6,910) I,H,BR,BL,C,STRNTH
    IF(NOPLOT) GO TO 1
    NPLCT = NPLCT+1
    IF(WIDE.GT.WIDEST.OR.MOD(NPLCT,3).EQ.1) WIDEST=WIDE
    CALL PLOT(XPLOT(WIDEST,NPLCT),YPLOT(NPLCT),-3)
24 WRITE(6,911)
    GO TO 1
C END PLOTS.
25 IF(NPLCT.EQ.0) GO TO 26

```



```

CALL PLOT(0.0,0.0,999)
WRITE(6,912) NPLOT
STOP
26 WRITE(6,913)
STOP
900 FORMAT(1EA4.4I5/7F10.0,E10.0)
901 FORMAT(8F10.0)
902 FORMAT(15A4,F10.0,I5/(8F10.0))
903 FORMAT('1',40X,'*** SPECTRAL ANALYSIS - PROGRAM BIGAUSS ***'//32X,
115A4//59X,'* * * *'//12X,'WAVELENGTH RANGE =',F8.1,' TO',F8.1,' AN
2GSTROMS',4X,'INPUT NUMBER OF COMPONENTS =',I3//12X,'INTERVAL OF DI
3GITIZATION =',F6.1,' ANGSTROMS',9X,'CONCENTRATION OF SOLUTION =',
41PE10.3,' MOLES/LITRE'//12X,'NUMBER OF INPUT DATA POINTS =',.0PI4,
518X,'CELL PATH LENGTH =',F6.2,' CENTIMETERS'//12X,'NUMBER OF POINT
6S ON RESCALED SPECTRUM =',I4.8X,'ZERO =',F8.3,' ABSORBANCE UNITS'/
7//12X,'DISPLAY OPTION PARAMETER, ISEE =',I2.17X,'UNCERTAINTY IN ABS
8ORBANCE READINGS =',F6.3,' ABSORBANCE UNITS'//12X,'PLOT OPTION PAR
9AMETER, IPLOT =',I3.18X,'RELATIVE TOLERANCE PARAMETER, TAU =',F8.5
X//12X,'BASELINE OPTION PARAMETER =',I3.21X,'WAVENUMBER RANGE =',
XF6.2,' TO',F6.2,' KILOKAYSERS')
904 FORMAT(/12X,'ENERGY SCALE =',F6.2,' KILOKAYSERS/INCH',14X,'ABSORPT
1IVITY SCALE =',F6.2,' DIVISIONS/INCH'//12X,'ENERGY AXIS LENGTH =',
2F6.2,' INCHES',18X,'ABSORPTIVITY AXIS LENGTH =',F6.2,' INCHES')
905 FORMAT('CITERATION',I3,: SUM OF SQUARED RESIDUALS X10('',I3,'') ='
1,E14.7/6X,'PEAK',11X,'HEIGHT X10('',I2,''),7X,'WIDTH PARAMETER
2 WIDTH PARAMETER POSITION OF MAXIMUM'//21X,'(ABSORPTIVITY)',13
3X,'(-)',19X,'(+)',14X,'(KILOKAYSERS)'//(I9,3F22.4,F21.2))
906 FORMAT(' RESIDUALS X10('',I2,''):'//(10F12.4))
907 FCRMAT(///' CONVERGENCE OF SUMS OF SQUARED RESIDUALS WAS NOT ACHIE
1VED WITHIN THE LIMITATIONS SET BY M AND TAU. IF A CHECK OF THE IN
2PUT DATA'/' REVEALS NO ERRORS, RE-EVALUATE M AND TAU.'')
908 FORMAT(/12X,'NUMBER OF ITERATIONS =',I4.25X,'SUM OF SQUARED RESIDU
1ALS X10('',I2,'') =',E14.7//0 THE RESIDUALS X10('',I2,'') AT THE PO
2INTS ON THE RESCALED INPUT SPECTRUM ARE:'//(10F12.4))
909 FORMAT(/48X,'CALCULATED PEAK PARAMETERS'/'+',47X,'_
1_____''//6X,'PEAK',11X,'HEIGHT X10('',I2,''),8X,'HALF-WIDTH ('
2-). HALF-WIDTH (+) POSITION OF MAXIMUM OSCILLATOR STR
3ENGTH'//21X,'(ABSORPTIVITY)',8X,'(KILOKAYSERS)',9X,'(KILOKAYSERS)',
49X,'(KILOKAYSERS)'//)
910 FORMAT(I9,3F22.4,F21.2,1PE25.3)
911 FORMAT(/'OPLOTTING INSTRUCTIONS CALCULATED.')
912 FORMAT('1DATA FOR A TOTAL OF',I3,' PLOTS WERE CALCULATED.'//41X,
1'***** END OF EXECUTION *****')
913 FORMAT('1',40X,'***** END OF EXECUTION *****')
END

```



```

SUBROUTINE PKFD(KK)
C
C PKFD DETERMINES PEAK PARAMETERS.
C
COMMON A(500),X(500),N,N1,PH(10),PWL(10),PWR(10),PC(10),MAX(10),
1T(10),ERR,ASYM,REFINE,BACK,TOL,RFLECT
REAL A*8
LOGICAL T,ASYM,TAIL,IR,DOWN,Y,TKK,FREE,REFINE,BACK,RFLECT
C LOCATE PEAK CENTER AND MAXIMUM.
FREE = ASYM
N = 2
1 IMAX = M
M = M+1
DO 2 I=M,N1
IF(A(I).GT.A(IMAX)) IMAX=I
2 CONTINUE
IM = IMAX-1
AIM = A(IM)
AI = A(IMAX)
AIP = A(IMAX+1)
R = AIM-AI
Q = 50.0*(AIP-AI+R)
TAIL = Q.GE.0.0
T(KK) = AIM.GT.AI
TKK = A(3).GT.0.000
IF(T(KK).AND.TKK) GO TO 14
IF(T(KK).AND..NOT.TKK) GO TO 1
TKK = .FALSE.
P = 10.0*R-Q*(X(IMAX)+X(IM))
C = -P/(Q+G)
H = AI+(C-X(IMAX))*(P+Q*(C+X(IMAX)))
CUT = 0.20*H
MAX(KK) = IMAX
C CALCULATE APPROXIMATE HEIGHT OF INFLECTION POINTS.
HI = 0.65*H
C DETERMINE PEAK WIDTH PARAMETERS.
3 II = IMAX
JJ = N1
K = 1
L = 1
IR = .TRUE.
GO TO 5
4 II = 1
JJ = IM
K = -1
L = IMAX
IR = .FALSE.
5 G = A(IMAX-K)
R = AI
N = II
SDMAX = -1.0E50
DO 6 I=II,JJ

```



```

J = I
F = Q
G = R
R = A(K*I+L)
C TEST FOR NATURAL DECAY.
IF(R.LT.CUT) GO TO 7
IF(REFINE) GO TO 6
SD = P-O-O+R
Y = Q.LT.HI
C TEST FOR SHOULDER.
DOWN = SD.LT.-ERR
IF(.NOT.TAIL.AND.(SD.GT.ERR.AND..NOT.Y.OR.DOWN.AND.Y).OR.TAIL.AND.
DOWN.OR.G.LE.R) GO TO 7
6 CCNTINUE
7 BACK = R.GT.CUT.AND.R.NE.SNGL(A(1))
IF(.NOT.IR.AND.J.LT.S.OR.IR.AND.J.LT.IMAX+S) FREE=.FALSE.
IF(TKK) GO TO 15
IF(IR) GO TO 8
IF(BACK) J=J-J/2+1
NM = IMAX-J+1
IF(FREE) NM=IMAX
GO TO 9
8 NM = IMAX
IF(BACK) J=J-(J-IMAX)/2+1
NN = J
IF(.NOT.FREE) GO TO 4
9 E = 0.0
S = 0.0
DO 10 I=NM,NN
D = (X(I)-C)**2
B = B+ALCG(H/SNGL(A(I)))
10 S = S+D
IF(.NOT.IR) GO TO 11
PWR(KK) = B/S
GO TO 4
11 PWL(KK) = B/S
IF(FREE.AND..NOT.RFLCT) GO TO 13
IF(FREE.AND.RFLCT) PWL(KK)=AMAX1(PWL(KK),PWR(KK))
12 PWR(KK) = PWL(KK)
MAX(KK) = N
13 PH(KK) = H
FC(KK) = C
RETURN
C DETERMINE PARAMETERS OF PEAK FITTING TAIL.
14 B = 50.0*ALOG(SNGL(A(2)*A(2)/(A(1)*A(3))))
IF(B.LT.0.05) B=0.05
C = X(1)+(5.0*ALOG(SNGL(A(1)/A(2)))/B-0.05)
H = A(3)*EXP(B*(X(3)-C)**2)
FI = 0.6*H
CUT = 0.20*A(1)
GO TO 3
15 IF(BACK) J=J-J/3
C LEAST SQUARES FIT TAIL FOR HEIGHT AND WIDTH.
SUMP = 0.0
SUMQ = 0.0
SUMP2 = 0.0

```



```

SUMPQ = 0.0
DO 16 I=1,J
  F = -(X(I)-C)**2
  Q = ALOG(SNGL(A(I)))
  SUMP = SUMP+P
  SUMQ = SUMQ+Q
  SUMP2 = SUMP2+P*P
16 SUMPQ = SUMPQ+P*Q
D = J*SUMP2-SUMP*SUMP
PWL(KK) = (J*SUMPQ-SUMP*SUMQ)/D
H = EXP((SUMP2*SUMQ-SUMP*SUMPQ)/D)
IF(REFINE) GO TO 12
IF(SNGL(A(1))-H*EXP(-PWL(KK)*(X(1)-C)**2).LT.TOL) GO TO 12
PACK = .TRUE.
GO TO 15
END

```

```

SUBROUTINE PKOP(KK,L)
C
C PKCP ADDS (L.GE.0) OR SUBTRACTS (L.LT.0) THE KK-TH PEAK (AS FOUND BY
C PKFD) FROM THE SPECTRUM EXISTING AT TIME OF CALL.
C
COMMON A(500),X(500),N,N1,PH(10),PWL(10),PWR(10),PC(10),MAX(10)
REAL A*8
C PEAK PARAMETERS OBTAINED FROM PKFD.
  AA = PH(KK)
  IF(L.LT.0) AA=-AA
  EB = PWL(KK)
  CC = PC(KK)
  N1 = 1
  N2 = MAX(KK)
1 DO 2 I=M1,M2
  E = -EB*(X(I)-CC)**2
  IF(E.LT.-40.0) GO TO 2
  A(I) = A(I)+AA*EXP(E)
2 CONTINUE
  IF(M2.EQ.N) RETURN
  M1 = M2+1
  N2 = N
  EB = PWR(KK)
  GO TO 1
END

```



```
SUBROUTINE WRYTE(NAME,NN,JJ,X,Y,TITLE)
C
C WRYTE PRESENTS SPECTRUM DATA POINTS IN ROWS OF TEN.
C
      REAL X(1),Y(1),NAME(15),TITLE(5)
      LOGICAL INPUT,BASLN
      INPUT = JJ.EQ.130
      BASLN = JJ.EQ.170
      LL = 500*(130/JJ)
      MM = 500*(160/JJ)
      JM = JJ-1
      N = (NN+JM)/JJ
      DO 2 I=1,N
      WRITE(6,900) NAME,TITLE,I,N
      KK = JJ*I
      J = KK-JM
      IF(KK.GE.NN) KK=NN
1   K = J+9
      IF(K.GT.KK) K=KK
      WRITE(6,901) (Y(L+MM),L=J,K)
      IF(INPUT.OR.BASLN) WRITE(6,902) (X(L),L=J,K)
      IF(.NOT.BASLN) WRITE(6,903) (X(L+LL),L=J,K)
      J = J+10
      IF(K.LT.KK) GO TO 1
2   CCNTINUE
      RETURN
900 FORMAT('1',40X,'*** SPECTRAL ANALYSIS - PROGRAM BIGAUSS ***',//32X
     1,15A4//59X,'* * * *'//53X,5A4,41X,'PAGE',I2,' OF ',I2//59X,'* * * *
     2')
901 FORMAT('0 AESCRBANCE ',10F11.3)
902 FORMAT(' ANGSTROMS ',10F11.2)
903 FORMAT(' KILOKAYSERS',10F11.2)
END
```



```
SUBROUTINE INTRP(XP,AP,NP,MAX,B,J)
```

```
C
C INTRP DOUBLES THE POINT DENSITY OF THE WHOLE SPECTRUM (EXCEPT AT THE
C ENDS), OR BETWEEN THE INFLECTION POINTS OF THE I-TH GAUSSIAN PEAK.
C DEPENDING ON WHETHER J IS ZERO OR NOT, BY USE OF A FOUR POINT CUBIC
C POLYNOMIAL INTERPOLATION METHOD. THE INDEX OF THE MAXIMUM DISCRETE
C POINT OF THE I-TH PEAK (FOUND BY PKFD) IS CONTAINED IN MAX. THE TOTAL
C NUMBER OF POINTS ON THE INTERPOLATED CURVE IS RETURNED IN NP. INTRP
C IS WRITTEN FOR A CONSTANT ABSISSAL INTERVAL OF 0.1 AND ABSISSAL
C VALUES IN DECREASING ORDER.
```

```
C
```

```
COMMON A(500),X(500),N,N1
REAL A*8,XP(1),AP(1)
IF(J.EQ.0) GO TO 1
IW = SQRT(50.0/B)+1.5
L = MAX-IW
IF(L.LT.2) L=2
M = MAX+IW
IF(M.GT.N1) M=N1
GO TO 2
1 L = 2
M = N1
2 DO 3 I=1,L
XP(I) = X(I)
3 AP(I) = A(I)
Q = A(L-1)
R = A(L)
S = A(L+1)
K = M-L
DO 4 I=1,K
LI = L+I
L2 = LI+I
LI = L2-1
XLI = X(LI)
XP(L1) = XLI+0.05
XP(L2) = XLI
P = Q
C = R
R = S
S = A(LI+1)
AP(L1) = (9.0*(Q+R)-(P+S))/16.0
4 AP(L2) = R
MP = M+1
DO 5 I=MP,N
NP = K+I
XP(NP) = X(I)
5 AP(NP) = A(I)
RETURN
END
```



```

SUBROUTINE AXES(NAME,WIDE,XDIM,XMIN,SCY,YD,IY,TWICE)
C
C AXES DRAWS THE AXES, HEADING, AND BOUNDARY, FOR EACH PLOT.
C
      REAL NAME(15)
      LOGICAL TWICE
C DRAW RECTANGLE.
      CALL PLOT(0.0,8.5,2)
      CALL PLOT(WIDE,8.5,2)
      CALL PLOT(WIDE,0.0,2)
      CALL PLOT(0.0,0.0,2)
C DRAW AND LABEL X-AXIS.
      CALL PLOT(0.5,0.5,-3)
      NDIV = 2.54*XDIM+0.5
      DO 1 I=1,NDIV,2
      K = I
      IF(TWICE) K=(I+1)/2
      X = XMIN+K
      ND = ALOG10(X)+I.001
      CALL NUMBER(I/2.54-0.1*ND,-0.17,0.1,X,0.0,2)
1 CCNTINUE
      CALL SYMBOL(XDIM,0.0,0.06,13,0.0,-1)
      DO 2 I=1,NDIV
      CALL SYMBOL(XDIM-I/2.54,0.0,0.06,13,0.0,-2)
2 CCNTINUE
      CALL SYMBOL((XDIM-1.32)/2.0,-0.39,0.12,'ENERGY (KK)',0.0,11)
C DRAW AND LABEL Y-AXIS.
      NDIV = 7.0*YD
      UPD = SCY/YD
      CALL NUMEER(-0.07,-0.1,0.1,0.0,90.0,2)
      DO 3 I=2,NDIV,2
      Y = I*UPD
      CALL NUMEER(-0.07,I/YD-0.1,0.1,Y,90.0,2)
3 CCNTINUE
      CALL PLOT(0.0,7.0,3)
      R = NDIV/YD
      CALL SYMBOL(0.0,R,0.06,13,90.0,-2)
      DO 4 I=1,NDIV
      CALL SYMBOL(0.0,R-I/YD,0.06,13,90.0,-2)
4 CCNTINUE
      CALL SYMRC(0.25,2.6,0.12,'ABSORPTIVITY X10',90.0,16)
      CALL NUMBER(-0.31,4.27,0.11,FLOAT(IY),90.0,-1)
      CALL SYMEOL(1.2,7.7,0.15,NAME,0.0,60)
      RETURN
      END

```





B30019